REPUBLIQUE DU CAMEROUN
Paix – Travail – Patrie
****
UNIVERSITE DE YAOUNDE I
FACULTE DES SCIENCES
DEPARTEMENT DE SCIENCES DE LA TERRE
****
Laboratoire de Geosciences des Formations Superficielles et Applications

REPUBLIC OF CAMEROUN
Peace – Work – Fatherland
****
UNIVERSITY OF YAOUNDE I
FACULTY OF SCIENCE
DEPARTMENT OF EARTH SCIENCES
****
Laboratory of Geosciences of Superficial Formations and Applications

GEOCHEMICAL SURVEY OF SULPHUR, GOLD AND PLATINUM GROUP ELEMENTS IN AMPHIBOLITES AND THEIR WEATHERED PRODUCTS IN AKOM II, SOUTH CAMEROON

A THESIS SUBMITTED IN PARTIAL FULFILMENT OF THE REQUIREMENTS FOR THE AWARD OF A DOCTOR OF PHILOSOPHY (Ph.D) IN EARTH SCIENCES.

Par : **AYE Anehumbu BEYANU**
MSc Earth Sciences

Sous la direction de
Paul-Désiré NDJIGUI
Professor

Année Académique : 2018

UNIVERSITE DE YAOUNDE I
THE UNIVERSITY OF YAOUNDE I

FACULTE DES SCIENCES *FACULTY OF SCIENCE*

DEPARTEMENT DES SCIENCES DE LA TERRE

ATTESTATION DE CORRECTION

Nous, membres du jury de soutenance de **thèse de Doctorat/PhD** de l'Etudiante **AYE ANEHUMBU BEYANU** matricule **05W050**, intitulé : « ***Geochemical Survey of Sulphur, Gold and Platinum Group Elements in Amphibolites and their Weathered Products in Akom II, South Cameroon*** » certifions que la candidate a effectué les corrections conformément aux remarques et recommandations formulées lors de la soutenance de ladite thèse.

En foi de quoi, nous lui délivrons cette **Attestation de Correction**, pour servir et valoir ce que de droit.

Fait à Yaoundé, le 10 07 2018

PRESIDENT DU JURY

Prof. NZENTI Jean Paul

RAPPORTEURS

Prof. NDJIGUI Paul-Désiré

MEMBRES

Prof. NGUETNKAM Jean-Pierre

Prof. NJILAH Isaac KONFOR

Prof. YONGUE-FOUATEU Rose

DEDICATION

TO

My beloved Parents, Peter IHIMBRU and Prodencia MBUNG AYE

ACKNOWLEDGEMENTS

The realisation of this work has been thanks to the collective effort of different people.

My sincerest appreciation goes to Prof. NDJIGUI Paul-Désiré for his supervision, patience, critical judgement, and assistance during the course of this study. His thoughtful advice and wise academic contributions helped in shaping this work. Thank you Prof.

I am indebted to Prof. Sarah-Jane Barnes of Université du Québec à Chicoutimi (UQAC) for Funding part of this project and for analyzing part of the samples in her laboratory.

My sincere gratitude goes to Clement Merilla of the Geoscience Laboratories at Sudbury (Canada) for analysis of the other part of the samples for this work.

My genuine appreciations go to Prof. SUH Emmanuel CHEO of University of Bamenda, his unselfish advice and relevant scientific contributions added the taste to this work.

My weighty recognitions go to Dr TCHOUANKOUE Jean-Pierre for kindly assisting during petrographic studies.

I wish to extend my special thanks to all the Lecturers of the Department of Earth Sciences (NJILAH Isaac Konfor, YONGUE FOUATEU Rose, NGO BIDJECK Louise Marie, TEMDJIM Robert, GHOGOMU Richard Tanwi, NKOUMBOU Charles…) for the patience they took to impart me with the knowledge I needed in order to fulfill this academic exercise.

I am most appreciative to my Darling husband Elias NUM and supportive children Petra, Blaise, Blessing, Praise and Nathan NUM, for permitting me to study; their encouragements, constant prayers, support and understanding during my absence.

I am very grateful to my mother Mama AYE Prudencia, and adopted parents Mr. and Mrs. KANYIMI IHIMBRU for building up my personality, for encouragements and prayers.

My heartfelt regards equally go to my seniors Dr. EBAH ABENG Appolonie Sandrine of blessed memory, Dr. SABABA Elisé and Dr. TESSONSAP TEUTSONG, your kind directives and wise contributions were enormous.

To my sister in the faith and closest friend Mrs. SHEY Grace and family, I say a big thank you. Your hospitality and ceaseless prayers counted a lot for the success of this work.

My profound gratitude also goes to my brother and colleague YOISIMBOM Keneth, your prayers, support and sacrifices are worth recognition. I am grateful to Papa NTONGA Gaston's family of Nyabitande for hospitality. May the Good Lord replenish.

Am the most thankful to my teacher and wife Pr. and Dr. FANTONG Wilson for their encouragements and wonderful scientific contributions.

I appreciate deeply the collaboration I had from Laboratory mates (MBIH Paul, MBANGA Jules, MBABI André, ASSOMO Gaelle, NGO MANDENG…) my regards to them all.

I owe ultimate thanks to God for my life, good health, protection, strength, provision and Divine interventions at different phases of this work.

ABSTRACT

The quest for this work is to find out the behaviour of S, Au-PGE in amphibolites and their weathered products. To achieve this, a petrologic and metallogenic study was done in the Nyabitande and Zingui areas (Akom II), South Cameroon.

Amphibolites of Akom II area are medium-grained and dark-coloured. They are made up of green hornblende, plagioclase, garnet, quartz, and accessory apatite, epidote, spinel, sericite and opaque minerals (pyrite, chalcopyrite). The presence of apatite, sericite, and two generations of opaque minerals suggests that they might be affected by hydrothermal alteration. Amphibolites present a granoblastic heterogranular texture.

The distribution of major, trace and rare earth elements in amphibolites of Nyabitande and Zingui confirms the basic nature of these rocks. However, the rocks of Nyabitande are richer in SiO_2, V, and Cu with rather lower Fe_2O_3 and Al_2O_3 contents. The chondrite normalised REE patterns are very flat for amphibolites from Nyabitande, while those from Zingui are inclined. This suggests that amphibolites from Nyabitande were derived from a depleted mantle source, whereas those from Zingui were from some enriched mantle source.

According to the sulphur contents, amphibolites can be grouped into two: those with low contents, ranging between 380 and 520 ppm; and those with elevated contents, varying from 1140 to 1710 ppm. The variability in sulphur contents is due to hydrothermal alteration. Cu contents are high while Ni contents are low and variable. The total Au-PGE contents in amphibolites are low (2 to 113 ppb). The rocks are richer in PPGE than in IPGE. The PPGE abundance might be relative to the oxidation of primary minerals into goethite. The PGE ratios show that Ir, Ru, Rh, and Pt have very high mobility compared to Pd in amphibolites of Nyabitande and Zingui areas.

The Au-PGE normalised patterns show positive Pd and negative Pt and Ru anomalies for samples from Nyabitande, whereas those from Zingui show negative Pd anomalies. This suggests that Pd in amphibolites of Nyabitande could have been leached out from other sources.

The weathered amphibolites occur in blocks and were obtained from Nyabitande. They present a centripetal weathering and are composed of amphibole, feldspars, quartz, garnet kaolinite, gibbsite, goethite, hematite, and spinel.

Major and trace elements like SiO_2, CaO, MgO, Na_2O, TiO_2 MnO Zn, Ga, Co and Sr were depleted during weathering. Rather, there was an accumulation in Zr, Ba, Th, U, and Mo. The contents of V, Cu, Sc, Nb, Rb, Hf, and Ta were stable during weathering. Trace element contents normalised with the primitive mantle show distinct positive anomalies in Pb and negative anomalies in Th. Despite the overall low contents in REE, normalized patterns show positive cerium anomaly (Ce/Ce^{*}= 4.24). Positive Ce anomalies could result from variability of oxidizing conditions.

The weathered samples show variable S (238- 902 ppm) and Cu (520 – 2150 ppm) contents**.** The contents of Cu, Ni and Au-PGE are higher in weathered samples than the fresh ones. Gold, Ru, Rh, Pt, Pd, and Cr are positively correlated. This confirms that Cr and Au-PGE are associated in mafic rocks. Chondrite-normalized base metal patterns confirm the abundance of Pd and the slight enrichment of Au-PGE in weathered rocks. Palladium, Rh and Ir are positively correlated with S. Conversely Pt and Ru are negatively correlated with S and Au is not correlated with S. Despite the high and variable S and Cu contents, the garnet amphibolites possess low Au-PGE and other base metals contents.

Key Words: South Cameroon, Amphibolites, sulphur, gold, platinum group elements.

RESUME

Ce travail a pour objectif de comprendre le comportement du soufre, de l'or et des éléments du groupe du platine dans les amphibolites et leurs produits d'altération. Pour cela, une étude pétrologique et métallogénique a été menée dans les localités de Nyabitandé et Zingui (Akom II), Sud Cameroun.

Les amphibolites d'Akom II ont des grains moyens à grossiers et de couleur noire. Elles sont constituées de hornblende verte, plagioclase, grenat, biotite, quartz, épidote et minéraux opaques (chalcopyrite et pyrite). La présence d'apatite, de séricite et de deux générations de minéraux opaques indiquent que ces roches auraient subi une altération hydrothermale. Ces amphibolites présentent généralement une texture granoblastique à hétérogranulaire.

La distribution des éléments majeurs, traces et terres rares dans les amphibolites de Nyabitande et de Zingui confirme leur nature basique. Cependant, les amphibolites de Nyabitande possèdent des teneurs plus élevées en SiO_2, V, Cu et plus faibles en Fe_2O_3 et Al_2O_3. Les spectres des terres rares normalisées par rapport à la chondrite sont plats à Nyabitande et en pente à Zingui. Ceci montre que les amphibolites de Nyabitande proviennent d'un manteau appauvri tandis que celles de Zingui résultent d'un manteau enrichi.

En fonction des teneurs en soufre, les amphibolites de Nyabitande sont de deux types: l'un pauvre en soufre, variant de 380 à 520 ppm et l'autre riche en soufre avec des teneurs comprises entre 1140 et 1710 ppm. L'altération hydrothermale serait à l'origine de la variabilité des teneurs en soufre. Les concentrations en cuivre sont élevées tandis que celles en nickel sont faibles et variables. Les teneurs en Au-EGP sont faibles dans les amphibolites (2-113 ppb). Les roches sont plus riches en PPGE qu'en IPGE. Les teneurs relativement élevées en PPGE seraient liées à l'oxydation des minéraux primaires en goethite. Les rapports entre les EGP montrent que Ir, Ru, Rh et Pt sont plus mobiles que le palladium dans les amphibolites de Nyabitande et Zingui.

Les spectres des Au-EGP présentent des anomalies positives en Pd et négatives en Pt et Ru dans les roches de Nyabitande, tandis que les spectres des roches de Zingui montrent des anomalies négatives en Pd. Ceci suggère que le palladium dans les amphibolites de Nyabitande pourrait provenir d'une autre source.

Les amphibolites altérées affleurent en boules dans la localité de Nyabitande. Elles montrent une altération centripète et sont constituées d'amphibole, de feldspaths, de kaolinite, de goethite, d'hématite, de gibbsite, de quartz, de grenat et de spinel.

Les éléments majeurs et traces tels que SiO_2, CaO, MgO, Na_2O, TiO_2, MnO, Zn, Ga, Co et Sr sont évacués au cours de l'altération tandis que Zr, Ba, Th, U, et Mo s'accumulent. Les teneurs en vanadium, Cu, Sc Nb, Rb, Hf et Ta sont stables au cours de l'altération. Les teneurs en éléments traces normalisées par rapport au manteau primitif montrent des spectres avec de fortes anomalies positives en Pb et des anomalies négatives en Th. Malgré les faibles teneurs en terres rares, les valeurs normalisées montrent des anomalies positives en cérium (Ce/Ce^{*}= 4.24). Les anomalies positives en Ce pourraient résulter d'une variabilité des conditions oxydantes.

Les matériaux d'altération ont des teneurs variables en S (238- 902 ppm) et Cu (520 – 2150 ppm). Les teneurs en Cu, Ni et Au-EGP sont plus élevées dans les matériaux d'altération que dans les roches saines. Ceci confirme que le Cr et les Au-EGP sont associées dans les roches mafiques. Les spectres des métaux de base normalisés par rapport à la chondrite confirment l'abondance du Pd et le léger enrichissement de Au-EGP dans les roches altérées. Pd, Rh et Ir sont positivement corrélés avec le soufre. Inversement, Pt et Ru sont négativement corrélés avec le soufre et Au ne présente pas de corrélation avec S. Malgré les teneurs élevées et variables en S et Cu, les amphibolites à grenat possèdent de faibles teneurs en Au-EGP et autres métaux de base.

Mots-clés : Sud-Cameroun, Amphibolites, Soufre, Or, Eléments du Groupe du Platine.

LIST OF ABREVIATIONS

Amp	Amphibole
Ap	Apatite
Au	Gold
Bt	Biotite
Cpx	Clinopyroxene
Ep	Epidote
Grt	Garnet
Mc	Microcline
Or	Orthoclase
Opq	Opaque
Pl	Plagioclase
Prt	Perthite
Qz	Quartz
Ser	Sericite
Spn	Sphene
Zrn	Zircon

TABLE OF CONTENTS

LIST OF TABLES

LIST OF FIGURES

GENERAL INTRODUCTION

The African continent ranks first worldwide with concentrations of platinum, gold, chromium, diamond, cobalt and manganese (Coakley and Mobbs, 1999). The substratum of Cameroon is highly supplemented with the above elements; various mineral resources and valuable noble metals (iron, nickel) which are cooperatively known as strategic and critical minerals. Ultramafic and mafic rocks are typically known as repository for transitional metals (iron, cobalt, chromium, nickel and platinum group elements (PGE)) which are among the rarest elements of the earth crust. PGE are almost completely confined to these rocks (Satyanarayanan *et al*., 2011).

Some mechanisms such as hydrothermal activity, metamorphism, or weathering can modify the concentrations of the above elements from the initial magmatic rock, resulting in subeconomic or economic amounts of platinum group elements (Prichard *et al*., 1986; Boudreau *et al*., 1986; Zaccarini *et al*., 2005; Wang *et al*., 2008; Ndjigui and Bilong, 2010). The weathered materials developed on ultramafic rocks under humid tropical conditions have been proven to be characterized by high contents that may go above 1000 ppm for gold and platinum group elements (Traoré *et al*., 2008).

Owing to the scarcity, but enormous industrial demand for gold and platinum group elements, there is significant interest in understanding the rare occurrence of these mineable Au-PGE concentrations in the highly depleted crust.

Consequently, several petrological and geochemical surveys for Ni, Cu, Au, and PGE have been carried out in Southern Cameroon on mafic–ultramafic rocks and their weathered products (e.g., Maurizot *et al.*, 1986; Ngo Bidjeck, 2004; Yongue Fouateu *et al*., 2009; Ndjigui *et al*., 2009; Ebah Abeng *et al*., 2012). The results show high Ni contents in peridotites and moderate Pt and Pd contents in amphibolites from Nyabitande area. In pyroxenites from Lolodorf area, Au-PGE contents are rather low. Palladium and Pt have the highest contents which attain 83 ppb and 26 ppb in amphibolites of Nyabitande (Aye, 2010; Ebah Abeng *et al*., 2012).

When basaltic rocks are subjected to high temperatures (550–750°C) and slightly greater pressure range than that which yields green schist, they are transformed into amphibolites. Therefore, amphibolites do retain platinum group elements derived from their protolith.

In Cameroon, amphibolites have been encountered in: Abiete- Yenjok, where they occur together with gabbro and peridotites precisely harzburgites (Ngo Bidjeck, 2004); Eséka, NE border of the Nyong unit, amphibolites occur as mafic/ultramafic xenoliths in gneissic rocks. They also co-exist with pyroxenites and talcschists in the same area (Bayiga *et al*., 2011). At Pouth-Kelle area, they outcrop in the form of metric blocs on the flanks of hills, together with talcschists in a gneissic environment (Minyemeck, 2006; Oumarou, 2006; Nkoumbou *et al*., 2008). Meanwhile, in Nyabitande, they appear in the form of rounded and spherical blocks of variable dimensions under the rain forest of Nyabitande. They occur in a terrain that is rich in gneisses and quartzite (Aye, 2010; Tessontsap, 2010).

The banded and intrusive series of the Ntem complex in South Cameroon also hold amphibolites which occur together with metagraywackes, ironstone, and sillimanite bearing paragneisses. In this case, amphibolites considered as remnants of supracrustal rocks. They occur as large elongated xenoliths in both intrusive and banded series as well as in foliated charnockite portions (Shang, 2001; Tchameni *et al*., 2004; Takam *et al*., 2009).

The above authors denote amphibolites as typically dark-colored and massive, with a flaky structure. They can exist as ortho-amphibolites in which case they are derived from basalts or mafic rocks (the case of this work) or para-amphibolites in which case they are derived from other chemically appropriate lithologies (certain “dirty marls” and volcanic sediments).

For all petrological and geochemical studies in South Cameroon, extensive exploration on Au-PGE in amphibolites and the weathered materials issued has not been realized (Aye, 2010; Tessontsap, 2010). Little has been achieved on the research for sulphur in amphibolites and their weathered products. The presence of insufficient or no data in these elements ignited their research. This work investigates on sulphur and Au-PGE contents in amphibolites and the weathered products developed upon them.

I. Problem Statement

Up to the beginning of the 20th century the total world production of PGE was principally from nuggets of alluvial deposits of platinum group minerals (PGM) mainly located downstream of mafic-ultramafic magmatic complexes of Colombia and Russia (Cabri *et al*., 2002; Garuti, 2004). According to these authors, since the discovery and exploitation of PGE in the last century in layered rocks of South Africa, Siberia and the extraction of by-products of PGE in sulphur and metal mines of Canada, there has been a strong growth in global demand for platinum group elements (PGE). Consequently, researchers in Cameroon recultivated interest in platinoids which had been long abandoned since 1950s due to poor analytical results (Ndjigui *et al*., 2003, 2004, 2008; Ebah Abeng 2006; Minyemeck 2006; Bilong *et al*., 2010).

Platinum group elements are principally known to occur within intrusions associated with high degree of mantle melting (Keays, 1995). They tend to concentrate mostly in basic and ultrabasic rocks (Gruenevaldt *et al*., 1986; Augé *et al*., 1995; Godal *et al*., 2007 Naldrett *et al*., 2008). Thus, these elements result directly from a mantle source through a mechanism in which plume melting is required. Sulphur bearing phases (pyrrhotite, pyrite (marcasite), chalcopyrite and pentlandite) have been proven as the carrier minerals for Au-PGE (Puchtel *et al*., 1995; Zaccarini *et al*., 2011). However, little has been achieved on the research for sulphur in mafic and ultramafic rocks of Cameroon.

Preliminary data on Au-PGE in amphibolite rocks of south Cameroon (Aye, 2010) reveal that these rocks though of metamorphic origin have moderate PGE contents. These contents range from 26 ppb to 83 ppb for platinum and palladium, respectively. But metamorphic rocks are formed through recrystallization of pre-existing rocks in the solid state, when these rocks are subjected to agents such as heat, pressure and chemically active fluids (Whitten and Brooks, 1972). This implies that the initial magmatic rock that contains PGE is modified when subjected to metamorphic processes, consequently, the carrier minerals of PGE are recrystallized during metamorphism. It is from these somehow conflicting ideas that the following questions arise:

- What are the processes that concentrate Au-PGE in amphibolites?
- What are the carrying minerals of PGE in amphibolites?
- Are there any sulphur contents in amphibolites of South Cameroon?

- How do sulphur and Au-PGE behave in amphibolites?

II. Objectives

The main focus of this work will be to carry out petrological studies on amphibolites and their weathered products. To achieve this:

- The petrography of the rock will be examined to understand the mineral associations;
- Mineralogical studies will also be done to find out the carrying minerals for gold and platinum group elements in these rocks;
- A geochemical survey will be done on amphibolites to understand the behaviour of major, trace as well as gold and platinum group elements.
- The behaviour of sulphur and its association with gold and platinum group elements, as well as a couple of metals will be developed.
- Also a geochemical survey on another mafic rock type (pyroxenites) found in the same area will be done and contents compared with those of amphibolites.

III. Significance of the work

From the second half of the twientieth century onwards, platinum group elements have become essential to modern industry, assuming such a relevant role in a number of advanced technologies that they have gained the reputation of "miracle metals" (Garuti, 2004). Their innumerable applications are based on physical properties such as: electrical conductivity and high resistance to heat, oxidation and chemical corrosion. What makes some of the PGE even more extraordinary is their rather unique ability to act as extremely efficient catalyst in several chemical reactions. These metals are indispensably used in the electronic, automobile, pharmaceutical, chemical dental industries and other diverse industrial sectors as semi-conductors, jewelleries and as good anti-pollutants in the environment. Owing to their scarcity but enormous industrial demand, there is significant interest in understanding the rare occurrence of mineable PGE concentrations in the highly depleted crust.

Further expansion of demand for platinoids is expected as a result of the development of the fuel-cell technology which will certainly play a prominent role in the production of clean energy and the construction of electrical vehicles in the not too distant future; this

renders platinum metals strategic commodities for human life (Garuti, 2004). Gold and platinoids are metals with very high marketing values and of very high demand in the world market. Hence, there is a worldwide increase in the search for Au- PGE (Matthey, 2006).

Despite the recent increase in South African production, supply of these metals is likely to be below demand in the nearest future (Matthey, 2006). For this reason the search for Au-PGE in the entire world is very imperative. Also, the fact that little or nothing has been achieved on the research for sulphur in amphibolites and their weathered products in this area, it becomes very necessary to add sulphur in our investigation. Since platinum group elements have become essential to modern industry, their discovery in the country will not only boast the nation's economy, but also furnished available raw materials for the various developing industries.

IV. Methodology

The methods adopted which furnished the data necessary to attain the main objectives of this work are as follows:

IV.1. Field investigations

Different field trips were carried out in the Nyabitande and Zingui areas. A total of thirty-three samples were collected in view of chemical analysis. The macroscopic description of the different samples started on the field, after which they were packaged for laboratory investigation.

IV.2. Petrographic Analyses

Thin sections of some relatively fresh samples were made in the University of Lorraine (France). The observation of these samples under polarized light was done in the Department of Earth Sciences (University of Yaounde 1), after which the mineral paragenesis were taken. These observations permit to describe the minerals and identify their genetic relationship.

IV.3. Geochemical analytical methods

The geochemical analyses were carried out in two laboratories, for a suite of major, trace, rare earth elements, as well as sulphur and Au-PGE.

The major, trace and rare earth elements were analysed at the Geoscience Laboratories (Sudbury, Canada). Geochemical analyses for Au-PGE, S, and Cu were carried out in the Earth's Materials Laboratory of University of Quebec –LabMaTer (Canada) and in the Geoscience Laboratories (Sudbury, Canada). The analytical procedures used in LabMaTer were previously described by Savard et al. (2010).

IV.3.1. Analyses of major elements using X-ray Fluorescence

Major element concentrations were determined by X-ray fluorescence after sample ignition. Sample powders were ignited and melted with a lithium tetraborate flux before analyses using an AXIOS Advanced PW 4000 analytical PAN. International standards BIR-1-0949, SDU-1-0295 and SDU-1-0296 as well as in-house standards were run with the unknowns.

IV.3.2. Trace element Analyses by ICP-MS

Rock powders were prepared for Inductively Coupled Plasma Mass Spectrometry (ICP-MS) analyses for lithophile trace element concentration by acid digestion in closed beakers. Powders were treated in a mixture of HCl and $HClO_4$ acids at 120˚C in sealed Teflon containers for one week, after which they were rinsed out of their containers with dilute HNO_3 and boiled to dryness. The residue was re-dissolved in HCl and $HClO_4$ and evaporated to dryness a second time, before being re-dissolved in a mixture of HNO_3, HCl and HF at 100˚C.

The dissolved solution of sample was analyzed in a Perkin-Elmer Elan 9000 ICP-MS instrument. At first, the analyses was performed using the IM100 analytical package, in which a weighted average of instrument responses for three certified reference materials prepared in the same manner as the unknown was compared with the instrument response of the unknown solution for each element. The nominal zero concentration was assumed to be equal to the measured response from an acid blank. Standard solutions were run between each batch of 30 samples along with a check sample for every 10 samples.

Data are replaced for a wide range of transition metals. Due to uncertainties in the element concentrations in the certified reference materials at the lowest concentrations, the detection limits for the IM100 package are higher than limits of the instrument capabilities. When some data for this study were found to be below the detection limit for the IM100 analytical package, the solutions were re-analyzed using a second set of four synthetic

calibrating solutions containing 14 rare earth elements Y, U, Th, Hf, Zr, Nb, Ta, Rb and Sr. The resulting detection limits were much lower, but this package does not report results for as many elements as were measured using the IM100 package.

The concentrations of rare earth elements were realized in the Geoscience Laboratories (Canada). The samples were crushed using a jaw crusher with steel plates and pulverized in a planetary ball mill made of 99.8% Al_2O_3. A two-step loss on ignition (LOI) determination was employed. Powders were first heated to 105˚C under nitrogen to drive off adsorbed water, before being ignited at 1000˚C under oxygen to drive off remaining volatiles and oxidized Fe.

IV.3.3. Analyses of Au-PGE in LabMaTer (Canada)

Gold and platinum group elements (Au-PGE) were determined by the Nickel Sulfur Fire Assay technique (NiS-FA), followed by $SnCl_2Æ2H_2O$–Te co-precipitation (NiS-FA). Fire assay is a neoclassical technique for PGE determination in geological materials. Many variants of the NiS-FA exist. This technique has three advantages: (i) it is capable of determining rhodium and gold; (ii) the relatively large test portion mass (15 g) reduces the nugget effect; and (iii) it is faster and less expensive than isotope dilution with high-pressure Asher acid digestion (HPA-ID) (Savard et al., 2010).

A NiS bead was produced by mixing 15 g of powdered geological material in a ceramic crucible with analytical grade fluxes: sodium carbonate (10 g), sodium tetraborate (15 g), silica (5 g), nickel (5 g) and sulfur (3 g). A further 15 g of sodium tetraborate was added on top after mixing. After fusion in a muffle furnace (1050°C) for 90 min, the NiS bead was separated from the cooled slag and dissolved for 24 hr in 160 ml of 12 mol l-1 HCl (environmental grade) in a 180 ml closed PFA jar placed in a vented oven (110°C). After complete dissolution of the NiS bead, stannous chloride dihydrate ($SnCl2Æ2H_2O$) (4 g) previously dissolved with 9 ml of 3.24 mol l-1 HCl and 3 ml of 2000 lg g-1 tellurium solution was added to the dissolved bead. The PFA jars were placed in the oven (110°C) for 24 hr. After cooling, the black precipitate was recuperated on a 0.45 lm cellulose membrane filter, thoroughly rinsed with ca. 50 ml of 1 mol l-1 HCl and then dissolved in a mixture of 2 ml HCl and 2 ml HNO_3 (concentrated environmental grade) in the PFA jar with the lid sealed, on a hot plate (at 120°C) for 12 hr. After complete digestion, the acid solution was diluted with de-ionized water (18.2 MX cm) to a total volume of 25 ml and the PGE and Au were determined by ICP-MS (Thermo Elemental X7 series; Thermo Fisher Scientific, Waltham,

MA, USA) using thallium as a drift monitor. A multiple PGE-Au and Restock solution (SCP Science, Baie D'Urfé, QC, Canada) was used for external calibration. Modification of sample and sulfur mass was necessary for S-rich samples, such as the massive sulfide WMS-1a, because the natural S concentration (28% m/m) significantly changes the S/flux ratios. The sample mass was reduced to 7.5 g and the sulfur added was adjusted to 0.9 g so that the total mass of S in the mixture was 3 g. The accuracy of each technique was verified by comparing the results obtained with the values for international RMs.

IV.3.4. Analyses of Au-PGE in Geoscience Laboratories (Canada)

The concentration of platinum group elements and gold were determined by a NiS fire assay with ICP-MS finish according to procedures described by Richardson and Burnham (2002). Fifteen grams were fused with sodium carbonate and sodium tetraborate in the presence of a NiS melt. After quenching of each sample, a bead of NiS was broken out of the crucible and digested in Teflon vessel using concentrated HCl. Tellerium coprecipitation was used to ensure that the insoluble residue to acid digestion retained all the PGE.

Solutions were vacuum-filtered, after which the precipitate was re-dissolved in aqua regia and de-ionized water. The resulting solutions were analyzed by ICP-MS using a Perkin Elmer Elan 9000 instrument. The precision of these results is in the order of 5% (2θ).

IV.3.5. Analytical methods for sulphur and copper

Whole-rock sulfur was determined using an infrared HORIBA EMIA 220V sulfur analyzer, using the method described by Bedard et al. (2008). The detection limit is < 18 ppm and the relative standard deviation is less than 5% for samples with more than 500 ppm. Copper was determined by atomic absorption spectrophotometry after aqua regia digestion. The HORIBA EMIA 220-V is a latest generation instrument with a programmable high frequency furnace. The plate current control heated the sample in small steps (up to ten) which allowed fine control over sulfur extraction. The sample was placed in a porous crucible with accelerators covering the rock powder. The sample was heated in an O_2 flux by an induction furnace. Volatilized gases were oxidized (S to SO_2) and passed through glass wool in order to filter dust, followed by Mg $(ClO_4)_2$ to dry gases. Gases then flowed to the infrared detector for quantification. Some samples did not fuse entirely, but could be identified easily by the lack of an orange glow in the sample chamber, and the powdery appearance of the sample after fusion, instead of the normal dull grey metallic surface.

IV. 4. Mineralogical analyses

This was done through x-ray diffraction (XRD). The sample powders pulverized with an agate mortar and pestle and smear mounts were prepared on low background silicon disks for analysis. This is done using a diffractometer of the PAN analytical X' PERT PRO type.

V. Thesis Outline

This work is presented in six chapters. It begins with a general introduction which includes generalities, problem statement, objectives and significance of this work. The work ends with a general conclusion.

Chapter one present the environmental setting of the study areas. This involves a presentation of the environmental parameters such as climate, vegetation, geomorphology and hydrography as well as the geological context.

Chapter two deals with the literature review. It handles the geology of the Southern part of Cameroon; a synthesis on past works on the geochemistry of gold and platinum group elements in rocks and their weathered materials; past research results obtained on the nature of sulphur and its relationship with platinoids; finally, the domains of application of gold, platinoids and sulphur.

Chapter three is a presentation on the petrology of amphibolites and country rocks. It covers the petrography, mineralogy and geochemistry of rocks. The distribution of major, trace, rare earth elements, gold and platinum group elements is presented in two groups: the rocks of Kolasseng I and the rocks of Kolasseng II.

Chapter four highlights the morphologic, mineralogical and geochemical characterization of weathered amphibolites.

Chapter five treats the behaviour of sulphur, copper, nickel, chromium, gold and platinum group elements in the rocks and their weathered amphibolites.

Chapter six first of all presents a recap of the main results on the petrology of amphibolites and country rocks; then, a discussion of the results.

Finally, a general conclusion is presented which covers the main findings of this work and the possible recommendations for future research.

CHAPTER ONE:

ENVIRONMENTAL SETTING

Introduction

This involves a presentation of the environmental parameters of the studied area such as climate, vegetation, geomorphology and hydrography. This is closely followed by the geology of the study area and the soil types developed upon these rock types. All the above mentioned factors engender the chemical weathering of rocks, the remobilization of chemical elements in the surface environment and their subsequent precipitation to form secondary mineral phases.

I. Localisation

The study areas are situated in the Akom II Sub-division, Ocean division, South of Cameroon. It is found along the road mid-way between Ebolowa and Kribi. The actual location chosen for sample collection is found in two villages (Nyabitande and Zingui), located at about 7 km and 12 km west of Akom II. The areas fall within the following geographical coordinates: longitudes 10˚09' and 10˚30' E and latitudes 2˚ 42'- 2˚ 51' N (Fig 1).

II. Physical Geography

II.1. Climate

South Cameroon is characterized by humid equatorial climate. The climate of Nyabitande and Zingui areas which form part of the coastal plain is mainly of equatorial type (Suchel, 1988). It is a hot rainy climate globally characterized by four seasons:

- Two rainy seasons, the long rainy season covers August to November and the short rainy period goes from April to June;

-Two dry seasons, the long dry season (December to March), and a short dry season (July to August). (By dry we mean that the sum of precipitation in millimeters is less than or equal to twice the average temperatures measured in degrees).

There is abundant precipitation; the total annual precipitation varies from 1746.4 to 2919.4 mm. Temperatures are high and vary slightly throughout the year; the average annual temperature is 24˚C. Minimum temperatures are observed in the months of July and August (22.9˚C) which indicate dry season while February (25˚C) is the hottest month.

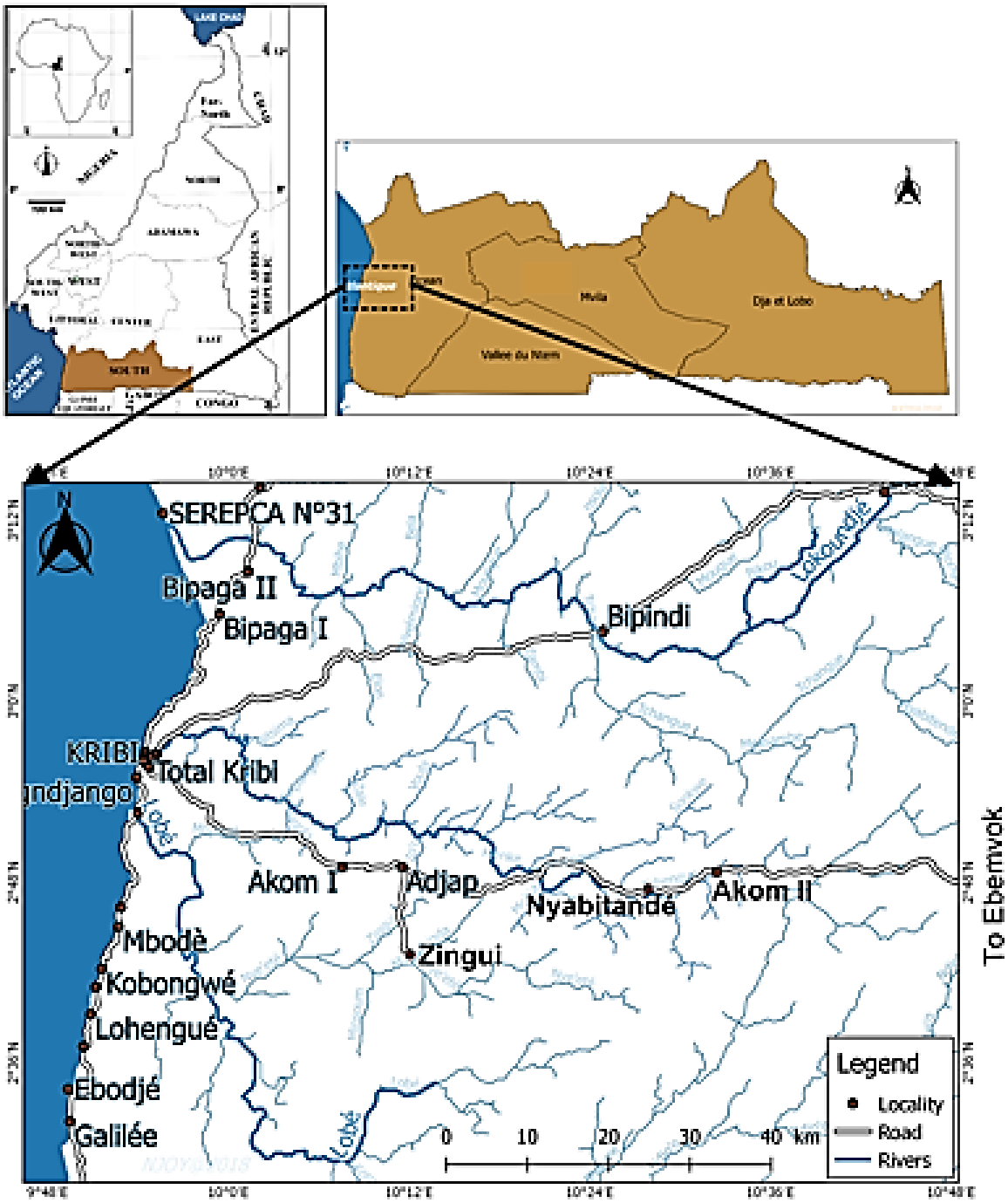

Figure 1 : Location map of study areas

II.2. Vegetation

The vast regions of the coastal plain contain two main vegetation types:-The mangrove forest around the estuaries; the thick Atlantic evergreen forest on lowlands (Letouzey, 1985).

The sampling sites are characterized by a dense equatorial evergreen forest which covers about 80% of the coastal plain. The vegetation in these areas can be distinguished in to two:

-The thick primary evergreen forest with poor undergrowth made up of huge trees with broad stems. This type is generally encountered along rivers and hill tops and is easy to penetrate.
-The sparse secondary forest results from the degradation of the primary forest through dense anthropogenic action. It is represented by small trees, palm trees with relics of a primary forest and raphia bushes in swampy areas. This type is issued by human action and contains numerous woody savanna strips which make up the thick undergrowth that renders access in to the forest difficult (Fig. 2).

II.3. Geomorphology

South Cameroon is a broad region that stretches from the Atlantic Ocean to the Congo basin. This zone is essentially low lying, the sampling sites form part of these broad coastal plain. According to Segalen (1967), the coastal plain makes up the region with the lowest altitudes (0-350 m). It is made up of a succession of three levels of altitudes increasing towards the plateau of South Cameroon (Njiké Ngaha, 1984):

The areas of Nyabitande and Zingui can be sub-divided in to 5 geomorphologic units (Fig. 3)

- A unit with altitude ≤ 200 m which falls within the coastal plain. It includes the Zingui area.
- A unit with altitude between 200 and 400 m, it extends toward the NW of Akom II. This unit makes up the low lands of the region; the hydrographic network strictly follows the spatial disposition of this unit. The main direction of water flow is thus SE-NW; this unit contains the Nyabitande area.
- A unit with altitude between 400 and 600 m, it is widely distributed in the region and stretches following the SW-NE direction.
- A unit with altitude from 600-800 m, it is mostly represented at the South and SE of Akom II; some portions are also represented in the NE of the region. Most streams in the South take their rise from this morphologic unit.
- Altitudes of 800-1000 m characterize the summit of hills found at the south of Akom II such as Ndagueng, Nkolbissoum. Streams generally follow the paths with the least altitudes between the above summits (Fig. 4).

II.4. Geology

The Nyabitande and Zingui areas belong to the Nyong series which corresponds to the North Western remobilized and restructured border of the Archean Congo Craton (Shang *et al.*,

2010; Ndema *et al*., 2015). The Congo craton is very well exposed in Southern Cameroon represented by the Ntem group (Goodwin, 1991).

The Nyong Unit constitute the greenstone belt characterized by pyroxenites, migmatites, gneisses, quartzites, peridotites, talcschists, amphibolites and banded iron formation), (Tonalite – Trondhjemite - Granodiorite (TTG), gneiss), and magmatic rocks (granodiorites and synites) (Lerouge et al., 2006; Owona et al., 2013; Ndema Mbongue et al., 2015; Ganno *et al*., 2015; Ganno *et al*., 2017; Teutsong *et al*., 2017). Most of these rocks outcrop enormously in the studied area. The above rocks are locally intercepted by mafic and ultramafic veins represented by gabbros, dolerites and peridotites (Toteu *et al*., 1994; Fig 5).

Figure 2 : Secondary forest-type vegetation in Nyabitande

II.5. Soils

A synthesis of the pedologic study of South Cameroon shows that the humid forest is developed on two main soils types: the reddish brown ferrallitic soils and the hydromorphic soils (Yongué, 1986; Bitom 1988; Bekoa 1994; Nguetnkam 1994).

The ferrallitic soils are reddish brown and are found on hills. There are differentiated from bottom to top in to three sets *(*Bilong, 1988; Ndjigui *et al*., 1998, 1999; Tessontsap, 2010*)*:

- An alteritic set at the bottom ;
- A middle set made up of nodular horizons with blocks of iron duricrust.
- Superior clayey, sand to clay set.

Mineralogically, the soils are made up of gibbsite, haematite, geothite, kaolinite, chlorites, smectites and interstratified chlorite-vermiculite and muscovite-vermiculite (Ndjigui *et al.*, 1998, 1999; Oumarou, 2006).

The hydromorphic soils are formed due to the flooding and accumulation of water over the land for a long period of the year. Two types of these soils are common in the region: the organic hydromorphic soils and the mineral hydromorphic soils.

- The organic types are formed in the valleys or low lying regions and are characterized by partially decomposed organic materials and lie above a sandy and clayey horizon (Segalen, 1967; Bekoa, 1994).
- The mineral hydromorphic soils are found in the portions of land sandwiched between the interfluves. They are humified at the surface, grey or yellowish with reddish or yellowish spots. Therefore the area of study is composed of reddish brown ferrallitic soils on the interfluves and hydromorphic soils in the submerged valley bottoms.

Conclusion

Studies on the environmental setting reveal that Nyabitande and Zingui villages are found in the coastal plain, situated at about 7 and 12 km to the west of Akom II, in Akom II Sub division Ocean Division, South region of Cameroon. The areas are marked by a hot rainy equatorial climate of four seasons. There is abundant precipitation (1746.4 to 2919.4mm) and the average annual temperature reaches 24˚C. The vegetation is of the dense equatorial forest type, characterized by the relics of a primary forest encountered along rivers and hill tops and a secondary forest with thick undergrowth represented by small trees, palm trees raphia bushes in swampy areas. The study areas form part of the coastal plain with altitudes of 0-350 m but some mountain chains in the North and South may reach 400, 600 and up to 800 m. The drainage pattern is dense and of dendritic type. The lithologic substratum is that of the greenstone belt of Nyong unit. It consists of gneisses, quartzites, migmatites, and amphibolites. The soils developed upon the above rocks are the yellowish brown ferrallitic soil type found on the interfluves and dark hydromorphic types in the valleys and low lands.

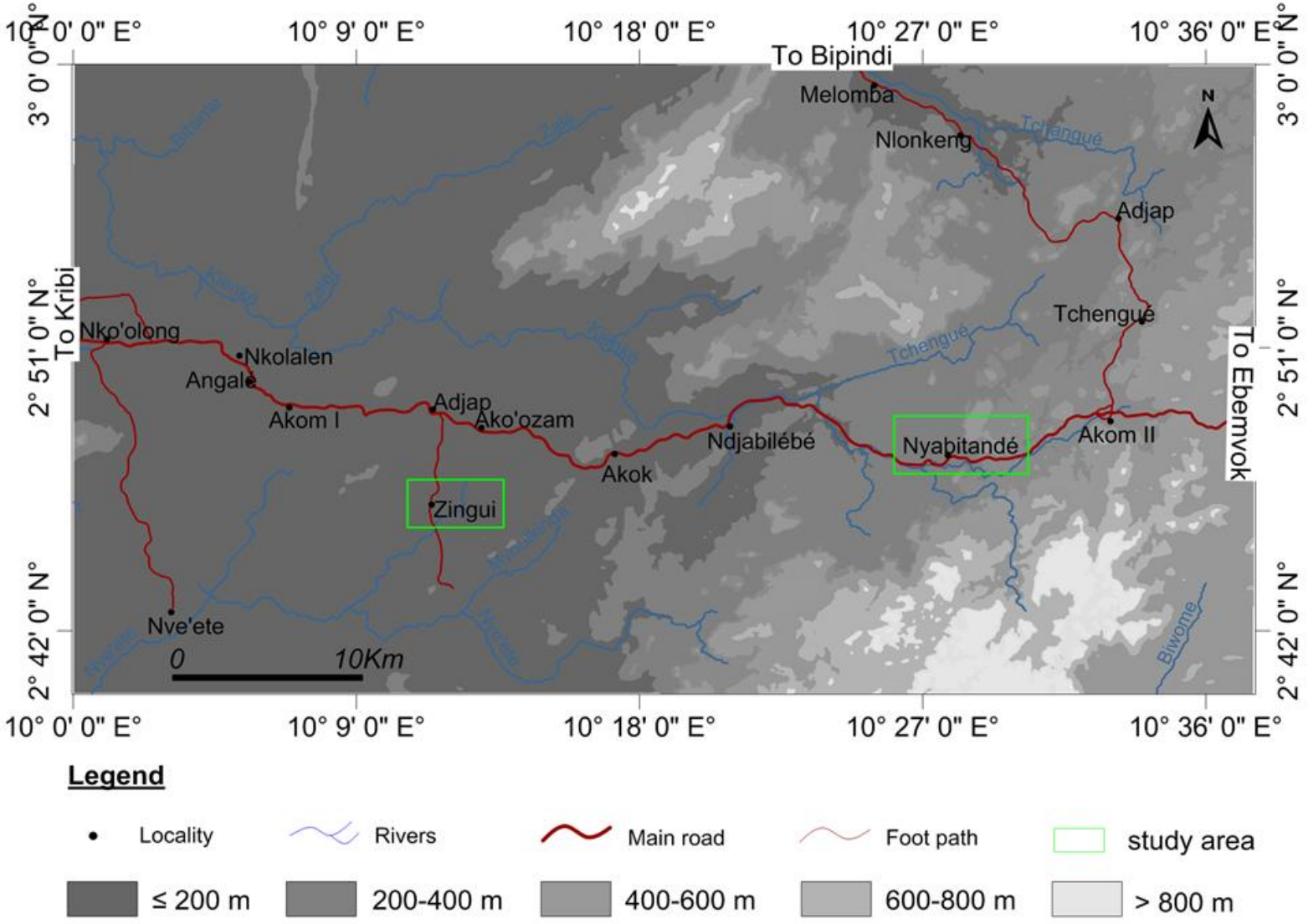

Figure 3 : Geomorphologic Map of the study areas

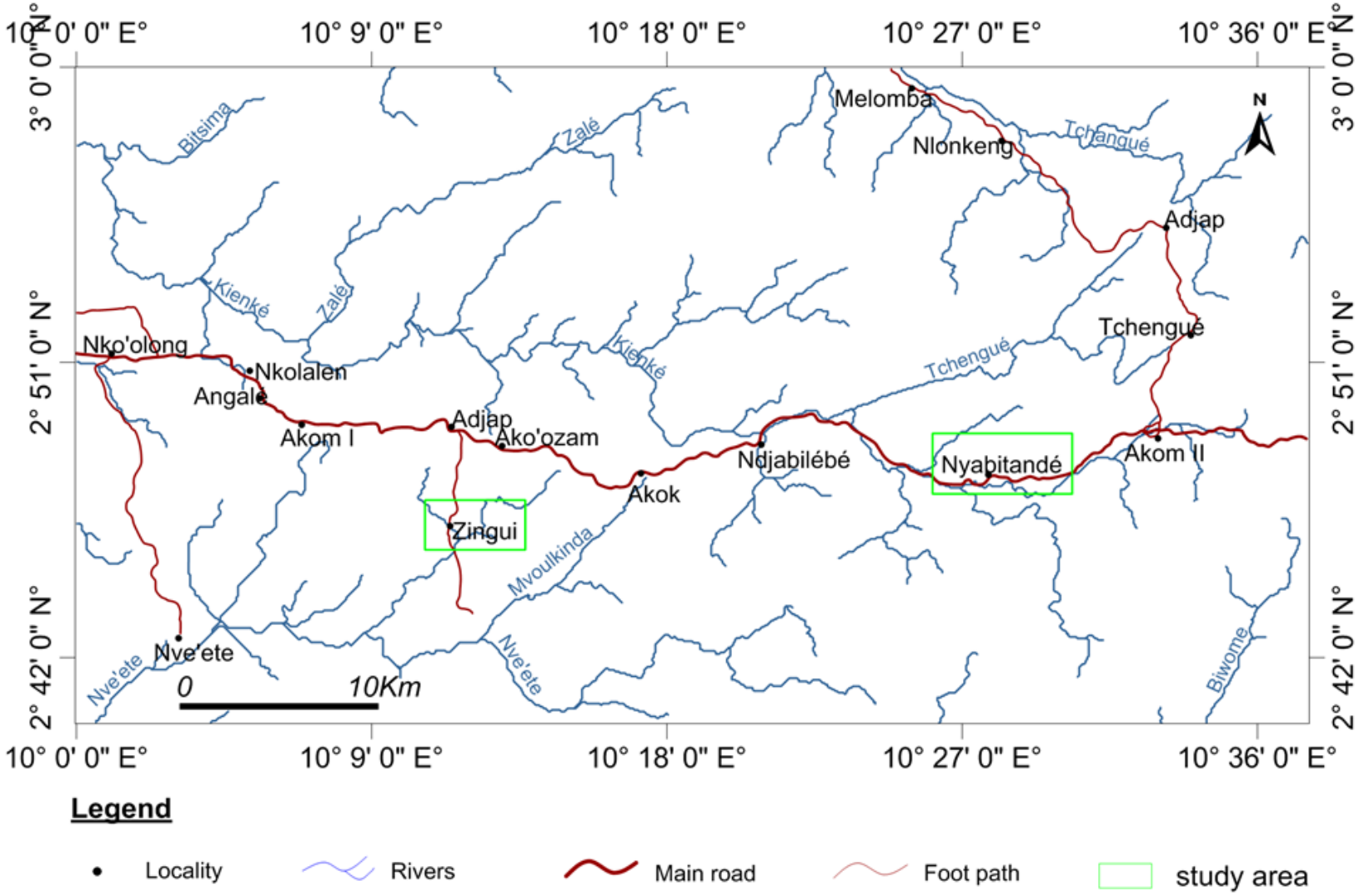

Figure 4 : Hydrographic network of the study areas

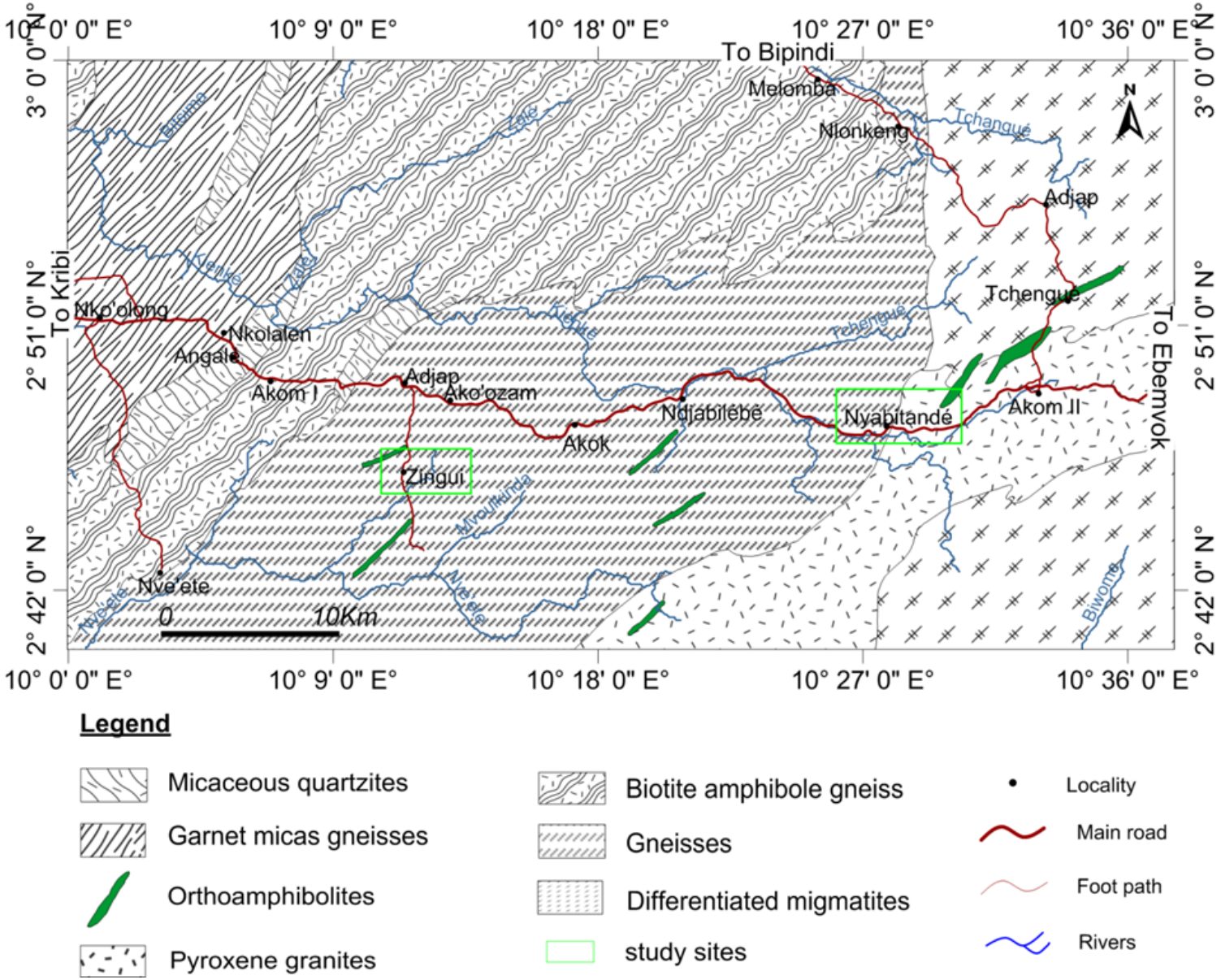

Figure 5 : Geologic map of Nyabitande and Zingui areas modified after (Champetier de Ribes and Aubague, 1956)

CHAPTER TWO

LITERATURE REVIEW

Introduction

This chapter handles the geology of the Southern part of Cameroon in general; a synthesis on past works on the geochemistry of gold and platinum group elements in rocks and their weathered materials and past research results obtained on the nature of sulphur and its relationship with platinoids.

I. Geology of South Cameroon

The Nyabitande and Zingui areas are situated in the Nyong unit. They form part of the north western border of the Congo Craton. The northwestern margin of the Archaean Congo craton in Southern Cameroon is commonly known as the Ntem complex (Maurizot *et al.,* 1986; Nédélec *et al.*, 1990; Shang *et al.,* 2010). The Ntem complex is bordered in the north by the Yaounde Group (e.g. Nzenti *et al.,* 1988; Toteu *et al.,* 2006), of the Pan-African orogenic belt in Central Africa. The two entities are delimited by a major thrust fault of Pan-African age (600 Ma). The Ntem complex consist of Palaeoarchaean to Mesoarchaean and Late Archaean charnockites, Mesoarchaean greenstone formations, Late Archaean TTG basement, dolerite dykes and high-K granites (Shang *et al.,* 2010).

Several studies have been carried out in this region by different authors over the years whose data is presented below:

I.1. Ntem Group

The Ntem group is a granulitic complex formed during the Archaean and Eburnean times (Tchameni *et al*., 2004; Takam *et al.,* 2009). It consists of the Precambrian basement which outcrops in South Cameroon and it comprises from East to West three tectonic units based on their ages and lithology: the Ntem unit, the Nyong unit and the Ayina unit.

I.1.1. Nyong unit

The studied amphibolites occur in the Nyong unit which belongs to the Northwestern remobilized and restructured border of Congo Craton (Maurizot *et al.,* 1986; Minyem and Nédélec, 1990; Penaye *et al.,* 2004). According to Maurizot *et al.* (1986), the Nyong unit is made up of a foliated series and a greenstone belt:

- The foliated series include gneisses, amphibolites, amphibolitic gneisses and calcic gneisses which outcrop enormously in the studied areas. This series is intercepted locally by mafic and ultramafic veins represented by gabbros, dolerites and peridotites.
- The greenstone belt is comprised of ferriferous quartzites, garnet amphibolo-pyroxenites, granitiferous gneisses, leucocratic to mesocratic gneisses.

The above rocks constitute the greenstone belt of the Nyong unit oriented NE-SW (Champetier de Ribes and Aubague, 1956; Toteu *et al.*, 1994).

The geochronologic studies (Toteu *et al.*, 1994, Lerouge *et al*., 2006) show that the Nyong unit is Eburnean (Lower Proterozoic).

I.1.2. Ntem unit

According to Maurizot *et al.* (1986), the Ntem unit is Archaean in age and is distinguished in to:

- Iron formations characterized by association of mafic facies (ortho-amphibolites with or without garnet and amphibolite gneisses);
- The greenstone complexes made up of mafic rocks, ferriferous quartzites and metabasites (ortho-amphibolites rich in garnet), the metabasites occurs as sills in the ancient metasediments (Tchameni, 1997).

I.1.2. Ayina unit

- The Ayina unit is considered to be of paleoproterozoic in age and is situated to the east of the Ntem Complex. It contains rocks which are grouped under the foliated series, and the rocks of this unit are similar to those of Ntem unit (Maurizot *et al.*, 1986; Toteu *et al.*, 1994).
- According to these authors, the Ayina unit is intruded by granodiorites which are dated to be 2 Ga. The Paleoproterozoic cover of the Congo Craton in the south East of Cameroon lies discordantly on the Ayina unit and disappears under the nappe of the Yaounde series (Vicat *et al*., 1998).

II. Research on gold in the world

Deposits of gold are encountered in Canada (Boyle, 1979), Australia (Carville *et al*., 1990), Russia (Tolstykh *et al*., 2000), United Kingdom (Shepherd *et al*., 2005), Brazil

(Cabral, 2006), Morocco (Ghorfi *et al*., 2006), the Withwaterand of South Africa which produces about 58 % of all the world's auriferous stock in detrital gold deposits to name a few.

Average contents of gold in ultramafic rocks are in the order of 79 to 93 wt.%, (Ghorfi *et al*., 2006). Primary mineralization of gold occurs in quartz veins outcropping in amphiboloschist and gold generally occurs as open-space filling in fragments of hematite-rich materials (Bourges *et al.*, 1994; Ghorfi *et al*., 2006). It is further associated with variable amounts of barite, calcite, quartz, epidote and chlorite.

Gold is optically homogenous; however, it locally contains inclusions of a suite of platinum group metals or is intergrown with a distinct suite of platinum group metals. Ghorfi et al. (2006) showed that the composition of gold ranges from 79 to 93 ppb, 6 to 19 ppb of Ag and 0.5 to 6.29 ppb Pd. While maximum noble metal contents of the investigated ore samples are 169.9 ppm Au, 17.8 ppm Ag, 5.57 ppm Pd and 177 ppm Pt.

Gold mineralizations are usually put in place by hydrothermal activities, with mineralization temperatures being mostly of epithermal range between 100 and 300˚C (Barakat *et al*., 2002; Gasquet *et al*., 2005; Cabral, 2006).

Gold exploited in Africa is found in Precambrian rocks (Eno Belinga, 1984). According to the above author quartzites and schists of West Africa (Mali, Sierra Leone, Ivory Coast, and Ghana) are intruded by several auriferous quartz veins. Also some alluvial gold deposits are exploited in Central African Republic, Cameroon and Democratic Republic of Congo.

II.1. Research of gold deposits in Cameroon

Gold mineralization in Cameroon is best known in the eastern region (Batouri area) Here, primary gold mineralization is related to structurally controlled discordant quartz veins/veinlets (Suh et al., 2006; Vishiti, 2009; Asaah et al., 2014); weathering profiles and altered wall rock restricted to NE-SW-trending shear zones (Suh et al., 2006) that cut across Pan African I-type granites (Asaah et al., 2014). Elsewhere, gold indices are localized in the South (Abiete Yenjok, Mintom, Mballam, Lolodorf), in the North West (Mayo Binka) and the North (Poli, Tcholliré). A majority of these deposits are exploited artisanally as eluvial and alluvial placer deposits (Ntep Gweth *et al*., 2001; Ngo Bidjeck, 2004).

Several reserves have been signaled after examination of several auriferous veins:

In Bétaré Oya (Mborguené) reserves vary from 5.6 to 170 g/t, while in Batouri (Kambele) contents of about 260 g/t are recorded.

Gold indices at Abiete-Yenjok are eluvial and are hosted in quartz veins while the alluvial type have blunt edges, small sizes and flat (Maurizot *et al.*, 1986).

Primary gold occurs as inclusions in sulphide notably sphalerite, as stringers in fractured quartz grains and as free gold associated with hematite. The primary gold grains are Au-Ag alloys (78.9-93.5 wt.% Au, 7-20.6 wt.% Ag, Suh et al., 2006). According to Asaah (2010), the concentration of gold in quartz veins from the Batouri area varies between 0.04 and >30 g/t within the range of 4.5-53.5 g/t reported by Suh et al. (2006) in the Dimako-Mboscorro area of the Batouri gold District

Ebah Abeng et al. (2012) reported Au assay values of 25.1 to 120.9 ppb within pyroxenites and amphibolites in the Lolodorf area , However, in 2013, Legend Mining Limited (www. legendminging.com.au) exploring for iron and gold in the Nyong Series reported gold grades of up to 8 g/t from stream sediments.

Vishiti et al. (2015) showed that gold values in quartz veins range from 2 to 557 ppb. Also, the electron microprobe analysis of the grains recorded high gold content in the rims (86.3-100 wt.%) and along fissures within the grains (95.1-100 wt.%). These contents were consistent with those of Ako et al. (2017). These authors indicated the gold contents of Meta-ultramafic rocks from the Paleoproterozoic Nyong Series to be 1.3 – 517.7 ppb. As a result the quantification of gold deposits up to date remains approximative.

II.3. Behaviour of gold in rocks

Gold mineralizations are usually put in place by hydrothermal activities, thus, it occurs in hydrothermal veins deposited by ascending solutions (Barakat *et al*., 2002; Gasquet *et al*., 2005; Cabral, 2006). It is generally associated with silver which gives to it a pale colour. It also form alloys with Ag, Cu or Platinum Group Elements. Gold generally occurs as open-space filling in fragments of hematite-rich materials and intergrown with specular hematite. It is further associated with variable amounts of barite, calcite, quartz, epidote and chlorite (Ghorfi *et al*., 2006). Ghorfi *et al*. (2006) also showed that the composition of gold ranges from 79 to 93 wt.%, 6 to 19 wt.% of Ag and 0.5 to 6.29 wt.% Pd. While maximum noble metal contents of the investigated ore samples are 169.9 ppm Au, 17.8 ppm Ag, 5.57 ppm Pd and 177 ppm Pt.

II.4. Behaviour of gold in weathered materials

Gold is chemically less mobile and has a high specific gravity. As a result it can concentrate in weathered materials or in placers by relative or absolute accumulation respectively. In humid tropical zones it has a high concentration in the saprolite zone (Zeegers and Leduc, 1991). The low mobility of gold is responsible for its concentration in eluvial deposits around gold veins and in stream sediments (Andrade *et al*., 1991; McCready *et al*., 2003).

The supergene mobility of Au and Au particles (mostly Ag-bearing Au) has been demonstrated either chemically or mechanically with variable degrees, as a function of time, tectonic stability, and climate, types of protores as well as host rocks, and chemical composition of Au (Mann, 1984; Butt and Zeegers, 1992; Colin, 1992; Bowell *et al*., 1993). The unique properties of Au particles, the very high specific gravity, the partial solubility and the high malleability led Colin *et al*. (1997) to propose Au as a tracer of the laterites dynamics.

In most cases, lateritic weathering implies a net mass loss of Au compared to fresh mineralizations (Colin *et al*., 1993; Freyssinet, 1994). Au^{+} and/or Au^{+++} can be complexed by ligands present within the supergene environment. Hydroxy±chloride AuCl(OH)y complexes and organo-metallic complexes have been proposed by Colin and Vieillard (1991), Krupp and Weiser (1992), Bowell *et al*. (1993), to explain the Au mobility in acid highly oxidizing lateritic environments.

The increasing chemical weathering induced morphological and chemical changes of primary Au particles. Partial dissolution produces microscopic pits at the surface of gold particles which leads to spongy aspects (Wilson, 1984; Colin *et al*., 1989; Santosh and Omana, 1991; Colin and Vieillard, 1991; Sanfo *et* al., 1993). The intensification of dissolution processes may induce the microdivision of the primary Au particles. The resulting particles, continuously subjected to chemical attack by supergene solutions, become smaller and smaller (up to their probable complete dissolution). The residual tiny rounded and pitted particles remaining at the surface of the lateritic mantle may be short scale translocated and constitute dispersion haloes (Colin and Lecomte, 1988; Freyssinet *et al*., 1989), easily detectable by regional Au surveys (Butt and Zeegers, 1992).

Gasquet *et al*. (2005) and Cabral (2006) showed that gold can be leached as well as put in place by hydrothermal activities. During weathering of primary silicates, the associated

gold grains are detached and their primary surfaces are altered, thus changing the appearance of gold (Ebah Abeng *et al*., 2012).

Petrological study indicates that the most weathered primary Au particles with rounded shapes and pitted surfaces were found, under the duricrust, within the upper friable saprolite. This layer however is not the most weathered part of the lateritic mantle, but it is where the quartz dissolution resulting porosity is the most developed. The distribution of Au contents in the weathered rocks is controlled by the hydrothermal primary pattern. No physical dispersion has been found. Most of the particles are residual and very weakly weathered (Varajão *et al*., 2000).

According to Bowles (1986, 1987), Au and PGE have similar chemical properties. As a consequence, the ligands able to complex Au are expected to complex PGE in similar conditions.

III.1. Research on Platinum Group Elements in the world

The platinum-group elements (PGE) comprise a geochemically coherent group of siderophile to chalcophile metals that includes osmium (Os), iridium (Ir), ruthenium (Ru), rhodium (Rh), platinum (Pt), and palladium (Pd). These elements generally occur in mineral, rather than metallic, form within an ore. The PGEs, especially platinum, are unusual in that they are largely concentrated in a single location (Cawthorn, 2010). Based on association, the PGE may be divided into two subgroups: the Ir-subgroup (IPGE) consisting of Os, Ir, and Ru and the Pd-subgroup (PPGE) consisting of Rh, Pt, and Pd. Their contents are generally stated in order of ppb or ppm, and they are typically encountered in mafic and ultramafic rocks and their weathered equivalents (Augé *et al*., 1995; Oumarou, 2006). On the bases of atomic weight they can be grouped in to two; the less dense platinoids which include: ruthenium, rhodium and palladium; the dense platinoids which include osmium, iridium and platinum

Ultramafic rocks are the repository for platinum group elements (PGE) (Satyanarayanan *et al*., 2011), as such, they contain the largest PGE deposits worldwide. Research works have shown that major deposits of mafic and ultramafic rocks rich in platinoids are principally found in South African Republic (Naldrett *et al*., 1986; Gruenevaldt *et al*., 1986; Naldrett *et al*., 2008); this is closely followed by Russia (Genkin and Evstigneeva, 1986); Zimbabwe (Oberthür *et al*., 2003), USA (Gray *et al*., 1986), Canada (Godel *et al*., 2007) France (Lorand *et al*., 2007; Lauguet *et al*., 2007).

PGE deposits are also encountered in Australia (Cowden, 1986), in Greece (Augé *et al.*, 1995). These deposits occur in Finland (Tuomo, 2010) to name a few. In the above deposits, different contents of PGE have been signaled:

According to Maier and Barnes, (1999), the concentration of PGE in ortho-pyroxenites is between 100 and 500 ppb but individual samples can attain 2700 ppb and the Pd/Ir ratios are approximately 70.

Godel and Barnes (2007) showed that only a minor quantity of PGE (about 10 to 140 ppb) were found in samples associated with small amounts of sulphur, while palladium and platinum are the most abundant PGE with contents of 244 ppm for Pd and 166 ppm for Pt.

Lorand *et al*. (2007) showed that the concentration of PGE in Iherzolites ranges from 1.4 to 7.1 ppb. While Naldrett *et al.* (2008) showed that the platiniferous dunite pipes of Bushveld Complex contain up to 2050 ppm total PGE.

Tuomo (2010) denoted that the marginal series of the Koillismaa intrusion in Finland contains up to 2650 ppb of Pd, 846 ppb of Pt while the cumulates of the Rometölväs Reef of the above intrusion contains 241 ppb of Pd, 263 ppb of Pt. This rock contains up to 1 ppm of Au+Pd+Pt.

It should be noted that of all platinoids only palladium and platinum are found in their pure forms in nature, while the others occur as natural alloys with platinum and gold hence, their name platinum group minerals.

III.2. Research on contents of platinoids in Cameroon

Interest on the mineralization of platinoids linked to mafic rocks had been indicated since 1950 by the BRGM and others.

Interesting research works in Cameroon were carried out in the South East (Ndjigui *et al*., 2008), coastal plain (Ndjigui *et al*., 2009), Nyos region (Bilong *et al*., 2011; Sababa et *al*., 2015). These authors working on the behaviour of PGE in mafic and ultramafic rocks showed that the contents of Pt and Pd in the fresh rocks are low and increase considerably in the weathered products, with the highest contents in the coarse saprolite.

Ndjigui *et al*. (2004) investigated the behaviour of PGE in the weathered mantle of serpentinites (South East Cameroon) and showed that the total PGE contents were 7.51 ppb in the unweathered rocks.

Ebah Abeng (2006) studied the garnet pyroxenites in Lolodorf (South Cameroon), the results were interesting for the contents of Pt, Pd and Au. The contents were 8.48 to 13.70 ppb for Pt, 9.20 to19.60 ppb for Pd and 4.10 to 9.10 ppb for gold.

Minyemeck (2006) studied the amphibolites and talcschists of Pouth-Kelle in the central part of Cameroon. The resulting contents were low, being 1-2 ppb for Pt,3 ppb for Pd and 2 to 4 ppb for Au in amphibolites.

Ebah Abeng et al., 2012 showed that the Au–PGE contents vary from 25.1 to 120.9 ppb in pyroxenites, amphibolites, and their weathered products from the Nyong unit. While Sababa et al 2015 showed that contents of Au-PGE in peridotites of Nyos and kumba area attain only 21ppb. Nevertheless, Ako et al. (2017) showed that the ∑PGE meta-ultramafic rocks from the Paleoproterozoic Nyong Series attain 5 – 11 ppm.

III.3. Behaviour of PGE in rocks

Platinoids are chalcophile elements which are generally inert and behave similarly but show certain compatibility and incompatibility in different milieu. Their behaviour in different rocks has been the focus of several authors.

According to Handler and Bennett (1999), the behaviour of PGE in the subcontinental mantle of Eastern Australia shows that individual PGE's partition into different trace phases results in a small scale heterogeneity of both PGE ratios and concentrations on an order of 8-2%. Analytical data in the main zone of the Eastern Bushveld Complex shows that PGE enrichment in that zone is attributed to a local enrichment by hydrothermal fluids. Also that incompatibility follows the sequence Ir< Rh <Ru < Pd < Pt, with Pt being approximately eight times more incompatible than Ir. In this complex, almost all samples contain less than 100 ppb total PGE (Harney *et al.*, 1990).

According to Bowles (1986), Platinum Group Elements tend to accumulate in the saprolite zone derived from the weathering of the PGE enriched rocks.

Ndjigui *et al.* (2003) showed that PGE have positive correlations with siderophile elements particularly Fe. This shows that PGE are fixed on the Fe oxy-hydroxides interfaces like some siderophile elements (Singh *et al*., 2002; Ndjigui and Bilong, 2010).

Ndjigui *et al*. (2009) proved that the concentrations of Pt and Pd in talcschists and amphibolites in Pouth-Kellé (South Cameroon) are low. It consists of 1-2 ppb for Pt and 3 ppb for Pd. while Ndjigui (2008) showed that platinoids are more concentrated in the

weathered materials than in the parent rock (serpentinites). Nevertheless contents of these elements in amphibolites of Nyabitande attain 113 ppb (Aye, 2010).

III.4. Behaviour of PGE in weathered materials

The behaviour of platinoids in weathered materials is not controlled by the same phenomenon as in the fresh rocks. These elements usually concentrate at the base of the weathered profile despite their poor contents in the parent rocks (Bowles, 1986, 1994). These concentrations can be matched with those of iron oxides and to certain siderophile elements such as chromium and nickel (Taufen and Marchetto, 1989; Ndjigui *et al*., 2003). Also Ndjigui *et al*. (2002, 2003), proved that metallic oxides are excellent indicators of platinoids in the weathered mantle.

At the base of the profile, these elements are inculcated in to carrier minerals like goethite (Singh *et al*., 2002), or made up of minerals that are different from those of the parent rocks (Salpeteur *et al*., 1995). In the upper parts of the weathered profile fluvic and humic acid are responsible for the release of platinoids in solution (Travis *et al*., 1976).

Bowles (1994) and Traoré (2005) showed that palladium is more soluble in surface and underground waters and is less stable than platinum. Platinum is subjected to a mechanical migration from top to bottom of the weathered mantle. It is this phenomenon that is responsible for the concentration of platinum or palladium in eluvial and alluvial deposits (Wood, 1996; Azaroual *et al*., 2001).

The work carried out by Traoré (2005), Ndjigui *et al*. (2005) and Ndjigui (2008) showed that platinoids also accumulate in hardened ferrugunous materials.

Platinoids were first considered as inert elements during weathering. This was due to their low solubility in supergene conditions (Anthony and Williams, 1994).

The high specific gravity of PGE has led to eluvial concentration of these elements in weathering profiles developed upon mafic and ultramafic rocks. These elements are usually affected by dissolution processes and thus concentrate as residual minerals along the weathering profiles of the above rocks (Traoré *et al*., 2006).

Weathering processes can dissolve the platinum-group elements and permit their transportation and deposition of PGM in eluvial deposits, in which the PGM are significantly different in grain size and morphology from those derived from an igneous source (Bowles *et al*., 1994). The cracks affecting the grains of PGM are interpreted as a change of volume, due

to chemical leaching in the oxidizing environment (Augé and Legendre, 1994; Oberthur *et al*., 2003; Traoré, 2005).

The high-Eh conditions of lateritic soils favour significant solution of platinum and palladium as chloride species. Also, organic acids may play an important role in controlling the dissolution of platinoids in natural, near-surface solutions (Bowles, 1986; Wood, 1990) The soil contains organic species that have a high affinity for the PGE, and these could provide a potential means of local transport in solution (Bowles, 1994).

The lateritic mantle developed at the expense of PGE mineralization shows a higher Pt and Pd concentrations compared to the bedrock. The decoupling between the PGE and chromite concentration in lateritic mineralization suggests that the PGE could have been dissolved, transported and reformed in the weathering mantle (Augé *et al*., 1995). Variation of the ratio Pt/Pd, are characteristic of the behavior of the PGE in supergene environments (Oberthür *et al*., 2003). The increase of Pt/Pd in the weathering profile reflects the preferential release of Pd compared to Pt (Varajao *et al*., 2000).

PGE have a higher concentration in the saprolite zone and in the hardened materials of some weathering profiles (Ndjigui and Bilong, 2010), this is due to due to vertical transfer and precipitation of these elements at the base of the weathering mantle. Thus, Pt-bearing rocks in lateritic environment are progressively dissolved and the Pt-group minerals (PGM) are released in the weathering mantle with a preferential depletion of Pd with regard to Pt (Traoré *et al.*, 2008a).

PGE oxides have been recognized in the chromitite horizons and in the placer deposits (Garuti, 2004). The formation of these PGE oxides is related to intense lateritization affecting the primary mineralization. Some oxides are the product of oxidation of pre-existing PGM, whereas others seem to have crystallized in laterite. This indicates a certain mobility of the PGE during the lateritic alteration (Augé, 1985).

Hydrothermal fluids were responsible for the release of the platinum-group elements (PGE) from the BMS to precipitate the PGM at low temperature during pervasive alteration (Wang *et al*., 2008). There is also evidence in many deposits that secondary hydrothermal activity can remobilize base metals and PGE (Ballhaus and Stumpfl, 1986; Boudreau *et al*., 1986).

IV. Research on sulphur

Sulphide phases are of two types: primary sulphides are scarce and either form rounded, globular inclusions or are commonly associated with interstitial oxide minerals; the secondary ones form a larger proportion of sulphides, disposed mostly in veins and patches resulting from the alteration of the monosulphide solid solution cumulates by late magmatic/hydrothermal fluids (Dare *et al.*, 2011). Less commonly, sulphides were found as inclusions in early crystallized minerals, in which case they replaced primary sulphides.

Sulphur bearing phases are usually identified as pyrrhotite, pyrite (marcasite), chalcopyrite and pentlandite by microscopy and electron microprobes (Puchtel *et al.*, 1995), they are also locally accompanied by millerite, heazlewoodite and violarite (Baumgartner *et al*., 2012)

The average range of sulphur content in analyzed rocks are as follows: gabbros 1590 ppm (< 100-10340 ppm); gabbronorites 760 ppm (<100-3100 ppm); troctolites 680 ppm (<100-1700 ppm); harzburgites, 200 ppm (<100-700 ppm); and dunites 400 ppm (<100-1200 ppm) (Puchtel *et al.*, 1995).

In most cases, the contents of S, in rocks containing greater than 800 ppm S can be modeled by segregation of a Fe–Ni–Cu sulfide liquid from a fractionating magma. As the magma evolved, there was the continual segregation of sulfide liquid.

IV. 1. Relationship between PGE and sulphur

Platinum-group element-dominated deposits are more commonly associated with sulfide-poor (0.5–5 vol.%) orebodies such as those occuring in the Merensky Reef and Platreef in the Bushveld complex in the Republic of South Africa (Naldrett *et al*., 2008), the Great Dyke in Zimbabwe (Wilson *et al.*, 2000), and the Stillwater complex in the USA (Godel and Barnes, 2008).

Sulfides are considered to be collectors of PGE (Barnes, 1990). Base metal sulphides (BMS) host the bulk of the PGE, except Pt, in solid solution. Sulphide deposits of magmatic origin consist of pyrrhotite, pentlandite, chalcopyrite (± pyrite), and platinum-group minerals (PGM). Understanding the distribution of the chalcophile and platinum-group element (PGE) concentrations among the base metal sulfide phases and PGM is important to know the origin of the rock and for the efficient extraction of the PGE (Dare *et al.*, 2011).

Sulphur bearing phases (pyrrhotite, pyrite (marcasite), chalcopyrite and pentlandite) identified by microscopy and electron microprobes (Puchtel *et al*., 1995), have also been proven as the carrying minerals for Au-PGE (Zaccarini *et al*., 2011).

Previously, pyrite has been rather neglected during the in situ analyses of BMS from magmatic ore deposits, but Dare *et al*. (2011) have demonstrated that pyrite of both primary and secondary origin can host PGE.

According to several authors (Naldrett *et al*., 1982; Barnes *et al*., 1997, 2001; Prichard *et al*., 2004; Mungall *et al*., 2005; Sinyakova and Kosyakov, 2007), base metal sulphide (BMS) liquid collects the platinum-group elements (PGE) and other chalcophile elements (Ag, As, Au, Bi, Cd, Co, Cu, Mo, Ni, Pb, Re, Sb, Se, Sn, Te, and Zn) from magmatic Ni–Cu–PGE sulfide ore deposits and that during sulfide fractionation these elements partition between early crystallizing monosulfide solid solution (MSS) and the remaining fractionated Cu-rich liquid. Typically, pyrrhotite and pentlandite host much of the PGE, except Pt. Thus, platinum-group element ores are thought to be formed by precipitation from sulfur-deficient, depleted mantle magmas. Immiscible sulfide melt usually host platinum-group elements, the very high sulfide melt-silicate melt partition coefficients of the platinum-group elements result from strong fractionation of these metals into the accessory sulfide component during the melting event.

The results for most deposits show that: pyrrhotite and pentlandite contain the bulk of the IPGE (Os, Ir, Ru, Rh), Re and Co but with Co, and in some cases Rh, largely hosted by pentlandite; the bulk of Pd is in pentlandite and Pd minerals (Li *et al*., 1993; Huminicki *et al*., 2005; Dare *et al*., 2010b) and Aguablanca, Spain (Piña *et al*., 2011).

Also, according to Naldrett *et al*. (2009, and references therein), and Zaccarini *et al*. (2011), PGE are massively contained in sulphides up to a concentration of 22972 ppb of total PGE (Zaccarini *et al*., 2011). According to these authors during the formation of an immiscible sulfide liquid at the magmatic stage, PGE available in the system is collected, especially the PPGE, and that this precipitation takes place under a relatively high S fugacity.

Gold and platinum group elements are definitely associated with sulphides right from the mantle. Dare *et al.* (2011) explained that all of the Pt and Au and a moderate proportion of Pd exsolve from the monosulphide solid solution (MSS) as discrete, small grains which are then hosted in pyrrhotite and pentlandite. This indicates that a small amount of these

incompatible elements partitioned originally into MSS and were expelled during cooling (Dare *et al*., 2011).

The PGE have much higher partition coefficients between silicate and sulfide liquid Barnes and Lightfoot (2005). Therefore, the first sulfide liquid to segregate from magma will be rich in PGE. The silicate liquid from which this sulfide liquid segregated will be PGE depleted and any sulfide liquid that subsequently forms from it will also have PGE-depleted patterns (Barnes and Lightfoot, 2005).

In some cases (Bell River Complex, Taborda, 2010) sulphides are present in disseminated form, however the PGE are not associated with them. The PGE are present as PGM mainly bismuth-tellurides and arsenides of Pt and Pd. It is suggested here that, in the magmatic chamber a sulphide liquid collected Ni, Cu and PGE. Then gravity settling gathered together all of the sulphide droplets in a layer. Sometime later during metamorphism S and Cu were mobilized, but left the PGE as PGM phases. This point to the fact that original suphide liquids that exsolve from magma carry along PGE which are left to themselves as fractionation of the sulphide liquid continues.

The above references and others prove clearly that sulphur in the form of sulphides is associated with PGE and that immiscible sulfide liquid in the magmatic chamber can play an important role in collecting and subsequent precipitation of the PGE available in the system.

Conclusion

Contents of Platinum group elements are usually expressed in ppb. These are elements of high potentials and increased demand. Their usage is essesntial both in developed and developing countries and covers several industrial domains. These elements are principally hosted in rocks such as basalts, gabbro, pyroxenites, serpentinites and their metamorphosed forms such as amphibolites, just to name a few. Platinoids are often associated to stratiform deposits of sulphur and are usually found with metals such as chromium, nickel, cobalt, copper, gold etc. These mafic and ultramafic rocks dominantly outcrop in South Cameroon. They form part of the Nyong Unit and can be dated PaleoProterozoic in age.

CHAPTER THREE: PETROLOGY OF AMPHIBOLITES AND COUNTRY ROCKS

Introduction

This chapter handles the petrography and geochemistry of amphibolites, pyroxenites and granodiorites from Nyabitande and Zingui areas.

I. Petrography of amphibolites, pyroxenites and granodiorites

Amphibolites appear as rounded and spherical blocks of different dimensions under the thick vegetation cover of Nyabitande as well as under the primary forest (Fig. 6). In the Zingui area, they occur as blocks and as xenolith in granodiorites (Fig. 7). Pyroxenites outcrop in the Nyabitande area, they also appear in the form of blocks. Granodiorites too outcrop as blocks in the Zingui area. They occur on the field as partly weathered large blocks of several meters wide.

I.1.Macroscopic view of rocks

Amphibolites are medium-grained, dark-coloured, and dense rocks (Fig. 8). They are made up of garnet, ferromagnesian minerals, and few quartzofelspathic minerals when observed with the naked eye. The rock display a preferential alignment of minerals which is more pronounced in some samples than others. Pyroxenites are dense, melanocratic and massive. On the field, they appear as blocks of different diameter. They possess more compact mineral grains than amphibolites. Observable minerals are garnet and quartz. Granodiorites are coarse-grained and light coloured. Minerals observed with the naked eye are feldspars and dark coloured minerals.

Figure 6 : Macroscopic view of an amphibolite outcrop (Nyabitande)

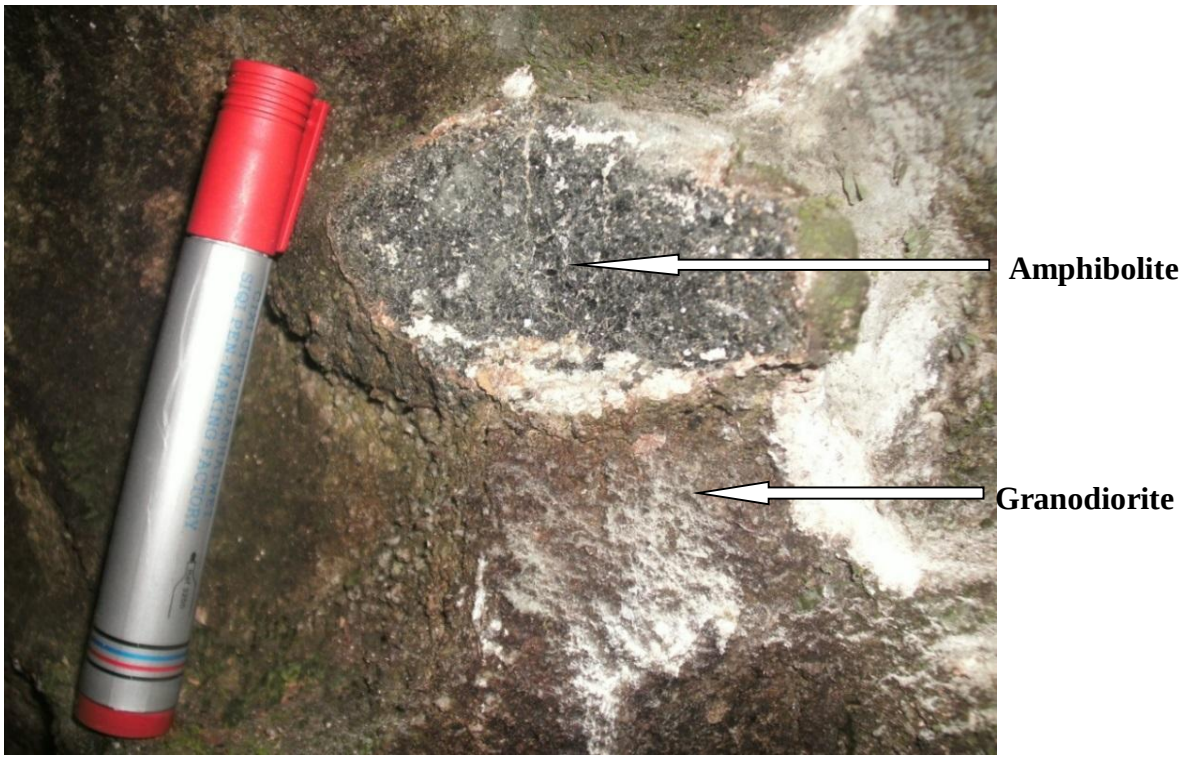

Figure 7 : Amphibolite as xenolith within granodiorite

Figure 8 : Macroscopic view of amphibolites

I.2. Microscopic view of rocks

Under the optical microscope, amphibolites appear as greenish dark rocks. They are made up of amphibole hornblende, plagioclase, garnet, biotite, quartz and accessory epidote, sphene, apatite and opaque minerals. The crystal size of amphibole occurs as microblast and phenoblast which can attain 2 mm (Fig. 9 a). They generally present a granoblastic heterogranular texture with associations of amphibole, plagioclase, garnet, quartz, oxides mineral paragenesis (Fig. 9 a and b). Pyroxenites appear as dark rocks composed of pyroxene, feldspar, biotite, garnet and and accessorily quartz and opaque minerals (Fig. 9 c). The granodiorite appears as a light coloured rock with mainly plagioclase, green hornblende, epidote and accessorily zircon, apatite, sphene and opaque minerals (Fig. 9 d).

I.2.1. Amphibolites

Three types of amphibolites are distinguished: the oriented micro granular type, the non-oriented micro granular one and the coarse grained amphibolites.

I.2.1.1. Oriented micro granular amphibolites

They are greenish dark rocks with preferential orientation of all mineral grains in a particular direction (Fig. 10 a). They present a granoblastic texture and are composed of amphibole, plagioclase, garnet, and accessory minerals like, quartz. Two types of amphiboles are distinguished: primary and secondary amphiboles: Primary amphibole is principally green hornblende which shows a green colour under polarized and cross polarized light. They occur as xenomorphic crystals of all sizes with a range of about 40 to 60 % in abundance of the total volume of rock. The amphibole grains are mostly found in association with minerals like garnet, plagioclase, quartz and opaque minerals. Crystal sizes vary from 0.06 to 1 mm, with sizes of some phenoblast reaching 2 mm (Fig. 10b). The secondary amphibole show shades of red, brown and yellowish colours under cross polarized light. They are bigger than primary amphibole and are formed from the alteration of pyroxene. Secondary amphibole occupies an average volume of about 35 to 70% of the rock. Crystal grains attain 1.5 to 2 mm (Fig. 10c). The most developed sections of both amphiboles contain inclusions of quartz and/or feldspars, apatite and opaque minerals and are associated with plagioclase and garnet.

- Plagioclase crystals are the most represented feldspars. They are characterized by small crystals and are principally recognized by their polysynthetic twinning.

Plagioclase crystals present xenoblastic forms and sizes that vary from microblast to phenoblast. They occur together with garnets, opaque minerals and amphiboles. They occupy about 10 – 15 % in abundance, and crystal sizes range between 0.04 and 1 mm, the crystals occur mainly at the interstices of the amphibole grains (Fig. 10d).

- Garnet shows globular and sub-rounded crystals that are dark under cross polarized light and brown under polarized light (Fig. 10d). The garnet crystals occur in all grain sizes, as microliths, microphenoblasts and phenoblasts giving the rock a granoblastic heterogranular texture. They have range from 15 to 26 % in the rocks though less represented in some samples with only 3 % in abundance. Its xenoblastic chains of crystals are cracked and the cracks contain inclusions of sub-rounded grains of plagioclase (Fig. 11a and b). Garnet crystals also occur as inclusions in amphiboles, they vary from 0.16 to 2 mm (Fig. 11c).

- Opaque minerals occur as amas in certain spots and have globular and fine grains in others. Whereas they are found as isolated grains in inclusions of amphibole, plagioclase and garnet. Opaque minerals occupy about 5 to 10 % - (Figs. 9 and 10b, 11d).

- Quartz presents xenomorphic crystals, some grains are rounded, sub rounded, and elongated. The grains are less abundant ranging from 2 to 5% of the total volume of rocks. Crystal sizes vary from 0.06 to 0.3 mm; it frequently occurs as inclusions in amphibole, plagioclase and garnet crystals (Figs. 10b and c). They also appear to occupy the interstices between amphibole grains (Fig. 11a, b and d).

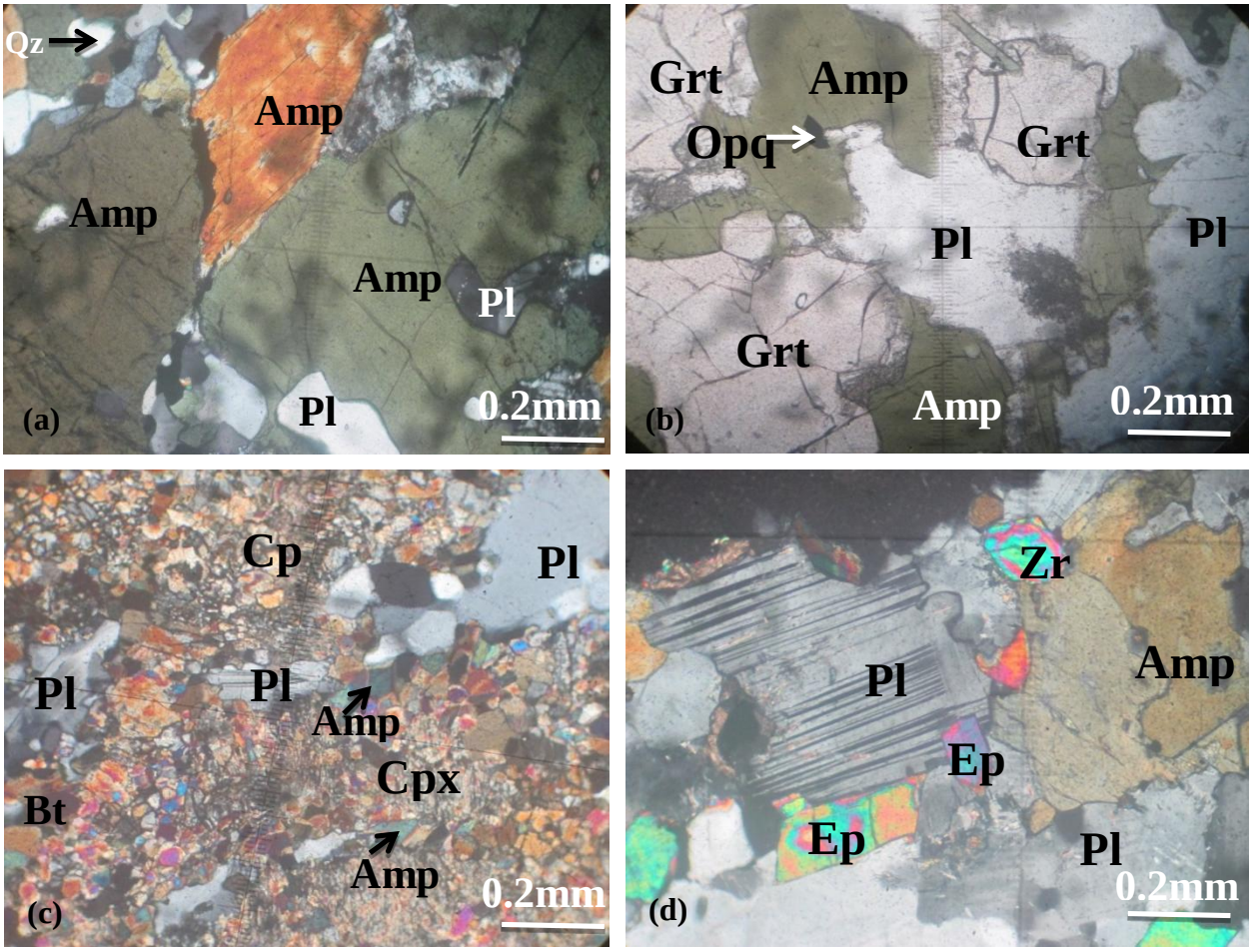

Figure 9 : Photomicrographs in cross polarized light showing amphibolites, pyroxenites and granodiorites of Nyabitande and Zingui. (a) Amphiboles (Amp) with plagioclase and quartz (Qz) (b) Garnet (Grt) associated with amphibole and plagioclase (Pl); opaque minerals (Opq) shown as inclusions; (c) Clinopyroxene (Cpx) crystals associated with plagioclase, amphibole and biotite (Bt); (d) Plagioclase associated with amphiboles and microblast of epidote (Ep) and zircon (Zrn).

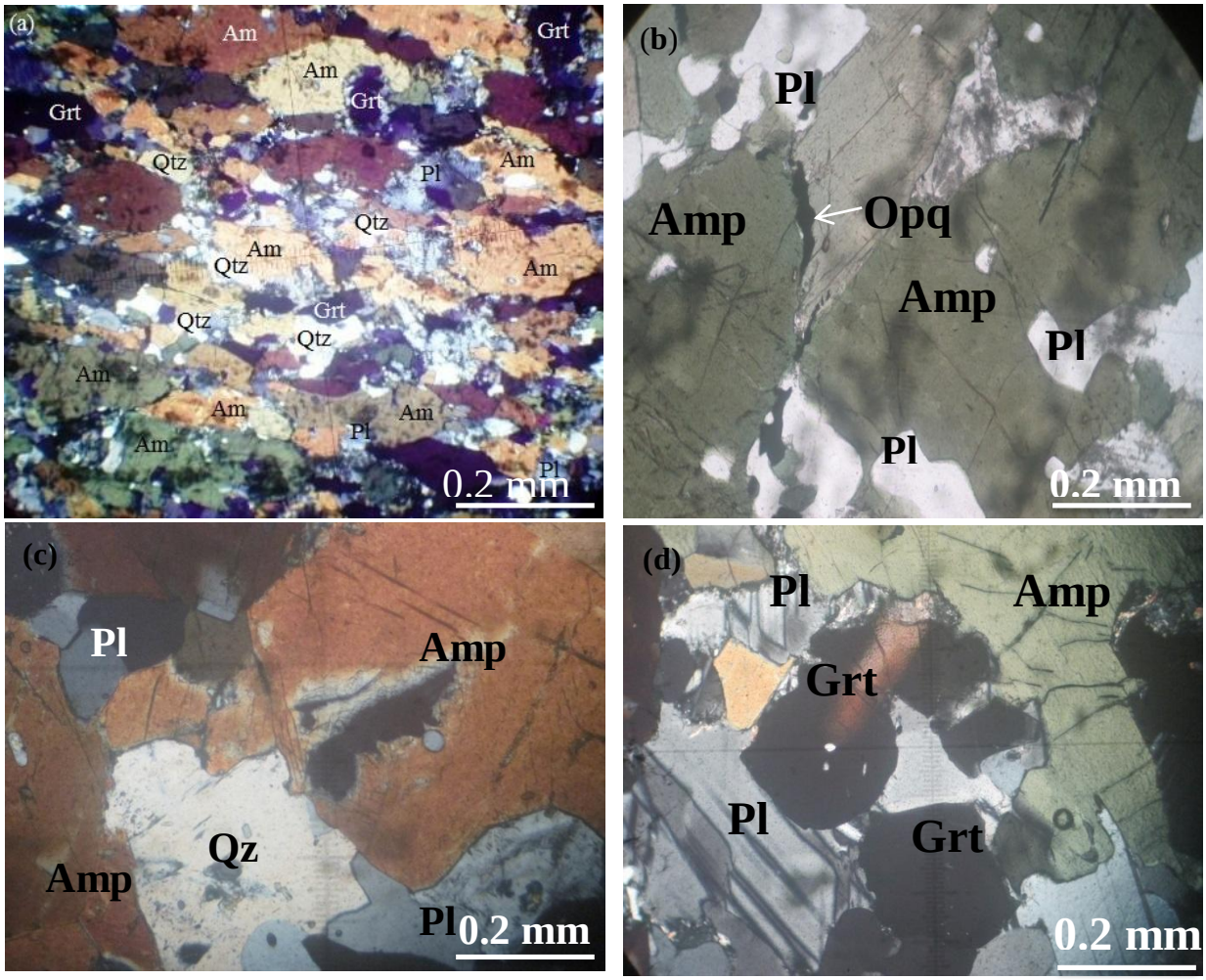

Figure 10 : Photomicrographs showing amphibolites of Nyabitande under polarized and cross polarized light. (a) Amphiboles grains under cross polarized light. (b) Primary amphiboles with opaque minerals under polarized light. (c) Crystals of secondary amphiboles associated with quartz under cross polarized light. (d) Plagioclase and garnets, asso ciated with amphiboles under cross polarized light.

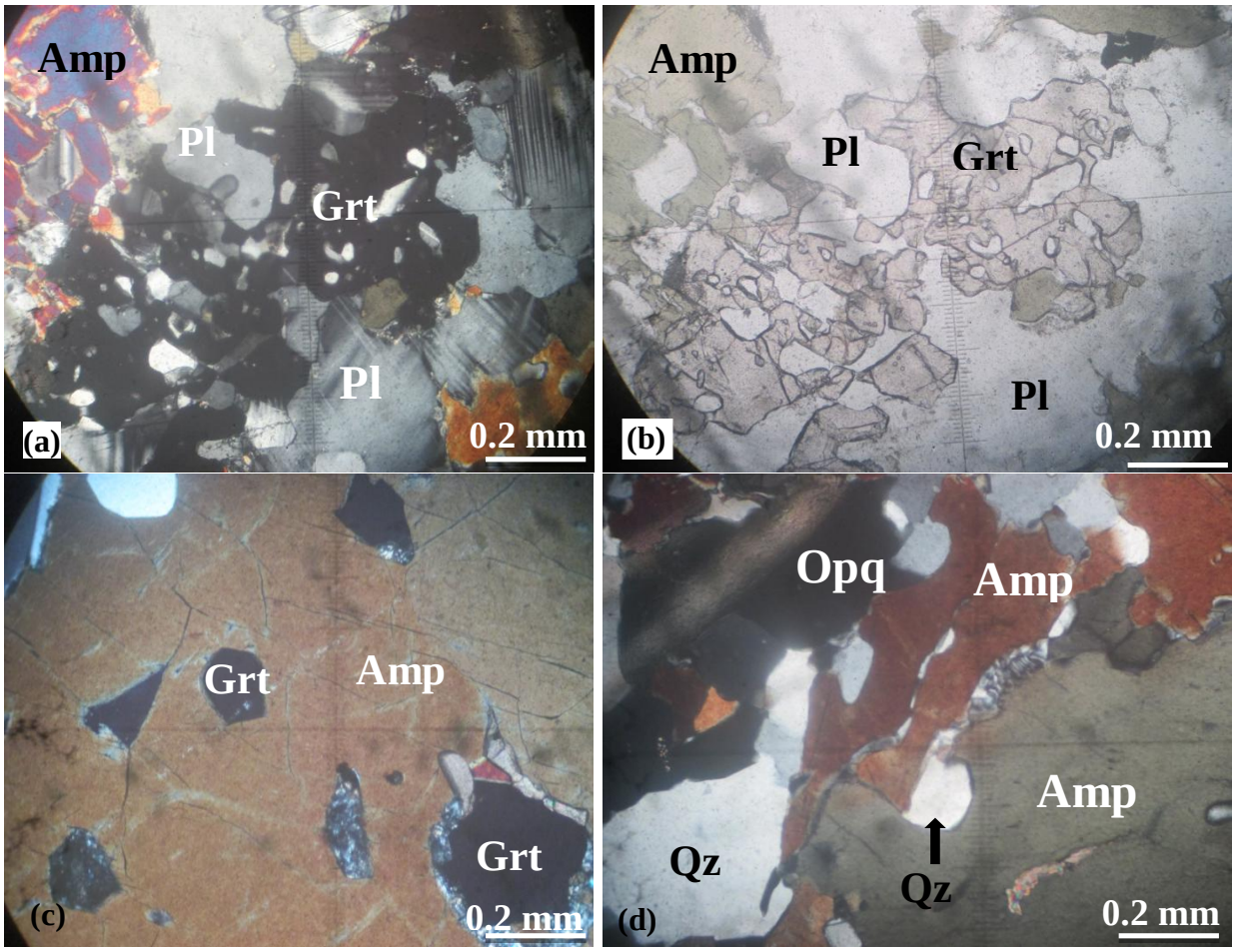

Figure 11 : Photomicrographs showing amphibolites of Nyabitande under polarized and cross polarized light. (a) Garnet with inclusions of plagioclase under cross polarized light. (b) Garnet with inclusions of quartz and plagioclase under polarized light. (c) Garnet crystals as inclusions in amphiboles under cross polarized light. (d) Quartz and opaque minerals as interstitial grains associated with amphiboles.

I.2.3. Non - oriented amphibolites

They are also greenish dark rocks but show no preferential orientation of mineral grains. They have coarser grains than the oriented amphibolites. They present several accicular grains made up of crystals of amphiboles, plagioclases, garnets and accessorily quartz, sphene, apatite and opaque minerals. The mineral grains (blast) are linked to each other and crystals are rarely isolated. This facie is different from others in that its grains are not oriented, with a maximum of 2 mm (Fig. 12a and b).

- Sphene occurs as a rare accessory crystal presenting an automorphic form. It is held between crystals of amphiboles, quartz and feldspars. Crystal size attains 0.04 mm (Fig. 12a and c).
- Apatite is identified as thick white crystals that changes from colourless to dark grey under crossed polarized light. They occur as small grains which are easily identified when they are found as inclusions within feldspars because they are thicker (Fig. 12b).

1.2.4. Coarse grained amphibolites

They contain relatively coarse grains of minerals, most of which occur as phenoblast. They appear to be pyroxenites that have been altered to amphibolites. They also contain the biggest amphiboles formed from the weathering of pyroxenes. The coarse amphibolites also contain some alkali feldspar grains. They are made up of green hornblende, plagioclase, abundant garnet and accessorily opaque minerals, little quartz, zircon (Fig. 12d).

- Zircon occurs rarely in the rock presenting automorphic grains; they occur held between amphibole grains (Fig. 12d).

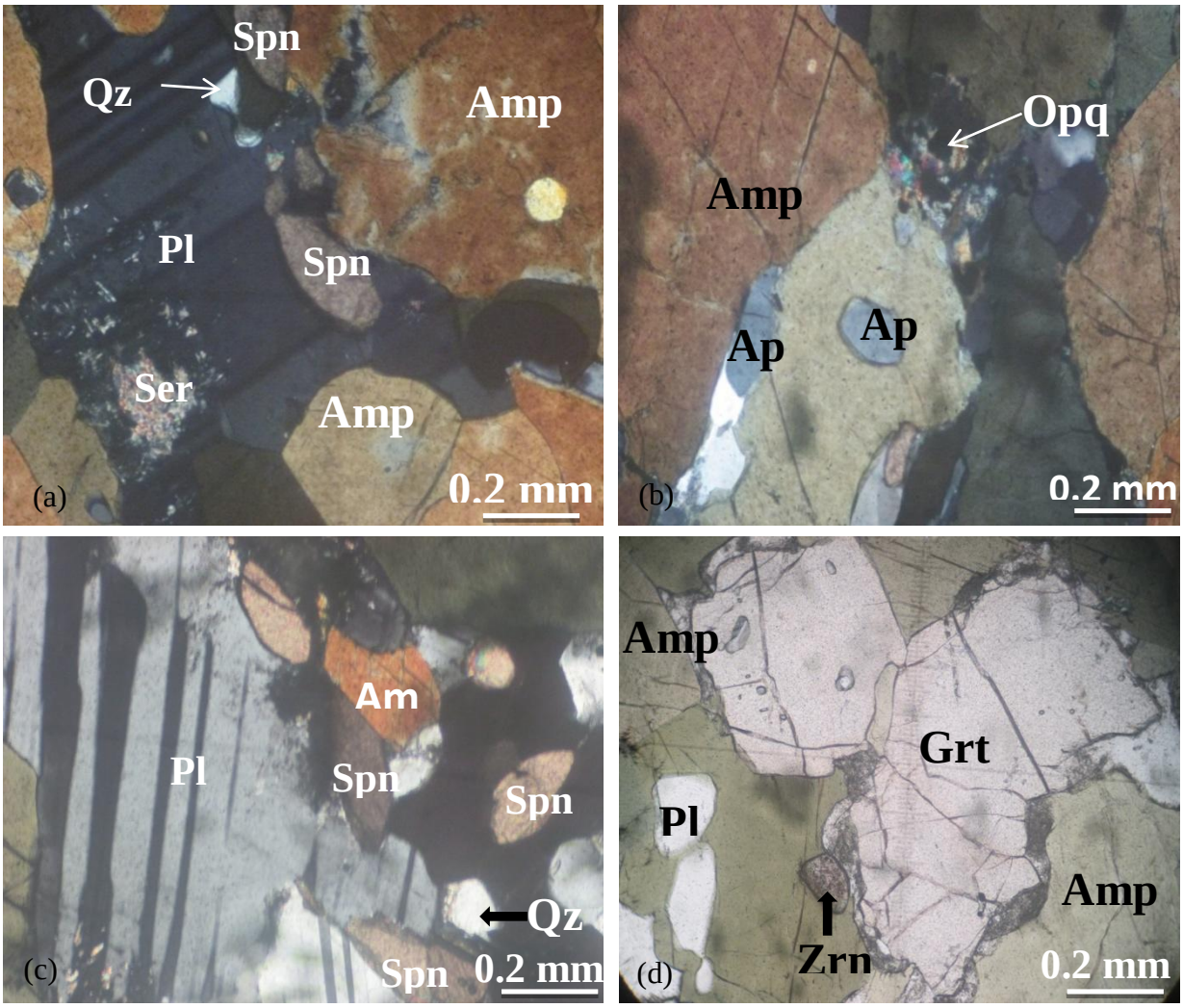

Figure 12 : Photomicrographs showing non-oriented and amphibolites of Nyabitande under polarized and cross polarized light (a) Non-oriented amphibolite with amphibole, plagioclase and accessory mineral crystals. (b) Amphiboles with inclusions of apatite (Ap) and opaque minerals. (c) Sphene (Spn) associated with plagioclase, quartz and amphiboles under cross polarized light. (d) Amphiboles and garnets with zircon (Zrn) as inclusion in coarse grained amphibolites, under polarized light.

.

I.3. Pyroxenites

They occur as melanocratic rocks composed of pyroxene, plagioclase, biotite, amphibole, garnet and accessorily opaque minerals (Fig. 13a).

Pyroxene crystals are mainly the clinopyroxene (augite). They occur as dismantled grains a phenomenon that occurs under pressure. Some of the augite grains still show their automorphic crystal grains showing an average abundance of 50 %, some other augite grains are being transformed in to biotite a sort of granulitisation in which water is not playing a role. The dismantlement of augite give rise to biotite and in the end concentrates as oxides.

- Augite grains occur in association with plagioclase, biotite and garnet. (Fig. 13a and b).
- Biotite presents elongated crystal forms and is brown in colour. The sizes vary from 0.05-0.1mm. The biotite is sub automorphic to automorphic and is formed from the transformation of the augite. Biotite occurs attached at the borders of the augite grains with an abundance of about 5 %. They are found together with pyroxene + plagioclase + opaque minerals. Biotite also appears to contain iron, revealed by their weak pleochroic nature (Fig. 13a and d).
- Garnet is found as numerous brown crystals under polarized light and dark grains under cross polarized light. They show globular grains with cracks on their surfaces, and an abundance of 20 % (Fig. 13c).
- Plagioclase feldspar is represented in the rock with an abundance of about 15 %. They are recognised by their polysynthetic twinning. They occur together with amphibole, pyroxene and garnet and are coarse grained (Fig. 13d).
- Opaque minerals occur as coarse crystals between augite grains (Fig. 13f).

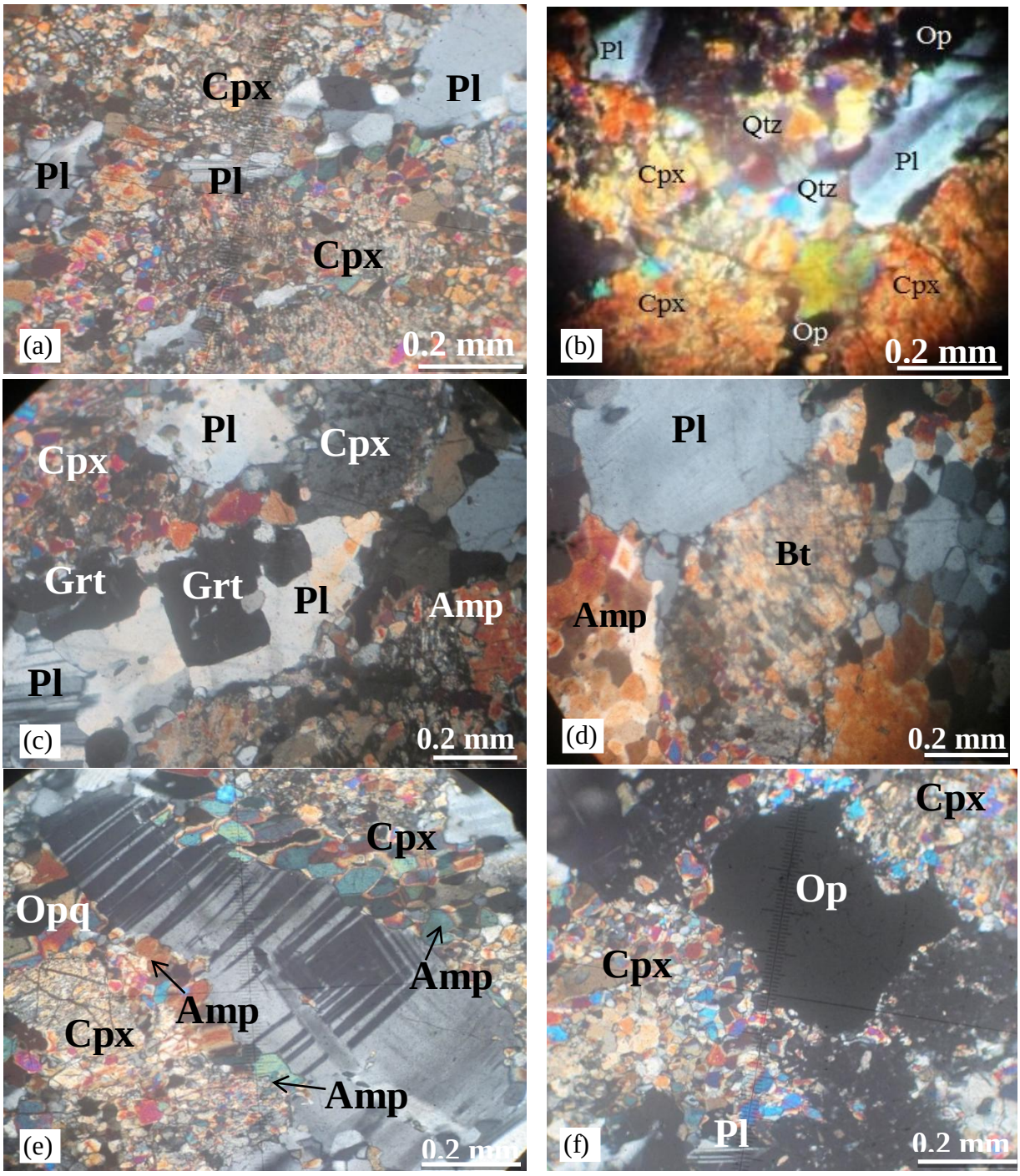

Figure 13 : Photomicrographs showing pyroxenites of Nyabitande under and cross polarized light. (a) Pyroxenite under cross polarized light. (b) Dismantled crystals of clinopyroxenes (augite) associated with plagioclase. (c) Globular garnet crystal associated with clinopyroxenes. (d) Iron –rich biotite crystals associated with clinopyroxenes and plagioclases. (e) Plagioclase between augite crystals (f) Opaque minerals between augite crystals.

I.2.3. Granodiorites

They appear as light coloured rocks with cyrstals of plagioclase, microcline, perthite amphibole, epidote and accessorily zircon, apatite, sphene, and opaque minerals (Fig. 14a).

- Plagioclases are abundant and occur as large crystals. Some crystals clearly display polysynthetic twinning, while a few of them do not show clear twinning. Plagioclases occupy about 20 %. They form an association with grains of green hornblende, and accessory minerals some of which occur as inclusions (Fig. 14b).
- Amphiboles are principally green hornblende. They are formed from the transformation of pyroxenes. They occupy about 10 % and occur together with epidotes, feldspars, and accessory minerals. Their sizes vary from about 0.5 to 0.8 mm (Fig. 14a).
- Microcline is easily identified by its double direction of twinning. They occupy about 20 % and occur in association with amphibole, plagioclase and accessory minerals (Fig. 14e).
- Epidote occur under the optical microscope as numerous small crystals that are sharp green and also reddish in colour under cross polarized light. They remain light brown under natural light. They show an abundance of about 5 %, and occur together with feldspars and hornblende (Fig. 14d).

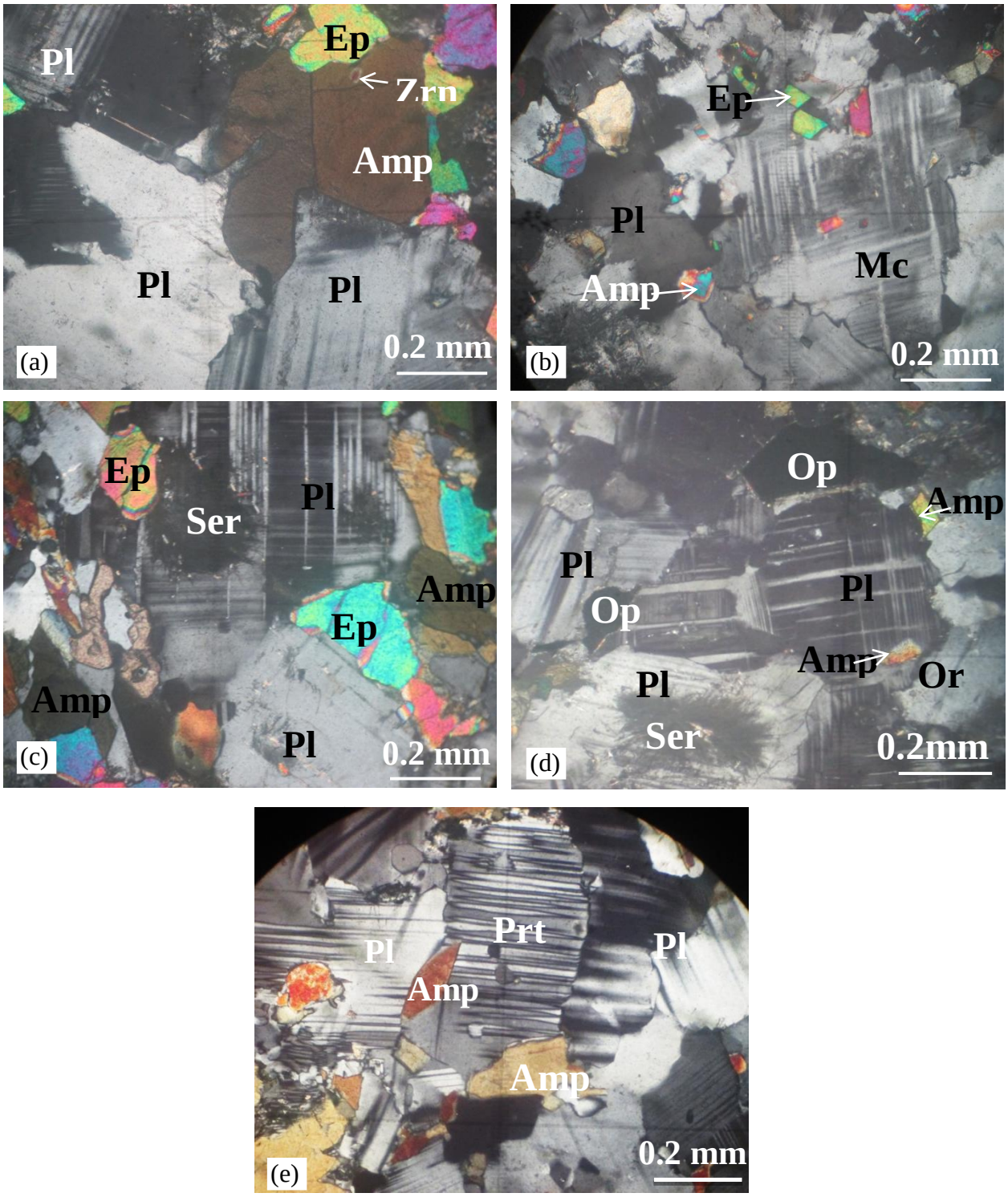

Figure 14 : Photomicrographs showing granodiorites under cross polarized light. (a) granodiorites with plagioclases, amphiboles and accessory minerals (b) Plagioclase crystals (c) Granodiorites with different feldspar crystals (Or – orthoclase) (d) Crystals of epidotes associated with feldspars (e) Coarse plagioclase crystals.

II. Geochemistry of amphibolites and country rocks

This part focuses on the geochemical behaviour of major, trace and rare earth elements in amphibolites, pyroxenites and granodiorites. Samples of amphibolites in Nyabitande were collected at different localities such as Folack Nvos, Kolasseng I and Kolasseng II.

II.1 Behaviour of major elements in rocks of Zingui and Kolasseng I

Silica is the most abundant oxide constituting about 49.95 wt.%. Contents vary from 44 to 50 wt.%. Maximum contents of silica are recorded in amphibolites of Kolasseng I while moderate contents occur in those of Zingui (Zn_1= 47.11 wt.%). Al_2O_3 which is often the most abundant oxide after silica also shows high contents. Contents of alumina attain about 15.41 wt.% of the whole rock. The rocks are also rich in Fe_2O_3 (11 to 18.83 wt.%); CaO ~11.85 wt.% and MgO about 9.36 wt.%. Amphibolites are marked by very low alkali contents K_2O (0.21 wt % and Na_2O (0.25 wt.%). They are poor in other oxides like TiO_2, P_2O_5, and MnO. Most contents of the latter are less than or equal to 1 wt.% (Table 1). Amphibolites from Nyabiande are richer in silica than those from Zingui.

II.2. Behaviour of major elements in pyroxenite and granodiorites

Contents of silica are especially high in granodiorites (GZn) of Zingui and pyroxenites of Kolasseng I (NK6). Their respective contents of silica are 68.07 wt.% and 56.56 wt.%. These contents are in sharp contrast with all the other samples (Table 1). The high silica contents of granodiorites are consistent with its acidic nature.

Table 1 : Major element contents (wt.%) in rocks of Zingui and Nyabitande

		Zingui			Folack Nvos				Kolasseng I									Kolasseng II						
		1		2	1				1								3	1						3
	d.l.	Zn1	Zn2	GZn	FN3	AY1	AY2	AY3	AV1	AV2	NK1	NK2	NK3	NK4	NK5	NK7	NK6	K4	K8R	K10	K11	K13	EA	K5
SiO2	0.04	47.11	44.79	68.07	48.76	49.00	49.29	48.84	48.68	47.81	49.30	48.39	49.95	47.75	49.20	48.49	56.56	48.38	48.14	49.49	44.68	49.17	49.12	47.08
Al2O3	0.02	15.41	11.04	15.28	15.08	12.18	14.02	13.34	12.81	13.37	12.95	13.94	14.36	13.95	14.99	13.62	21.04	14.43	14.32	17.21	14.63	13.25	14.16	13.39
Fe2O3	0.01	11.48	18.83	3.15	13.63	17.40	14.00	14.85	13.35	14.56	17.09	14.72	12.31	15.20	14.83	14.65	5.45	16.45	14.26	15.45	20.03	19.80	14.99	16.67
CaO	0.01	11.47	11.85	3.73	11.11	10.57	10.79	10.81	11.08	11.14	8.91	10.42	11.56	10.51	10.94	10.87	7.37	9.58	10.69	10.45	11.22	8.73	10.22	10.10
MgO	0.01	9.36	7.80	1.10	6.86	6.62	6.73	6.72	8.13	7.17	5.07	6.50	7.75	6.48	5.56	6.86	1.27	5.87	6.97	3.81	5.78	4.70	6.44	6.55
Na2O	0.02	2.10	1.27	4.67	0.25	1.62	2.58	2.51	2.47	1.90	2.15	1.99	1.97	2.03	1.85	2.64	6.93	1.99	1.89	1.75	1.10	0.70	2.69	2.62
K2O	0.01	0.33	1.15	1.00	0.21	0.27	0.40	0.38	0.50	0.51	0.68	0.34	0.28	0.36	0.24	0.26	0.23	0.71	0.26	0.11	0.12	0.11	0.35	0.34
MnO	0.01	0.13	0.28	0.04	0.22	0.32	0.15	0.13	0.19	0.30	0.25	0.21	0.20	0.26	0.23	0.21	0.06	1.74	1.01	1.31	1.75	1.85	1.65	1.51
P2O5	0.01	0.07	0.72	0.06	0.09	0.20	0.15	0.16	0.09	0.09	0.18	0.17	0.07	0.16	0.09	0.16	0.18	0.31	0.22	0.22	0.29	0.29	0.21	0.24
TiO2	0.01	0.73	1.03	0.33	1.19	1.74	1.31	1.92	1.25	1.40	1.64	1.47	1.08	1.45	1.14	1.45	0.48	0.18	0.07	0.10	0.12	0.11	0.19	0.16
LOI	0.05	0.80	1.03	1.15	0.64	0.49	0.74	0.62	0.72	0.85	0.95	0.62	0.61	0.69	0.65	0.27	0.62	0.60	0.88	0.64	0.59	1.65	0.22	1.16
Total		98.97	99.80	98.59	100.02	100.40	100.16	100.41	99.28	99.10	99.18	98.77	100.14	98.84	99.71	99.47	100.20	100.26	98.73	100.53	100.32	100.27	100.27	99.84

d.l.: detection limit; LOI: Loss on Ignition

1: Amphibolites; 2: Granodiorite; 3: Pyroxenite; Ay1, Ay2, Ay3= Aye 2010 (Masters Dessertation)

II.3- Behaviour of major elements in rocks of Kolasseng II

The representative major element analyses are given in Table 1. Both rocks have similar major element concentrations. Silica concentrations in pyroxenite attains 47.08 wt.%. Amphibolites have slightly higher contents (48 to 49.49 wt.%). Except the K_{11} sample whose silica values are only 44.68 wt.%.

Contents of Al_2O_3 are moderately high; they vary from 13 to 17.21 wt.% (Table 1). Amphibolites are richer in alumina (17.21 wt.%) than pyroxenites (13.13 wt.%). Contents of Fe_2O_3 are high. They attain 20.03 wt.% in amphibolites and 16.67 wt.% in pyroxenites (Table 1). Both rocks show increasing silica content with a corresponding decrease in magnesia contents. This is a common characteristic of rocks in the Neoarchean greenstone terrains (Barnes et al., 2007; Manikyamba et al. 2008).

CaO contents range from 8.73 to 11.22 wt.%. These contents are highest in the K_{11} and are lowest in the K_{13} samples of amphibolites. CaO values are equally higher in amphibolites than in the pyroxenites (10.10 wt.%). Contents of MgO (3 to 6.97 wt.%) are rather low in both rocks (Table 1).

The concentrations of alkalis are less than or equal to one for amphibolites except for the EA sample. These concentrations are higher in pyronenites (2.62 wt.% for Na_2O). Values of alkalis in amphibolites range from 0.70 to 1.99 wt.% for Na_2O and 0.11 to 0.71 wt.% for K_2O. Meanwhile in pyroxenites, the concentration for K_2O is 0.34 wt.% (Table 1).

The rocks of Kolasseng II are very poor in MnO and P_2O_5. The contents of these oxides are all less than 1 wt.%. TiO_2 contents are also very low and range from 1.01 to 1.85 wt.% (amphibolites) and are 1.51 wt.% (pyroxenites). The loss on ignition is low; it ranges from 0.22 to 1.65 wt.% for amphibolites and are 1.16 wt.% for pyroxenites (Table 1).

II.4 Major element geochemical variations

II.4.1. Binary diagrams of Al2O3 with other major elements

Major oxide contents were plotted against those of Al_2O_3 (Fig. 15). The results were slight positive correlations for SiO_2 and the alkalis, negative correlations for Fe_2O_3 and no correlations with CaO.

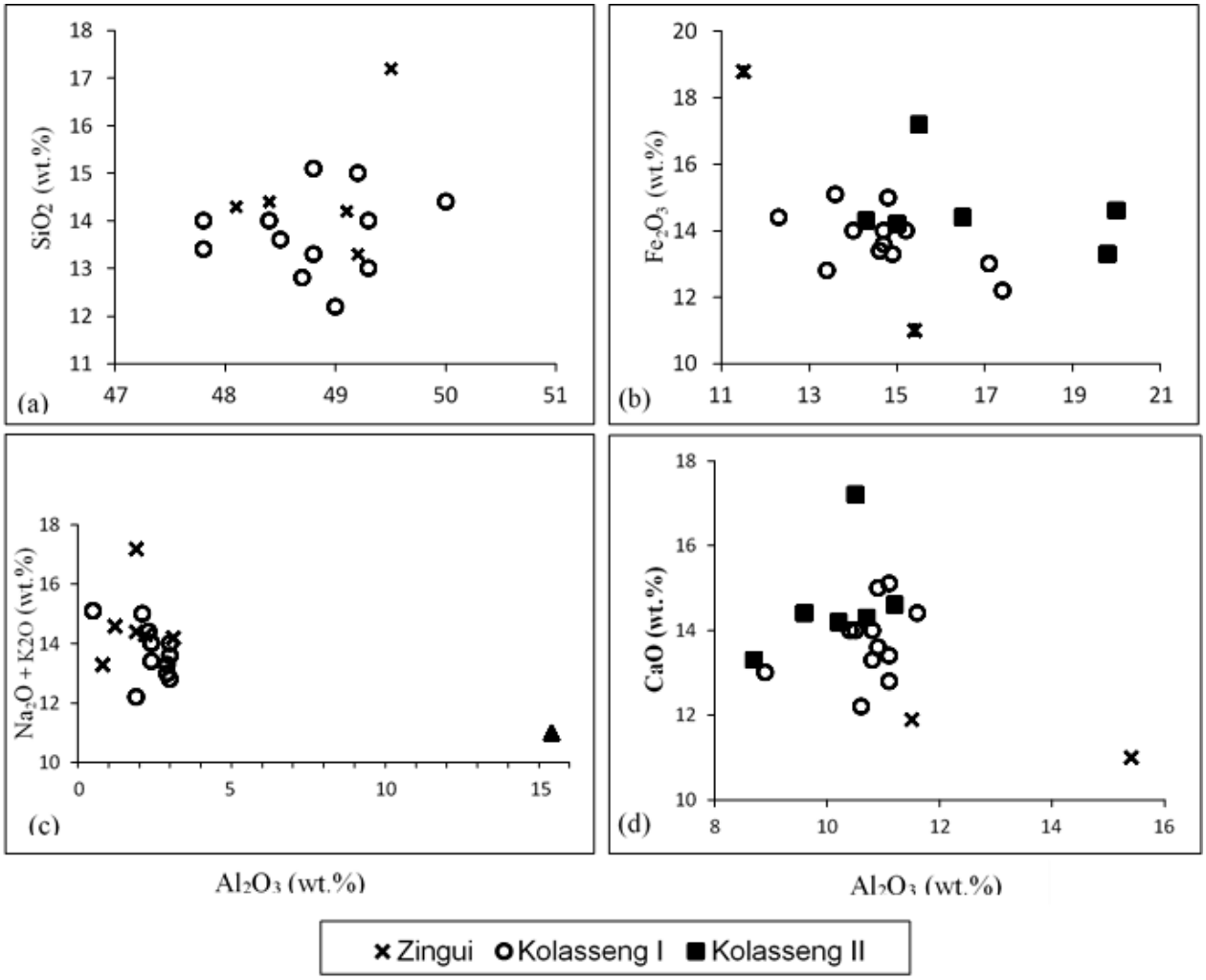

Figure 15 : Figure 15: Binary diagrams of Al2O3 with other major elements (a) Al2O3 vs SiO2; (b) Al2O3 vs Fe2O3; (c) Al2O3 vs alkalis; (d) Al2O3 vs CaO.

II.4.2. Binary diagrams of MgO with other major oxides

MgO contents were also compared to those of other oxides. CaO and Fe_2O_3 show an overall positive relationship with MgO (Fig. 16).

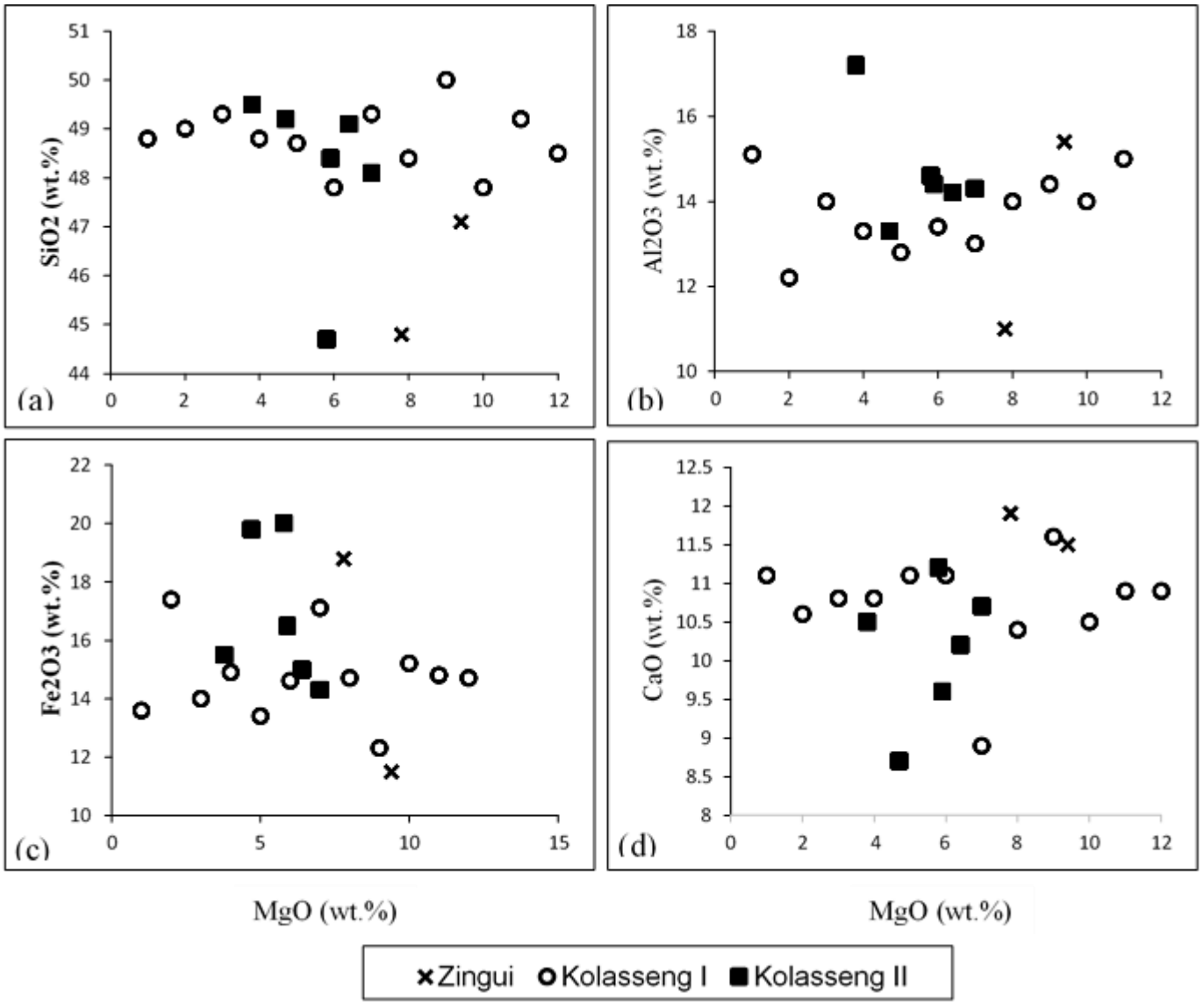

Figure 16 : Binary diagrams of MgO versus other major oxides (a) MgO vs SiO2; (b) MgO vs Al2O3; (c) MgO vs Fe2O3; (d) MgO vs CaO

II.4.3. Binary diagrams of Fe2O3 and other major oxides

Fe_2O_3 shows positive correlations with manganese and phosphorus oxides. It is rather negatively correlated with magnesium oxides. Fe_2O_3 is not correlated with alumina and silica (Fig. 17).

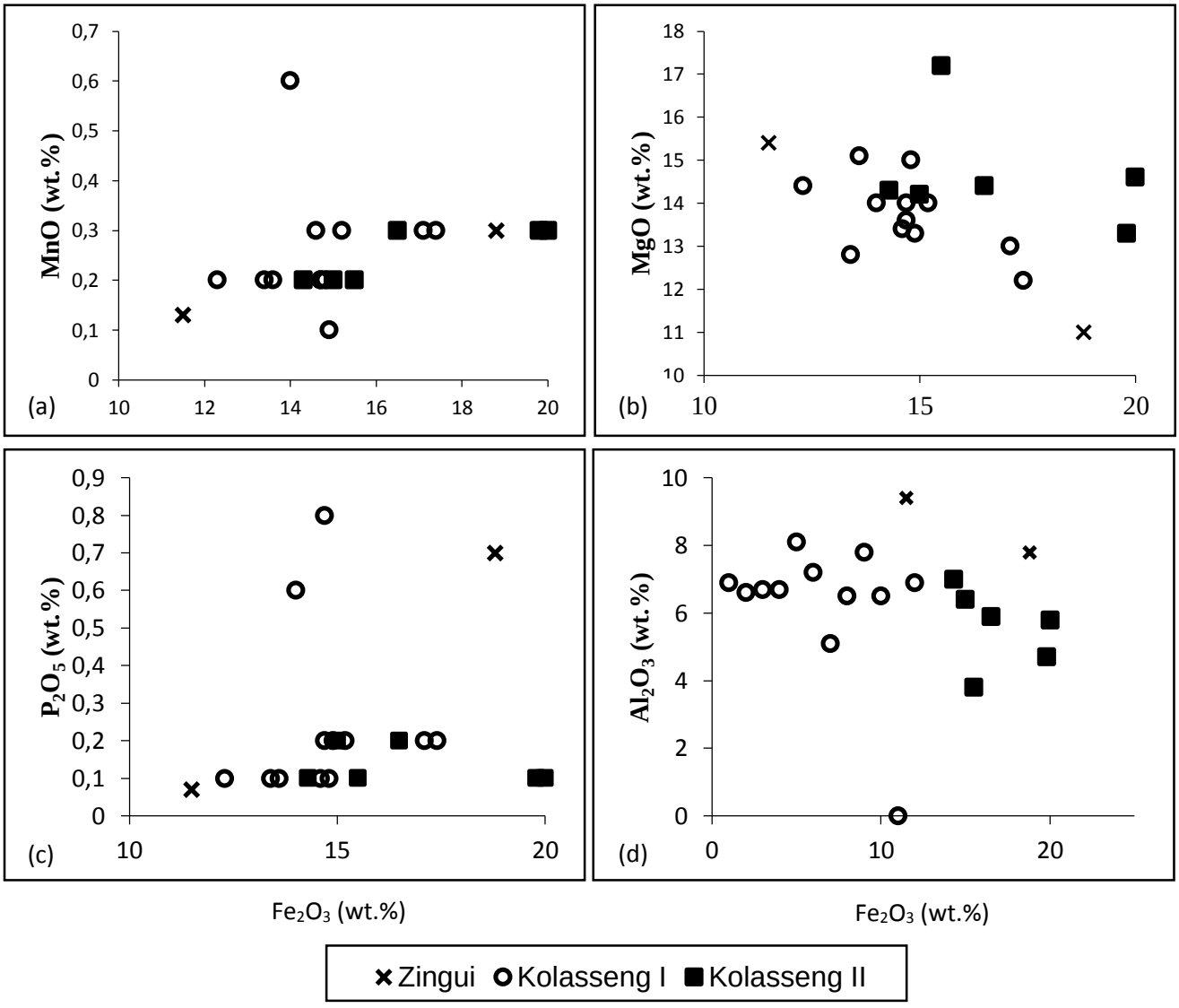

Figure 17 : Binary diagrams of Fe2O3 and other major oxides a) Fe2O3 vs MnO (b) Fe2O3 vs MgO (c) Fe2O3 vs P2O5 (d) Fe2O3vs Al2O3

II.5. Behaviour of Trace Elements in Amphibolites, Pyroxenites and Granodiorites

Trace element behaviour was observed in amphibolites of Kolasseng I and Zingui areas. The contents of these elements were also studied in the country rocks of the Kolasseng I area. Trace elements are usually partitioned in to three subgroups as follows;

II.5.1. First group of transitional elements

The amphibolites (Table 2) are rich in the first group of transitional trace elements which include Cr, V, Ni, Zn, Cu, Co and Ga. The chromium contents are outstanding in amphibolites of Zingui, they attain 591 ppm. In Nyabitande, samples collected from Kolasseng I also show high chromium contents (Table 2). The contents in most samples are greater than 200 ppm except of NK1 sample from Kolasseng (81 ppm). Contents of vanadium range from 205.20 to 347.40 ppm while contents of copper are greater than 134 ppm except for some samples.

Nickel contents (66.70 to 218.60 ppm), are variable and similar to those of zinc ranging from 66 to 236 ppm. Contents of cobalt and scandium in amphibolites are rather low. They range from 44 to 62.90 ppm for cobalt and 36 to 45.50 ppm for scandium. Most of the lowest scandium contents are obtained from one of the Zingui samples (Table 2). Amphibolites have very poor contents of galilium. Its contents vary from 15 to 25.11 ppm.

The country rocks (granodiorites and pyroxenites) are very poor in element of the first group of transitional elements. Their contents only attain a maximum of 45 ppm, except contents of vanadium which attains a hundred ppb.

This first group of trace elements has the most representative contents compared to all other trace elements (Table 2).

II.5.2. Second and third series of transitional elements

Amphibolites have moderate contents of the second and third groups of transitional trace elements. These include Zr, Y, Nb, Hf, Sb, Ta and Mo. Contents of zirconium range from 38 to 140 ppm. The highest content occurs in amphibolites from Kolasseng I. Contents of yttrium range from 17.21 to 69.14 ppm. Apart from Zr, and Y, other trace elements of this

series have low concentrations. The maximum and minimum content are found in amphibolites from Zingui. Nb and Pb have generally low contents less than 5 ppm (Table 2). Amphibolites are marked by very poor contents of Hf, Mo, Sn, Tl, Ta, Cd, and Cs. These contents are principally lower than 1 ppm. The other elements (Sb and Cd) have contents that are lower than their detection limits (Table 2).

II.5.3. Alkali and alkaline earth metals

The alkali and alkaline earth metals are represented by Li, Rb, Be, Sr, Ba. Strontium and barium are the most represented. Contents of strontium vary from 90 to 242 ppm. Amphibilites from Zingui have the highest contents. Also, most of the samples have contents that are superior to 100 ppm (Table 2). Contents of barium range between 35 and 178 ppm except NK7 sample. Lithium (2 to 11.00 ppm) and Rubidium (2 to 22 ppm) behave in a similar manner as some elements of the second and third groups of transition (Table 2).

Amphibolites have very poor Be contents. These contents are less than 2 ppm (Table 2). The rocks are also very poor in uranium (0.08 to 0.44 ppm) and thorium (0.28 ppm). Thorium exceptionally has relatively high contents of 9.60 ppm in Zn2 sample from Zingui.

II.5.4. Behaviour of trace elements in pyroxenites and granodiorites

Granodiorites and pyroxenites are marked by completely different trace element behaviour compared to all amphibolite samples. They show low contents in trace elements. The rocks are distinguished by very high Sr contents attaining 1008.60 ppm in pyroxenites and 638.80 ppm in granodiorite. They show high contents in zirconium which are rather low in amphibolites. Granodiorite shows particularly high contents in barium (665.60 ppm) which is low in the other rocks (Table 2).

Generally, the amphibolites of Zingui are richer in chromium than those from Nyabitande. Also, amphibolites from Kolasseng I of Nyabitande are more distinguished in trace element contents for several samples. With the exception of the above mentioned elements, all amphibolite samples show higher trace element contents than the country rocks (Table 2).

The contents of trace elements are generally variable and does not show much contrast. All the amphibolite and pyroxenite samples contain garnets. An exception here is the amphibolites from Zingui.

II.6. Behaviour of trace elements in rocks of Kolasseng II

The garnet amphibolites were noted for their high contents in the elements of the first group of transition (V, Cr, Ni, Zn, and Cu) compared to contents of other trace elements (Table 2). Vanadium had contents that attain 370 ppm and above while Cu contents in some samples were as high as 493.5 ppm. Cr, Zn and Ni show average contents of 123 ppm, 115 ppm and 94.79 ppm respectively.

Contents of Co were outstanding in EA sample attaining 543 ppm, while its contents in other samples vary between 46 and 66 ppm. Scandium showed rather lower contents, they range from 36 to 50 ppm (Table 2).

The garnet amphibolites of Kolasseng II show variable contents in elements of the second and third groups of transition (Table 2). Zr show contents that vary from 41 to 153 ppm, maximum contents were obtained from K4 sample. Y contents range from 23 to 43 ppm, while those of Nb, and Hf, show average contents that attain only 5 and 2 ppm respectively. Ta and Mo both show contents that are all less than 1 ppm.

The alkalis and alkaline earth metals (Li, Rb, Be, Sr, Ba) behave in a similar way as those of second and third groups of transitional elements. Sr and Ba (alkaline earth metals) have maximum contents of 145 and 135 ppm respectively while their average contents attain 94 and 66 ppm respectively. Beryllium contents are less than 1 ppm, while those of Rb and Li (alkali metals) are all less than 16 ppm (Table 2). Other elements such Th, U and Pb have contents of 2 ppm and below.

Garnet pyroxenites on the other hand also show high contents in elements of the first series of transition. However, elements like Cr, Zn and Ni have higher contents in garnet pyroxenites than in garnet amphibolites (Table 2). The elements of the second and third series of transition show varying contents, these include 110 ppm for Zr, 16 ppm for Y, and 5 ppm for Nb, and the other elements of this groups have contents less than 1 ppm.

Table 2 : Trace element contents (in ppm) in rocks of Zingui and Nyabitande.

d.l.= detection limit

		Zingui			Kolasseng I													Kolasseng II						
		1		2	1												3	1						3
	d.l.	Zn1	Zn2	GZn	FN3	AY1	AY2	AY3	AV1	AV2	NK1	NK2	NK3	NK4	NK5	NK7	NK6	K4	K8R	K10	K11	K13	EA	K5
Cr	3	591	558	34	174	199	198	203	389	285	81	199	278	234	96	222	11	110	159	43	75	73	194	208
V	0.8	239	205	39	347	307	290	309	283	293	334	261	285	260	338	273	113	335	327	314	>370	>370	248	272
Cu	1.4	134	3.9	25.6	178	363	290	107	243	214	106	398	204	296	205	356.	10.2	494	314	181	263	165	362	270
Ni	1.6	218	158	15.7	130	132	142	134	184	144	66.7	134	143	129	89.1	143	11.2	112	104	50.5	86.3	57.1	122	132
Zn	7	63	206	41	99	113	107	107	108	97	126	236	91	94	97	129	45	130	103	84	130	100	111	150
Co	0.1	62.9	44.03	8.38	53.7	61.9	60.9	62.7	58.4	57.2	53.8	56.6	53.19	54.9	56.0	57.6	9.78	60.7	57.2	46.4	66.7	49.2	544	58.4
Sc	1.1	39	36.8	6.3	45.3	47.5	43.2	44	39	37.5	45.5	40.9	44.4	41.8	44.1	42.7	9.3	37.2	46	36.3	50.8	47.3	38.2	39.5
Ga	0.04	15.2	25.11	16.6	18.0	20.2	19.3	20.7	17.7	19.0	19.4	18.5	16.9	17.6	17.8	17.6	24.6	19	16.7	21.5	20.3	18.2	19.0	19.9
Zr	6	43	129	101	44	140	82	105	38	47	120	75	46	83	39	94	189	153	41	52	52	67	92	110
Y	0.05	17.2	69.14	8.17	25.3	47.4	29.6	28.2	22.2	27.3	39.4	36.6	20.25	39.4	25.5	34.1	10	43.3	23.2	26.9	33.4	26.8	37.5	33.1
Nb	0.03	2.26	14.68	3.62	3.25	5.95	4.17	5.13	3.38	3.92	6.68	4.86	3.26	5.06	3.35	4.66	4.2	7.09	2.87	4.07	5.07	5.56	5.57	5.04
Mo	0.08	0.19	0.16	0.16	0.33	0.52	0.34	0.44	0.34	0.38	0.57	0.64	0.35	0.98	1.12	0.38	< dl	0.76	0.37	0.34	0.39	0.47	0.4	0.38
Hf	0.14	1.22	3.32	2.55	1.4	3.6	2.19	2.76	1.32	1.53	3.2	2.13	1.37	2.3	1.27	2.53	4.76	3.37	1.25	1.64	1.68	2.06	2.45	2.82
Pb	0.6	0.9	7.8	8.4	11.1	0.8	2.6	2.1	6.7	5	1.8	0.9	1.5	< dl	1.5	1.5	7.8	2.4	1.5	1.4	1.1	2.1	0.8	5.6
Ta	0.02	0.14	0.46	0.18	0.23	0.41	0.26	0.32	0.23	0.26	0.46	0.32	0.22	0.32	0.23	0.3	0.14	0.46	0.2	0.28	0.35	0.38	0.36	0.32
Li	0.4	2.5	4	4.2	5.3	9	11.9	11.3	8.5	9.1	5.5	6.1	6.7	2.1	3.2	11	2.6	10.5	2.5	3.7	2.2	2	6.4	16.5
Be	0.04	0.28	1.97	1.06	0.31	0.61	0.59	0.53	0.4	0.39	0.65	0.53	0.38	0.53	0.39	0.49	0.73	0.6	0.4	0.38	0.38	0.38	0.72	0.53
Ba	0.8	59.7	178	665	47.3	66.4	80.7	84	143	108	174	47.5	44.4	55.5	35	10.4	47.2	135.	41.2	18.5	35.2	36.3	79.2	120
Sr	0.6	122	241.9	638	111	64.7	136	114	153	172	107	204	124	90	114	107	1009	136	80.1	145	53.3	27	120.3	102
Rb	0.23	2.22	20.91	22.0	7.75	6.29	6.71	6.53	2.95	18.6	15	4.7	8.79	5	3.51	9.38	2.8	15.2	2.69	2.8	2.04	3.58	7.92	11.3
Th	0.02	0.37	9.6	1.96	0.34	0.8	0.52	0.69	0.46	0.45	3.11	0.73	0.28	0.61	0.45	0.66	11.8	2.86	0.32	0.51	0.56	0.63	0.74	0.67
U	0.01	0.11	0.44	0.35	0.11	0.22	0.13	0.2	0.15	0.13	0.78	0.18	0.08	0.21	0.12	0.17	1.81	0.83	0.13	0.16	0.15	0.19	0.19	0.18

1: Amphibolites; 2: Granodiorite; 3: Pyroxenite; Ay1, Ay2, Ay3= Aye 2010

II.7. Trace elements geochemical variations

Trace element data are presented in conventional bivariant plots. They help to define the relationship between elements and permit us to better study the rocks. Trace elements like Zr are positively correlated with Nb, Sr and Ni. Zr is rather negatively correlated with Cu. Uranium on the other hand is positively correlated with Zr and is not correlated with the other elements (Figs. 18 and 19).

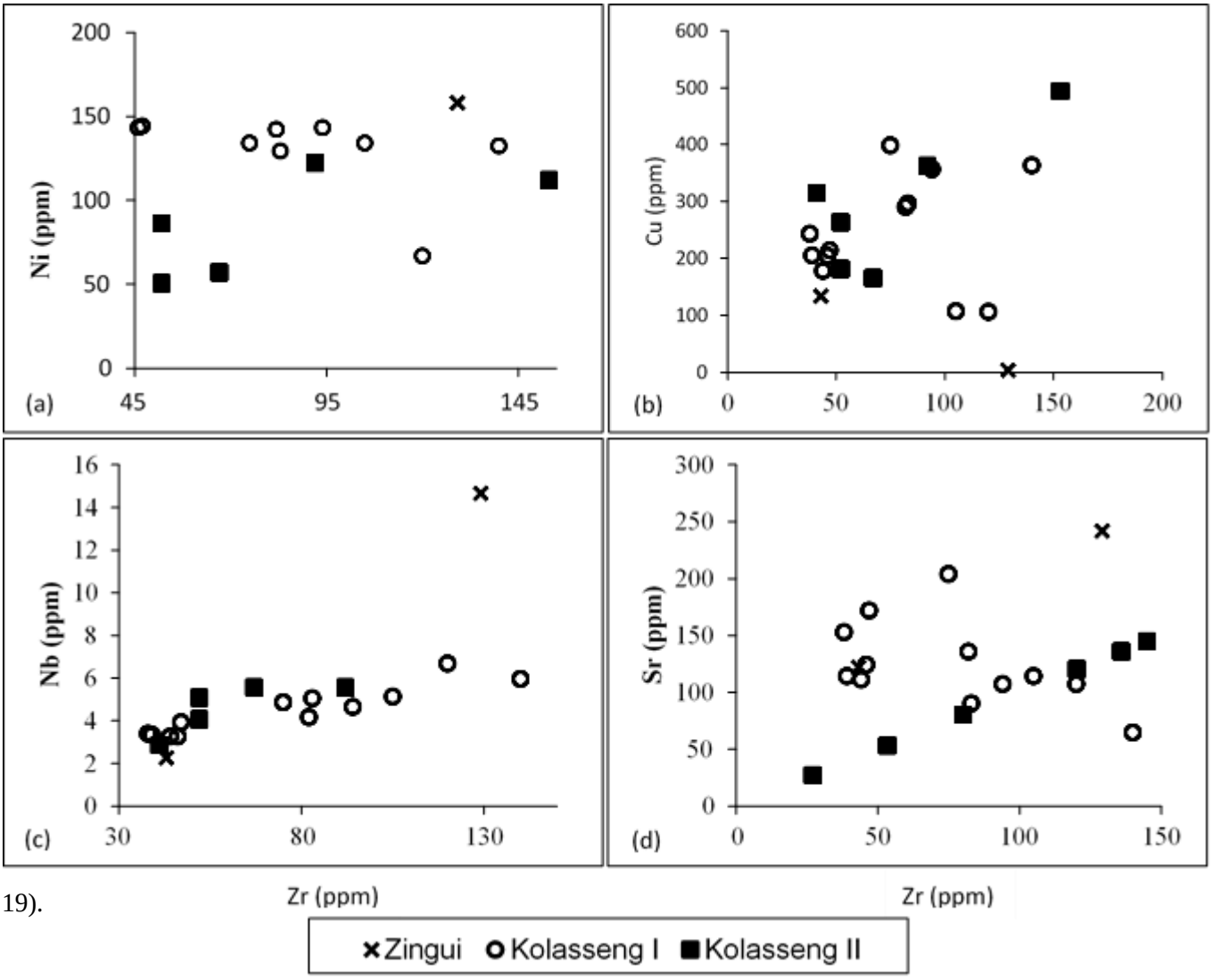

Figure 18 : Binary diagrams for selected trace elements (a) Zr vs Ni; (b) Zr vs Cu (c) Zr vs Nb (d) Zr vs Sr.

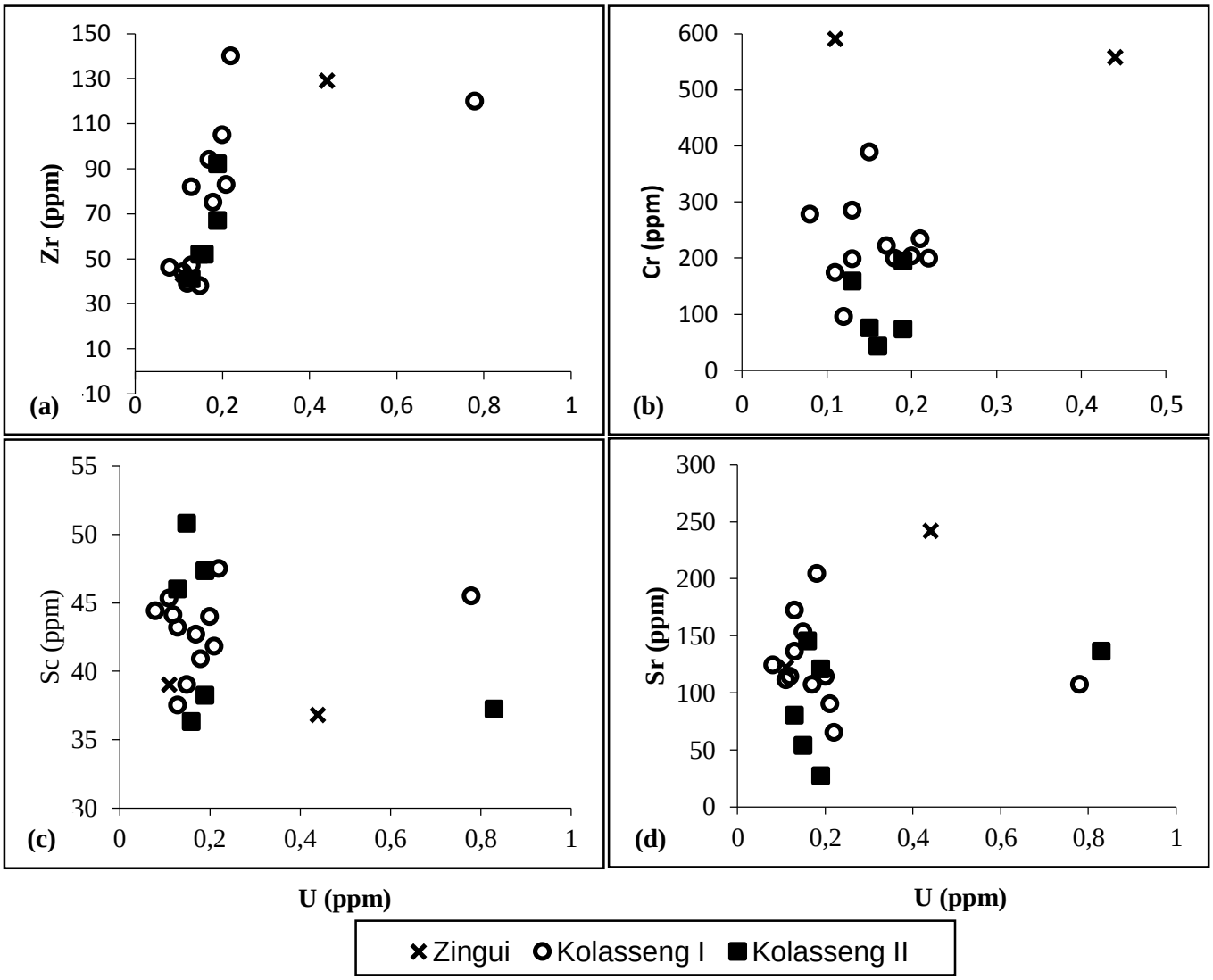

Figure 19 : Binary diagrams for selected trace elements (a) U vs; Zr (b) U vs Cr (c) U vs Sc (d) U vs Sr.

Binary diagrams were also established between silica and various groups of trace elements. Silica correlates negatively with the elements of the first and second groups of the periodic table (Cr, Ni and Zr, Y) respectively. It has slight positive correlations with the alkalis (Fig. 20).

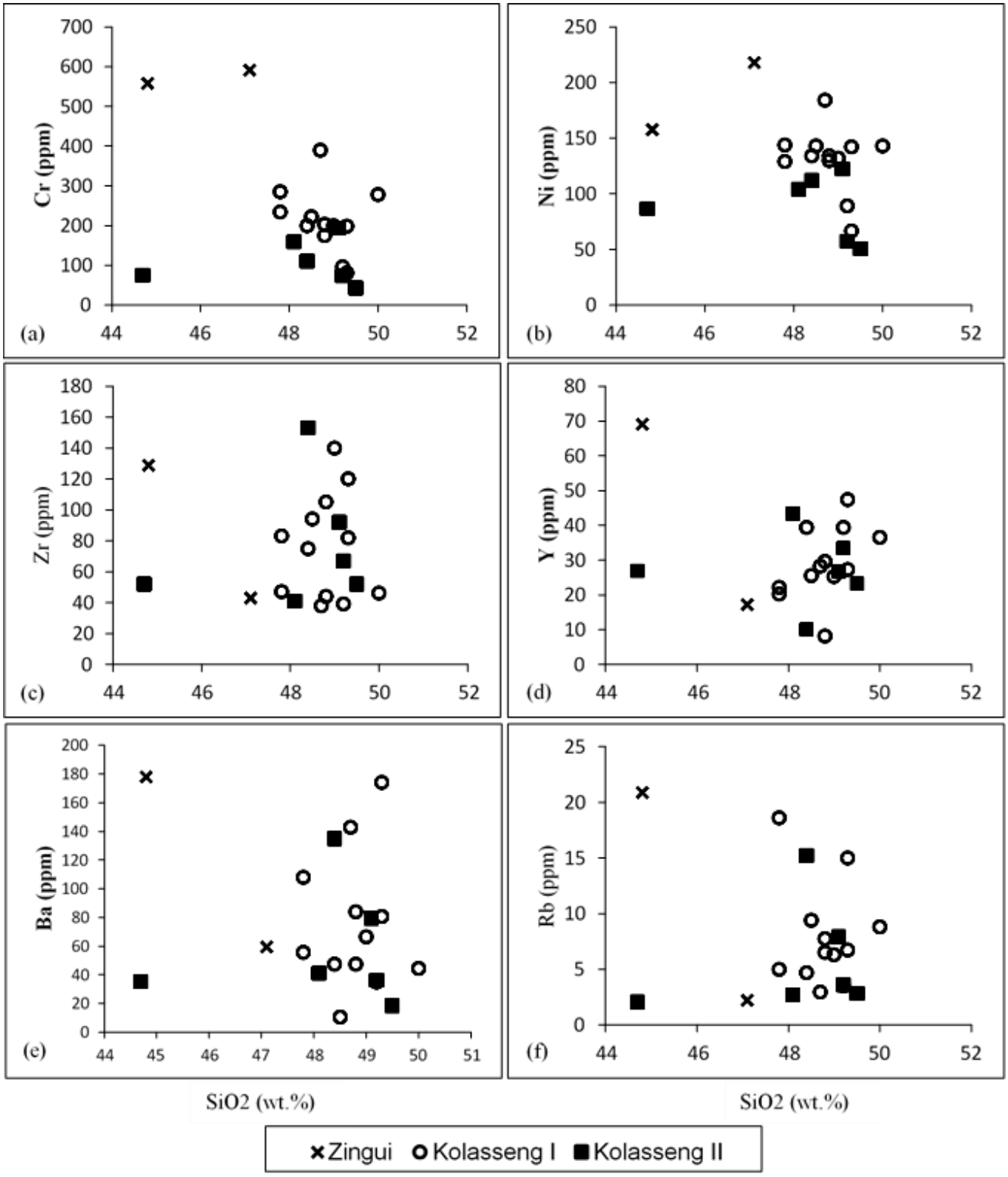

Figure 20 : Binary diagrams for silica and selected trace elements (a) SiO2 vs Cr; (b) SiO2 vs Ni; (c) SiO2 vs Zr; (d) SiO2 vs Y; (e) SiO2 vs Ba; (f) SiO2 vs Rb.

II.8. Geochemistry of rare earth elements

The rare earth element contents in amphibolites of Nyabitande and Zingui are variable. They show moderate concentrations as a whole. The total of REE content in the rocks varies between 36 and 272 ppm.

II.8.1. Light rare earth elements (LREE)

Cerium and neodymium are the most represented among the LREE. Cerium contents vary from 10 ppm to 97 ppm while those of neodymium range from 6 to 55 ppm. The samples with the highest contents are the amphibolites from Zingui (Table 3). Contents of Pr are rather low. However, they are higher in amphibolite of Zingui (13 ppm) compared to amphibolites of Nyabitande (4.66 ppm) (Table 3).

The Lanthanum contents range from 3.64 to 42.85 ppm, minimum and maximum contents occur in the Zn2 and the FN3 samples of Nyabitande and Zingui areas (Table 3). The Sm contents range from 1 to 5 ppm in all the amphibolite samples, but an outstanding content of 14 ppm is observed in the Zingui area. The europium contents are mainly less than 2 ppm.

II.8.2. Heavy rare earth elements (HREE)

The HREE are reprentend by Gd, Tb, Dy, Ho, Tm, Er, Yb and Lu. HREE show low concentrations in amphibolites (Table 3). Dysprosium and gadolinium have similar variations, contents of dysprosium vary from 3.02 to 13.08 ppm, while those of gadolinium range from 2 to 13.64 ppm (Table 3). Terbium contents show similar variations as holmium. Their contents are less than 2 ppm. Contents of Tb vary from 0.45 to 1.62 ppm while contents of Ho vary from 0.65 to 1.75 ppm. Contents of erbium are rather higher and variable; they range from 1.93 to 7.16 ppm and are similar to those of ytterbium which oscillates between 1.84 and 6.10 ppm (Table 3). Amphibolites are marked by very low thulium and lutetium contents. Their contents are similar and are all less than 1 ppm. The contents range from 0.28 to 0.99 ppm for thulium except for AY2 sample (4.41 ppm), while those of lutetium consist of 0.28 to 0.85 ppm with maximum and minimum contents similarly occurring in Zn2 and Zn13 samples, respectively (Table 3).

Generally the HREE have contents that are scarcely greater than 7 ppm except of some few contents which reached 13 ppm. It is also observed that the most significant HREE contents are seen in Zingui rocks (Table 3). Also, the rocks are richer in light rare earth

elements (25 - 226.4 ppm) than the heavy rare earth elements (11 - 46.53 ppm). The values of the LREE/HREE ratios are low. They range between 1.70 and 4.87. The higher value (4.87) occurs in Zn2 sample while the lower value occurs in Zn1 sample (Table 3).

II.8. 3. Normalisation of Rare Earth Elements

The rare earth elements are normalized following two parameters: the concentrations of the element in amphibolites compared to the concentrations of the same element in chondrite according to McDonough and Sun (1995). This is obtained through the following formula:

$$N = X_{amphibolites} / X_{chondrite} \quad (1)$$

$X_{amphibolites}$ = concentration of element in amphibolites.

$X_{chondrite}$ = concentration of element in chondrite.

The normalized data presented, shows europium anomalies in most of the amphibolite samples from Kolasseng I (Fig. 21). The spectra also show flat patterns (Fig. 21b). The amphibolites from Zingui have inclined patterns with a negative europium anomaly. There is enrichment in REE within amphibolites due to the high normalized values (> 10). Data from the country rocks (granodiorites and pyroxenites) were also nornalized with chondrite (McDonough and Sun, 1995). The granodiorite sample show a slight positive cerium anomaly while the pyroxenites show slight negative europium anomalies (Fig. 22)

Table 3 : Rare earth element contents (in ppm) in amphibolites and country rocks

		Zingui			Folack Nvos				Kolasseng I									Kolasseng II						
		1		2	1				1								3	1						3
	d.l.	Zn1	Zn2	GZn	FN3	AY1	AY2	AY3	AV1	AV2	NK1	NK2	NK3	NK4	NK5	NK7	NK6	K4	K8R	K10	K11	K13	EA	K5
La	0.04	4.4	42.9	12.6	3.64	7.93	5.43	6.14	5.24	5.52	17.1	7.65	3.77	7.44	4.55	6.67	59.2	17	4.79	4.7	6.06	4.15	6.69	6.65
Ce	0.12	10.3	97.2	40.9	10.0	20.3	13.5	17.8	12.1	12.5	36.2	19.2	10.2	17.3	11.9	16.93	104	35.3	11.95	12.2	14.1	8.67	17.5	17.46
Pr	0.01	1.5	13.1	2.64	1.6	3.16	2.08	2.7	1.93	2.16	4.66	2.89	1.62	2.62	1.78	2.55	9.12	4.65	1.86	2.0	2.43	1.56	2.75	2.66
Nd	0.06	6.9	55.8	9.61	8.5	15.7	10.2	13.3	10.0	11.3	20.3	14.4	8.41	13.2	9.25	13.0	29.0	20.9	9.21	10.1	12.2	7.35	14.1	13.1
Sm	0.01	2.0	14.0	1.93	2.85	4.78	3.36	4.13	3.15	3.6	5.22	4.49	2.69	4.23	2.98	4.06	4.23	5.46	2.97	3.23	3.87	2.45	4.45	4.03
Eu	0.01	0.8	3.4	0.67	1.07`	1.54	0.99	1.37	1.07	1.31	1.59	1.44	0.99	1.32	1.1	1.29	1.39	1.78	1.1	1.3	1.4	0.87	1.36	1.27
Gd	0.01	2.6	13.6	1.65	3.77	6.4	4.43	5.37	4.1	4.8	6.31	5.74	3.39	5.64	3.88	5.23	3.02	6.85	3.79	4.31	5.04	3.21	5.71	5.19
Tb	0.01	0.5	2.2	0.26	0.68	1.62	0.77	0.9	0.67	0.81	1.09	0.99	0.59	1.01	0.69	0.91	0.4	1.12	0.65	0.74	0.87	0.63	0.98	0.9
Dy	0.01	3.0	13.1	1.54	4.52	7.94	5.12	5.42	4.36	5.41	7.05	6.57	3.75	6.84	4.57	6.07	2.04	7.34	4.23	4.85	5.85	4.61	6.53	5.87
Ho	0.01	0.7	2.6	0.29	0.97	1.75	1.07	1.04	0.87	1.09	1.49	1.41	0.78	1.47	0.97	1.29	0.36	1.51	0.86	0.99	1.24	1.02	1.34	1.21
Er	0.01	1.9	7.2	0.84	2.82	5.44	3.2	2.8	2.39	3.05	4.22	4.08	2.26	4.35	2.87	3.83	0.92	4.45	2.49	2.91	3.66	3.22	4.02	3.62
Tm	0.01	0.3	1.0	0.12	0.42	0.8	4.47	0.38	0.33	0.41	0.63	0.59	0.32	0.62	0.41	0.54	0.12	0.63	0.35	0.42	0.54	0.48	0.58	0.52
Yb	0.01	1.8	6.1	0.77	2.73	5.1	3.03	2.27	2.04	2.5	4	3.84	2.03	3.98	2.7	3.54	0.73	3.99	2.29	2.69	3.51	3.15	3.79	3.31
Lu	0.01	0.3	0.9	0.11	0.41	0.77	0.45	0.33	0.29	0.36	0.59	0.56	0.3	0.57	0.4	0.52	0.11	0.59	0.34	0.4	0.53	0.48	0.57	0.49
∑REE	-	36.8	272	73.9	44.0	83.2	54.1	63.9	48.5	54.8	110	73.8	41.1	70.6	48.0	66.4	215	111	46.9	50.8	61.3	41.9	70.4	66.28
LREE	-	25.8	226	68.3	27.7	53.4	35.5	45.4	33.5	36.4	85.0	50.0	27.7	46.1	31.5	44.5	207	85.1	31.9	33.4	40.1	25.1	46.8	45.17
HREE	-	11	46.5	5.58	16.3	29.8	18.5	18.5	15.1	18.4	25.4	23.8	13.4	24.5	16.5	21.9	7.7	26.5	15	17.3	21.2	16.8	23.5	21.11
LREE/ HREE	-	2.3	4.9	12.3	1.7	1.79	1.92	2.45	2.22	1.97	3.35	2.1	2.06	1.88	1.91	2.03	26.9	3.21	2.13	1.93	1.89	1.49	1.99	2.14
$(La/Yb)_N$	-	1.4	4.14	9.65	0.79	1.06	1.22	1.84	1.51	1.3	2.52	1.17	1.1	1.1	0.99	1.11	45.4	2.89	1.42	1.17	1.71	0.89	1.2	1.36
Ce/Ce*	-	1.0	1.06	1.84	1.08	0.98	0.96	1.05	1.0	0.94	1.05	1.06	1.07	1.02	1.08	1.07	1.17	0.96	0.97	0.98	0.89	0.82	1	1
Eu/Eu*	-	1.0	0.75	1.14	0.99	0.85	0.78	0.89	0.2	0.96	0.84	0.86	0.99	0.82	0.99	0.85	1.19	0.89	1	1.06	0.97	0.95	0.82	0.85

d.l. =detection limit

1: Amphibolites; 2: Granodiorite; 3: Pyroxenite; Ay1, Ay2, Ay3= Aye (2010)

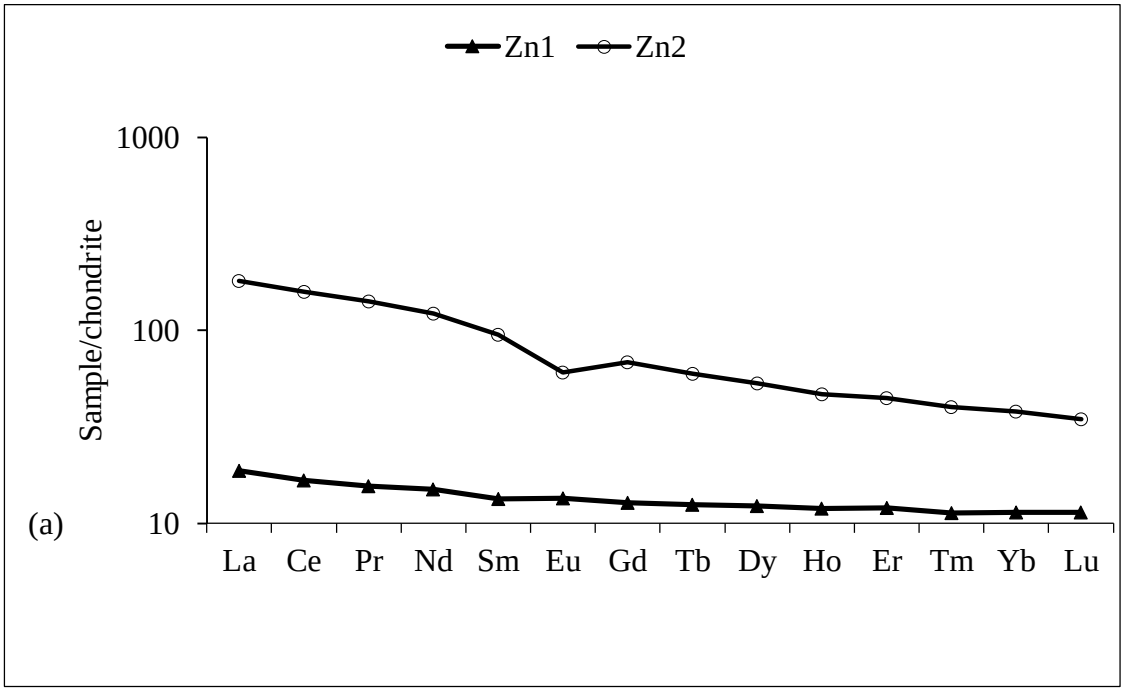

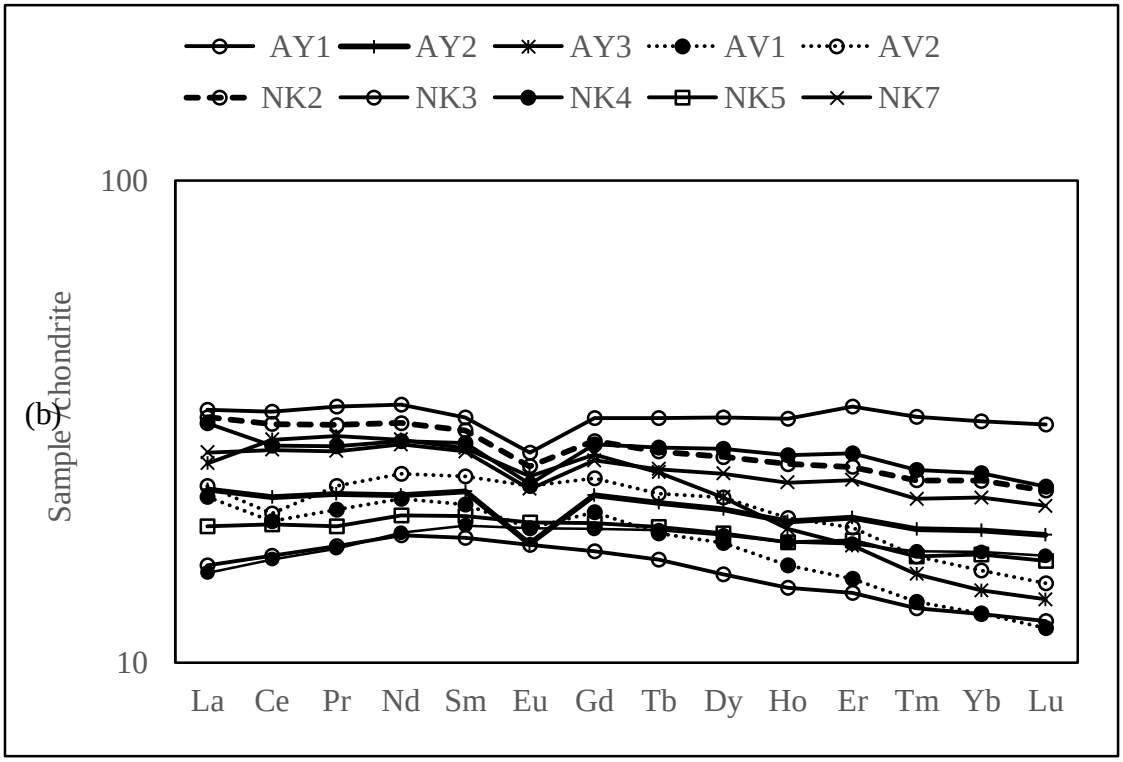

Figure 21 : Chondrite normalized REE patterns for amphibolites (a) Zingui area (b) Kolasseng I area.

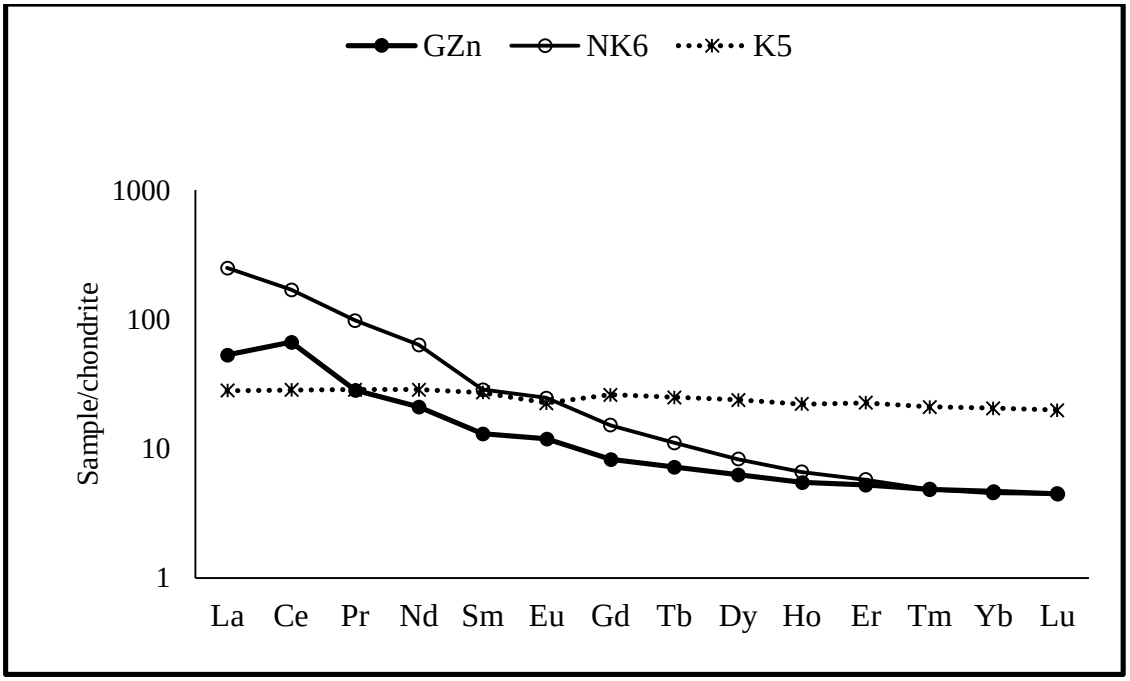

Figure 22 : Chondrite normalized REE patterns for country rocks: granodiorites (GZn); Pyroxenites (Nk6 and K5).

II.8.4. Fractionation of rare earth elements

The fractionation indice is usually gotten from the ratios of concentration of La and Yb normalized with chondrite according to McDonough and Sun (1995), through the following formula:

$$(La / Yb)_{normalized} = (La_{amphibolite} / La_{chondrite}) / (Yb_{amphibolite} / Yb_{chondrite}) \qquad (2)$$

These indices aid in determining the behaviour of REE in amphibolites and its country rocks. The ratios of $(La/Yb)_n$ are high, that is, they are above 1 for all the samples except NK5 and FN3 samples with contents less than one (Table 3).

II.8.4.1- Behaviour of rare earth elements in rocks of Kolasseng II

The REE contents were examined in amphibolites and pyroxenites from Kolasseng II. Both rocks show low REE contents. The total REE contents in amphibolites range from 41 to 111 ppm, while those of pyroxenites attain 66 ppm. However these contents are about twice higher than those of pyroxenites of Lolodorf (21.76 and 64.49 ppm; Ebah Abeng *et al.*, 2012) and more than ten times higher than those of serpentinites of Lomié ultramafic complex (0.48 and 1.33 ppm; Ndjigui *et al* 2008). The rocks are richer in the light rare earth elements than in the heavy ones, the LREE/HREE values vary from 1.49 and 3.21. The LREE concentrations range from 25.05 to 85.11 ppm (Table 3.

Within the amphibolites cerium, neodymium and lanthanum are the LREE with the highest concentrations. The concentrations of Sm are slightly higher than those of Pr, europium concentrations are lowest among light rare earth elements (Table 3). On the other hand, Dy and Gd are the heavy rare earth elements (HREE) with elevated concentrations. Their maximum contents include 7.34 ppm and 6.85 ppm respectively. Tb and Ho behave in a similar way, their contents are below 1 ppm (Table 3). Contents of erbium and ytterbium are rather higher and variable; they range from 2.49 to 4.45 ppm for Er and oscillate between 2.29 and 3.99 ppm for Yb. The contents of Tm and Lu are similar, these contents are all less than 1 ppm (Table 3).

Garnet amphibolites are richer in REE as a whole than garnet pyroxenites. Pyroxenites are also richer in LREE than the HREE, their contents of LREE doubles those of HREE (Table 3). Cerium has the highest content while Lu is the least.

II.8.4.2. Normalisation of Rare Earth Elements of Kolasseng II

The spectra of REE of amphibolites of Kolasseng II normalized with chondrite according to McDonough and Sun (1995) reveal pronounced negative Eu anomalies for EA and K4 samples while the other samples show only slight negative Eu anomalies (Fig. 23). Most of the samples show slight negative cerium anomalies, but these anomalies are well distinguished in K11 and K13 samples (Fig. 23). Both amphibolites and pyroxenites show negative europium anomalies (Fig. 23).

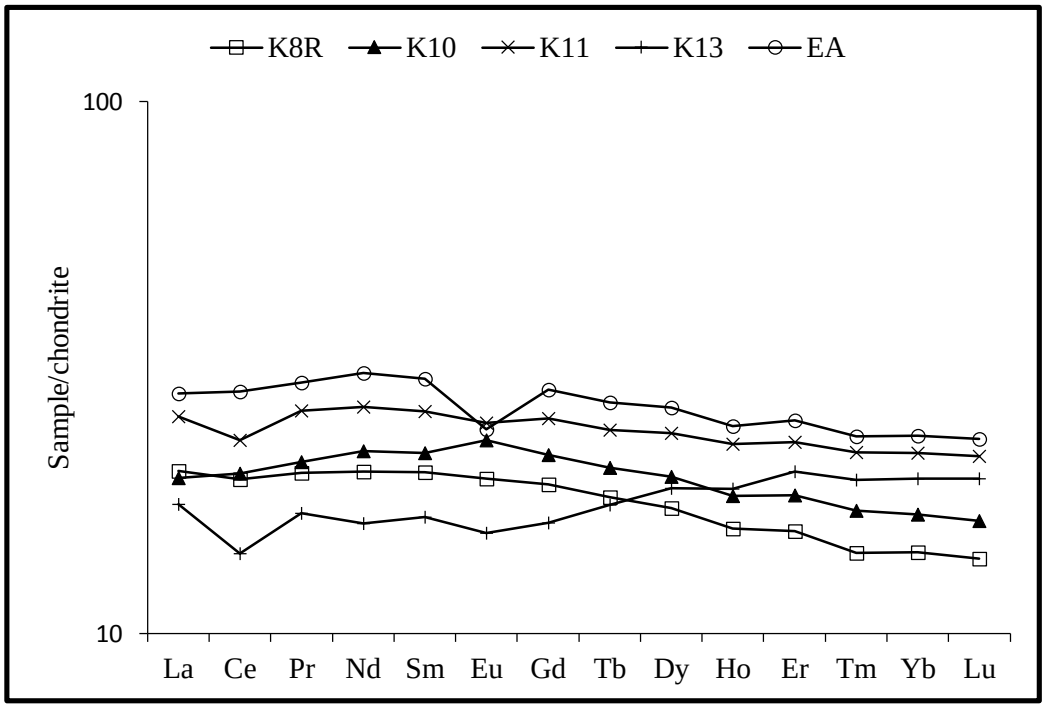

Figure 23 : Chondrite normalized REE patterns for amphibolites of Kolasseng II.

II.8.5. Fractionation of rare earth elements (REE)

The ratios of the fractionation indice (La/Yb)n for amphibolites of Kolasseng II are all above 1 except K13 sample with a ratio of 0.89. The maximum ratio attains 2.89 in the K4 sample. This stipulates that the K13 sample have undergone more fractionation compared to the K4 sample. Also, the enrichment of the elements above 10 for both amphibolites and pyroxenites confirms the fact that they have undergone a lower rate of fractionation (Table 3, Fig. 23).

II.8.4. Calculations of anomalies in cerium and europium

Calculations to determine cerium and europium anomalies (Table 3), reveal that the ratios for cerium are all lower than 1 except for the EA sample and the pyroxenite country rock whose ratios are 1. Ratios for Eu on the other hand are also less than 1. The low Eu/Eu* ratios for most of the samples points to the presence of negative europium anomalies for many samples as confirmed by the normalisation spectra (Table 3; Fig. 23).

The fractionation indices of amphibolites of Kolasseng I and II areas are all greater than 1 except for a few disperities. Their Ce/Ce* ratios are all less than or equal to 1, while their Eu/Eu* ratios in most samples are both less than 1 (Tables 3).

Generally, amphibolites are characterised by negative europium and cerium anomalies while pyroxenites show positive cerium anomalies.

Conclusion

Amphibolites are medium-grained, dark-coloured, and dense rocks. They generally present a nemato-granoblastic heterogranular texture. Amphibolites composed of amphibole, plagioclase, garnet, quartz, and accessory apatite, spinel, sericite, pyrite, chalcopyrite and non-identified opaque minerals. The presence of apatite, sericite, and two generations of opaque minerals suggests that they might be affected by hydrothermal alteration. X-ray diffrations of relatively fresh amphibolites show primary minerals like amphibole, feldspar, pyroxene, garnet and quartz. The major, trace and rare earth elements contents, are consistent with the mafic nature of amphibolites. Amphibolites from Nyabiande have higher contents of silica than those from Zingui area. Amphibolites of Kolasseng II have particularly high TiO_2 contents. Their silica content increases with a corresponding decrease in MgO. The loss on

ignition values is also low. SiO_2, alkalis and MgO have positive correlations with Fe_2O_3 and CaO. MnO and P_2O_5 also correlate positively with selected major oxides. Amphibolites have high contents of Cr, Ni, Zn and Sr. The chondrite normalized REE patterns for amphibolites reveals negative europium anomalies and slight negative cerium anomalies for selected samples. Calculations of fractionation indice $(La/Yb)_n$ show that amphibolites have a low degree of fractionation. The amphibolites from Zingui area are richer in contents of REE than those from Nyabitande. Xenoliths of amphibolites collected from the country rocks of Zingui are particularly rich in REE.

CHAPTER IV

PETROLOGY OF WEATHERED AMPHIBOLITES

Introduction

This chapter explains the morphology, mineralogy and geochemical characteristics of weathered amphibolites.

I. Morphological and mineralogical features of weathered amphibolites

Samples of weathered amphibolites were collected in Kolasseng II. The garnet amphibolites occur as dense centimetric weathered blocks of irregular shapes with variable stages of weathering. The blocks with incomplete weathered process leave behind the rocks with differentiated portions from the periphery to the core: a deeply weathered outer portion with a yellowish brown colour; a white patched portion; an inner thick dark portion and a slightly weathered core (relatively fresh) with the relic structure of parent rock (Fig. 24).

The weathered materials are also differentiated according to grain size. The mineral assemblage is confirmed by XRD analysis which shows that the weathered amphibolites are made up of amphibole, feldspars, quartz, garnet, kaolinite, and accessory gibbsite, goethite, hematite, and spinel (Fig. 25).

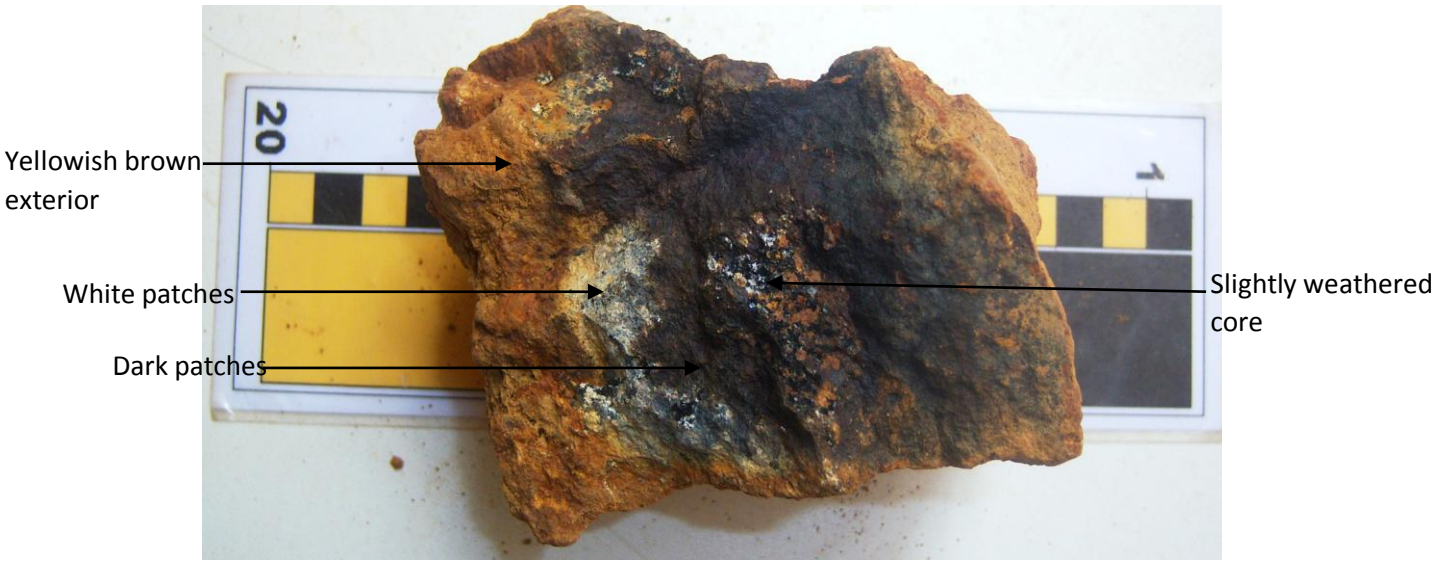

Figure 24 : Macroscopic view of weathered amphibolite block

The weathered amphibolite blocks were differentiated in to fine grained, medium grained and coarse grained facies as follow:

- The fine grained facies were deeply weathered presenting an intermingled yellowish and reddish colour, the relics of minerals are difficult to recognize. Some samples also show much white minerals and small lines with recrystallised quartz grains. Also some samples show slightly fresh interior containing relic structures, with some yellowish and white secondary minerals all of which are oriented.

- The medium grained facies are less weathered compared to the fine grained type, but nevertheless some had undergone intense weathering. They generally show intense weathering on the outside with relatively fresh interior with relics of ferromagnesian minerals.

- The coarse grained facies display a centripetal weathering. The entire surfaces of the samples are deeply weathered in to a yellowish to reddish brown. At the point of breakage facies present dark red spots and a few whitish portions, while the interior is black and shows large mafic slightly fresh grains. Also, these facies show granular grains.

The weathered facies with abundant garnet minerals show relatively fresh interiors with a weak schistocity, observable minerals include feldspar, and garnet.

II. Geochemistry

This section is concerned with the behaviour of major, trace and rare earth elements in weathered amphibolites. The weathered materials were collected at Kolasseng II. The rocks were all rich in garnet, but show different grain size distribution (Table 4).

II.1 Geochemistry of major elements

The weathered blocks of amphibolites have variable contents of SiO_2. These contents range from 26 to 49 wt.% in the fine grained variety; 34 to 48 wt.% in the medium grained amphibolites but attain a maximum of 25.3 in the coarse grained amphibolites (Table 4).

Weathered amphibolites have high contents of Al_2O_3. These contents oscillate between 13.15 and 24.17 wt.%; 14 .50 and 16.73 wt.%; 14.34 and 21.49 wt.% for the fine, medium and coarse grained rocks respectively (Table 4). Weathered amphibolites have high contents of alumina. These contents oscillate between 13.15 and 24.17 wt. %; 14 .50 and 16.73 wt.%; 14.34 and 21.49 wt.% for the fine, medium and coarse grained rocks respectively (Table 4).

Weathered amphibolites present a high concentration in Fe_2O_3 relative to the unweathered rocks. Thus, the weathered rocks are richer in Fe_2O_3 than the fresh rocks. Fe_2O_3 contents range from 24.66 to 32.75 wt.% in the fine grained rocks, 15.90 to 24.53 wt.% for the medium grained rocks and 20.55 to 30.99 wt.% for the coarse grained rocks (Table 4).

CaO contents are rather low and variable, most of the contents are less than 2 wt.% except for a few samples with contents of 9 wt.%. They vary from 0.04 to 9 wt.%. There is also a significant decrease in CaO contents from the fresh rocks to the weathered blocks, this decrease can be up to four times or more compared to the fresh rocks (Table 4).

MgO behaves similarly to CaO, maximum contents for MgO attain 6.10 wt.%, while minimum contents attain 0.39 wt.%. TiO_2 also have similar behaviour to that of MgO. Its contents range between 1 and 2 wt.%, except one sample (K14) with contents of 3.25 wt.% (Table 4).

Both weathered and fresh amphibolites are very poor in alkalis (Table 4). Contents of Na_2O are very close or equal to the detection limit, while contents of K_2O are all less than 1 wt.%. Other oxides like MnO and P_2O_5 are also significantly low; they consist of 0.03 to 0.33 wt.% for MnO and 0.07 to 0.25 wt.% for P_2O_5. The loss on ignition is by far higher than the detection limit and also significantly higher than those of the alkalis. It consists of 7 to 15 wt. %; 1 to 9.54 wt.% and 6 to 15 wt.% for the fine, medium and coarse grained amphibolites respectively (Table 4).

Generally, the weathered amphibolites show a partial depletion of SiO_2 and a strong depletion of CaO and MgO. Weathering also caused a relative accumulation of Al_2O_3 and Fe_2O_3 contents. Concentrations of Fe_2O_3 are several times higher than those of CaO and MgO, Al_2O_3 and iron have similar behaviour. Also, SiO_2, Al_2O_3 and Fe_2O_3 represent more than 70 % of all the major elements of weathered amphibolites (Table 4).

II.1.1. Major element bivariant plots

Bivariant plots enable us to understand the behaviour of major elements in amphibolites during weathering. The plots show positive correlation of silica with CaO, MgO, alkalis (Na_2O+K_2O) and MnO (Fig. 26 c, d, e, and g). Silica rather correlates negatively with Fe_2O_3, Al_2O_3 and TiO_2 (Fig. 27 a, b and f). On the contrary, Fe_2O_3 correlates positively with TiO_2 and P_2O_5 (Fig. 27 a and b). Fe_2O_3 has weak correlations with Al_2O_3 (Fig.

27 c). Fe_2O_3 has strong negative correlations with CaO, MgO, MnO and the alkalis (not shown) (Fig. 27 d, e and f).

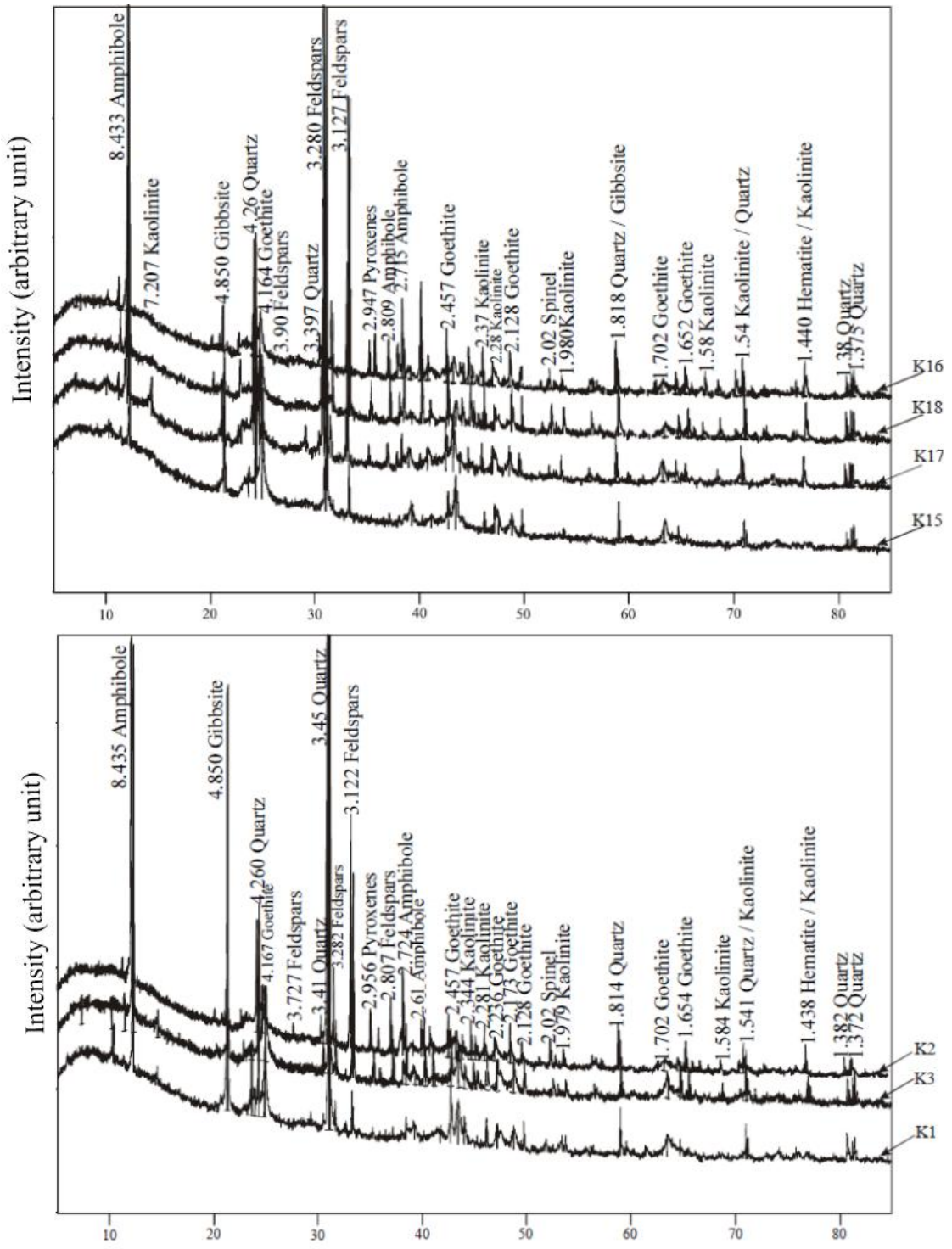

Figure 25 : XRD patterns for weathered amphibolites

Table 4 : Major element contents of the weathered garnet amphibolites

	Dl	Fine grained					Medium grained			Coarse Grained				
		K1	K3	K6	K7	K17	K2	K9	K12	K14	KI5	K16	K8W	K18
SiO_2	0.04	26.71	37.08	49.11	34.26	38.29	38.14	48.55	47.49	25.3	28.74	45.22	37.15	42.25
Al_2O_3	0.02	24.17	16.53	13.15	15.35	18.48	16.73	15.93	14.50	21.49	19.95	14.34	16.69	15.65
Fe_2O3	0.01	27.06	27.11	25.19	32.75	24.66	24.53	15.90	17.15	30.86	30.99	20.55	23.51	24.30
CaO	0.006	0.86	2.80	0.04	0.45	1.85	3.56	9.65	9.29	1.01	0.44	4.13	5.93	4.48
MgO	0.01	1.03	2.27	0.49	0.39	1.69	2.72	4.99	6.10	0.85	0.44	3.41	5.00	2.60
Na_2O	0.02	0.13	0.42	0.02	0.06	0.21	0.58	1.69	1.26	0.13	0.05	0.52	0.80	0.43
K_2O	0.01	0.69	0.24	0.81	0.41	0.21	0.19	0.17	0.17	0.15	0.30	0.32	0.24	0.41
TiO_2	0.01	2.79	2.02	1.96	2.93	1.88	2.52	1.34	1.28	3.25	2.98	1.76	1.59	2.68
MnO	0.0022	0.19	0.18	0.15	0.06	0.09	0.18	0.22	0.25	0.08	0.03	0.18	0.18	0.33
P_2O_5	0.002	0.25	0.17	0.15	0.24	0.11	0.15	0.07	0.08	0.22	0.23	0.09	0.08	0.15
LOI	0.05	15.39	10.75	7.13	12.46	12.04	9.54	1.62	2.39	15.75	14.91	8.07	8.90	6.59
Total	-	99.31	99.63	99.24	99.38	99.56	98.89	100.11	99.96	99.14	99.10	98.63	100.11	99.87

D l.: Detection limit
LOI: Loss on ignition

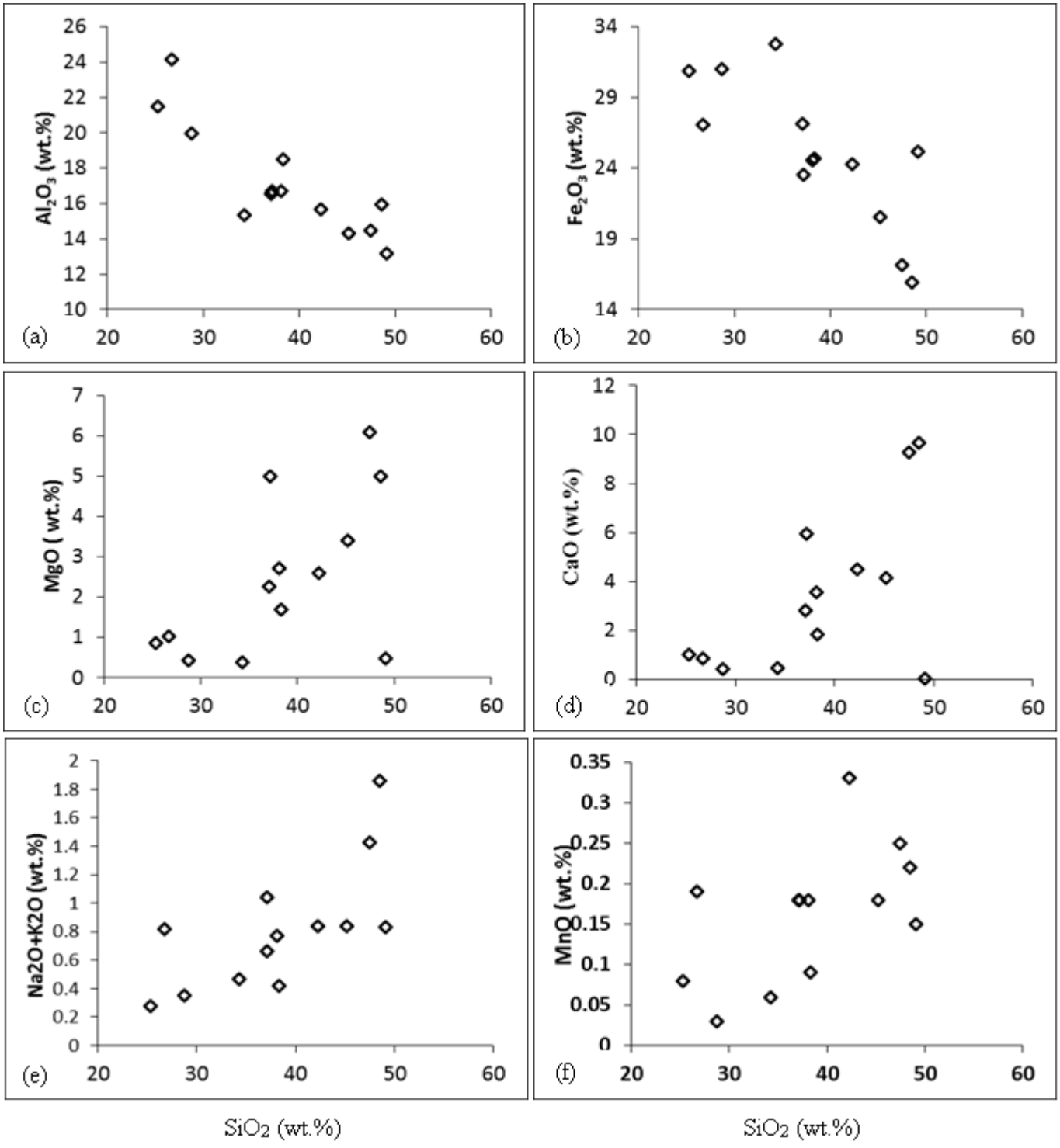

Figure 26 : Bivariant plots of silica and selected major elements in weathered amphibolites. (a) SiO2 vs Al2O3; (b) SiO2 vs Fe2O3; (c) SiO2 vs MgO; (d) SiO2 vs CaO; (e) SiO2 vs alkalis; (f) SiO2 vs MnO

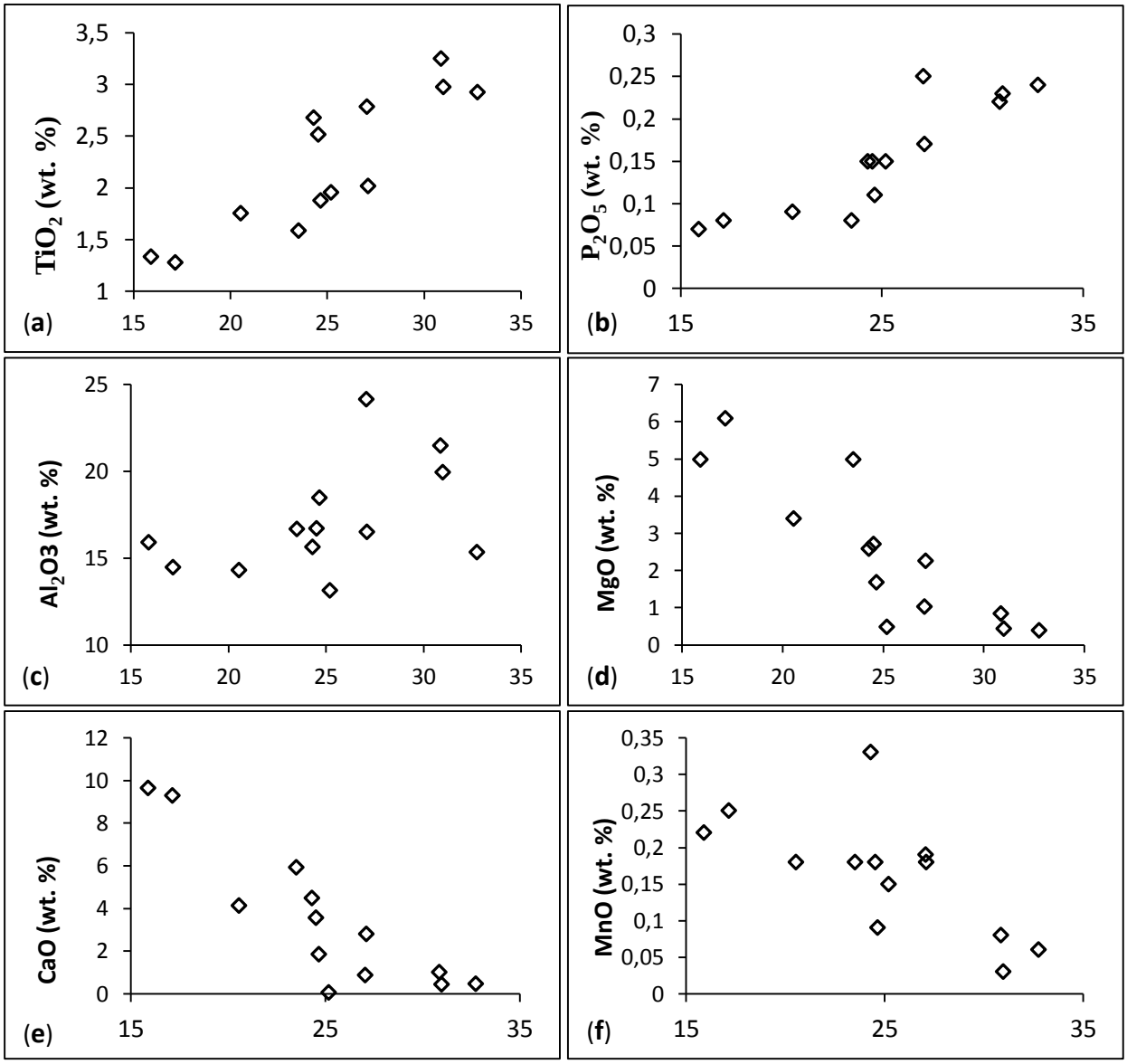

Figure 27 : Bivariant plots of Fe2O3 and selected major elements in weathered amphibolites. (a) Fe2O3 vs TiO2; (b) Fe2O3 vs P2O5; (c) Fe2O3 vs Al2O3; (d) Fe2O3 vs MgO; (e) Fe2O3 vs CaO; (f) Fe2O3 vs MnO.

II.2. Behaviour of trace elements in weathered amphibolites

This study of trace elements has been facilitated by grouping them into the first, second and third groups of transitional elements, the alkali metals, the alkaline earth metals and other metals.

Weathered amphibolites have low contents of trace elements. The trace elements of the first group of transition have the highest contents. Vanadium, chromium and copper have relatively higher contents compared to those of other elements in this group. Contents of V are all greater than 350 ppm except for one sample (K6=103 ppm). Contents of Cr are variable, they range from 60 to 358 ppm, and 70 to 295 ppm for the fine and medium grained rocks respectively, but are higher being 239 to 388 ppm in the coarse grained rocks (Table 5). Contents of Cu oscillate between 100 and 332 ppm except for one sample. Zinc and nickel also have significant concentrations in some samples; zinc behaves similarly with Ni in these weathered amphibolites. Zn contents oscilate between 35 and 155 ppm, while Ni contents are more variable; they ranging from 20 to 114 ppm. Concentrations of Co, Sc, and Ga are less than 60 ppm. They consist of 9 to 57 ppm for Co; Sc contents are less varied, they range from 34 to 55 ppm; while those of Ga vary between 18 and 37 ppm (Table 5).

- Second and third groups of transitional elements are characterized by Zr, Nb, Y, Mo, Hf, and Ta. Contents of zirconium are the most elevated within these groups. They oscillate between 40 and 209 ppm, Sr and Y contents attain a maximum of 99 and 20 ppm respectively (Table 5). Within the third group of transition, Pb contents are the highest. They vary between 10 and 110 ppm except for two samples with contents less than 5 ppm Contents of Nb are variable and less than 13 ppm, whereas those of Mo, Hf and Ta are significantly low. They include less than 1 ppm for Ta, less than 1 ppm for Mo except for K14 sample with contents of 13 ppm while contents of Hf vary from 1 to 5 ppm (Table 5).
- Alkali and alkaline earth metals (Li, Rb, Ba) generally have similar characteristics as those of the second and third series of transition elements. Within this group, Barium has very high contents that are comparable with those of the elements of the first group of transition; maximum barium contents are 305 ppm in the fine grained rocks, 128 ppm in the medium grained rocks, and 96 ppm respectively in the coarse grained rocks (Table 5).

The weathered rocks are very poor in the alkali metals (Li, Rb); Lithium concentrations are less than 10 ppm. On the contrary, Rb contents are close to 11 ppm, except for one outstanding sample (K6) with 46 ppm (Table 5).

Concerning other trace elements, the contents of the actinides (uraniun and thorium) are very low. Analyzed data shows that Th has contents of 0.45 to 3.68 ppm while uranium contents range from 0.14 to 1.59 ppm (Table 5).

II.2.1. Correlation between major and trace elements

Binary diagrams were established in order to check the affinity between some trace and major elements in the course of supergene alteration and to bring out their behaviour. Here correlations have been established between silica, manganese oxide, ferrous oxide and magnesia with selected trace elements to check their similarities during weathering.

II.2.1.1. Correlations between MnO and selected trace elements

The diagrams show positive correlations of MnO with Zn and Co (Fig. 28 c and d); negative correlations with Ga and Zr (Fig. 28 a and b). Binary diagrams reveal no correlations between MnO and Ni, V, Cu and Cr.

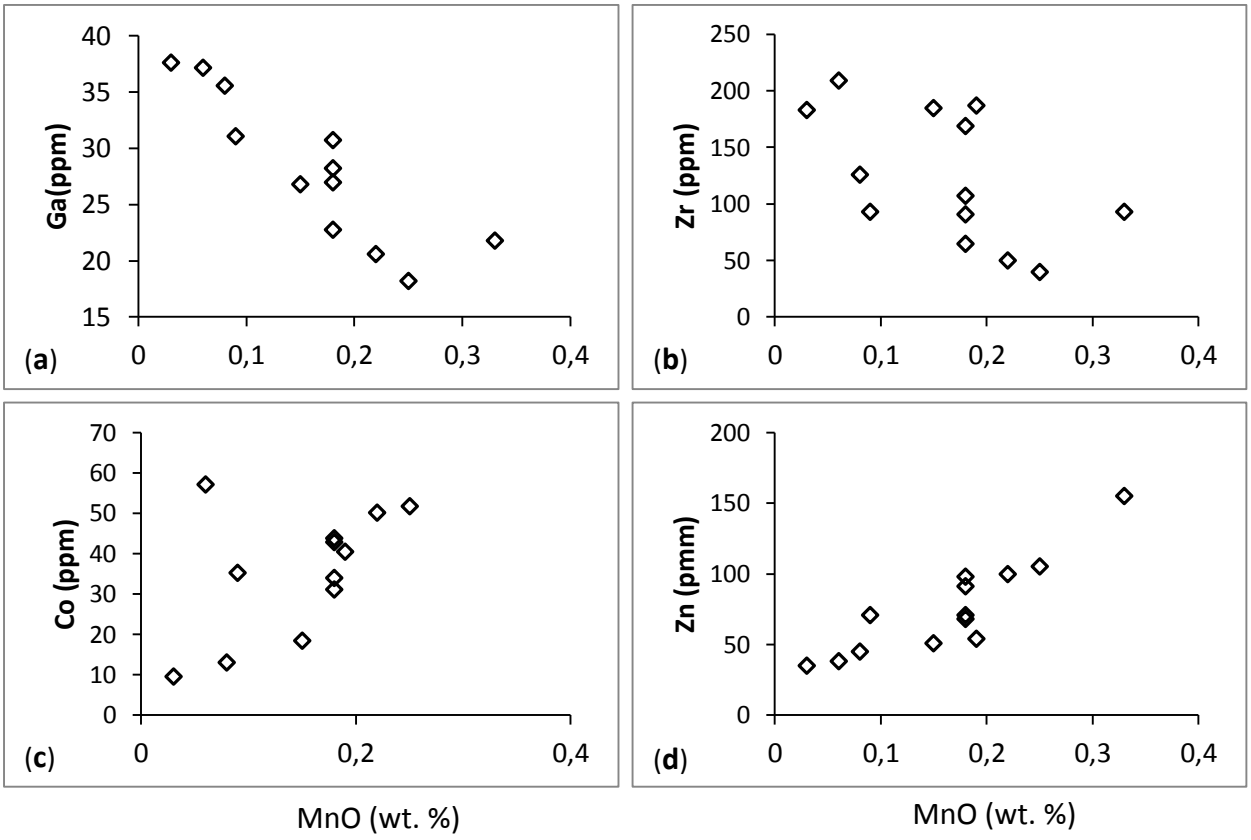

Figure 28 : Binary diagrams of MnO and some trace elements (a) MnO vs Ga; (b) MnO vs Zr; (c) MnO vs Co (d) MnO vs Zn in weathered amphibolites

Table 5 : Behaviour of trace element contents in weathered garnet amphibolites

		Fine grained					*Medium grained*			*Coarse grained*			*Coarse grained*	
Trace Eléments	d.l	K1	K3	K6	K7	K17	K2	K9	K12	K14	K15	K16	K8W	K18
Cr	3	213	358	60	131	200	295	70	96	388	275	239	261	63
V	0.8	>370	>370	103.6	>370	>370	>370	>370	355.6	>370	>370	353.0	>370	>370
Zn	1.8	54	71	51	38	71	98	100	105	45	35	68	91	155
Co	0.13	40.4	34.01	18.45	57.18	35.23	42.86	50.17	51.79	13.12	9.57	31.04	43.75	35.23
Sc	1.1	46.4	39.7	34.0	44.3	51.3	42.8	39.7	46.5	55.7	53.4	37.8	47.2	44.9
Ga	0.04	34.7	30.74	26.80	37.16	31.09	28.25	20.61	18.20	35.60	37.65	22.78	27.01	21.79
Zr	6	187	107	185	209	93	169	50	40	126	183	91	65	93
Sr	0.6	8.3	21.0	4.1	7.6	11.4	37.5	99.0	57.3	9.4	13.1	23.5	19.0	38.1
Y	0.05	4.87	13.42	1.70	3.53	6.23	16.54	20.17	20.69	5.12	7.57	14.84	10.26	18.11
Nb	0.03	12.0	5.68	8.10	11.34	8.87	7.9	3.64	3.62	10.14	9.08	5.62	4.54	6.75
Pb	0.18	39.8	27.3	18.0	24.1	17.3	110.7	2.2	2.4	19.3	17.9	10.1	16.4	11.4
Mo	0.08	1.53	0.84	1.06	1.34	0.46	0.95	0.25	0.32	13.37	1.49	0.94	0.80	0.37
Li	0.4	8.1	3.4	10.6	2.7	4.5	4.1	4.8	4.0	1.2	1.6	2.4	2.5	6.4
Rb	0.11	2.78	8.91	46.23	9.43	5.78	11.41	3.73	2.78	2.62	7.94	5.49	3.95	9.07
Ba	0.8	84.4	58.1	305.5	117.4	104.4	128.6	24.8	27.3	45.1	96.0	60.2	41.2	53.0
Hf	0.14	5.02	3.10	4.99	5.62	2.84	4.43	1.52	1.35	3.75	4.91	2.68	2.05	2.59
Th	0.02	3.68	1.44	1.70	6.71	1.82	1.83	0.57	0.45	1.67	1.58	2.35	1.40	2.82
U	0.01	1.24	0.67	1.01	1.59	0.90	0.78	0.16	0.14	0.73	0.86	0.71	0.52	0.86
Ta	0.01	0.77	0.39	0.42	0.80	0.69	0.51	0.24	0.25	0.63	0.56	0.39	0.31	0.45

d.l =detection limit

II.2.1.2. Correlations between SiO_2 and selected trace elements

The plots reveal negative correlations between s SiO_2 with Sc, Ga and Zr (Fig. 29 a, b and

c). SiO_2 however correlates positively with Zn (Fig. 29 d), but shows no correlations with Ni and Cu (Fig. 29 e and f).

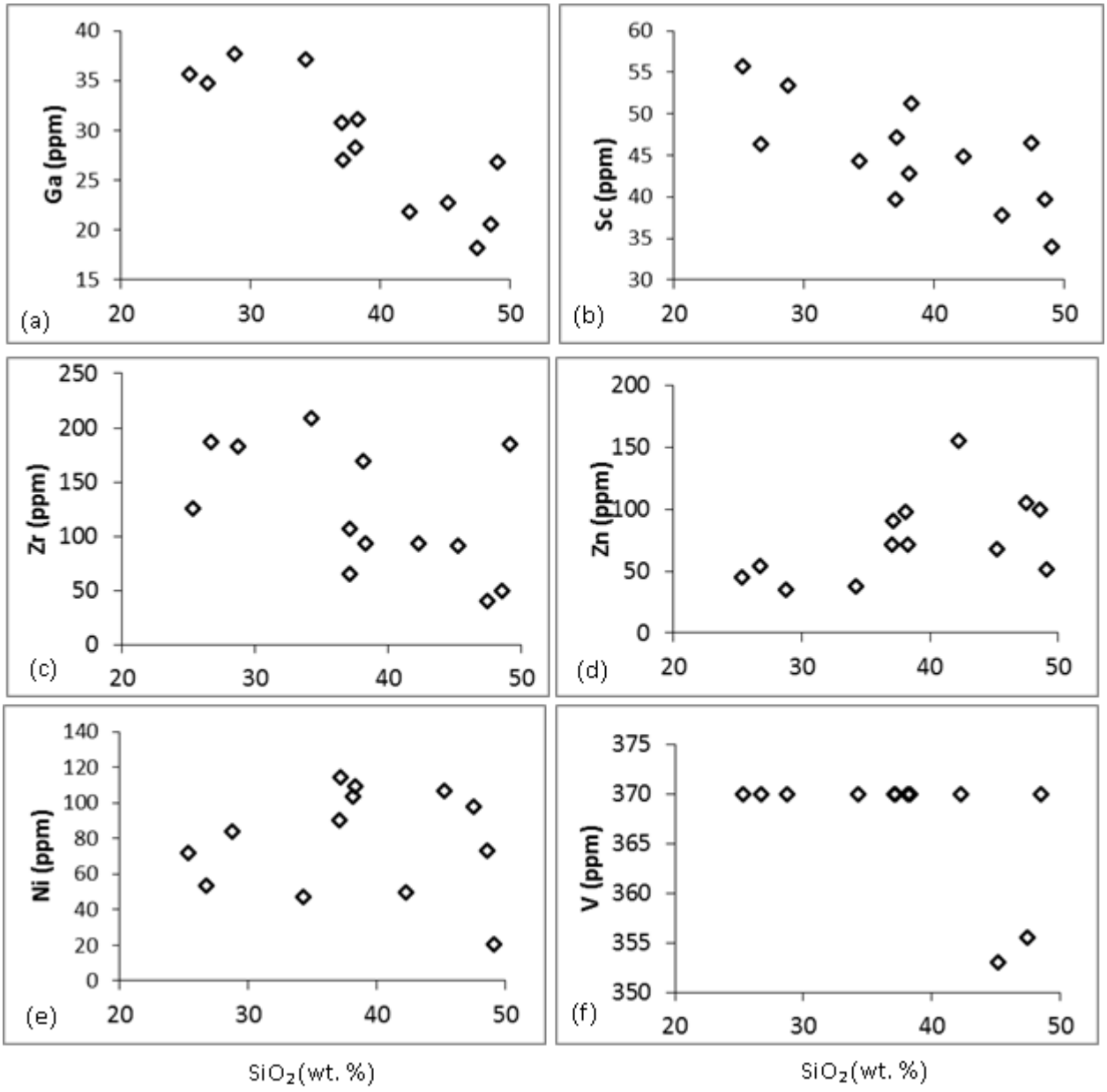

Figure 29 : Binary diagrams of silica and some trace elements (a) SiO2 vs Ga; (b) SiO2 vs Sc; (c) SiO2 vs Zr; (d) SiO2 vs Zn; (e) SiO2 vs Ni; (f) SiO2 vs V in weathered amphibolites

II.2.1.3. Correlations between Fe_2O_3 and selected trace elements

Ferrous oxides correlates positively with Ga, Zr and Cr (Fig. 30 a, b and c); correlates negatively with Co and Zn but is neutral with Cu (Fig. 30 c, d and e).

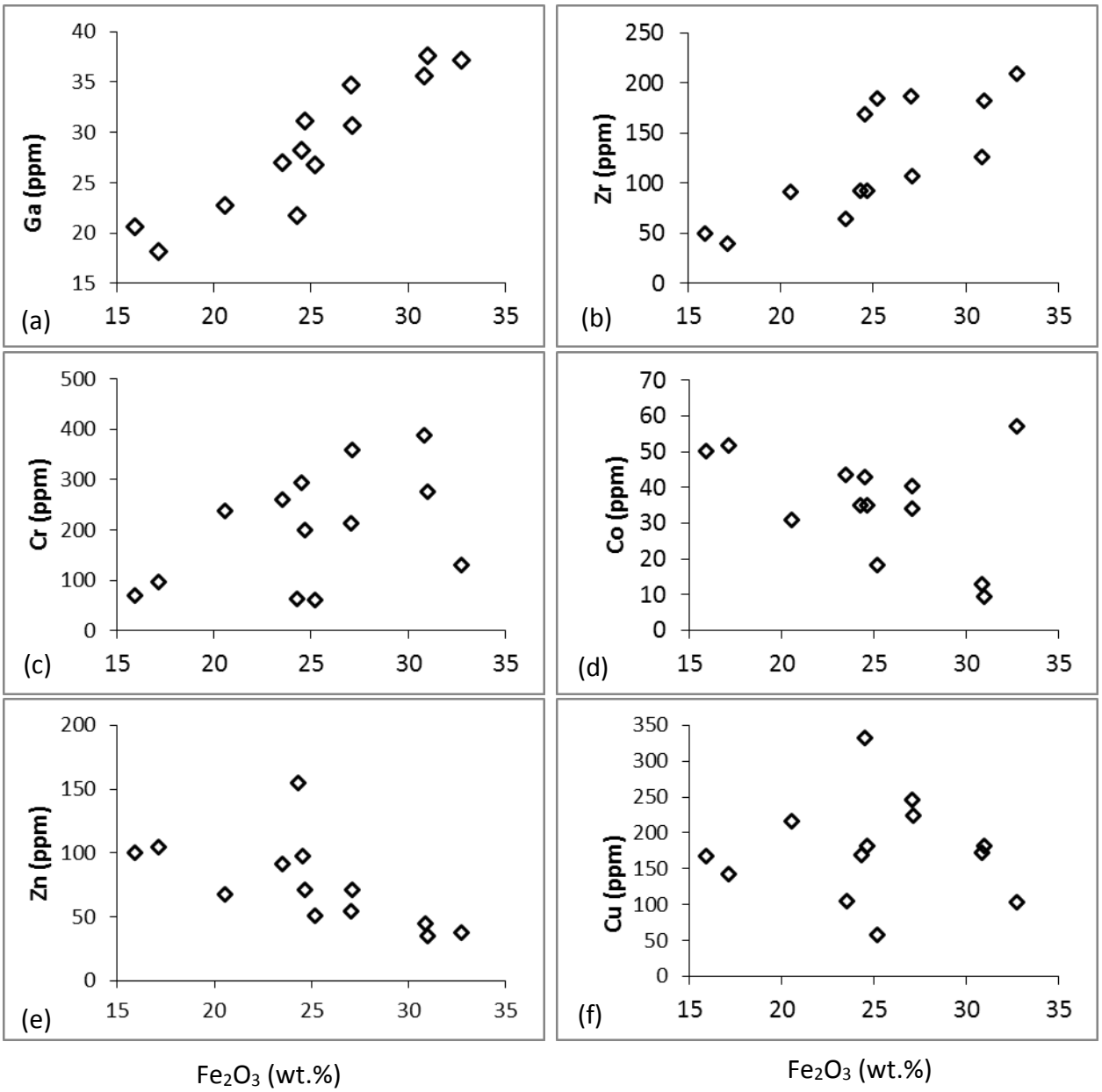

Figure 30 : Binary diagrams of Fe2O3 and selected trace elements in weathered amphibolites (a) Fe_2O_3 vs Ga; (b) Fe_2O_3 vs Zr; (c) Fe_2O_3 vs Cr; (d) Fe_2O_3 vs Co; (e) Fe_2O_3 vs Zn; (f) Fe_2O_3 vs Cu

II.2.1.4. Correlations between MgO and selected trace elements

The variations between MgO and trace elements are generally weak. Diagrams reveal weak positive correlations of MgO with Co, Zn and Ni, whereas it has weak negative correlations with Ga and Zr; it has no affinities with Cu (Fig. 31).

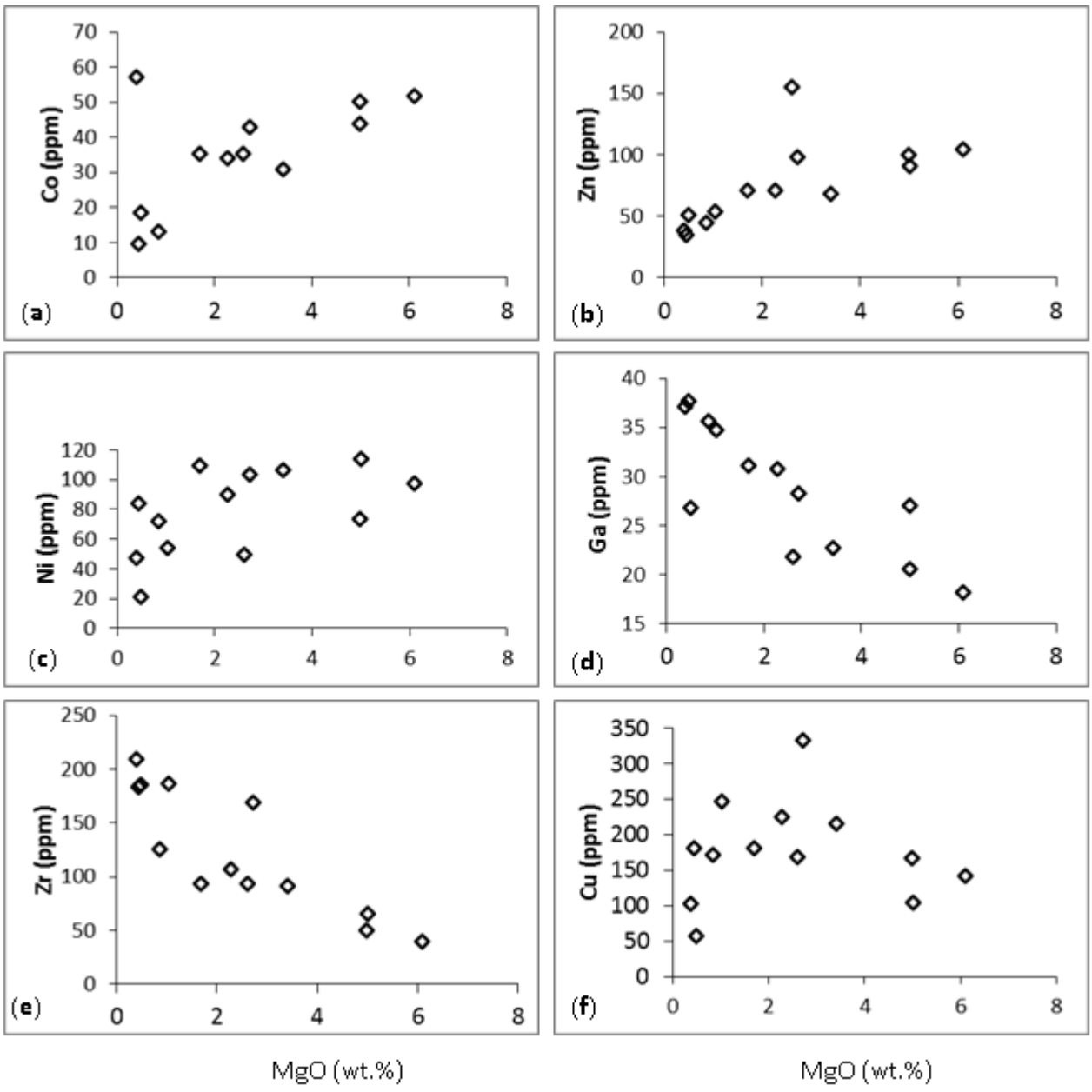

Figure 31 : Binary diagrams of MgO and selected trace elements in weathered amphibolites. (a) MgO vs Co; (b) MgO vs Zn; (c) MgO vs Ni; (d) MgO vs Ga; (e) MgO vs Zr; (f) MgO vs Cu.

II.2.2. Correlation between trace elements

Binary diagrams are established to highlight the degree of compatibility in trace elements and also their behavioural patterns in the course of weathering processes. Positive correlations therefore will signify that these elements are hosted by the same minerals or they are being weathered by the same processes.

Scatter plots show strong affinities as well as incompatibilities among of trace elements. Chromium correlates positively with Ga, Cu, and Sc, (Fig. 32 a, b, and c), it also has affinity for Ni and Pb. Chromium rather correlates negatively with Li (Fig. 32 d).

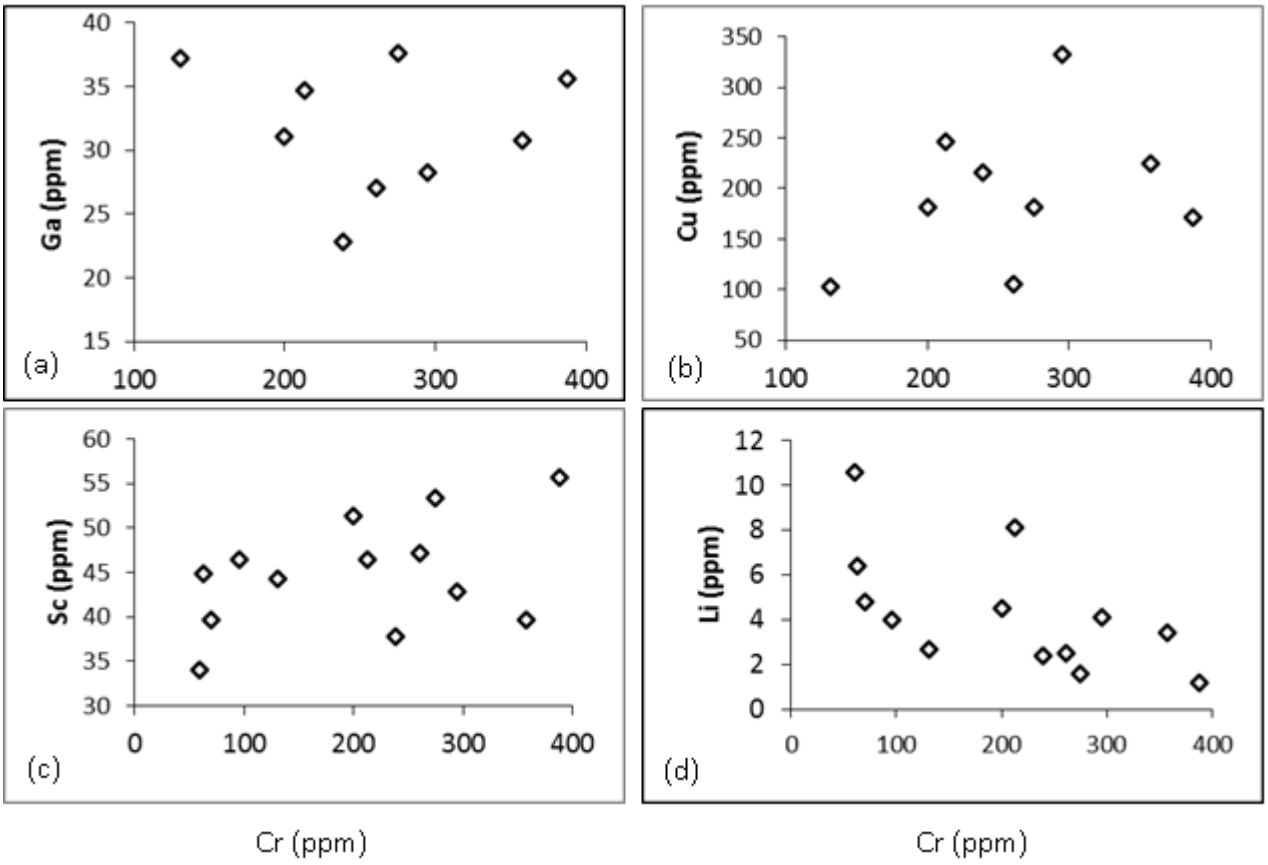

Figure 32 : Scattered plots of Chromium with selected trace elements in weathered amphibolites. (a) Cr vs Ga; (b) Cr vs Cu; (c) Cr vs Sc; (d) Cr vs Li.

Scatter plots of Zr and Cu with selected trace elements further proof strong positive correlations of Zr with Hf, and Nb (Fig. 33a and b); Cu with Ga, Pb and Ni (Fig. 33 e and f). On the other hand Zr correlates negatively with Y and Zn (Fig. 33 c and d).

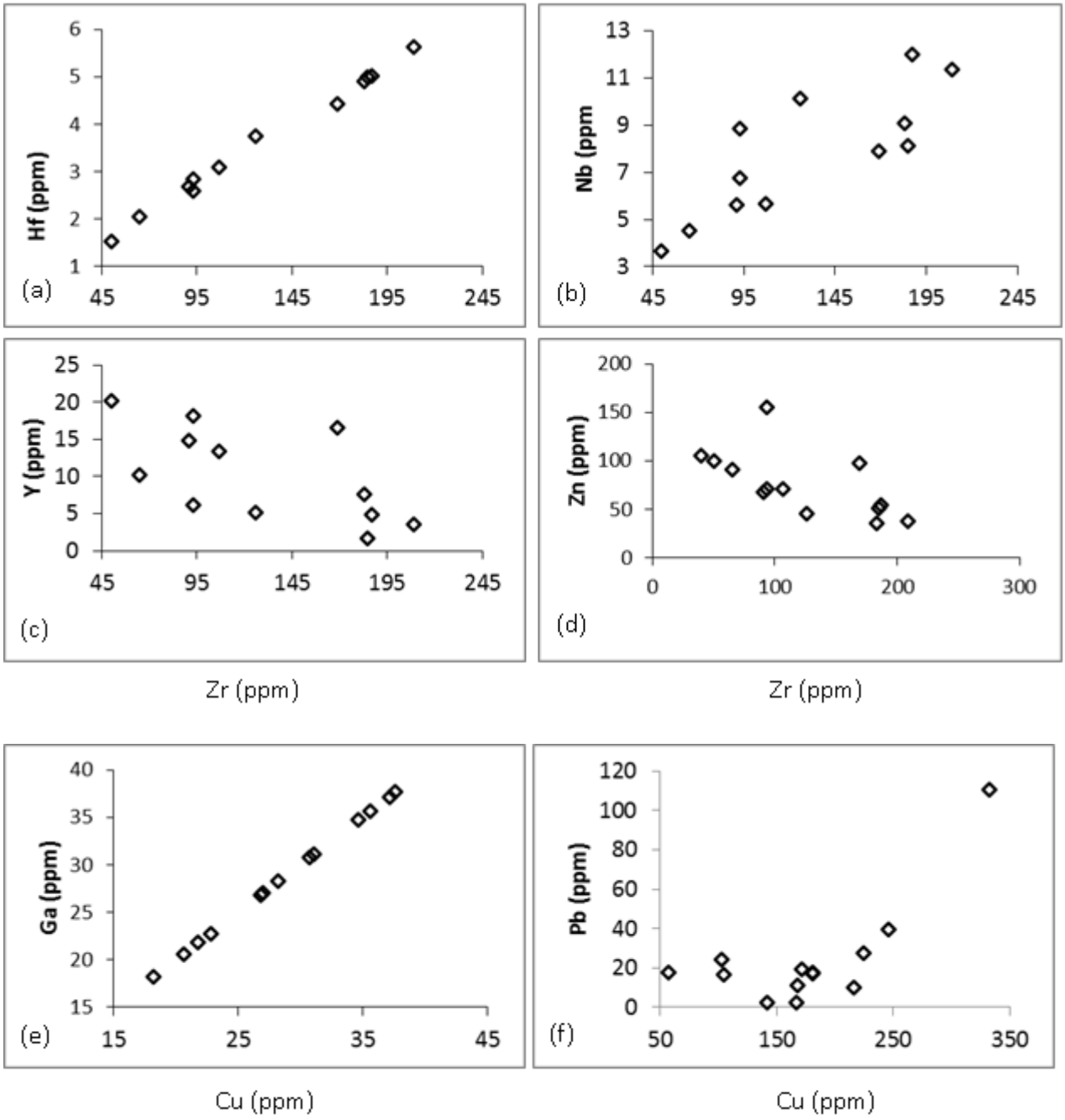

Figure 33 : Scattered plots of Zr and Cu with selected trace elements in weathered amphibolites. (a) Zr vs Hf; (b) Zr vs Nb; (c) Zr vs Y; (d) Zr vs Zn; (e) Cu vs Ga; (f) Cu vs Pb.

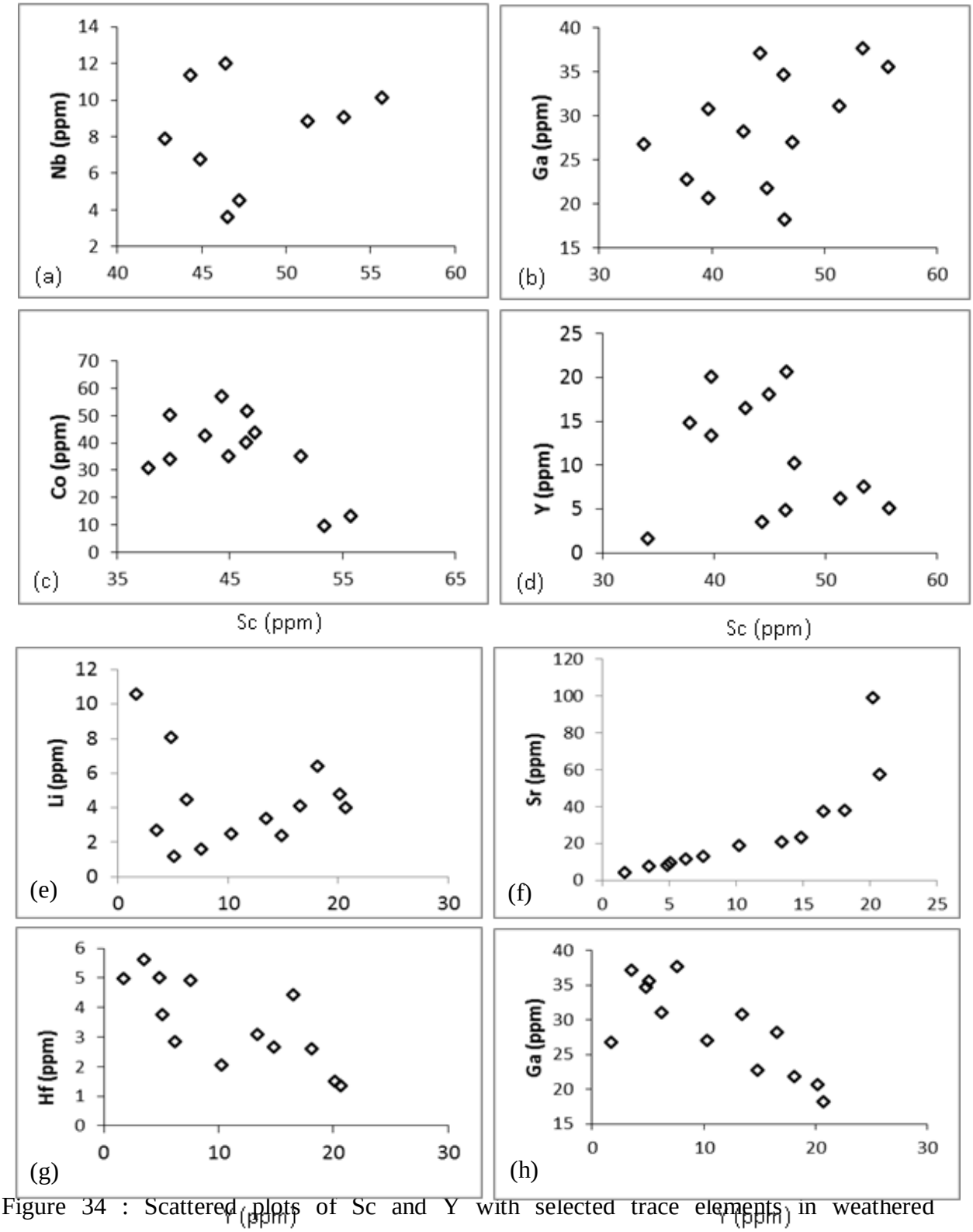

Figure 34 : Scattered plots of Sc and Y with selected trace elements in weathered amphibolites.(a) Sc vs Nb; (b) Sc vs Ga; (c) Sc vs Co; (d) Sc vs Y; (e) Y vs Li; (f) Y vs Sr; (g) Y vs Hf; (h) Y vs Ga.

In the scattered plots above (Fig. 34), scandium has positive correlations with Nb and Ga, but it rather has weak negative correlations with cobalt and yttrium (Fig. 34 a, b, c and d). Yttrium on the other hand has positive plots when correlated with Li and Sr and negative plots when associated with Hf and Ga (Fig. 34 e, f, g and h).

Zinc has positive plots with yttrium, strontium and negative correlations with Nb, and Hf (Fig. 35 a, b, c and d respectively).

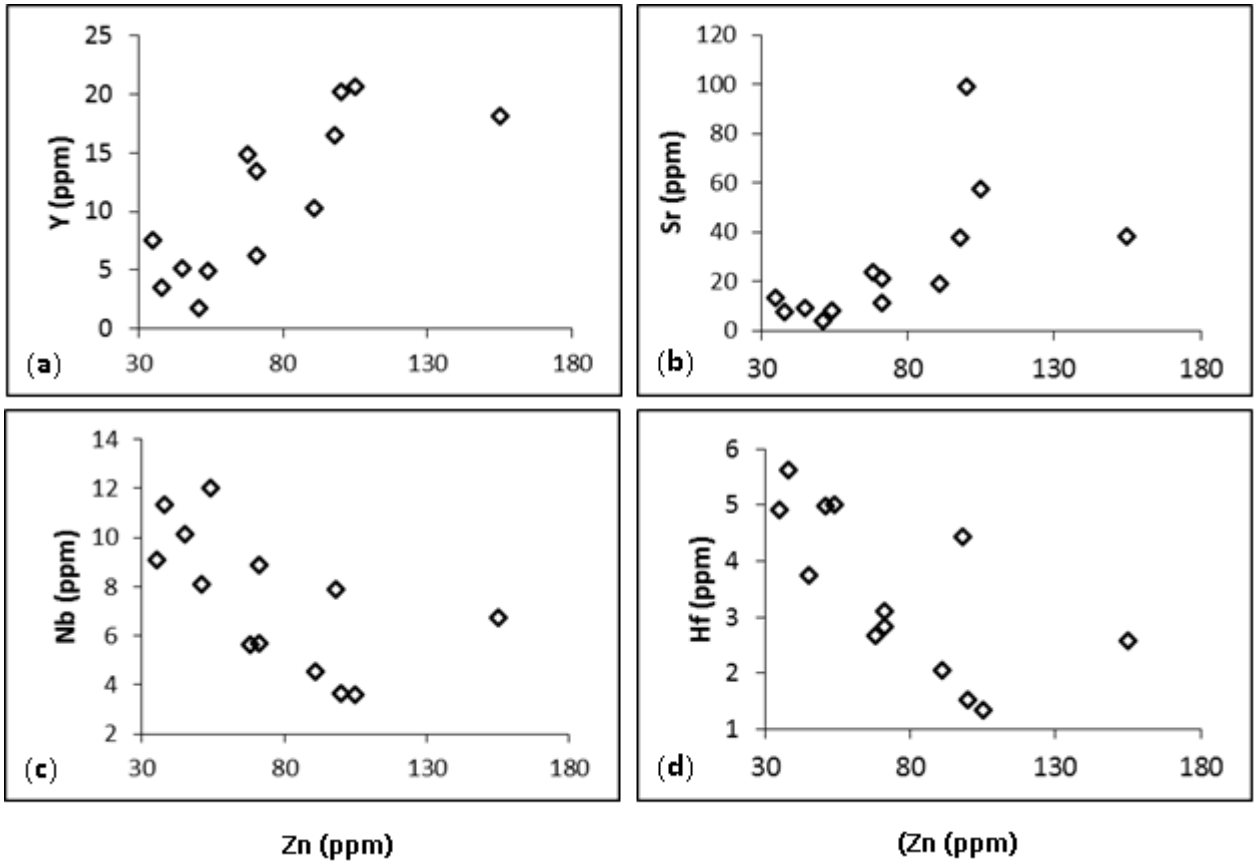

Figure 35 : Scattered plots of zinc with selected trace elements in weathered amphibolites. (a) Zn vs Y; (b) Zn vs Sr; (c) Zn vs Nb; (d) Zn vs Hf.

In general the positive correlations among groups of trace elements identified above may signify that (i) these groups of elements were laid down under the same physicochemical conditions; (ii) these trace elements may be hosted by the same secondary minerals (Sababa, 2015). Meanwhile those groups of elements with negative correlations proof that they are incompatible and consequently hosted by different mineral phases.

Trace elements were normalized with respect to primitive mantle values according to McDonough and Sun (1995). The normalized patterns were similar in form, but possessed

distinct positive anomalies in Pb and negative anomalies in Th compared to those of the chondrite normalized patterns (Fig. 36).

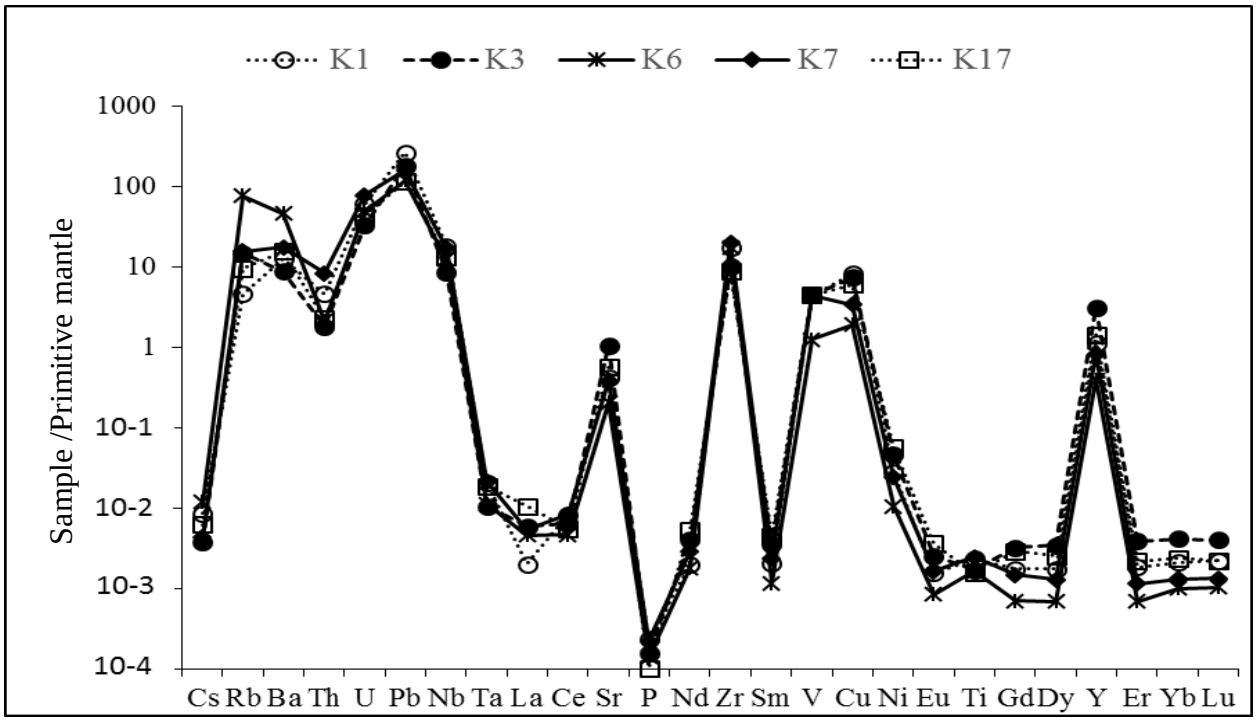

Figure 36 : Primitive mantle-normalized trace element patterns for weathered amphibolites.

II.3 Geochemistry of rare earth elements in weathered materials

The REE contents in weathered amphibolites have an overall low contents; these contents range from 16 to 32.86 ppm in the fine grained facies, 38 to 63 ppm for the medium grained facie and 22 to 70.5 ppm for the garnet facies. Average REE values attain 38 ppm (Table 6). The low contents of REE confirm the ultramafic nature (Perelomov et al., 2012). LREE are by far more abundant in the rocks than HREE. They consist of a maximum of 58 ppm, while the HREE consist of a maximum of 13 ppm, the LREE/HREE values are low, and they range between 1.87 and 7.61. The fractionation constant $(La/Yb)_n$ varies between 0.33 and 2.35 (Table 6).

II.3.1 Light rare earth elements (LREE)

The contents of LREE vary from 14 to 26 ppm in the fine grained rocks, from 25 to 51 ppm in the medium grained rocks and 18 to 58 ppm for coarse grained rocks. These contents generally oscillate between 14 and 58 ppm. Cerium contents are the greatest among

all rare earth elements. They have an increasing order of contents from fine to coarse grains and attain maximum contents of 26.48 ppm. The highest Ce contents are observed in the K2 sample which has undergone profound weathering, while the least contents are obtained in the K8W sample which is only slightly weathered (Table 6).

Contents of lanthanum are rather low and variable; they are about two to three times lower than those of Ce. Maximum La contents attain 15.58 ppm while those of praseodymium are lower, being 3.84 ppm as maximum. Here most samples have contents that are less than or equal to 1 ppm (Table 6). Neodymium behaves in a similar manner like La with only slightly higher values in some samples, its contents 2.26 ppm to 15.61 ppm (Table 6).

Samarium and europium show very low concentrations, maximum Sm contents (3.67 ppm) are observed in K16 sample while minimum contents (0.47 ppm) are obtained in K6 sample. The contents of europium are the lowest of all LREE. The contents are all less than 1 ppm with exception of two samples (Table 6).

II.3.2. Heavy rare earth elements (HREE)

This group of elements generally shows low concentrations in weathered amphibolites; all of which are less than 4 ppm.

Dysprosium is the HREE with the highest contents; its contents range from 0.4 to 3 ppm contents of gadolinium (0.38 and 3.63 ppm) have similar variations to those of Dy, Dy and Gd have the highest values among all the HREE. Erbium and ytterbium have similar behaviours, their concentration attain a maximum of 2 ppm, terbium, holmium, thulium and lutetium contain similar but very low contents that are all less than 1 ppm. These elements are the least represented of all HREE, their contents are also close to the detection limits (Table 6).

II.3.3. Normalization of REE

The rare earth elements were normalized following their concentrations in the weathered amphibolites in relation to the concentrations of the same element in fresh rock. The K4 sample was the fresh rock considered. The normalization of fresh and weathered amphibolites is acquired through the following formula:

$$\mathbf{R_1 = X_{WA} / X_{FR}}$$

Where $\mathbf{X_{WA}}$ = concentration of element in weathered amphibolites, and $\mathbf{X_{FR}}$ = concentration of element in the fresh rock. The results of these calculations are presented in the form of spectra. The normalized patterns were assembled according to the grain sizes of weathered amphibolites

II.3.3.1. Fine grained weathered amphibolites

The fresh rock normalized patterns for fine grained weathered amphibolites reveal positive cerium anomalies in all the samples except in one, and a slight negative Ce anomaly. The patterns also reveal a slight negative Eu anomaly; a depletion in REE with respect to the fresh rock and flattened curves from Gd to Lu (Fig. 37).

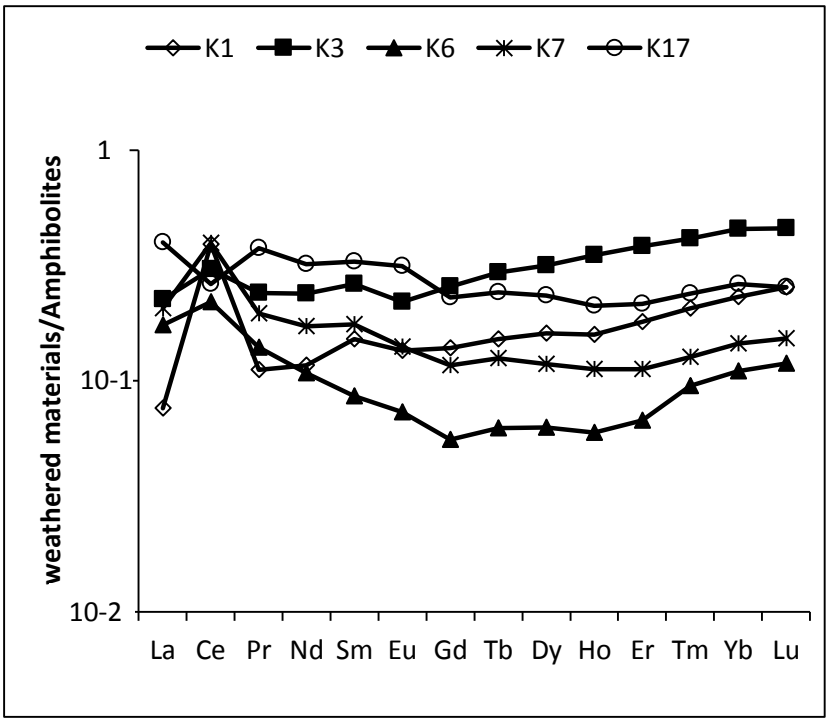

Figure 37 : REE patterns for fine grained weathered amphibolites normalized with fresh amphibolite

II.3.3.2. Medium grained weathered amphibolites

The fresh rock normalized patterns for medium grained weathered amphibolites reveal a positive Ce anomaly and a slight negative Eu anomaly for the same sample. Also, there is fractionation of LREE with respect to HREE, with a slight positive Eu anomaly. There is also parallelism and general platitude of HREE curves (Fig.38).

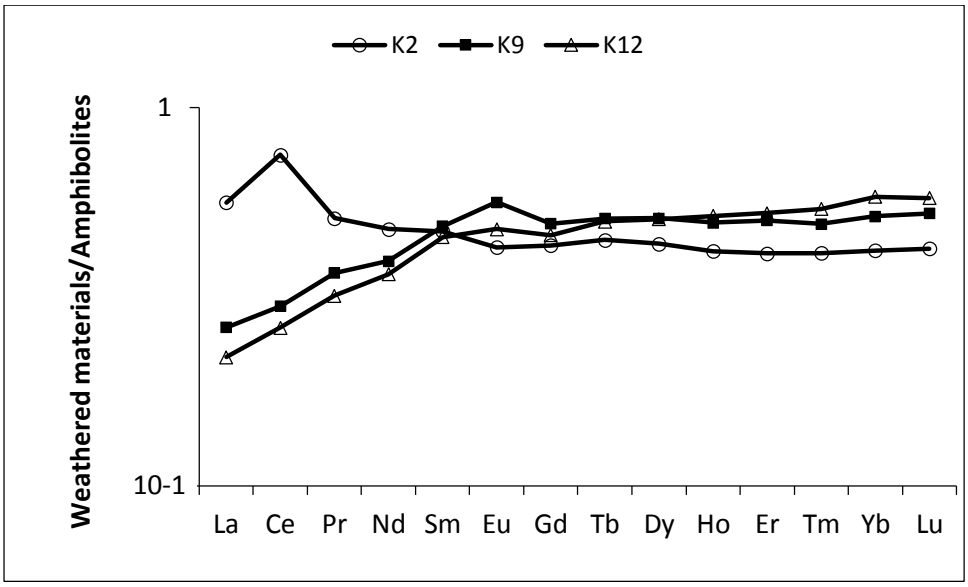

Figure 38 : REE patterns for medium grained weathered amphibolites normalized with fresh rock

II.3.3.3. Coarse grained weathered amphibolites

The normalized patterns here are heterogenous and are characterized by:

(i) Postive Ce anomalies in some samples, and negative Ce anomalies in others;

(ii) Slight positive Eu anomalies in some sample and fractionation of LREE with respect to the HREE in some samples;

(iii) An enrichment of LREE with regard to the HREE, and general platitude of HREE curves is also distinguished (Fig. 39).

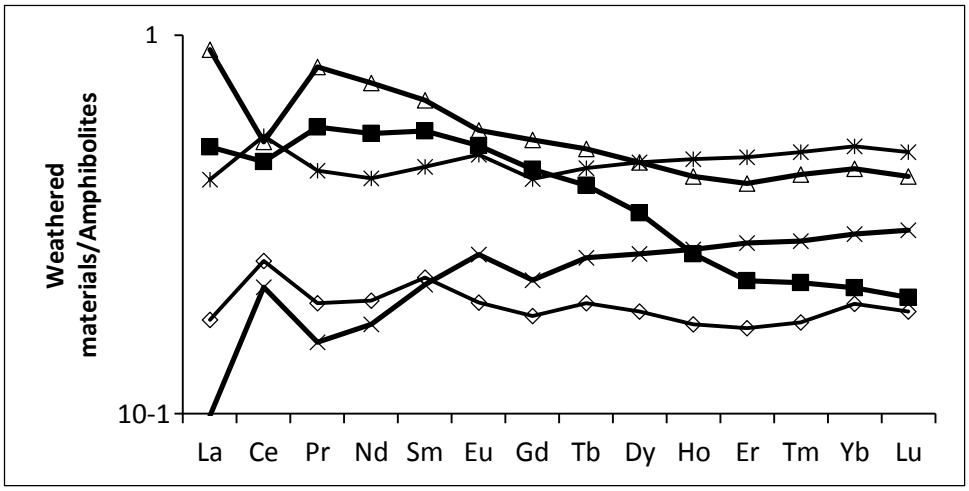

Figure 39 : REE patterns for coarse grained weathered amphibolites normalized with fresh amphibolites.

II.3.4. Fractionation of rare earth elements (REE)

The fractionation indice $(La/Yb)_N$ is often used to check the rate of fractionation of REE. The indice also aid in understanding the behaviour of REE. The values of $(La/Yb)_N$ are low and variable, they range from 0.33 to 1.58 for the fine grained weathered materials; 0.38 to 1.34 for the medium grained ones and 0.33 to 2.35 in the coarse grained weathered materials (Table 6). The values of fractionation index are in conformity with the nature or weathered amphibolites (Perelomov *et al*., 2012).

II.3.5. Correlation between rare earth elements

Correlation of these elements will give an understanding whether these elements moved together or differently. Positive plots of REE suggest a common origin for the samples (Bellot *et al*., 2010).

II.3.5.1. Correlations between major elements and rare earth elements

Contents of major (SiO_2, Al_2O_3, Fe_2O_3, MgO and CaO) and REE were compared to check whether these elements had the same source. The results are indicated in figures 40 to 44.

Al_2O_3 has no correlations for Ce (Fig. 40a). It has weak negative correlations with Gd, Eu, and the total REE contents. It rather shows negative plots with LREE than with the HREE (Fig. 40b, c, d, f and e).

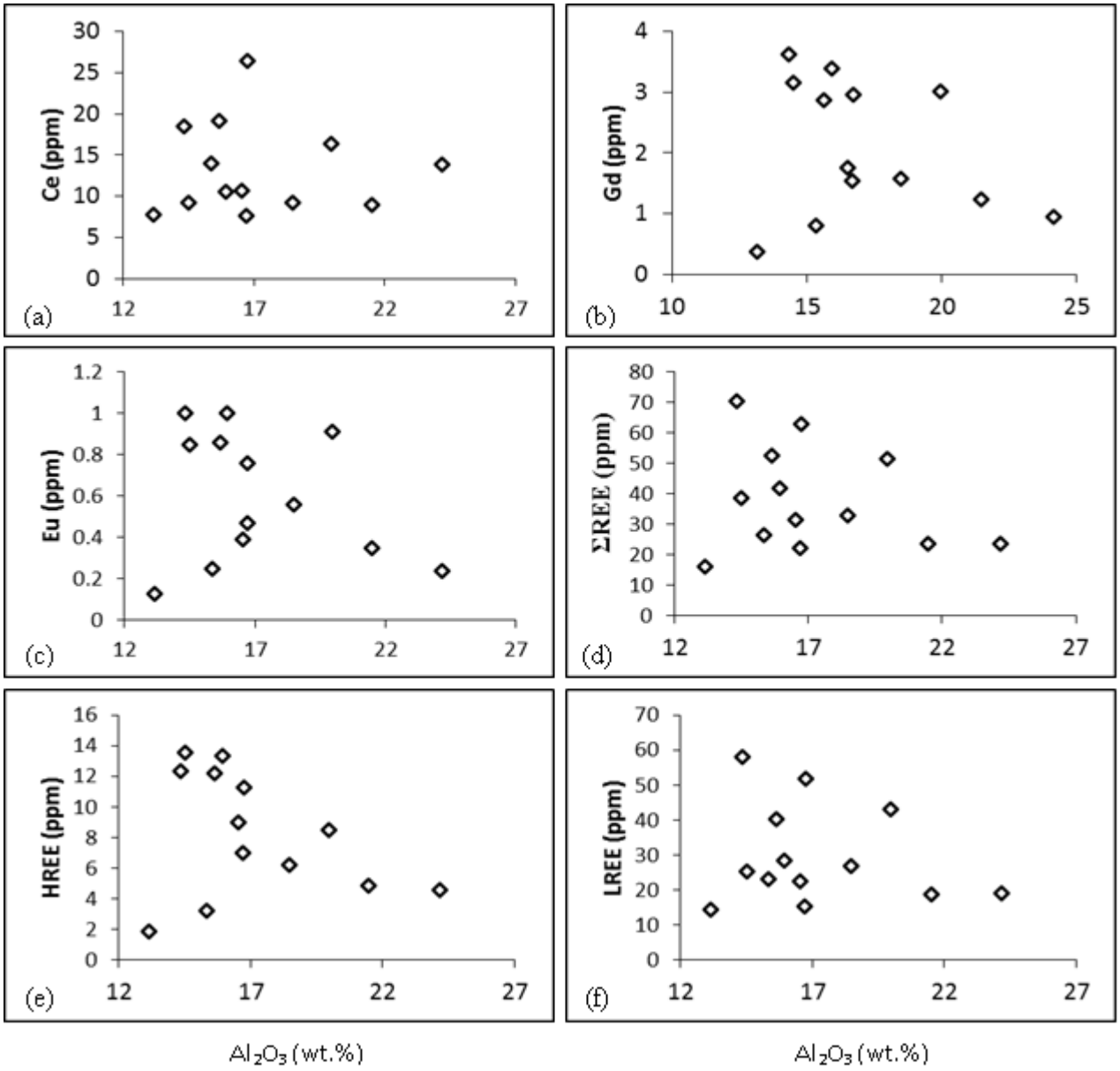

Figure 40 : Variation plots of Al2O3 with REE in weathered amphibolites (a) Al2O3 vs Ce; (b) Al2O3 vs Gd; (c) Al2O3 vs Eu; (d) Al2O3 vs ∑REE; (e) Al2O3 vs HREE; (f) Al2O3 vs LREE

.

Table 6 : Rare earth Element contents (in ppm) in weathered amphibolites

d.l. : detection limits

		Fine grained					Medium grained			Coarse grained				
REE	d.l	K1	K3	K6	K7	K17	K2	K9	K12	K14	K15	K16	K8W	K18
La	01	1.29	3.83	2.96	3.51	6.78	9.53	4.46	3.72	3.01	8.61	15.58	1.68	7.06
Ce	0.12	13.81	10.73	7.76	13.95	9.26	26.48	10.55	9.25	8.94	16.40	18.44	7.64	19.14
Pr	0.01	0.52	1.12	0.65	0.91	1.75	2.37	1.70	1.48	0.91	2.66	3.84	0.72	2.04
Nd	0.06	2.44	4.98	2.26	3.60	6.68	9.98	8.21	7.58	4.16	11.49	15.61	3.60	8.76
Sm	0.23	0.83	1.43	0.47	0.96	1.79	2.57	2.65	2.48	1.25	3.05	3.67	1.20	2.45
Eu	0.01	0.24	0.39	0.13	0.25	0.56	0.76	1.00	0.85	0.35	0.91	1.00	0.47	0.86
Gd	0.01	0.95	1.75	0.38	0.80	1.57	2.96	3.38	3.15	1.24	3.02	3.63	1.55	2.86
Tb	0.01	0.17	0.33	0.07	0.14	0.27	0.50	0.57	0.56	0.22	0.45	0.56	0.29	0.50
Dy	0.01	1.18	2.32	0.46	0.87	1.72	3.20	3.74	3.72	1.37	2.49	3.39	1.94	3.39
Ho	0.01	0.24	0.53	0.09	0.17	0.32	0.63	0.75	0.78	0.26	0.40	0.64	0.41	0.71
Er	0.01	0.80	1.70	0.30	0.50	0.96	1.83	2.24	2.34	0.75	1.00	1.81	1.26	2.12
Tm	0.002	0.13	0.26	0.06	0.08	0.15	0.26	0.31	0.34	0.11	0.14	0.27	0.18	0.31
Yb	0.01	0.92	1.82	0.44	0.58	1.05	1.67	2.06	2.32	0.78	0.86	1.77	1.19	2.03
Lu	0.002	0.15	0.27	0.07	0.09	0.15	0.25	0.31	0.34	0.11	0.12	0.25	0.18	0.29
REE	-	23.67	31.46	16.1	26.41	32.86	62.99	41.93	38.57	23.46	51.6	70.46	22.31	52.52
LREE	-	19.13	22.48	14.23	23.18	26.82	51.69	28.57	25.36	18.62	43.12	58.14	15.31	40.31
HREE	-	4.54	8.98	1.87	3.23	6.19	11.3	13.36	13.55	4.84	8.48	12.32	7	12.21
LREE/HRE	-	4.21	2.50	7.61	7.18	4.33	4.57	2.14	1.87	3.85	5.08	4.72	2.19	3.30
Ce/Ce^*	-	4.24	1.30	1.41	1.96	0.68	1.40	0.96	0.99	1.36	0.86	0.60	1.75	1.27
Eu/Eu^*	-	0.93	0.85	1.06	0.98	1.15	0.95	1.15	1.04	0.97	1.03	0.94	1.18	1.12
(La/Yb)n	-	0.33	0.49	1.58	1.42	1.52	1.34	0.51	0.38	0.91	2.35	2.07	0.33	0.82

$(La/Yb)_N = (La_{rock} / La_{chondrite}) / (Yb_{rock}/Yb_{chondrite.}$

$Ce/Ce^* = (Ce_{rock}/ Ce_{chondrite}) / (La_{rock}/ La_{chondrite})^{½} (Pr_{rock}/ Pr_{chondrite})^{½}$.

$Eu/Eu^* = (Eu_{rock}/ Eu_{chondrite}) / (Sm_{rock}/ Sm_{chondrite})^{½} (Gd_{rock}/Gd_{chondrite})^{½}$.

II.3.5.1.1. Correlations between Silica and Rare Earth Elements

Silica like alumina has no affinity for cerium (Fig. 41 a). It rather has strong correlations with Eu and Dy (Fig. 41b and c). Silica has very slight positive correlations with LREE and with the sum of REE as a whole (Fig. 41c and e), suggesting the high mobility of LREE during weathering. Whereas it has strong positive correlation with the HREE (Fig. 41f). This confirms the slight depletion of silica in the weathered amphibolites.

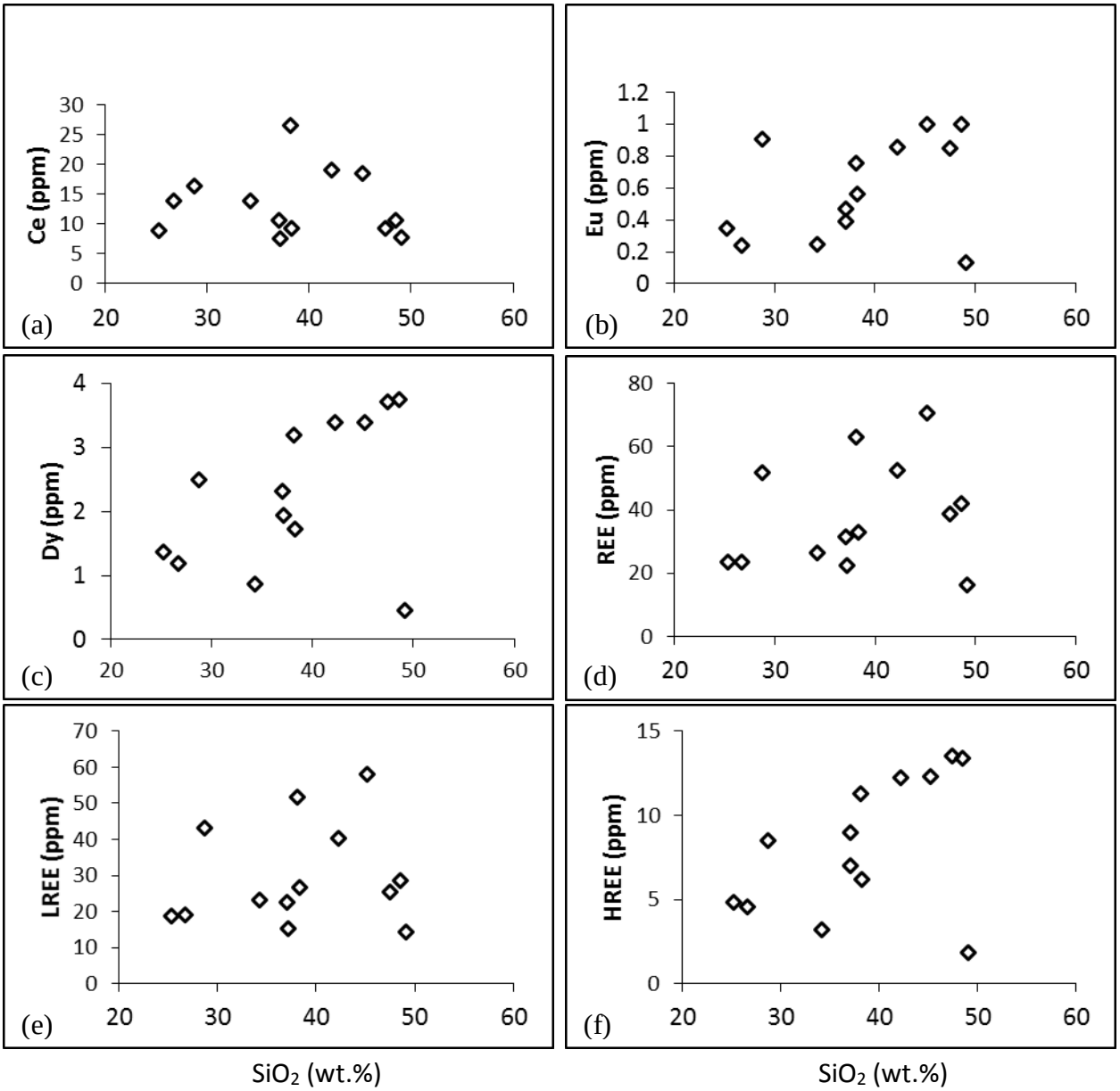

Figure 41 : Binary diagrams of silica with REE in weathered amphibolites. (a) SiO2 vs Ce; (b) SiO2 vs Eu; (c) SiO2 vs Dy; (d) SiO2 vs REE; (e) SiO2 vs LREE; (f) SiO2 vs HREE

II.3.5.1.2. Correlation between ferrous oxide and rare earth elements

Ferous oxide like silica has no correlation with Nd (Fig. 42 b). It correlates negatively with Gd and Eu (Fig. 42 a and c). Ferous oxide does not have correlations with the LREE, but rather portrays negative correlations the HREE (Fig. 42e and f). The total REE contents do not also correlate with Fe_2O_3 since the LREE form the dominant fraction (Fig. 42d).

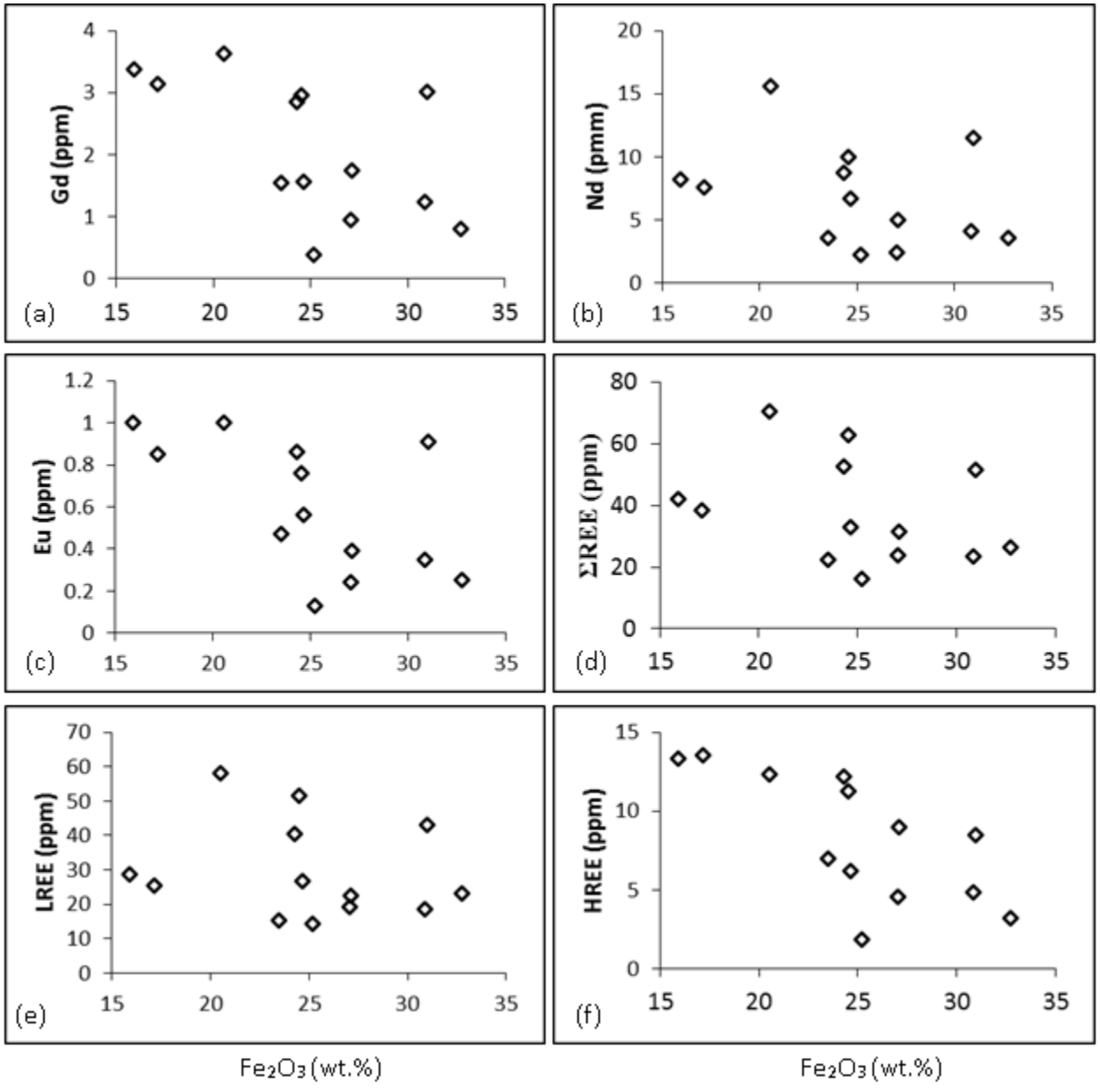

Figure 42 : Binary diagrams of ferrous oxide with REE in weathered amphibolites. (a) Fe2O3 vs Gd; (b) Fe2O3 vs Nb; (c) Fe2O3 vs Eu; (d) Fe2O3 vs REE; (e) Fe2O3 vs LREE; (f) Fe2O3 vs HREE.

II.3.5.1.3. Correlations between MgO and rare earth elements

MgO behaves differently from all other major elements when associated with REE. Its variation diagrams reveal positive correlations with individual and collective LREE and HREE. The only exception is that the positive correlations are stonger for HREE than for LREE (Fig. 43). The sum of REE is also positively correlated with MgO.

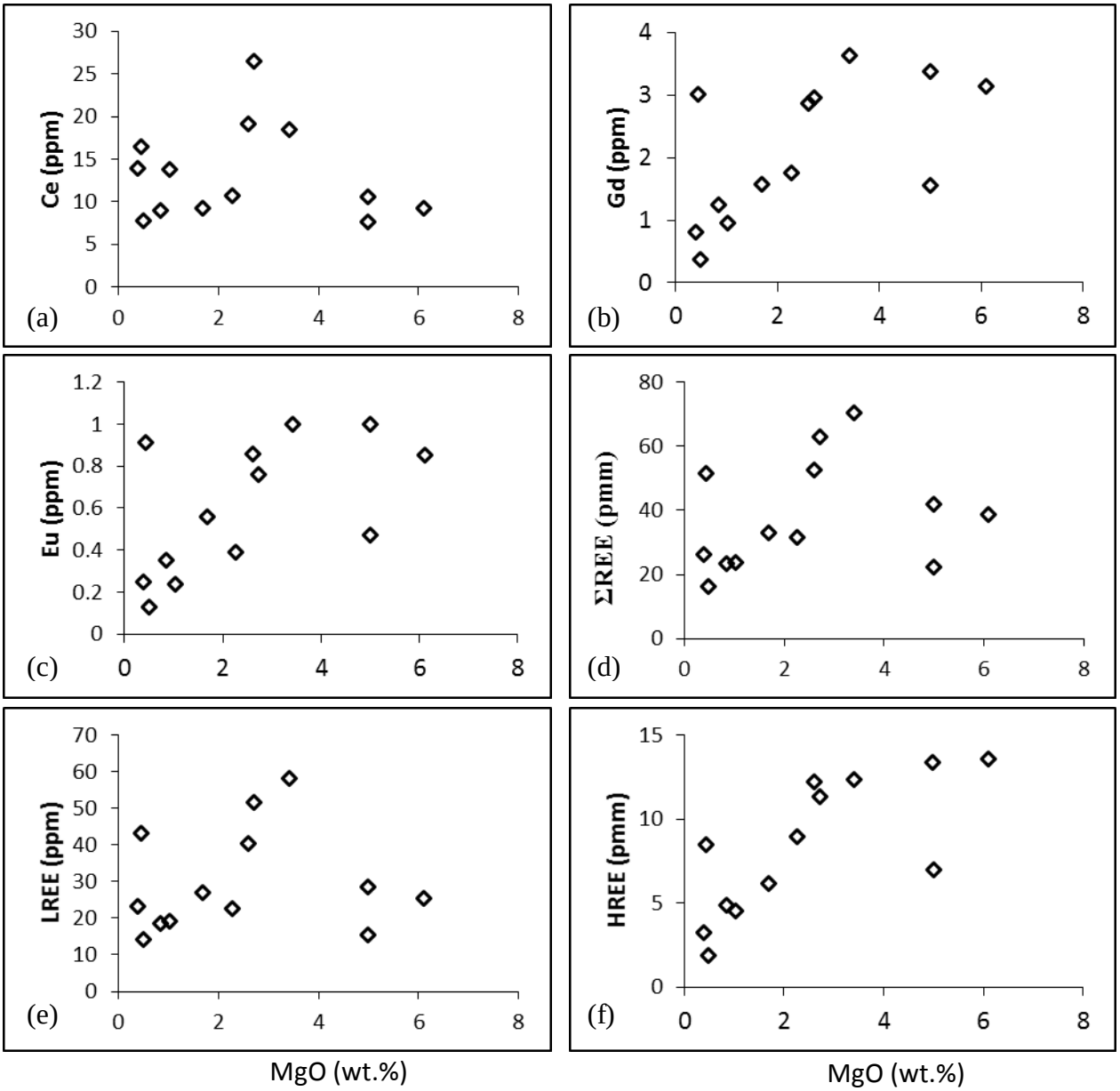

Figure 43 : Binary diagrams of MgO with REE in weathered amphibolites. (a) MgO vs Ce; (b) MgO vs Gd; (c) MgO vs Eu; (d) MgO vs REE; (e) MgO vs LREE; (f) MgO vs HREE.

3.5.1.4 Correlations between CaO and rare earth elements

CaO behaves in the same way as MgO in weathered amphibolites. It correlates positively with REE (Fig. 44a, b and c). Binary diagrams have positive correlations if CaO with the total of REE, (Fig. 44d, e and f). Also, like MgO, the correlation of CaO is stronger with HREE than with LREE.

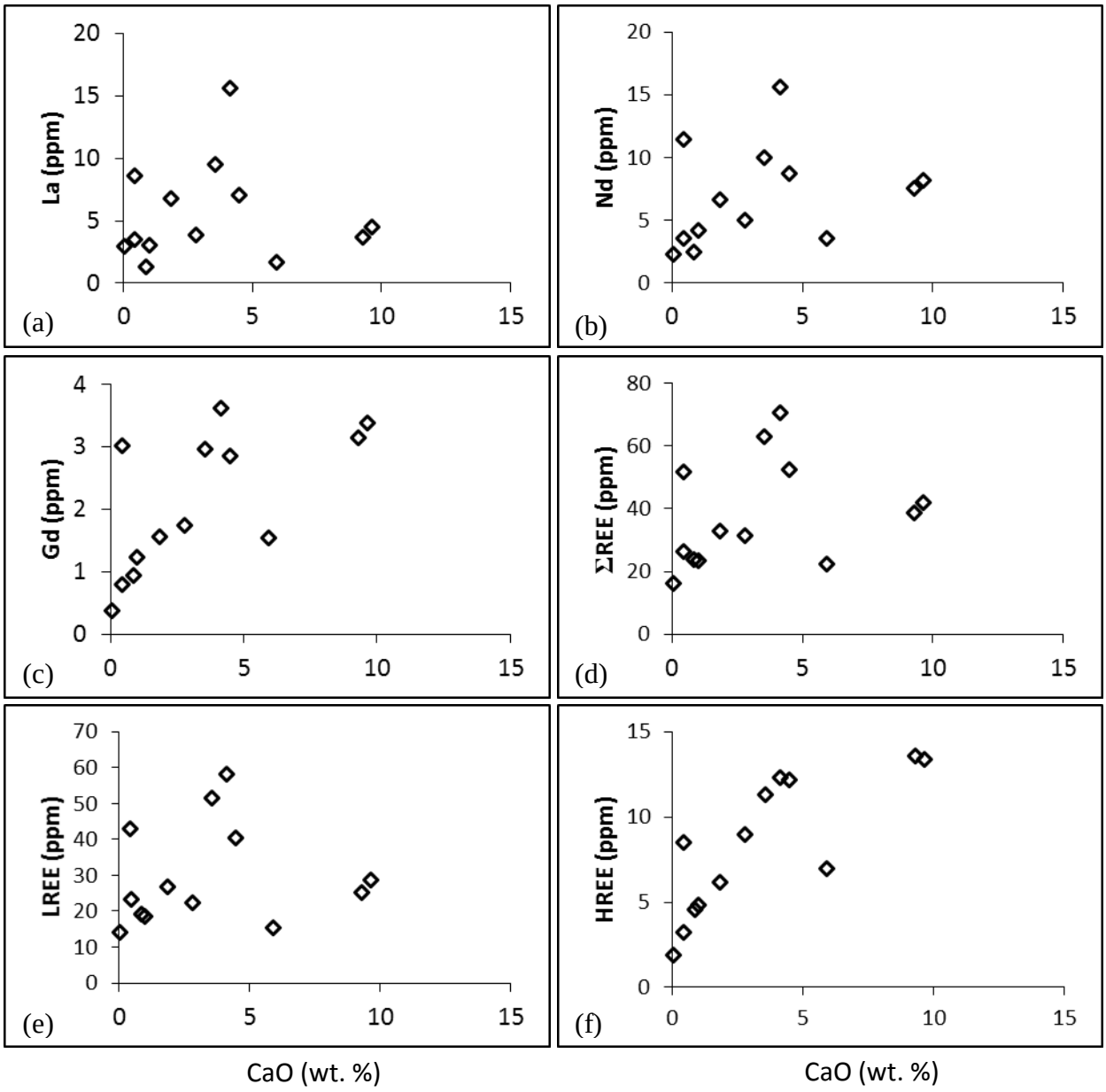

Figure 44 : Variation plots of CaO with REE in weathered amphibolites.

III. Mass-balance assessment

III.1. Method

Mass-balance assessment is an approach that helps to better understand the mobility of elements in weathering processes. This is expressed in the form of losses or gains. Two methods have been developed to estimate mass changes. (i) the first method is more frequently used and is expressed in kg/m^3. It requires bulk density, porosity and thicknesses of the materials. This method leads to the determination of the mass transported or deposited for each element (e.g., Kamgang Kabeyene Beyala et al., 2009; Ndjigui and Bilong, 2010). This method is not suitable for this study; (ii) the second method, expressed in percentage (%), takes into consideration only the element contents in samples (e.g., Wimpenny et al., 2007; Ndjigui et al., 2008).

Several elements are regularly used as immobile elements to quantify gains and losses within weathered materials these include: titanium (Beauvais, 2009; Kamgang Kabeyene Beyala et *al.,* 2009); thorium (Moroni et *al.,* 2001; Ndjigui et *al.,* 2008); zirconium (Wimpenny et *al.,* 2007; Beauvais, 2009) and cobalt (Sababa, 2015). The choice of an inert element (immobile element) is often dependent on the method selected for the mass-balance assessment (Ndjigui and Bilong, 2010).

Several methods have been suggested to do mass balance assessments. In this study, the method of Nesbitt and Wilson (1992), and amended by Moroni et al. (2001), is adopted:

$$\% \text{ change} = \{(X_{WS}/ Th_{WS}) / (X_{OS}/Th_{OS}) -1\}*100 \quad (1)$$

X_{WS} and X_{OS} are the element concentrations in the weathered sample and in the original sample (parent rock), respectively. Th_{WS} and Th_{OS} are the concentrations of thorium in the weathered sample and the original sample, respectively.

III.2. Choice of an invariant element

Here, the Gresen's equation which is based on isocons is applied to identify the immobile element or the most stable element during weathering (Chu et al., 2015; Grant, 2005): $C_{wi}=M_O/M_W (C_{Oi}+\Delta C_i)$. Where C_i is the concentration of species "i", "O"refers to the original rock and "W" to the weathered rock, M_O and M_W are equivalent masses before and after weathering. ΔC_i is the change in concentration of species "i". This may be done graphically by plotting the analytical data C_{Wi} against C_{Oi}, in which case the immobile

species define a straight line through the origin. This is the isocon, whose equation is $C_W = (M_O/M_W)\ C_O$. The slope of the isocon yields the overall change in mass relative to M_O. The slope may be determined from the clustering of C_{Wi}/C_{Oi} data (Table 1, Appendix). In Fig. 45, Th, Fe_2O_3, and Zr could reasonably be chosen as isocon. Thorium is the most suitable invariant element for amphibolites due to its low solubility under low temperature conditions. Also, its contents do not vary much between different rocks (Braun and Pagel, 1990).

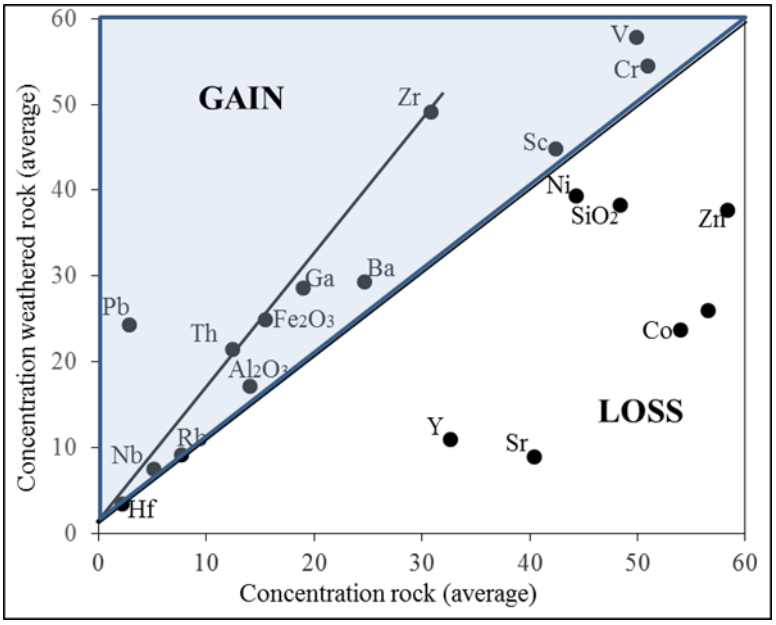

Figure 45 : Diagram showing the mobility of elements during weathering of amphibolites

III. 3. Mass balance assessment of major elements

In the fine grained weathered amphibolites, the application of Eq. (1) shows that Si, Al, Ca, Mg, Na, Ti and Mn are strongly leached. Fe and P are slightly accumulated, whereas K is strongly accumulated (Fig. 46a). In the medium grained weathered rocks most major elements remained more or less stable. Magnesium and potassium are strongly enriched; Fe and Mn are slightly enriched in some samples. Most major elements in the K12 sample have been leached out in varying degrees (Fig 46b). All the major elements were leached in the coarse grained weathered amphibolites. Nevertheless, Fe, Mg, K and P were only slightly leached (Fig. 46c).

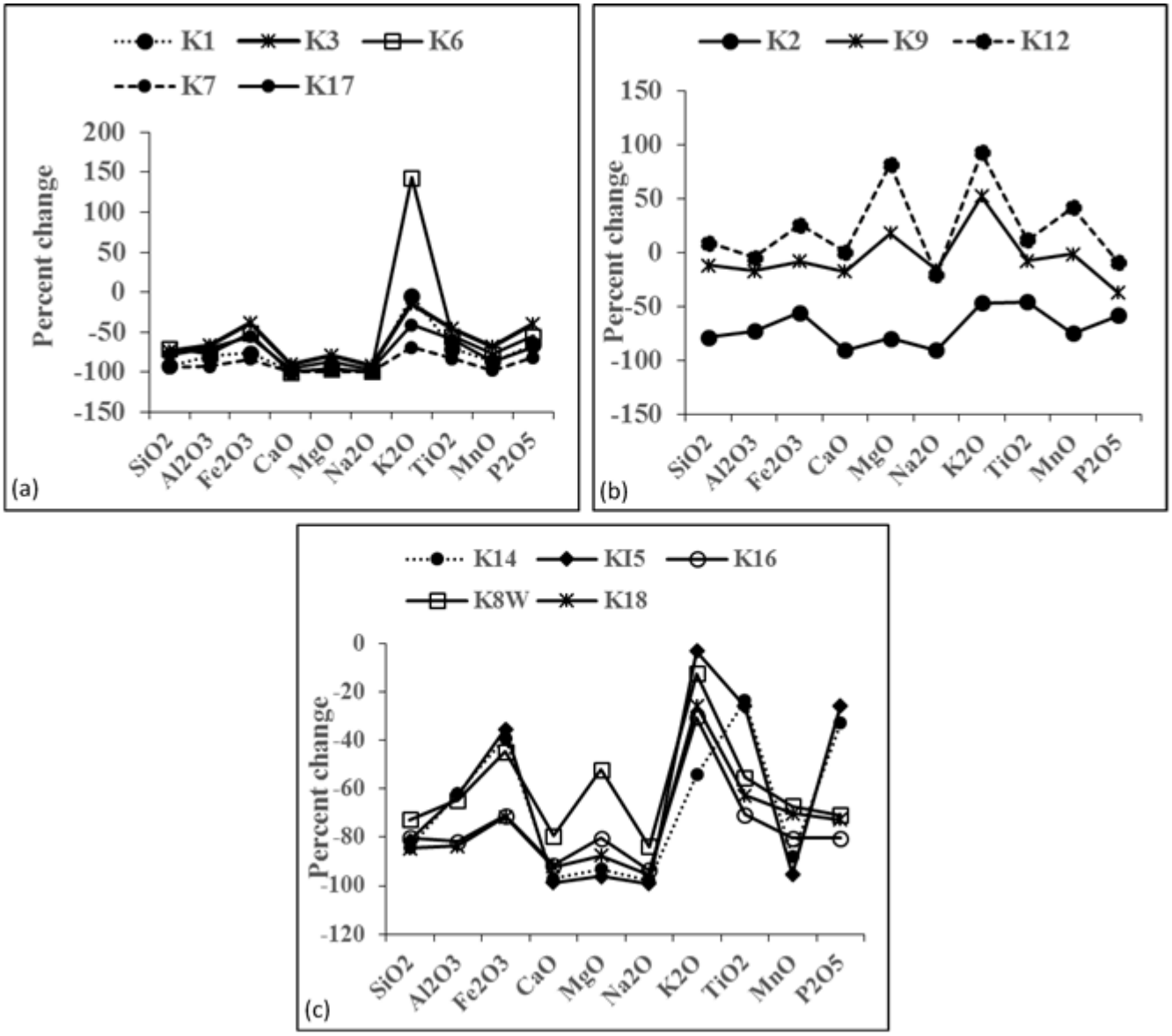

Figure 46 : Spectra showing relative chemical gains and losses of major elements (a) fine grained materials; (b) medium grained materials; (c) coarse grained materials, in the weathered samples.

III.4. Mass balance assessment of trace elements

Within fine grained weathered materials, the elements of the first and second groups of transition (V, Zn, Co, Sc, Ga, Y, and Nb) are leached. However, there exist some slight remobilization in Cr and Zr. Pb is abundant among the trace elements. With regards to the alkalis, Rb and Ba are strongly accumulated in some samples and leached in others. Uranium is slightly remobilized in all the samples (Fig. 47a). The patterns for the medium grained weathered materials reveal a strong accumulation in Pb in the K2 sample, meanwhile all the

other trace elements are slightly leached (Fig. 47b). Similarly, in the coarse grained weathered materials there is strong enrichment in Pb and Mo. Cr, Ba and U are only slightly remobilized (Fig. 47c).

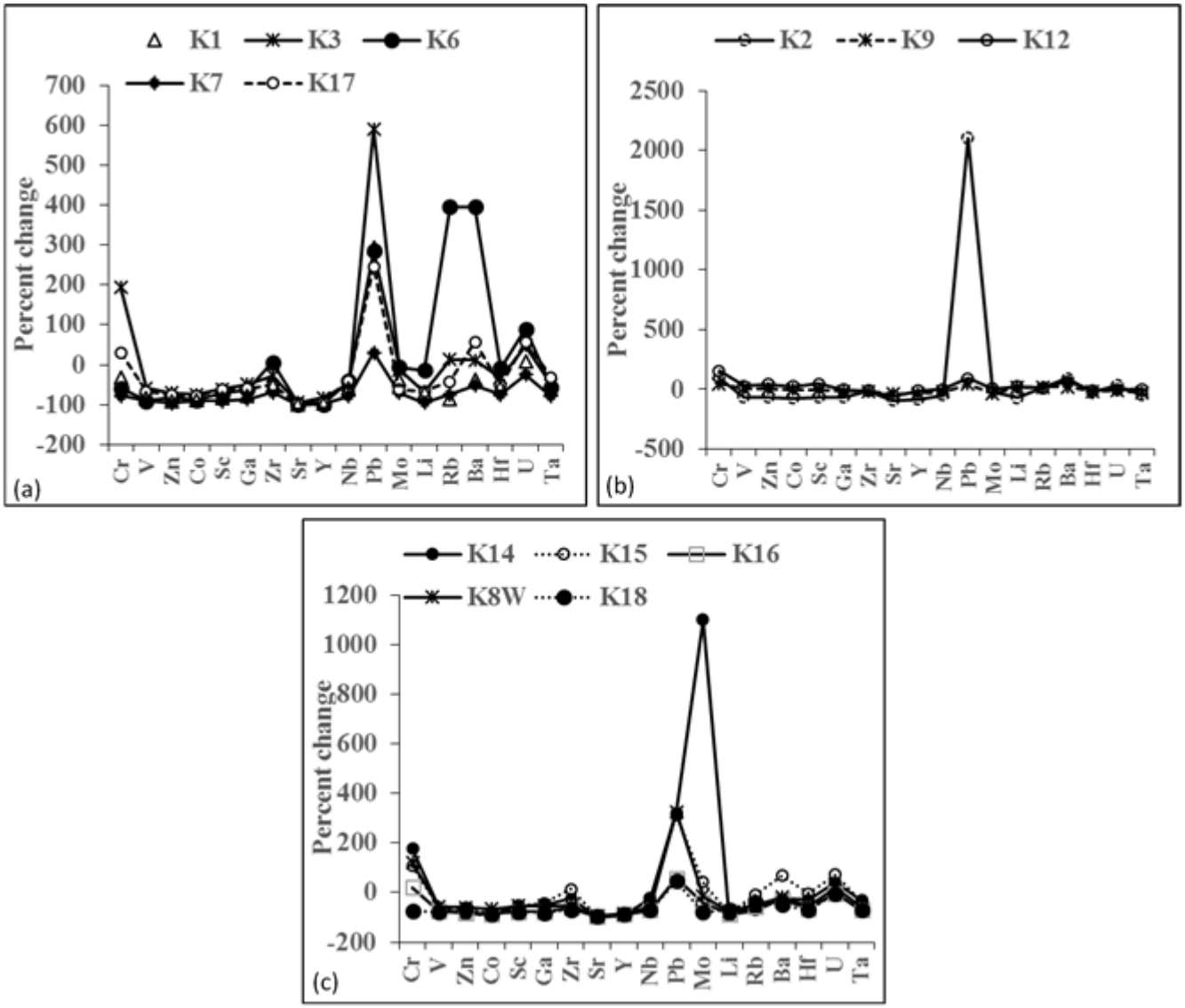

Figure 47 : Spectra showing relative chemical gains and losses of trace elements (a) fine grained materials; (b) medium grained materials; (c) coarse grained materials, in the weathered samples.

III.5. Mass balance assessment of rare earth elements

Mass balance assessment reveals strong leaching of rare earth elements in all the weathered materials (Fig. 48a b and c). The HREE are more leached out than in the LREE, except for the medium grained samples (Fig. 48b).

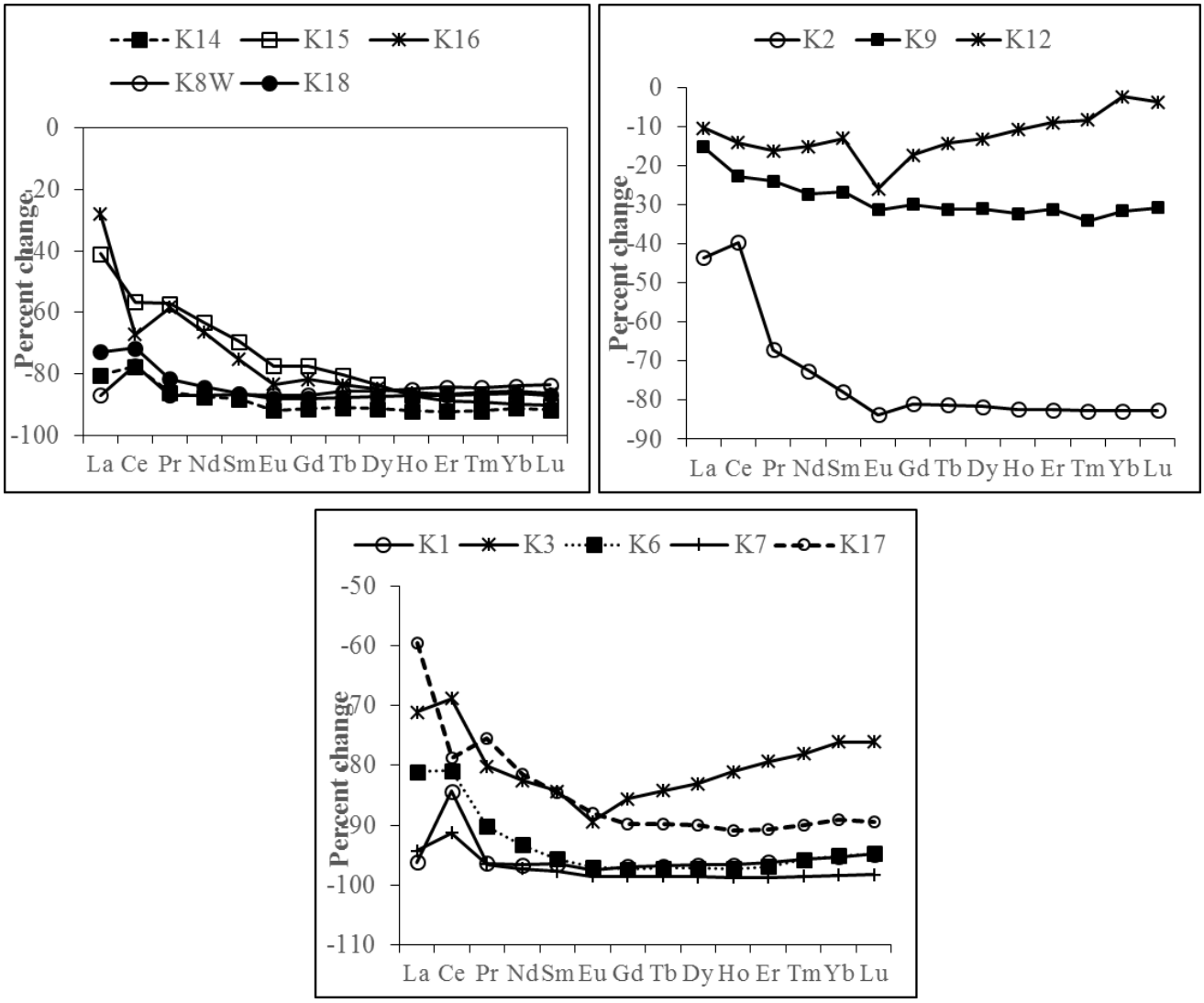

Figure 48 : Spectra showing relative chemical gains and losses of rare earth elements (a) coarse grained materials; (b) medium grained materials; (c) fine grained materials, in the weathered samples.

Conclusion

The weathered amphibolites blocks are dense and centimetric, they have undergone variable stages of centripetal weathering. They are made up of amphibole, feldspars, quartz, garnet kaolinite, gibbsite, goethite, hematite, and spinel. Most weathered samples experienced some relative enrichments and depletions of materials during weathering. We observe depletions in SiO_2, CaO, MgO, Na_2O, TiO_2 and MnO contents. Contrarily, there was enrichment in Fe_2O_3 contents. Fe_2O_3 correlates positively with TiO_2 and P_2O_5 but rather has strong negative correlations with CaO, MgO, MnO and the alkalis. Trace elements show

strong affinities with some major oxide. MnO and SiO_2 correlate positively with Zn and Co and negatively with Ga, Zr, Sc, Ga and Zr. Trace element patterns show pronounced positive anomalies in V, Cu and Zr; and distinct negative anomalies in Ni, Co, Sr and Li. Conversely, primitive mantle spectra reveal distinct positive anomalies in Pb and negative anomalies in Th. Despite the overall low contents in REE, normalized patterns reveal positive and negative cerium anomalies for some samples; slight negative and positive Eu anomaly for others. There is variable fractionation of REE in weathered amphibolites. The mass balance assessment of weathered materials shows a strong leaching of most major element. However, iron, Magnesium, potassium and Phosphorus are more enriched comparatively. Most trace elements (V, Zn, Co, Sc, Ga, Y, and Nb) have been leached out from the weathered materials. Cr, Zr and U and slightly remobilized, while Pb, Mo, Rb and Ba are strongly enriched within the materials. There is a strong leaching of rare earth elements in all the weathered materials, the HREE are more leached out than in the LREE.

CHAPTER FIVE

GEOCHEMISTRY OF S, Cu, Ni, AND Au-PGE

Introduction

Platinum group elements (PGE) are usually harbored in trace amounts in mafic and ultramafic rocks. Here, their contents are expressed in the order of ppb. When these rocks are exposed to tropical conditions, they are simultaneously weathered. This leads to the progressive destabilization and remobilization of PGE that existed in very small concentration forming deposits of economic interests. PGE (carried by platinum group minerals-PGM) are often associated with chromites or with interstitial Fe-Ni-Cu sulphides. Also, sulphur saturation in chromites forming systems is the only condition necessary for PGE precipitation (Garuti, 2004). In nature, PGE tend to exist in the metallic state or bond with sulfur (Brenan, 2008). This gives evidences that S, Cr, Ni, Cu and PGE have a common ground in mafic and ultramafic rocks.

The focus of this topic is firstly, to apprehend the behaviour of Au-PGE in amphibolites; then, to understand the distribution of sulphur, copper, nickel, gold and platinum group elements in weathered amphibolites.

V.1. Geochemistry of Gold and Platinum Group Elements in amphibolites of Kolasseng I

Contents of Au-PGE in amphibolites vary slightly from one sample to another. These contents range from 2 to 113.77 ppb. The rocks from Kolasseng I are richer in Au-PGE; their contents attain between 113.77 ppb. The NK2, NK7 and NK4 samples have the highest values (Table 7. Amphibolites of Zingui have the least Au-PGE contents; they vary only between 2.47 and 4.45 ppb.

The contents of gold are variable in amphibolites; they vary from 0.24 to 13.60 ppb. The highest gold content is observed in amphibolites of Kolasseng I (Table 7), while minimum contents (0.24 ppb) occur in amphibolites of Zingui. Gold contents attain 13.60 ppb, but these contents are significantly lower than those of Pd and Pt (Table 7). The contents of palladium in amphibolites vary between 0.69 and 83.10 ppb (Table 7). Maximum contents occur in samples of Folack Nvus, while minimum contents are observed in Zingui area. Average contents of palladium are in the order of 14.43 ppb. Palladium contents in amphibolites are relatively higher than those of platinum and all other PGE. Palladium has a maximum of 83.1 ppb (Table 7), therefore the rock tends to be more palladiferous.

The contents of platinum in amphibolites vary from 1.14 to 26 ppb (Table 7). Amphibolites of Folack Nvos have the most representative contents. These contents include 26.30 ppb in AY1 sample, 10.50 ppb in AY3 sample, 9.55 ppb in AY2 sample and 5.20 ppb in FN3 sample. Contents of PGE in the other samples are rather low, being less than 8 ppb (Table 7).

Contents of rhodium, ruthenium and iridium are very poor in amphibolites compared to gold, platinum and palladium (Table 7). These contents are mainly lower than 1 ppb for all the three elements. Maximum contents include 0.18 ppb for iridium, 3.69 ppb for rhodium and 0.66 ppb for ruthenium (Table 7). Ruthenium has the lowest contents when compared to gold and all other PGE. Contents of ruthenium are all less than 1 ppb with some of these contents lower than the detection limit (Table 7).

The concentration of Pt, Pd and Au ranges from 2.07 to 116.56 ppb (Table 7). While the sum of Pt and Pd contents vary between 1.83 and 109.40 ppb. The values of Au/ Pd + Pt are low (~ 0.50). The Pd/Pt values vary from 0.45 to 3.76, while those of Pd/Pd+Pt are less than 1 (Table 7).

V.1.2- Normalization of Au-PGE

The contents of Au-PGE were normalized with to chondrite according to McDonough and Sun (1995). The result reveal positive palladium anomalies ((Pd/Pd*) ranging from 2.68 to 4.14) for amphibolites from Kolasseng I, and Folack Nvos. However, negative platinum anomalies were observed for all samples. Amphibolites from Zingui rather show slight negative palladium anomalies (Fig. 49). The spectra show negative ruthenium anomalies for almost all samples. Nevertheless, the normalized patterns reveal that amphibolites contents are very low compared to those of chondrite.

V.1.3- Distribution of IPGE and PPGE

Platinum group elements have been grouped in to PPGE (Pt, Pd, Rh) and IPGE (Os, Ir, Ru), based on their affinities for sulphur and for olivine and spinel respectively. Amphibolites are several times richer in PPGE than the IPGE, their contents range from 1.97 to 113.09 ppb. The IPGE contents are very low; their contents are less than 1 except for one sample (Table 7).

V.1. 4: Mobility of gold and platinum group elements

The mobility of platinoids and gold is drawn from the values of Pd/Ir, Pd/Ru, and Pd/Pt and Pd/Au. The values are all greater than 1 (Table 7). The Pd/Ir values are extremely high for being 4155 represented in AY1 sample. This is followed by those of Pd/Ru (170.95). The values for Pd/Rh attain a maximum of 83.67 in NK3 sample, while that of Pd/Pt is rather low (Table 7). Iridium has the highest mobility ratios while platinum has the least. Also the rocks of Folack Nvos have higher ratios while those of Zingui have the least Table (7).

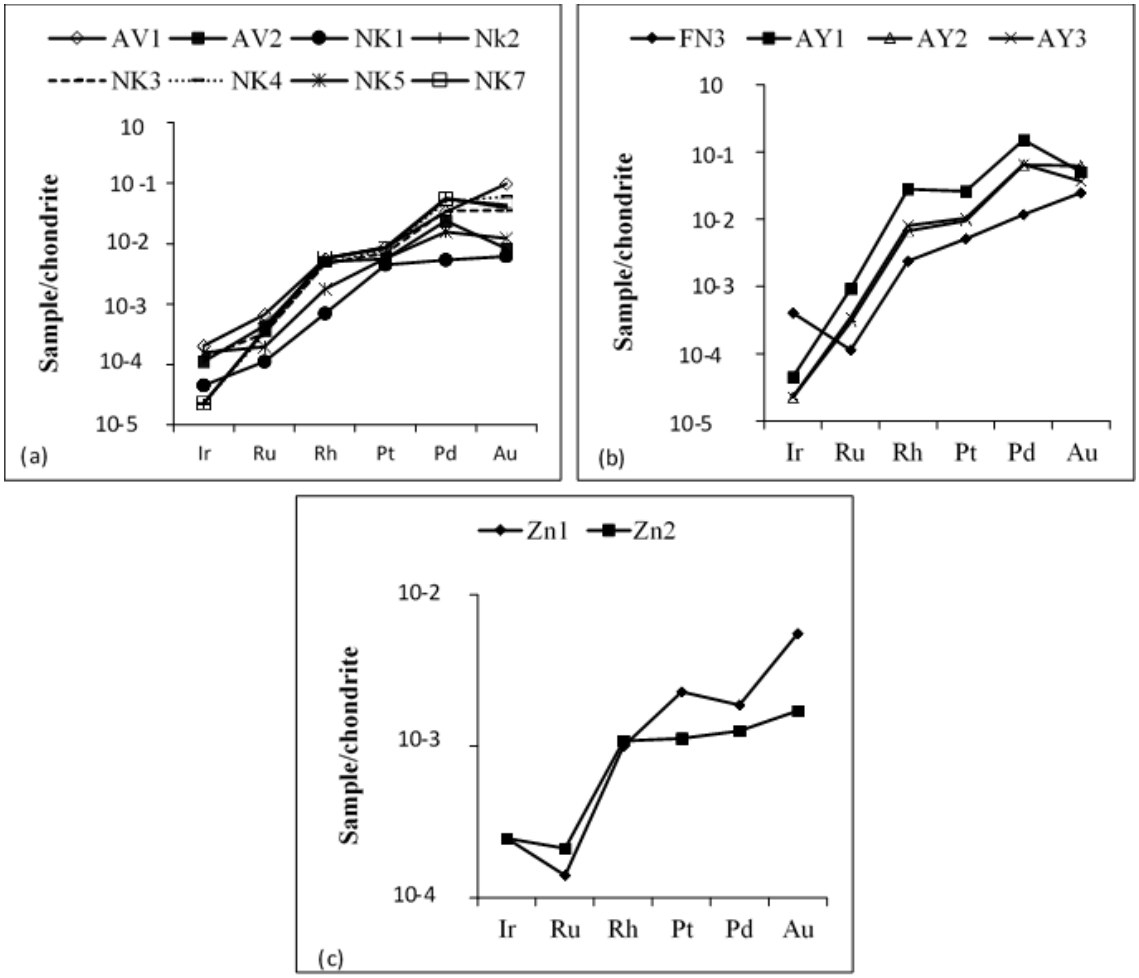

Figure 49 : Chondrite normalized Au-PGE plots for amphibolites (a) Kolasseng I (b) Folack Nvus (c) Zingui site

Table 7 : Binary diagrams of sulfur vs. selected base metals

		Zingui		Folack Nvus				Kolasseng I							
Elements	d.l.	Zn1	Zn2	FN3	AY1	AY2	AY3	AV1	AV2	NK1	NK2	NK3	NK4	NK5	NK7
Au	0.22	0.77	0.24	3.47	7.16	8.81	5.22	13.60	1.16	0.87	5.47	4.98	8.51	1.71	6.15
Ir	0.01	0.11	0.11	0.18	0.02	0.01	0.01	0.09	0.05	0.02	0.01	0.06	0.01	0.07	0.01
Pd	0.12	1.03	0.69	6.55	83.10	35.90	36.20	18.60	13.10	2.95	31.10	19.10	27.00	8.64	30.00
Pt	0.17	2.31	1.14	5.20	26.30	9.55	10.50	8.84	5.68	4.52	8.75	7.05	7.95	5.69	8.46
Rh	0.02	0.13	0.14	0.31	3.69	0.87	1.04	0.73	0.65	0.09	0.74	0.60	0.61	0.23	0.75
Ru	0.08	0.10	0.15	<dl	0.66	0.21	0.25	0.48	0.31	<dl	0.26	0.23	0.23	0.14	0.26
∑PGE	-	3.68	2.03	12.24	106.61	37.73	42.78	28.74	19.79	7.58	40.86	27.04	35.8	14.77	39.48
Pd+Pt	-	3.34	1.83	11.75	109.40	45.45	36.70	27.44	18.78	7.47	39.85	26.15	34.95	14.33	38.46
Pd+Pt+Au	-	4.11	2.07	15.22	116.56	54.26	54.97	41.04	19.94	9.21	45.32	31.13	43.46	16.04	44.61
Pd/Pd+Pt	-	0.31	0.38	0.56	0.76	0.79	0.78	0.68	0.70	0.05	0.67	0.73	0.77	0.60	0.78
Au/Pd+Pt	-	0.23	0.13	0.30	0.07	0.19	0.11	0.50	0.06	0.12	0.12	0.19	0.24	0.12	0.16
∑IPGE	-	0.21	0.26	0.26	0.68	0.22	0.26	0.57	0.36	0.1	0.27	0.29	0.24	1.99	0.27
∑PPGE	-	3.47	1.97	12.06	113.09	46.32	47.74	28.17	19.43	7.56	40.59	26.75	35.56	14.56	39.21
Au-PGE	-	4.45	2.47	15.71	113.77	46.54	48.00	42.34	20.95	8.45	46.33	32.02	44.31	16.48	45.63
IPGE/PPGE	-	$6.05*10^{-2}$	$1.32*10^{-1}$	$2.16*10^{-2}$	$6.01*10^{-3}$	$4.75*10^{-3}$	$5.45*10^{-3}$	$2.02*10^{-2}$	$1.85*10^{-2}$	$1.32*10^{-2}$	$6.65*10^{-3}$	$1.08*10^{-2}$	$6.75*10^{-3}$	$1.37*10^{-1}$	$6.89*10^{-3}$
Pd/Pt	-	0.45	0.61	1.26	3.16	3.76	3.45	2.10	2.31	0.65	3.55	2.55	3.40	1.52	3.55
Pd/Rh	-	7.92	4.93	21.13	22.52	41.26	34.81	24.88	20.15	32.78	42.03	83.67	44.26	37.57	40.00
Pd/Ru	-	10.30	4.60	81.88	125.91	170.95	144.80	37.83	42.26	36.88	119.6	83.04	117.4	61.71	115.3
Pd/Ir	-	9.36	6.27	36.39	4155	3590	3620	201.77	262.0	147.5	3110	318.3	2700	123.4	3000
Pd/Pd*	-	2.53	0.90	1.05	4.14	2.68	3.34	1.16	3.49	1.02	3.07	2.20	2.24	1.89	2.84
Pd/Au	-	1.34	2.88	1.89	11.60	4.07	6.93	1.37	11.29	3.39	5.69	3.54	3.17	5.05	4.88

d.l. : detection limit

V.2. Correlations

The platinum-group of elements and their ratios have been plotted against MgO in Figure 50. In this figure, Ir and Ru show a distinct positive relation with MgO. The other PGEs in the amphibolites show weak positive correlation with MgO.

All samples show an overall positive relationship for Cr versus Ir, Ru and Au (Fig. 51a–c) but there is much scatter in the plots of Cr versus Rh, Pt and Pd (Fig. 51. d–f). Amphibolites of Kolasseng I show very strong positive relationships between total PGE and Pd/Pt (Fig. 52); and total PGE versus Pd/Ir (Fig. 53).

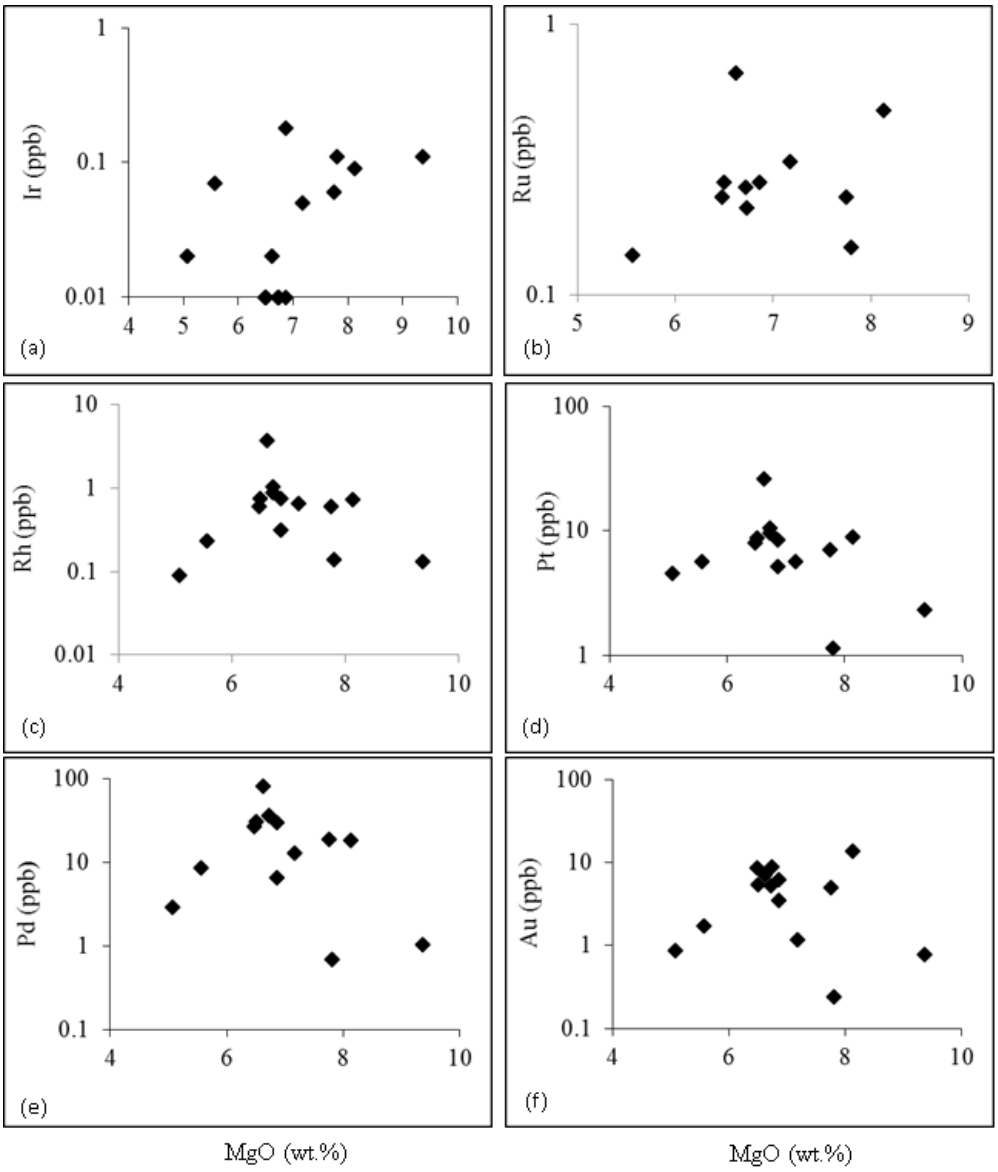

Figure 50 : Plots of MgO versus PGE for amphibolites from Kolasseng I.

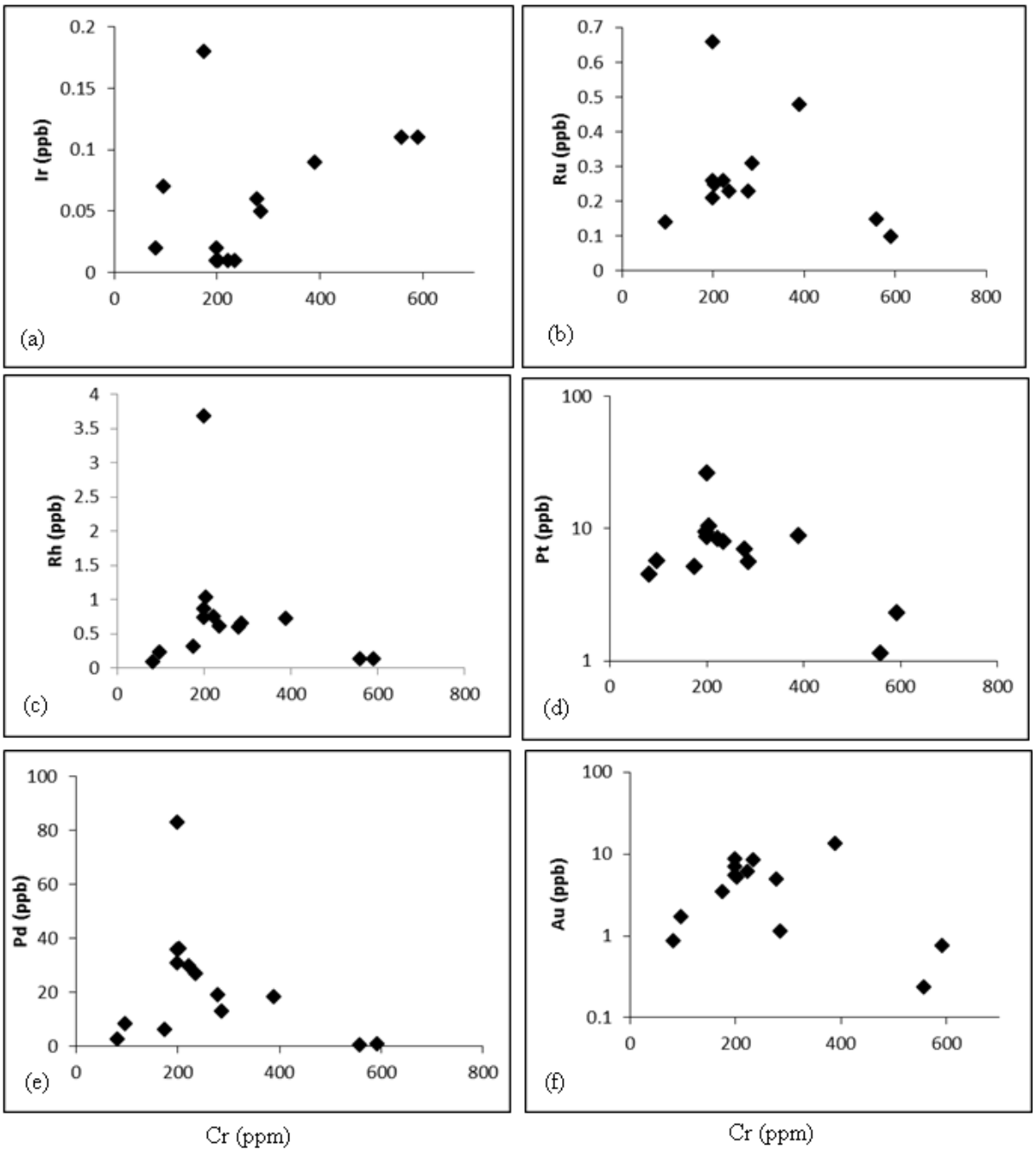

Figure 51 : Plots of Cr versus PGE for amphibolites from Kolasseng I

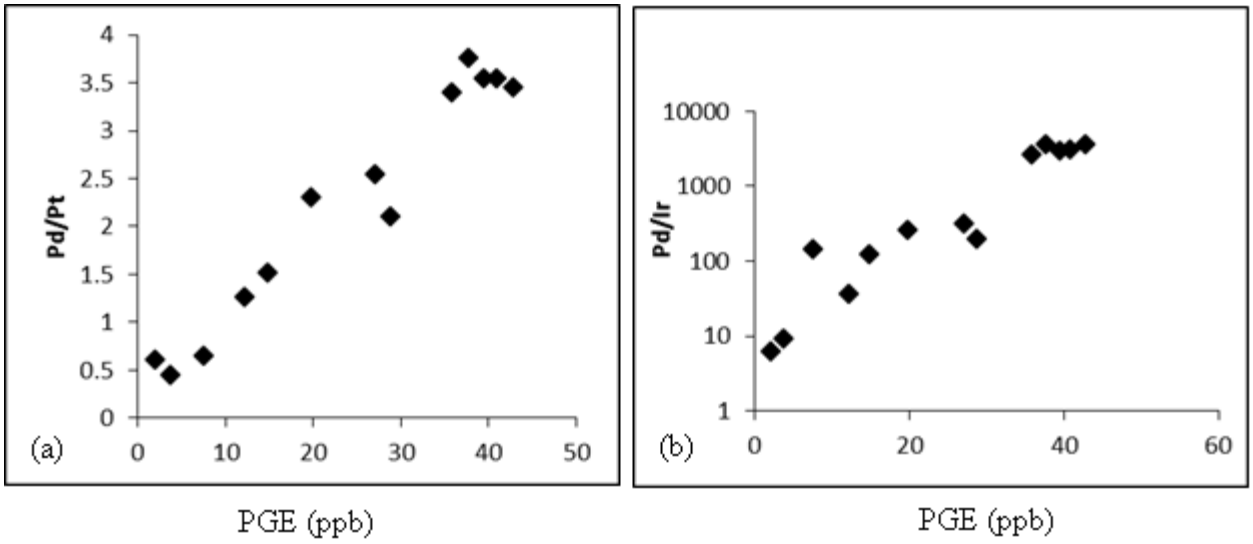

Figure 52 : Plots of (a) total PGE (ppb) versus Pd/Pt. (b) total PGE (ppb) versus Pd/Ir for amphibolites from Kolasseng I.

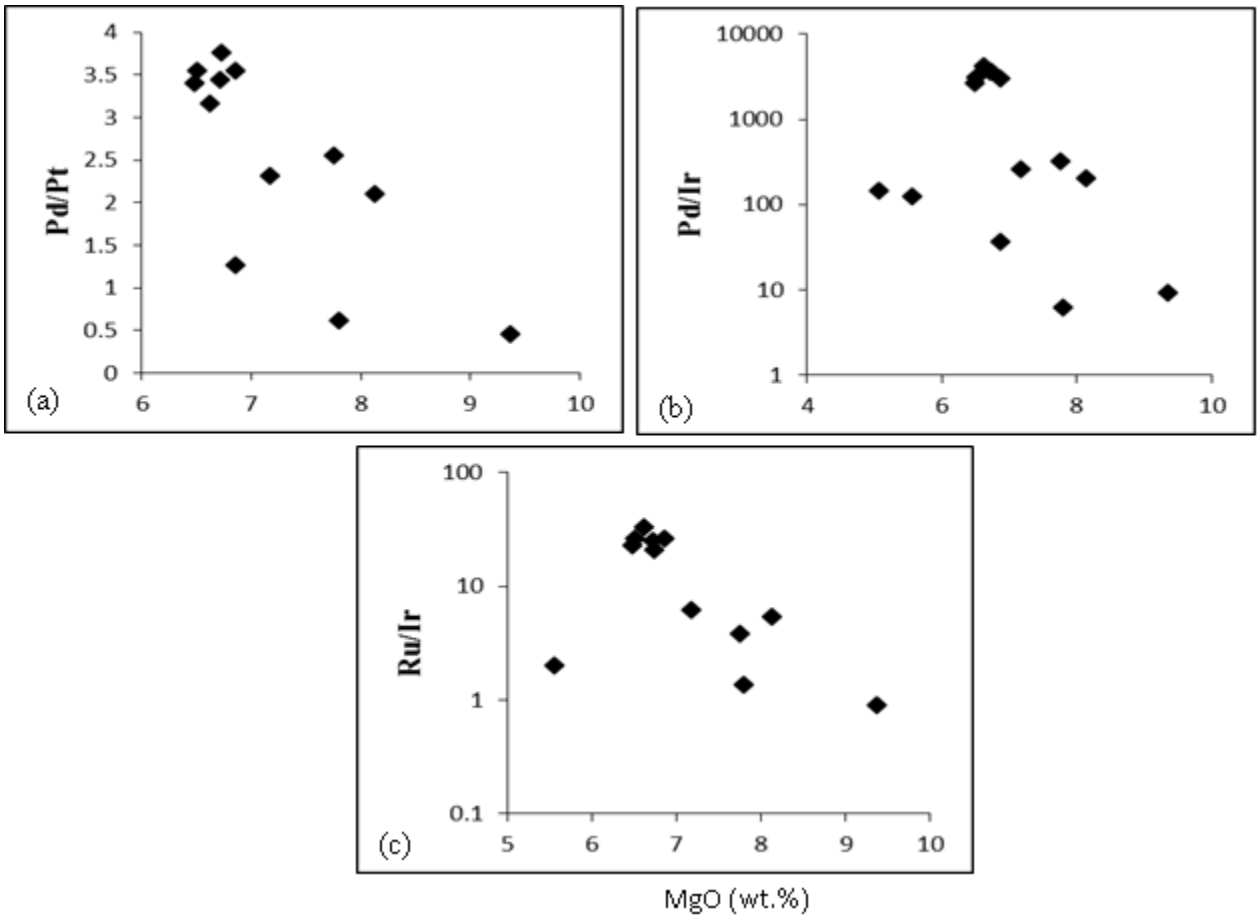

Figure 53 : Plots of MgO (wt. %) versus (a) Pd/Pt; (b) Pd/Ir; (c) Ru/Ir for amphibolites from Kolasseng I.

V.3. Geochemistry of rocks from Kolasseng II

A total of seven rock samples were collected from Kolasseng II in order to determine their contents in gold and platinum group elements.

V.3.1 Geochemistry of S, Cu, Cr, and Ni in amphibolites of Kolasseng II

The concentrations of S, Cu, Cr and Ni in amphibolites and pyroxenites are listed in Table 8. The contents are higher in the garnet amphibolites than in the garnet pyroxenites.

Nickel concentrations have a wide range in amphibolites; they vary from 50 to 121.9 ppm while the average concentration of Ni is 94.79 ppm. These concentrations are rather higher (132.0 ppm) in garnet pyroxenites. The EA sample has the most elevated concentration; Ni concentrations are about three to four times or more low than those of S and several times lower than Cu concentrations (Table 8).

The concentrations of Cu are clearly elevated in both garnet amphibolites and pyroxenites. In the garnet pyroxenites the concentrations attain 2820 ppm, whereas they have a broad range in amphibolites. Cu concentrations in amphibolites vary from 1800 to 5350 ppm while their average concentration attains 3069 ppm. The K4 sample contains the must elevated Cu content (350 ppm) while K13 sample contains the least (Table 8).

Garnet pyroxenites have very low sulphur contents, which are less than 1 ppm (0.046 ppm). Sulphur contents are high in garnet amphibolites and have a wide variation (380 to 1710 ppm). The average contents for S is 848.57 ppm, the K4 sample has higher contents of sulphur than the other entire rock samples (Table 8).

The base metals are negatively correlated with S except Pd and Ir, meanwhile Cu and Ni are not correlated with S (Fig. 54).

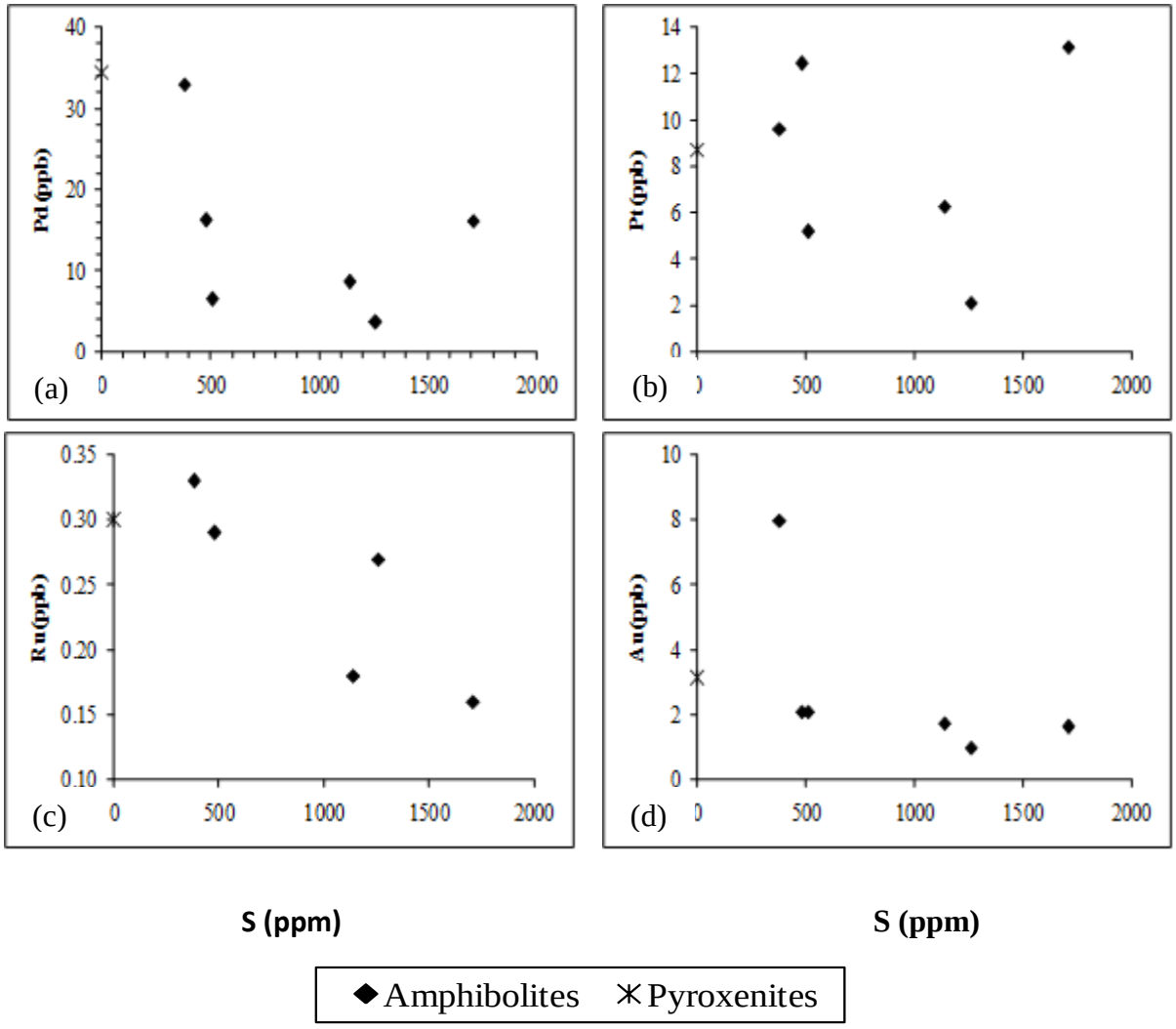

Figure 54 : Binary diagrams of sulphur versus precious metals in amphibolites of Kolasseng II.

V.3.2- Behaviour of Au-PGE in amphibolites and pyroxenites of Kolasseng II

The detailed Au-PGE concentrations in amphibolites and pyroxenites are confined in Table 8. The contents range from 8 to 59.54 ppb for garnet amphibolites and 50.35 ppb for garnet pyroxenites. The total PGE concentrations of garnet amphibolites have a wide range of 7 to 52 ppb whereas those of garnet pyroxenites are low (PGE = 47 ppb; Table 8). In details they include 34.36 ppb for Pd, 8.70 ppb for Pt as the dominant PGE, while the contents of Rh, Ru, Ir and Os are all less than 1 ppb. The PGE contents in pyroxenites are comparatively lower to those of amphibolites, but concentrations of palladium in pyroxenites are higher than those in amphibolites (Table 8). Concentrations of palladium are more than two times higher than those of platinum. The highest concentration in amphibolites is found in K11 sample while the lowest is in the K10 sample (Table 8).

Platinum contents are rather low, ranging from 2.11 to 13.18 ppb. Maximum concentrations in amphibolites are found in K4 sample. Gold contents are low. They include 7.97 ppb in amphibolites and 3.12 ppb in pyroxenites. The Au-PGE contents attain 59 ppm maximum in garnet amphibolites and 50 ppm in garnet pyroxenites.

The concentrations of the other platinoids (Ru, Rh, Ir and Os) are very low and less than 1 ppb. These concentrations are also less than detection limit for several samples (Table 8), they include 0.10 to 0.19 ppb for Os, 0.05 to 0.20 ppb for Ir, 0.18 to 0.33 for Ru and 0.13 and 0.93 ppb for Rh.

The contents of Pd+Pt are variable and range from 5.75 to 42.59 ppb, Pd/Pd+Pt and Au/Pd+Pt values are all less than 1. Both rocks are richer in PPGE than IPGE (5-42.9 ppb for PPGE and 0.59- 1.29 ppb for IPGE). The PPGE/IPGE values, are all greater than 8, they vary between 8.71 and 55.62 for amphibolites and are higher (117.03) in pyroxenites (Table 8).

V.3.3 Mobility of Au-PGE in rocks of Kolasseng II

The Pd/Pt, Pd/Rh and Pd/Os Pd/Ru, Pd/Ir and Pd/Au ratios are all higher than 1 (Table 8). This shows that all the other PGE as well as gold are more mobile than Pd, Pt being the least mobile and Ir the most mobile. All samples have higher Pd/Pt values (amphibolite average Pd/Pt = 1.72; pyroxenite samples = 43.06) than the mantle (Pd/Pt = 0.53; Barnes *et al*., 1988; Khatun *et al*., 2014). Also, Pd/Ir show very high values (amphibolites average = 73.23) which are several times higher than that of the mantle (Pd/Ir =1, Barnes *et al*., 1988).

V.3.4- Normalisation of Au-PGE in rocks of Kolasseng II

The plots of chondrite-normalized (McDonough and Sun, 1995) Au-PGE patterns reveal a slight positive Pd and negative Ru anomalies for the amphibolites, while the pyroxenites have slight negative and positive anomalies in Pt and Pd respectively (Fig. 55).

All patterns show strong enrichment in PPGE but are depleted in IPGE with positive anomalies in Pd and negative ones in Ru for both amphibolites and pyroxenites.

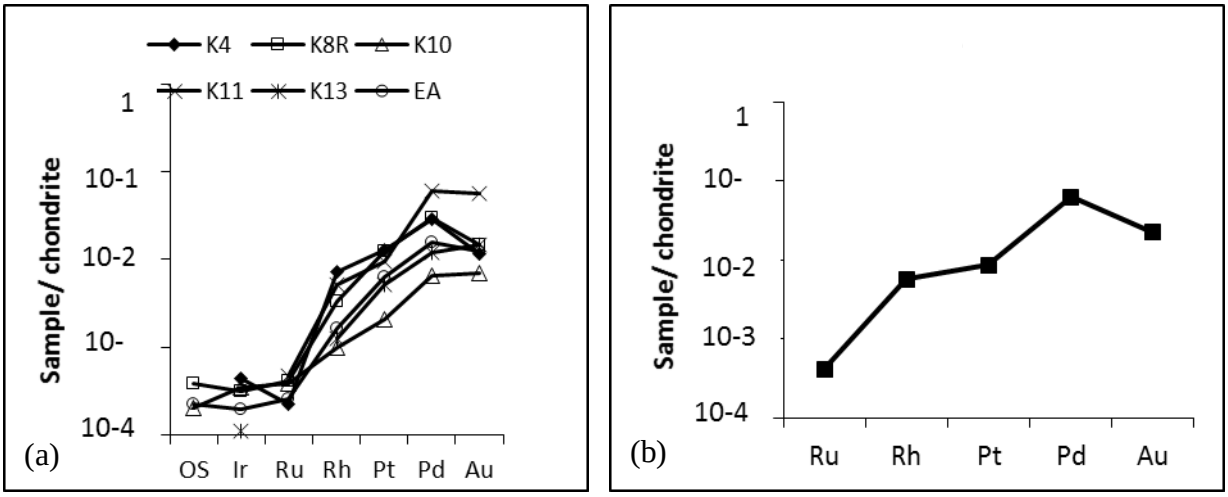

Figure 55 : Chondrite normalized Au-PGE patterns for amphibolites (a) and (b) Pyroxenites.

V.4 Distribution of Sulphur, Copper, and Nickel in weathered amphibolites

The weathered samples are marked by variable S and Cu contents**.** The S contents vary between 239 and 902 ppm. These contents are rather low compared to those of the fresh rocks. Cu contents range from 520 to 2150 ppm. These contents are greater than 1000 ppm except for 3 samples, K1 and K2 samples have the most representative copper contents (Table 9).

Ni contents are low, ranging from 109 to 114 ppm. Low Ni contents may indicate fractionation of their carrier minerals or partial melting of some mantle material containing extremely low proportions of olivine (Hoch, 1999). The low Ni contents in these samples can also be associated to a low degree of partial melting of the original magma (Barnes and Lightfoot, 2005).

Average contents of S, Cu, and Ni in weathered samples include 548.46, 1432 and 78.69 respectively. Sulfur correlates positively with Cu (Fig. 56a); negatively with Ni (Fig. 56b); and positively with Cr (Fig. 56c). The negative correlation occurs also between sulfur and Ni/Cr ratio in the weathered amphibolites (Fig. 56d).

Table 8 : S, Ni, Cu and Au-PGE contents in the Amphibolites of Kolasseng II

	d.l.	Amphibolites						Pyroxenites
		K4	K8R	K10	K11	K13	EA	K5
S (ppm)	-	1710	480	1260	380	510	1140	0.046
Ni	-	111.9	103.8	50.5	86.3	57.1	121.9	132.0
Cu	-	5350	2970	1990	3830	1800	2720	2820
Os (ppb)	0.07	<dl	0.19	0.10	<dl	<dl	0.11	<dl
Ir	0.03	0.20	0.14	0.16	<dl	0.05	0.09	<dl
Ru	0.12	0.16	0.29	0.27	0.33	<dl	0.18	0.30
Rh	0.08	0.93	0.44	0.13	0.68	0.16	0.21	0.75
Pt	0.08	13.18	12.45	2.11	9.63	5.18	6.28	8.70
Pd	0.47	16.11	16.21	3.64	32.96	6.50	8.63	34.36
Au	0.48	1.62	2.08	0.99	7.97	2.08	1.72	3.12
PGE	-	32.2	31.8	7.4	51.57	13.97	17.22	47.23
Pd+Pt	-	29.29	28.66	5.75	42.59	11.68	14.91	43.06
Pd+Pt+Au	-	30.91	30.74	6.74	50.56	13.76	16.63	46.18
Pd/Pd+Pt	-	0.55	0.57	0.63	0.77	0.56	0.58	0.80
Au/Pd+Pt	-	0.06	0.07	0.17	0.19	0.18	0.12	0.07
IPGE	-	1.29	1.06	0.66	1.01	0.21	0.59	0.30
PPGE	-	29.29	28.66	5.75	42.59	11.68	14.91	35.11
Au-PGE	-	33.82	33.88	8.39	59.54	16.05	18.94	50.35
PPGE/IPGE	-	22.7	27.04	8.71	42.17	55.62	25.27	117.03
Pd/Pt	-	1.22	1.30	1.73	3.42	1.25	1.37	43.06
Pd/Rh	-	17.32	36.84	28	48.47	40.63	41.10	45.81
Pd/Ru	-	100.69	55.90	13.48	99.88	-	47.94	114.53
Pd/Ir	-	1.74	115.79	22.75	-	130.00	95.89	-
Pd/Os		-	85.32	36.4	-	-	78.46	-
Pd/Pd*	-	0.16	0.02	0.15	0.60	0.19	0.18	0.40
Pd/Au	-	9.94	7.79	3.68	4.14	3.13	5.02	11.01

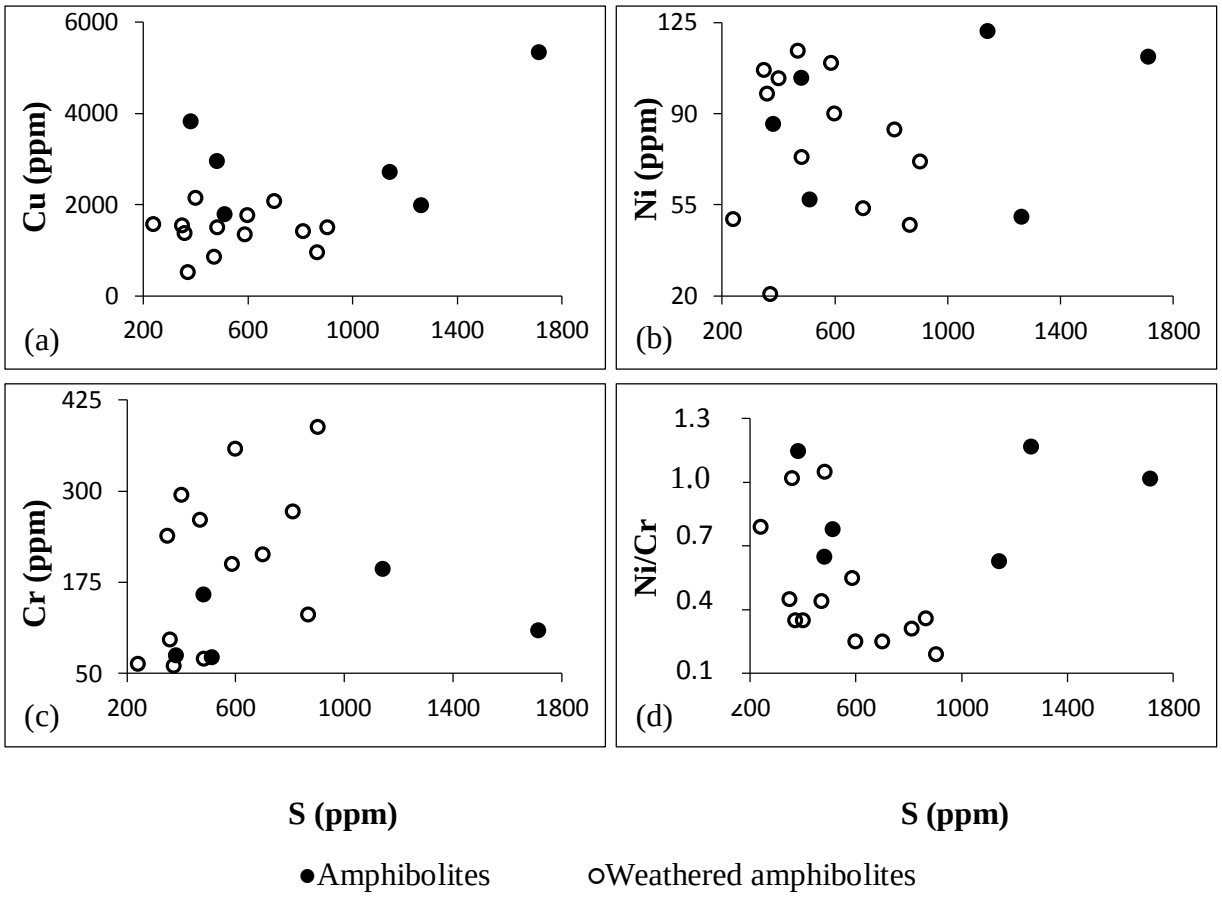

Figure 56 : Binary diagrams of sulfur vs. selected base metals (a) S vs. Cu; (b) S vs. Ni; (c) S vs. Cr, (d) S vs. Ni/Cr.

V.5. Distribution of Au and PGE in weathered amphibolites

The Au-PGE contents are higher in weathered samples compared to those of fresh ones. The total PGE contents are variable, ranging between 11 and 93 ppb with Pt and Pd abundances (Table 9). The contents of Ir are rather very low, the generally vary from 0.07 to 0.27 ppb with most of the samples contents being below detection limit. Contents of Os are closely similar to those of Ir, a cross section of the contents are less than detection limit. Ru contents are slightly higher than those of Ir, but all of these contents are less than 1 ppb. Rh contents vary from 0.16 to 1.51 ppb, thus also close in range with the other described PGE (Table 9).

The gold contents are very low and less than 1 ppb in three samples and up to 27 ppb in the others (Table 9). The total Au-PGE contents vary between 13 and 117 ppb.

V.5.1 Mobility OF Au-PGE

The values of Pd/Pt, Pd/Ru, Pd/Ir, Pd/Rh and Pd/Au ratios permitted the mobility of Au-PGE to be deduced within the weathered rocks (e.g., Bowles et al., 1994; Ndjigui and Bilong, 2010). The data for different ratios are shown in Table 9. The values of the different ratios are all greater than 1 except for two samples (Table 9). The ratio is very high for Pd/Ir being 141. This is followed by the ratios of Pd/Ru which attain 117 which is also relatively high. The maximum values of Pd/Rh and Pd/Au are respectively 46 and 44. Pd/Pt values vary from 0.41 to 3, thus Pd/Pt values are all higher than 1, but attain only a maximum of 3. Two of the Pd/Pt values are less than 1 (Table 9).

From these ratios we can be deduced that: (1) Ir, Ru, Rh and Au are more mobile than Pd in the weathered amphibolites; (2) Ir is highly mobile compared to other Au-PGE; (3) Ru is more mobile than Rh which is in turn mobile than Au in all the weathered samples; (4) Pt is slightly more mobile than Pd, except for K7 and K18 samples. However, the Pd/Pt values are higher than 1 in some samples. This indicates the contrast Pt behaviour in the supergene environment. The high values above 1 reveal a minimum fractionation of palladium compared to other PGE (Table 9). Also, K12 Sample shows values with the highest mobility of platinoids in relation to palladium, compared to the other samples. Globally the mobility ratios show palladium as the least mobile element in all platinum group elements in amphibolites of Nyabitande.

V.5.2 IPGE/PPGE ratios

Platinoids can be partitioned in to two subgroups: the high-melting IPGE, including Ir, Os and Ru characterized by relatively low solubilities in silicate melts and the low-melting PPGE (Pd, Pt, Rh) characterized by relatively more soluble character (Garuti, 2004). The sub groups are also based on their behaviour or affinity for certain minerals or elements (Mitchell and Keays, 1981). According to this grouping IPGE are closely linked to olivine, while the PPGE have an affinity for sulphur.

The weathered materials are enriched in PPGE (16 to 77 ppb) than IPGE (0.26 to 2.11 ppb). The high PPGE abundance might be relative to the oxidation of primary mineral into goethite (Ahmed *et al*., 2009). The strong depletion of IPGE can be attributed to retention of IPGE in the metal alloys of the original magma (Barnes *et al*., 1995). Palladium, Rh, Ru and

Ir are positively correlated with S (Fig. 57a, c, d, and e). Conversely, the correlation is negative between platinum and S (Fig. 57b).

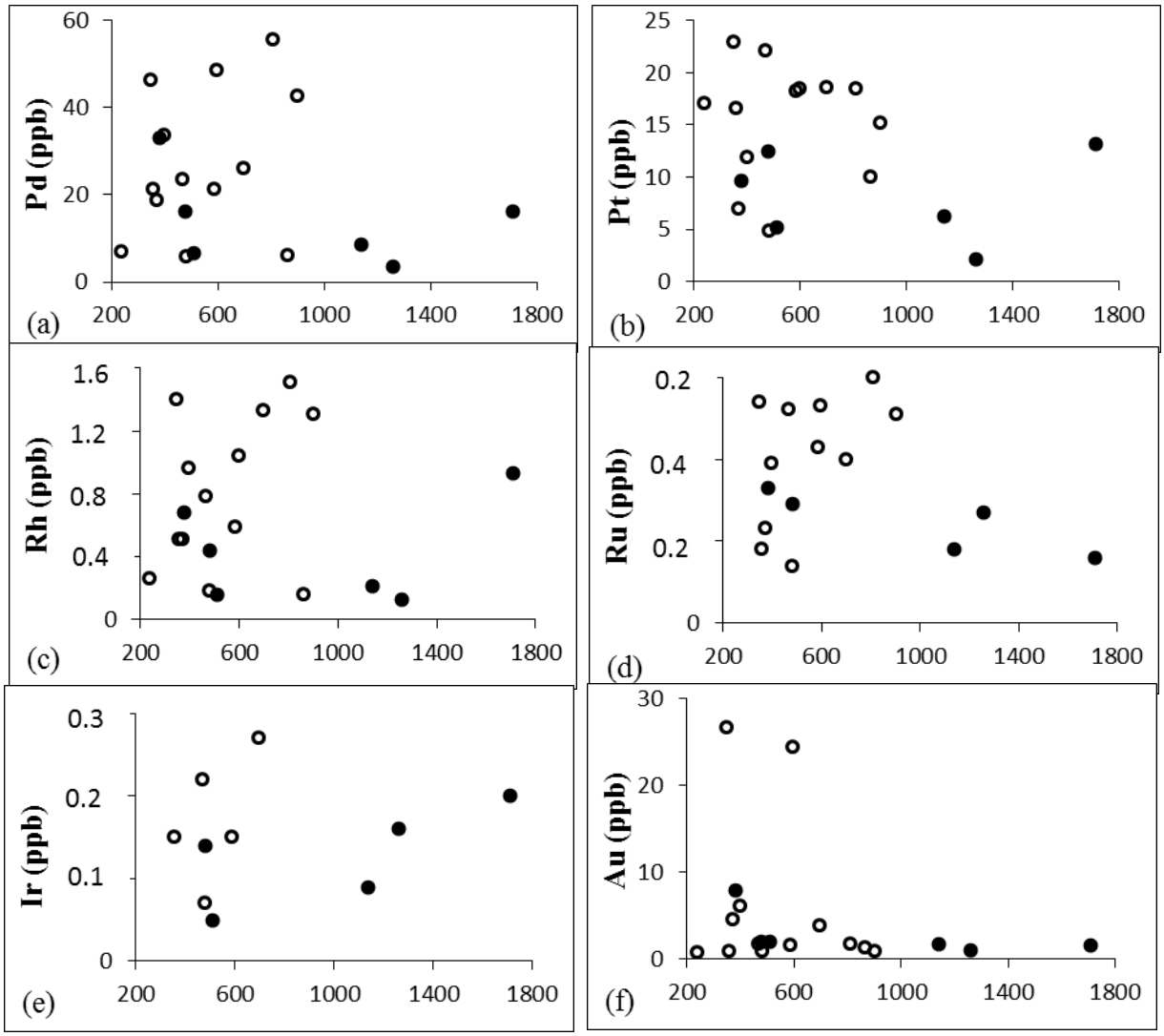

Figure 57 : Binary diagrams of sulfur vs. precious metals (a) S vs. Pd; (b) S vs. Pt; (c) S vs. Rh, (d) S vs. Ru; (e) S vs. Ir; (f) S vs. Au.

V.5.3: Normalization of Au-PGE

The chondrite-normalized (McDonough and Sun, 1995) base metal patterns reveal high enrichment in Cu, Pd and Ni in the weathered amphibolites (Fig. 58a). The chondrite-normalized (McDonough and Sun, 1995) patterns for average contents of the weathered and fresh rocks follow the same trends and reveal the slight enrichment in PGE due probably to the low degree of weathering (Fig. 58b). With respect to the fresh rocks, Os, Ir and Ru are depleted (Fig. 58a and b). In fact PPGE are more mobile (more soluble) than IPGE in the supergene environment (Garuti, 2004). These results suggest that the processes that lead to PGE, Ni- and Cu-enrichment are quite different.

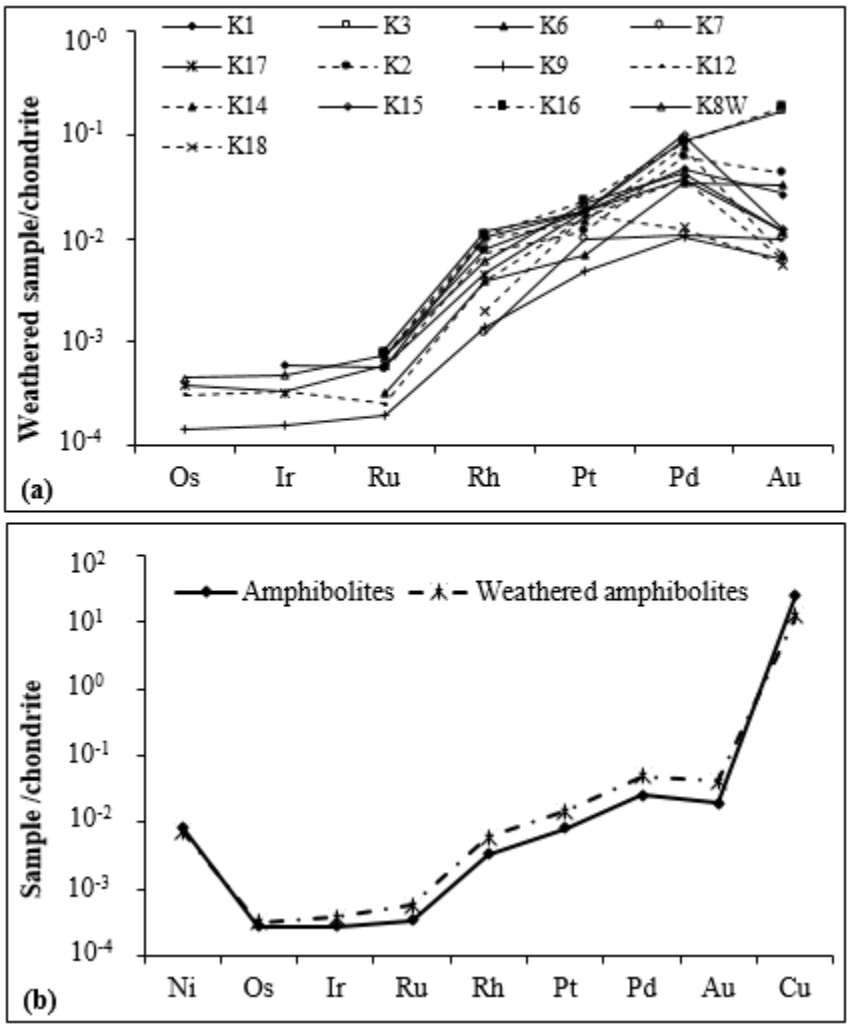

Figure 58 : Chondrite-normalized base metal patterns for (a) weathered amphibolites; and (b) average contents for the fresh and weathered amphibolites.

Table 9 : S, Cu, Ni, Cr, Au-PGE contents in weathered Amphibolites

	dl	K1	K3	K6	K7	K17	K2	K9	K12	K14	K15	K16	K8W	K18	Av
S (ppm)	-	699.45	598.04	370.72	865.06	586.91	399.55	482.61	358.52	902.18	810.58	348.03	469.13	239.15	548.46
Cu	-	2082	1770	520	950	1350	2150	1500	1380	1500	1420	1550	860	1580	1432
Ni	1.6	53.8	90.1	20.8	47.3	109.6	103.7	73.5	97.7	71.8	84.0	106.9	114.3	49.5	78.69
Cr	3	213	358	60	131	200	295	70	96	388	272	239	261	63	204
Ni/Cr		0.25	0.25	0.35	0.36	0.55	0.35	1.05	1.02	0.19	0.31	0.45	0.44	0.79	0.49
Cu/(Cu+Ni	-	0.97	0.95	0.96	0.95	0.92	0.95	0.95	0.93	0.95	0.94	0.93	0.88	0.97	0.94
Os (ppb)	0.07	<dl	<dl	<dl	<dl	0.19	<dl	0.07	0.15	<dl	<dl	<dl	0.22	<dl	0.16
Ir	0.03	0.27	<dl	<dl	<dl	0.15	<dl	0.07	0.15	<dl	<dl	<dl	0.22	<dl	0.17
Ru	0.12	0.40	0.53	0.23	<dl	0.43	0.39	0.14	0.18	0.51	0.60	0.54	0.52	<dl	0.41
Rh	0.08	1.33	1.04	0.51	0.16	0.59	0.96	0.18	0.51	1.31	1.51	1.40	0.78	0.26	0.81
Pt	0.08	18.58	18.51	6.99	9.98	18.24	11.90	4.85	16.53	15.12	18.44	22.87	22.04	17.00	15.47
Pd	0.47	26.14	48.61	18.79	5.95	21.14	33.64	5.79	21.16	42.57	55.59	46.31	23.45	6.94	27.39
Au	0.48	3.80	24.34	4.58	1.38	1.62	6.07	0.89	0.88	0.95	1.75	26.59	1.68	0.80	5.79
PGE	-	46.72	68.69	26.52	16.09	40.74	46.89	11.10	38.68	59.51	76.14	71.12	47.23	24.20	44.13
Au-PGE	-	50.52	93.03	31.10	17.47	42.36	52.96	11.99	39.56	60.46	77.89	97.71	48.91	25.00	49.92
IPGE	-	0.67	0.53	0.23	-	0.77	0.39	0.28	0.48	0.51	0.60	0.54	0.96	-	0.54
PPGE	-	46.05	68.16	26.29	16.09	39.97	46.50	10.82	38.20	59.00	75.54	70.58	46.27	24.20	43.67
PPGE/IPGE	-	68.73	128.60	114.30	-	51.91	119.23	38.64	79.58	115.69	125.90	130.70	48.19	-	92.86
Pd/Pt	-	1.42	2.63	2.69	0.60	1.16	2.83	1.19	1.28	2.82	3.01	2.02	1.06	0.41	1.78
Pd/Ir	-	96.81	-	-	-	-	-	82.71	141.07	-	-	-	106.59	-	106.80
Pd/Os	-	-	-	-	-	111.26	-	82.71	141.07	-	-	-	106.59	-	110.41
Pd/Ru	-	65.35	91.72	81.70	-	49.16	86.26	41.36	117.56	83.47	92.65	85.76	45.10	-	76.37
Pd/Rh	-	19.65	46.74	36.84	37.19	35.83	35.04	32.17	41.49	32.50	36.81	33.08	30.06	26.69	34.16
Pd/Au	-	6.88	2.00	4.10	4.31	13.05	5.54	6.51	24.05	44.81	31.77	1.74	13.96	8.68	12.88

V.5.4. Mass balance assessment of base metals

The method of mass balance evaluation for base metals is same as in the other elements shown in the previous chapter. The calculations are done following the approach of thorium is used as invariant element. The application of the equation of Nesbitt and Wilson (1992) reveals: (i) high leaching in S, Ni and Cu in all samples; however, there is a slight remobilization of Ni in some samples (Fig. 59a-d); (ii) strong IPGE leaching in most samples (Fig. 59a-d); (iii) leaching of Au-PGE in the fine grained rocks; however there is an enrichment in Au-PPGE in one sample (K3, Fig. 59a); (iv) strong PPGE enrichments in the medium and coarse grained rocks (Fig. 59b, c and d) and (v) leaching of Au-PPGE in some samples (Fig. 59 a and d).

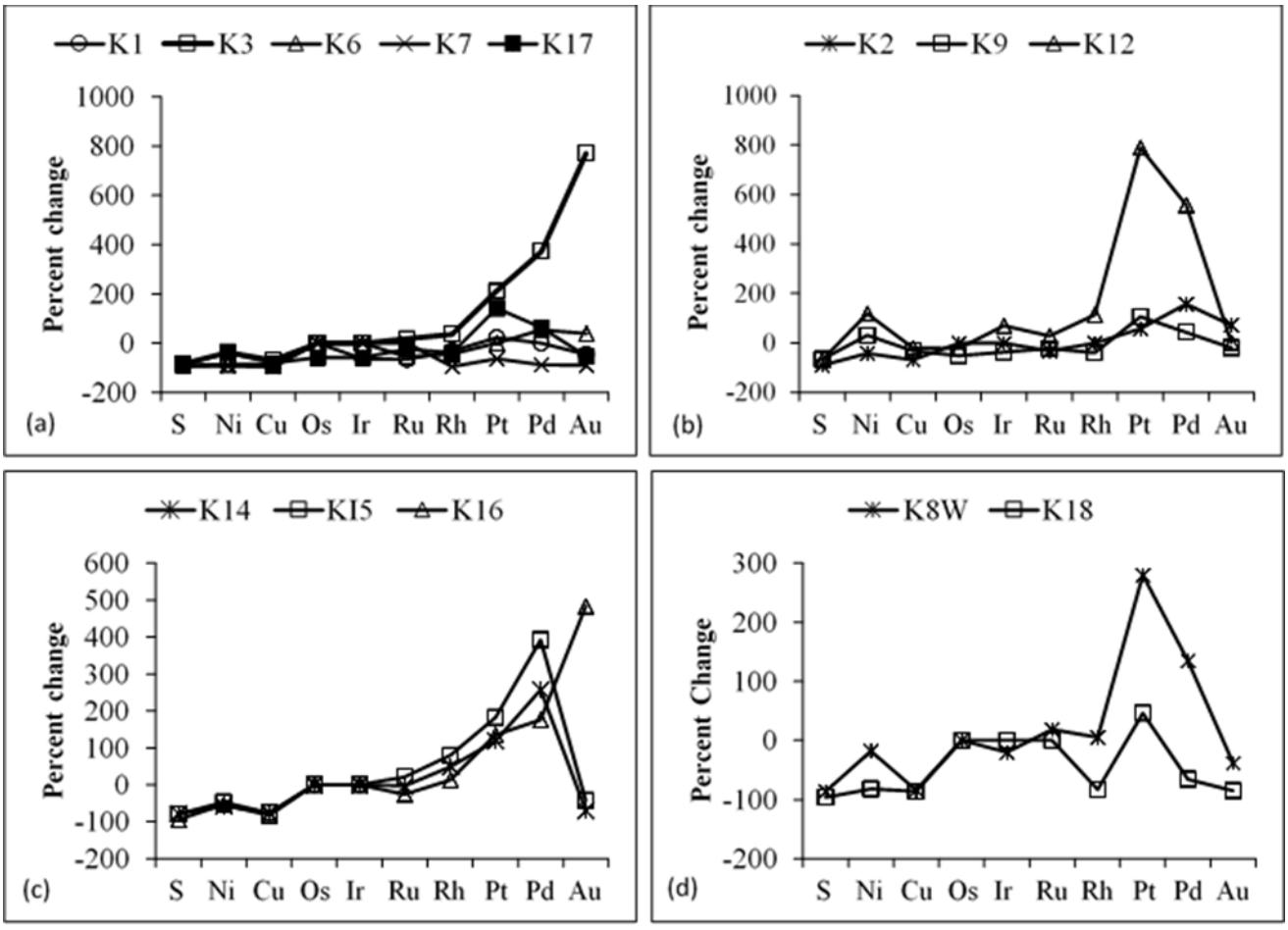

Figure 59 : Spectra showing relative chemical gains and losses of base metals (a) fine grained materials; (b) medium grained materials; (c and d) coarse grained materials, in the weathered samples.

V.5.5. Binary diagrams

Selected platinum group elements were correlated with some major elements, to match their behaviour during weathering. Correlations were also established between Cr, Ni and Cu with selected PGE to compare their affinities to those in other mafic and ultramafic rocks.

V.5.5.1. Correlations between chromium and some PGE

Scattered plots reveal strong positive correlations between Rh, Ru, Pt and Pd with Cr in weathered amphibolites (Fig. 60a to d). This confirms the findings of that chromium and PGE are associated in mafic and ultramafic rocks.

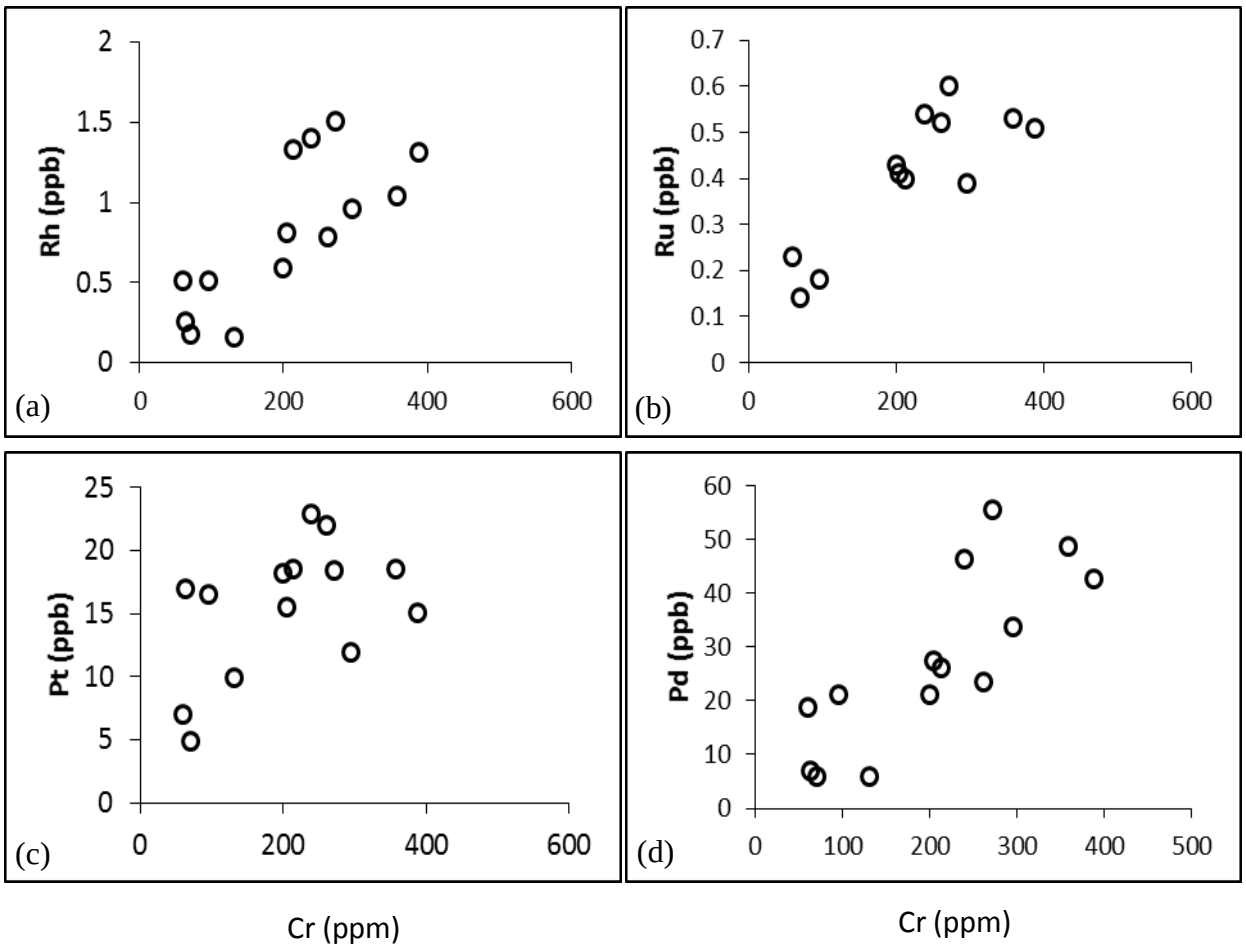

Figure 60 : Scattered plots of chromium and some PGE in weathered amphibolites.

V.5.5.2. Correlations between copper and selected PGE

Copper is positively correlated with Pt, Pd and palladium –like platinum group elements as a whole (Fig. 61a, b and d). On the contrary, Cu has to correlations at all with the iridium-like platinum group elements (Fig. 61c).

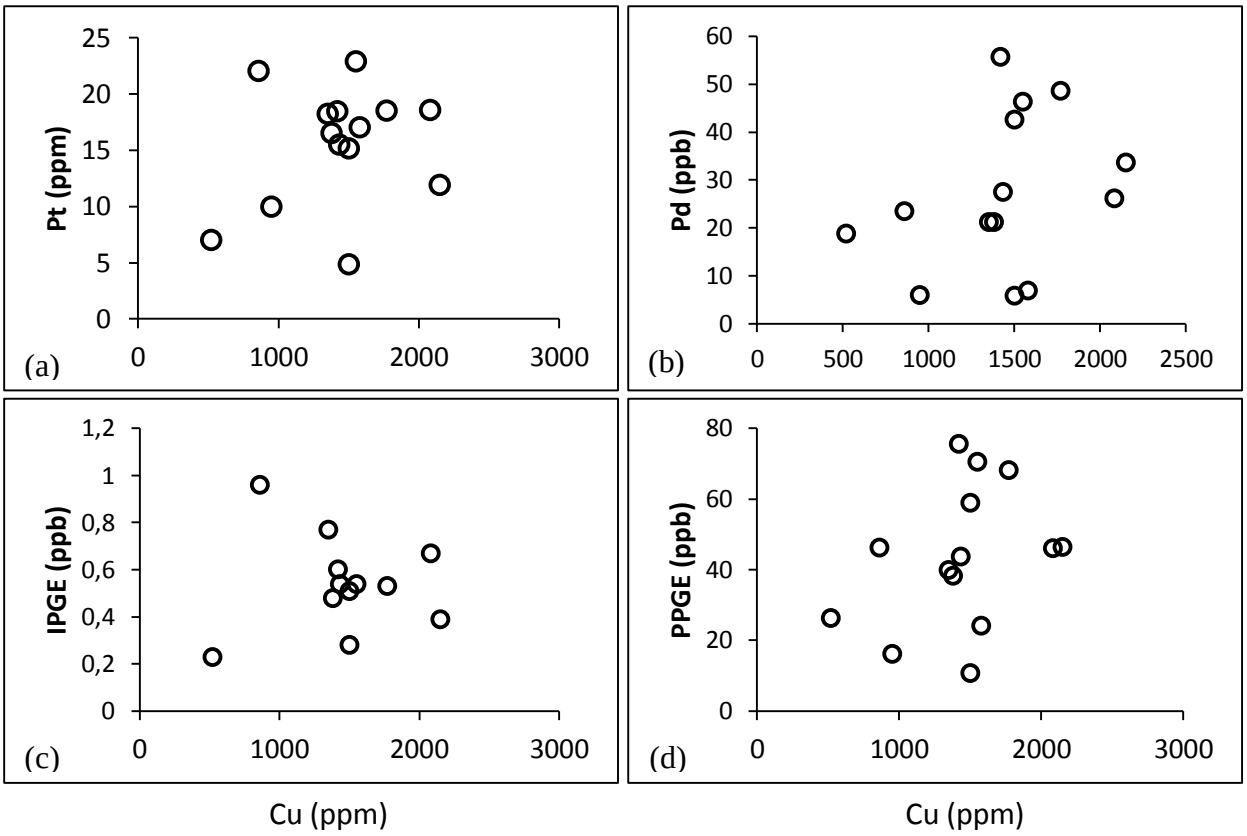

Figure 61 : Scattered plots of chromium and some PGE in weathered amphibolites.

V.5.5.3. Correlations between nickel and selected platinum group elements

Plots of nickel and platinum group elements reveal positive correlations between Ru (IPGE) and Ni (Fig. 62a). Similarly nickel has positive correlations with all the palladium – like platinum group elements (Fig. 62b, c and d). The positive correlation of Ni-PGE may suggest that these metals were originally components of a primary mineral assemblage (Zaccarini *et al.*, 2014)

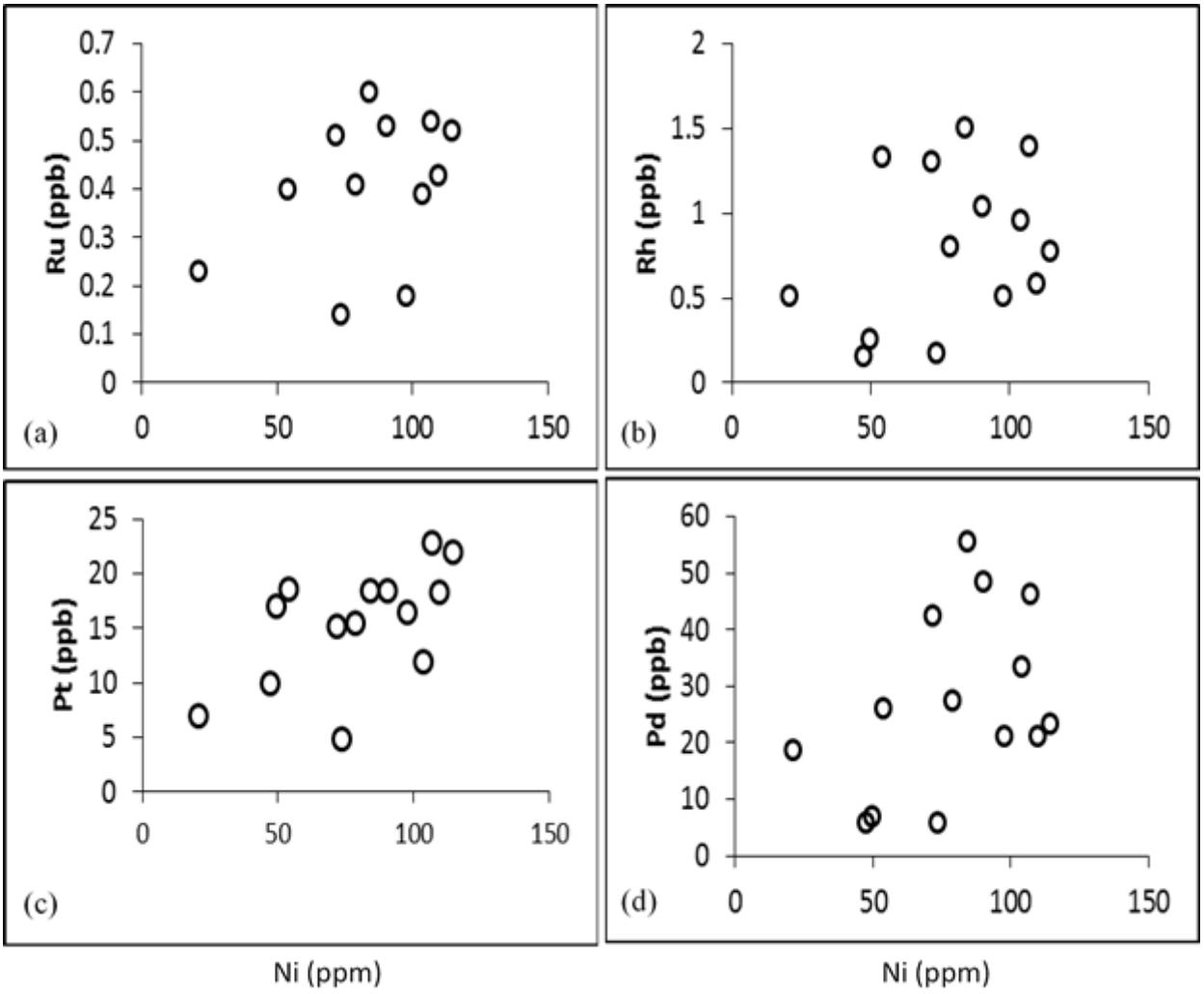

Figure 62 : Scattered plots of nickel and some PGE in weathered amphibolites.

V.5.5.4. Correlations between major elements and selected platinum group elements

Silica generally has very weak correlations with platinum group elements in weathered amphibolites. It has slight negative correlations with Rh, Ru and Pd (Fig. 63a, b and c). Silica rather has slight positive correlations with platinum (Fig. 63d). The PPGE have very small negative correlation with silica, while the IPGE do not correlate at all with silica (Fig. 63e and f).

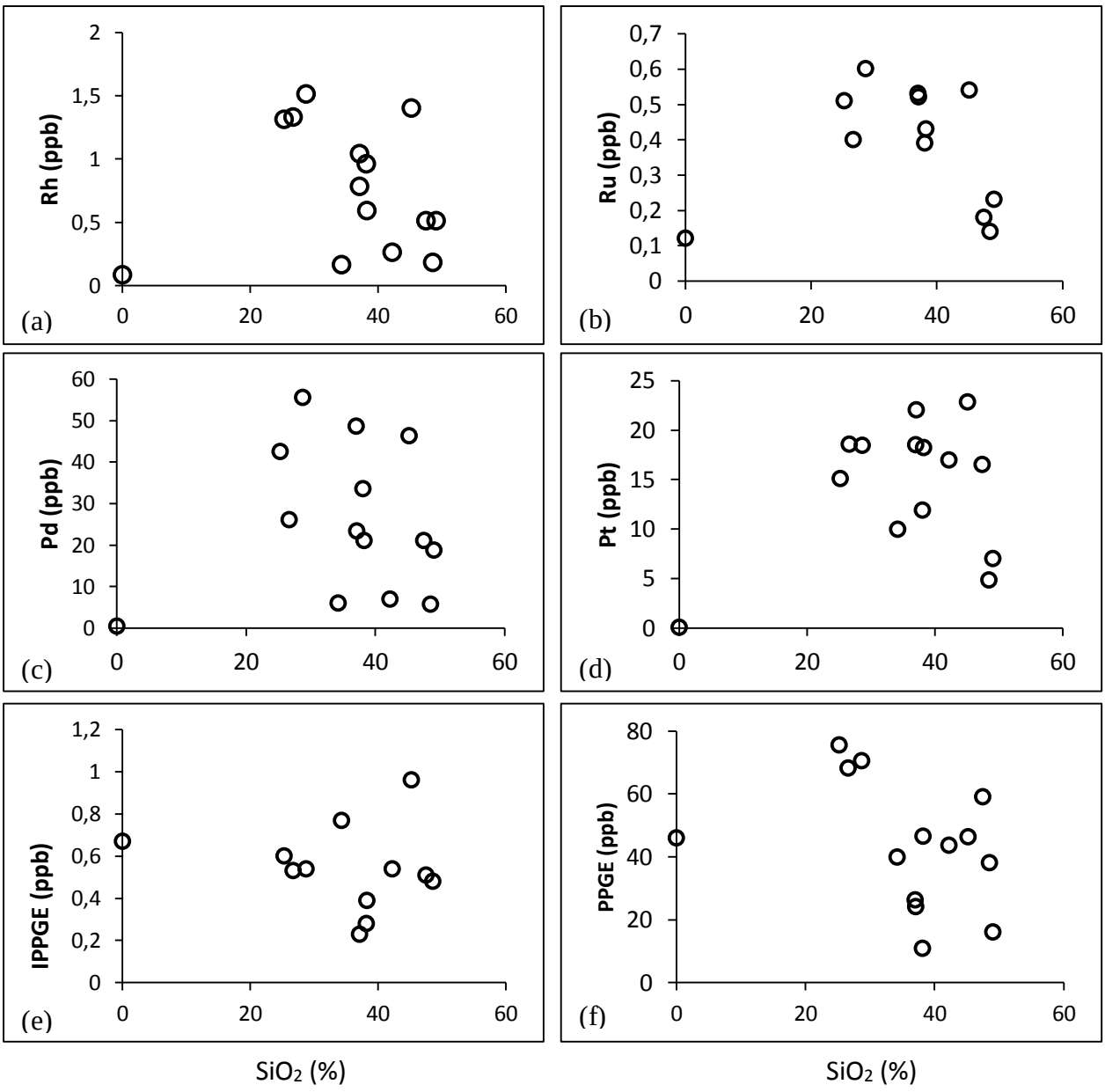

Figure 63 : Scattered plots of silica and some PGE in weathered amphibolites.

V.5.5.5. Correlations between alumina and selected platinum group elements

Ruthenium alone has negative correlations with alumina (Fig. 64). Rhodium, platinum and palladium form positive correlations with alumina (Fig. 64a, c and d). The iridium-like platinum group elements show only slight positive correlations with alumina, whereas the palladium-like platinum group elements have stronger positive correlations (Fig. 64e and f).

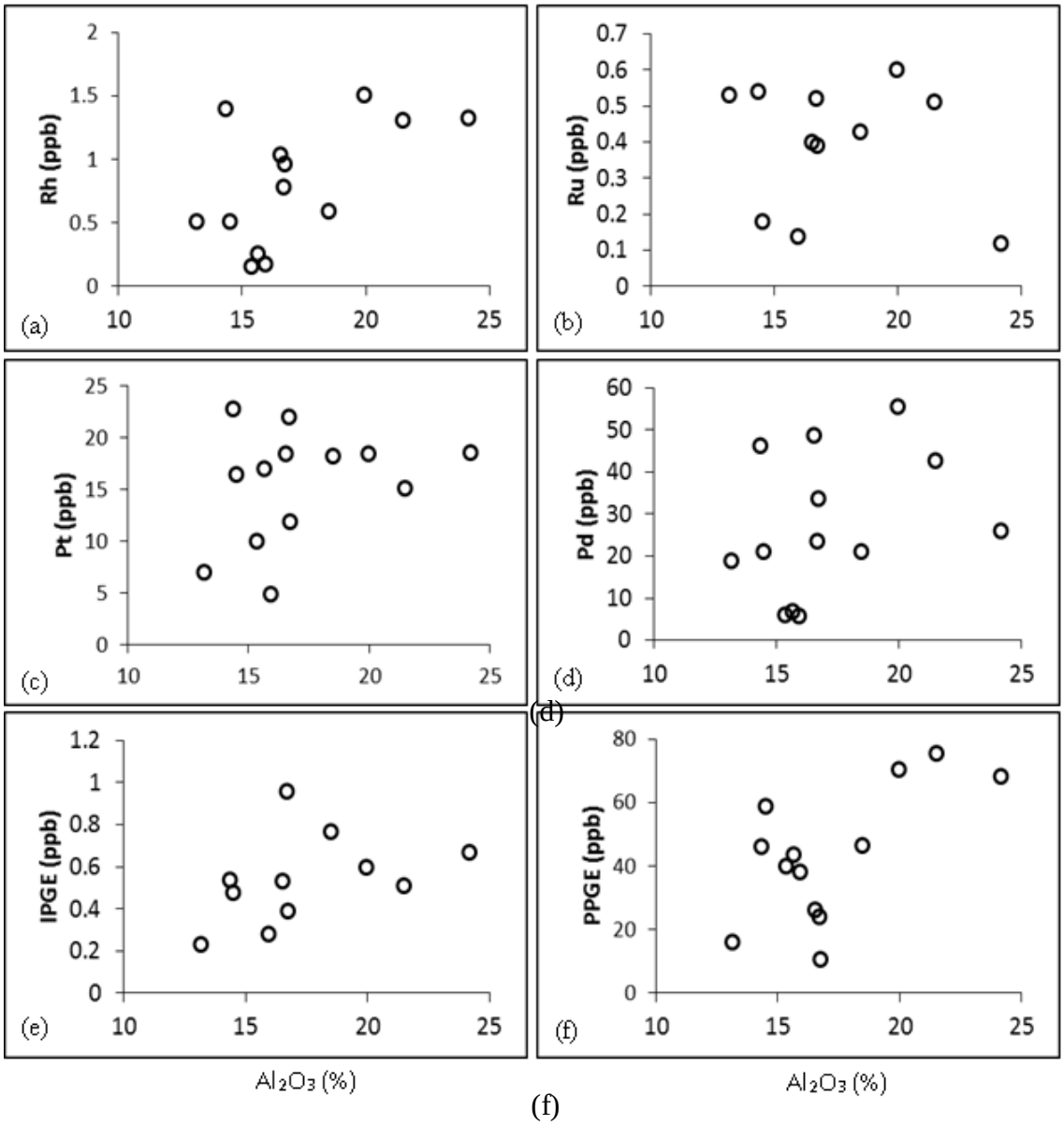

(c) (d)

(e) (f)

Figure 64 : Scattered plots of alumina and some PGE in weathered amphibolites.

V.5.5.6. Correlations between ferrous iron and selected platinum group elements

Scattered plots reveal ruthenium as the only PGE that correlates positively with ferrous iron (Fig. 65a). Rhodium, platinium and palladium donot correlate with ferrous iron (Fig. 65c and d). The IPGE and the PPGE both have very weak positive trends with ferrous iron (Fig. 65 e and f).

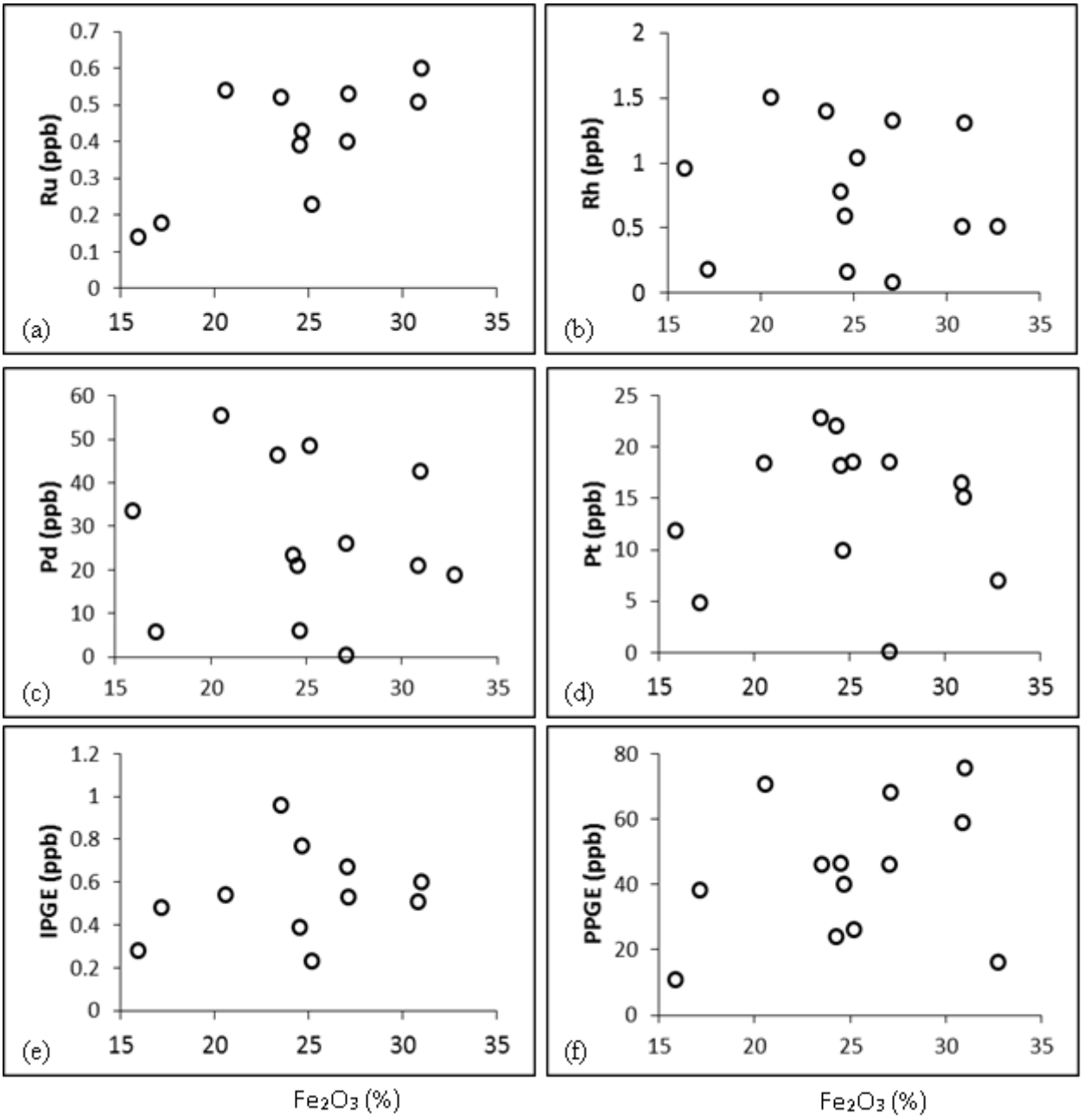

Figure 65 : Scattered plots of ferrous iron and some PGE in weathered amphibolites. (a) Fe2O3 vs Ru; (b) Fe2O3 vs Rh; (c) Fe2O3 vs Pd; (d) Fe2O3 vs Pt; (e) Fe2O3 vs IPGE; (f) Fe2O3 vs PPGE.

V.5.5.7. Correlations between MgO and selected platinum group elements

Only ruthenium represents slight negative correlations with magnesia (Fig 66a). Magnesia does not correlate at all with rhodium, platinum, and palladium (Fig 66 b, c, d). It does not also show any correlation with the IPGE and the PPGE in weathered amphibolites (Fig 66 e and f).

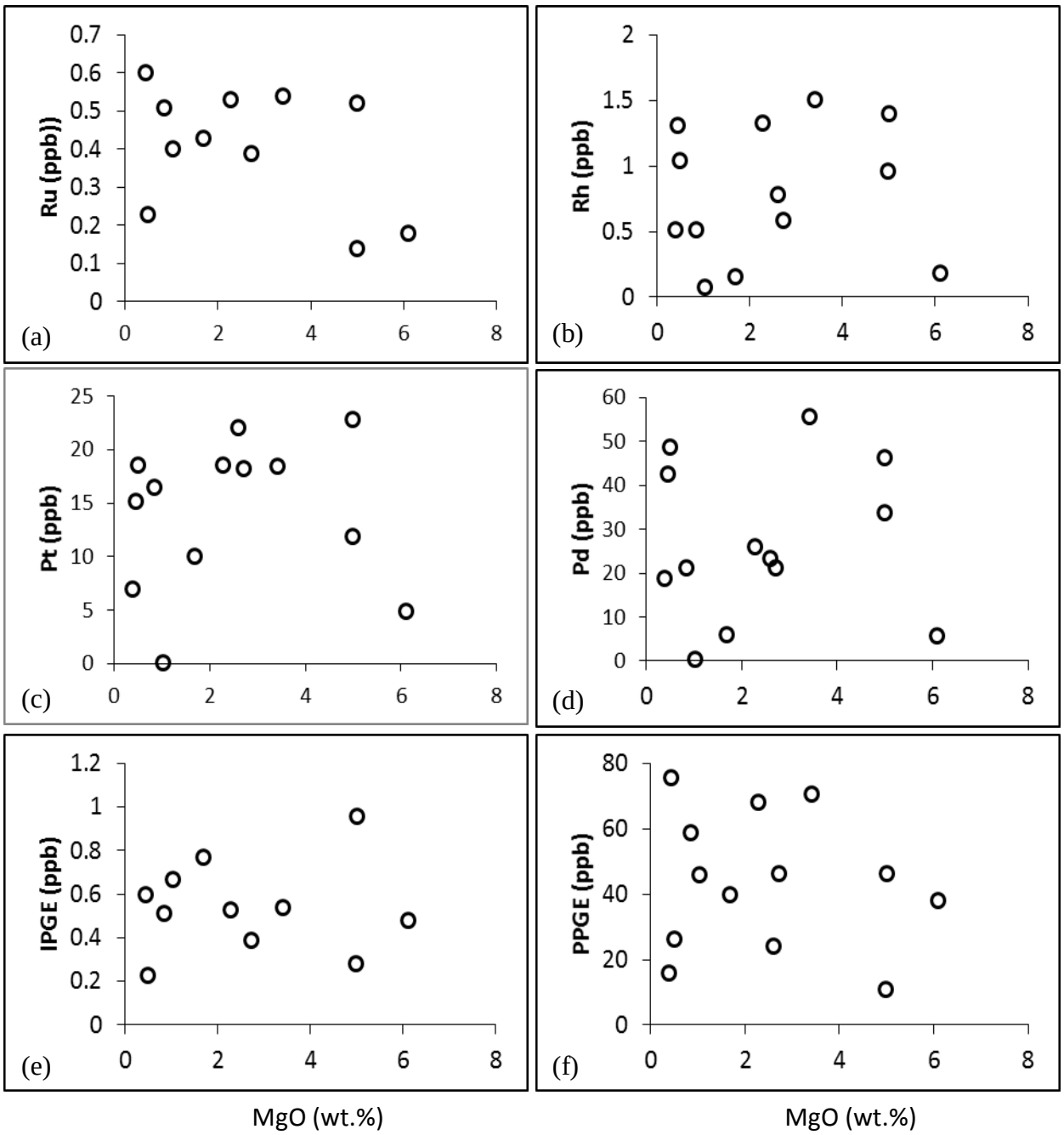

Figure 66 : Scattered plots of MgO and some PGE in weathered amphibolites. (a) MgO vs Ru; (b) MgO vs Rh; (c) MgO vs Pt; (d) MgO vs Pd; (e) MgO vs IPGE: (f) MgO vs PPGE.

Gold, Ru, Rh, Pt, Pd, and Cr are positively correlated on the Grant's isocon diagram (Grant, 1986; 2005), which is used to graphically identify the most immobile elements (Fig. 67). The diagram confirms PGE-enrichment in the weathered samples revealed by the chondrite- normalized base metal patterns (Fig. 67). Osmium, Ir, Au, Ru Rh, Pt, Pd, and Cr show enrichment, while Ni, Cu and S are slightly depleted (Fig. 67).

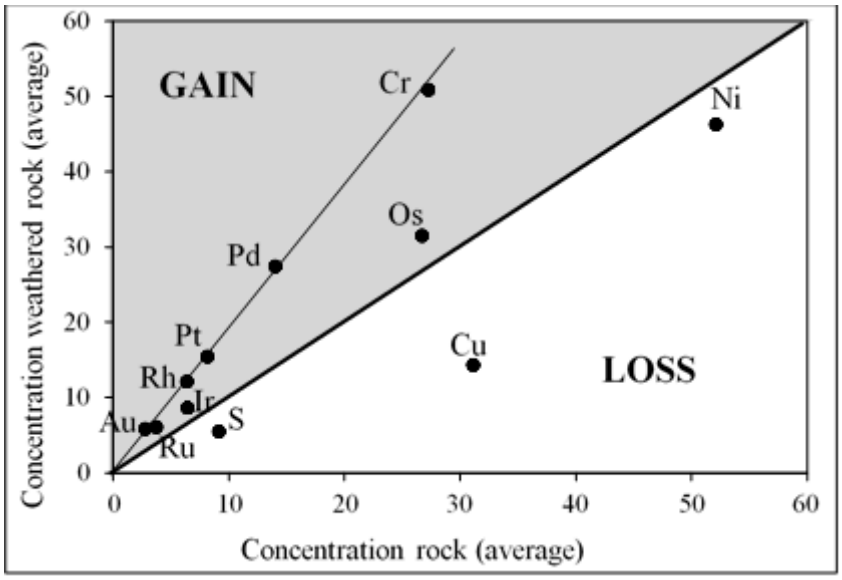

Figure 67 : Grant diagrams of weathered samples vs. amphibolites.The diagrams are constructed for S, Cu in ppm/100, Ni in ppm/1.7, Cr in ppm/4, Os in ppb*200, Ir in ppb/50, Ru, Rh in ppb*15, Pt, Pd and Au in ppb.

Conclusion

Two amphibolite types were distinguished based on sulphur contents; those with high S contents (Average = 1370 ppm) and others with low S contents (average of 457 ppm). Nickel concentrations vary from 50.5 to 121.9 ppm. The concentration of copper in amphibolites varies from 1800-5350 ppm (average =3069 ppm). Sulphur correlates positively with Cu, Ni, and Cr; and negatively with Ni/Cr ratio.

The total Au-PGE contents of amphibolites are low. They are particularly enriched in Pd and Pt. Gold contents are low and variable. The Au-PGE contents are low with respect to chondrite. The rocks are very rich in PPGE than IPGE. The mobility ratios of Au-PGE are very high (Pd/Ir = 4155; Pd/Ru = 170). Selected PGE groups have strong correlations with Cr and MgO. Sulphur correlates positively with Cu, Ni and Cr and negatively with Ir, Ru, Au and Ni/Cr ratio. The Au-PGE spectra show positive Pd anomalies and negative Pt and Ru

anomalies for samples from Nyabitande. Whereas, spectra of Zingui amphibolites all show negative Pd anomalies. Base metal patterns show a strong enrichment in Cu and Ni relative to Au-PGE and slight accumulation of Rh, Pt, Pd and Au relative to Os, Ir and Ru.

The weathered samples are marked by variable S and Cu contents**.** The hydrothermal alteration led to the leaching of sulphur, nickel and Chromium. Thus contents of these elements are rather low compared to those of the fresh rocks. The Au-PGE contents are higher in weathered samples compared to those of fresh ones. Platinum is more mobile than Pd contrary to Ir, Rh, and Ru

The chondrite-normalized base metal patterns reveal high enrichment in Cu, Pd and Ni. With respect to the fresh rocks, Os, Ir and Ru are depleted. Gold, Ru, Rh, Pt, Pd, and Cr are positively correlated on the Grant's isocon diagram. According to this diagram, Os, Ir, Au, Ru Rh, Pt, Pd, and Cr show enrichment, while Ni, Cu and S are slightly depleted. The mass balance assessment also shows that S, Ni and Cu have been leached out of the weathered amphibolites.

CHAPTER VI : DISCUSSION

Introduction

The main objective of this work was to carry out petrologic studies on amphibolites and their weathered products. Also, the content of a mafic country rock was to be investigated and compared with those of amphibolites. This is achieved in three ways. Firstly, the petrography of the rock is examined. Secondly, to investigate the carrier minerals for gold and platinum group elements in these rocks through mineralogical studies. Finally, to understand the behaviour of major, trace, rare earth elements as well as sulphur, gold and platinum group elements, through geochemical survey.

Different results have been obtained from the above analyses. This chapter handles firstly the presentation of the main results, then an attempt of discussion on the findings.

VI.1. RECAPITULATION OF MAIN RESULTS

VI.1.1. Amphibolites

Amphibolites are medium-grained, melanocratic and dense rocks. They are made up of amphibole, plagioclase, garnet, quartz, apatite, chalcopyrite and pyrite. They generally present a granoblastic heterogranular texture.

Among the major elements, SiO_2, Fe_2O_3 and Al_2O_3 are the most abundant oxides in amphibolites. Contents of CaO and MgO are moderate. The rocks have very low contents in alkalis, P_2O_5 and MnO. However, TiO_2 contents are particularly high in amphibolites of Kolasseng II. Geochemical variations between major oxides reveal positive correlation for SiO_2 with alkalis; MgO with Fe_2O_3 and CaO. MnO and P_2O_5 also correlate positively with selected major oxides. Nevertheless, there are negative correlations between TiO_2 and major oxides. Amphibolites have high contents of Cr, V, Zn, Ba and Sr, these contents attain several hundreds of ppm. The contents of other trace elements are rather low. The rocks from Zingui area have higher Cr, Sr and Ba contents. Contents of rare earth elements are generally low in amphibolites. The total REE contents vary between 36 and 272 ppm. Despite these low contents, the rocks are marked by enrichment in light rare earth elements (25- 226 ppm) than the heavy rare earth elements (11-46 ppm). The values of the LREE/HREE ratios are low (1.70 and 4.87). Cerium and neodymium contents are the most representative; they attain 97 and 55 ppm respectively. The normalization of REE with respect to chondrite for amphibolites reveals negative europium anomalies and slight negative cerium anomalies for

selected samples. The amphibolites from Zingui area are richer in contents of REE than those from Nyabitande.

Two amphibolite types were distinguished based on sulphur contents; those with high S contents (Average = 1370 ppm) and others with low S contents (average of 457 ppm). Nickel concentrations vary from 50.5 to 121.9 ppm. The concentration of copper in amphibolites varies from 1800-5350 ppm (average =3069 ppm). Sulphur correlates positively with Cu, Ni, and Cr; and negatively with Ni/Cr ratio. Contents of Au-PGE in amphibolites are variable (2-113 ppb). Palladium and platinum have the highest contents (Pd + Pt = 109 ppb). Au-PGE normalization reveal positive palladium and negative ruthenium anomalies (Pd/Pd*= 4.14. The rocks are several times richer in PPGE than IPGE.

The mobility ratios of Au-PGE are very high (Pd/Ir = 4155; Pd/Ru = 170). PGE show strong positive correlations with Cr and MgO. Sulphur has no correlation with Pd, Pt and Rh. It is rather positively correlated with Ir The chondrite-normalized (McDonough and Sun, 1995) base metal patterns show a strong enrichment in Cu and Ni relative to Au-PGE.

VI.1.2. Granodiorites

Granodiorites are light coloured rocks with abundant plagioclase crystals, orthoclase, epidote, amphiboles and accessorily zircon, apatite, sphene and opaque minerals. They have high SiO_2 (68.07 wt. %) and Al_2O_3 (15.28 wt. %) contents. The other oxides have very low contents. Amidst the low trace element contents, Sr (638.80 ppm) and Ba (665.60 ppm) contents are very high. As concerns rare earth elements, only cerium (40.89 ppm), lanthanum (12.60 ppm) and neodymium (9.61 ppm) have high contents. However, the rocks are richer in LREE with positive cerium and slight negative europium anomalies.

VI.1.3. Pyroxenites

Pyroxenites are melanocratic rocks with a granoblastic equigranular texture. They are composed of pyroxene, plagioclase feldspar, biotite, garnet, amphibole and accessorily quartz and opaque minerals. They have high SiO_2 (56.56 wt. %) and Al_2O_3 (21.04 wt. %) contents. The contents of other oxides are low. Pyroxenites have variable trace element contents. Nevertheless, they show outstanding Sr (1008.60 ppm) and titanium (9,575 ppm) contents. The total REE content of pyroxenites reaches 215 ppm. The rocks are richer in LREE (207 ppm) than the HREE (7.7 ppm). Pyroxenites have very low sulphur contents, which are less than 1 ppm (0.046 ppm). Nickel contents are rather higher in pyroxenites (132.0 ppm) than in amphibolites. The contents of Cu (2820 ppm) are high while those of Au-PGE attain 50.35

ppb. These Au-PGE contents are comparatively lower than those of amphibolites. The normalised patterns are strongly enriched in PPGEwith positive Pd and negative Ru anomalies.

VI.1.4. Weathered amphibolites

The weathered amphibolites occur as dense centimetric blocks that have undergone variable stages of weathering. The weathering is intense on the outside with relatively fresh interior. The mineral assemblage is made up of amphibole, feldspars, quartz, garnet, kaolinite, gibbsite, goethite, hematite, and spinel.

The weathered amphibolites experienced some relative accumulation and depletion of materials during weathering. We observe an evacuation in SiO_2 and CaO contents and a slight loss in contents of MgO, Na_2O, TiO_2 and MnO during weathering. On the contrary, there was a gain in Fe_2O_3 within the weathered blocks. Binary diagrams show positive correlation of silica and Fe_2O_3 with selected trace elements. They generally have low contents of trace elements. However, there are slight enrichment of trace elements like Zr, Ba, Th, U, and Mo within weathered amphibolite blocks.

Amidst trace elements, there are strong affinities as well as incompatibilities. Chromium Cu and Zr show strong positive correlations with selected trace elements. Primitive mantle normalized (McDonough and Sun, 1995) patterns show pronounced positive anomalies in V, Cu, Pb and Zr; and distinct negative anomalies in Ni, Co, Sr, Th and Li.

The weathered amphibolites have overall low contents in REE. The fresh rock normalized patterns for fine, medium and coarse grained weathered amphibolites reveal positive and negative cerium and Eu anomalies.

The mass balance assessment of weathered materials show a strong leaching of most major element. However, iron, Magnesium, potassium and Phosphorus are more enriched comparatively. Most trace elements (V, Zn, Co, Sc, Ga, Y, and Nb) have been leached out from the weathered materials. Cr, Zr and U and slightly remobilized, while Pb, Mo, Rb and Ba are strongly enriched within the materials. There is a strong leaching of rare earth elements in all the weathered materials, the HREE are more leached out than in the LREE.

The weathered samples are marked by variable S and Cu contents**.** The S contents (239 - 902 ppm) are rather low compared to those of the fresh rocks. Cu contents range from 520 to 2150 ppm. Ni contents are low, ranging from 109 to 114 ppm. Sulfur correlates positively with Cr and Cu, but negatively with Ni.

The Au-PGE contents are higher in weathered samples than the fresh ones. Ir, Ru, Rh and Au have high mobility ratios with respect to Pd. Hence, palladium is the least mobile element within the weathered blocks. The chondrite-normalized base metal patterns reveal enrichment in Cu, Pd and Ni in the weathered rocks. With respect to the fresh rocks, Os, Ir and Ru are depleted. Also, according to the Grant's isocon diagram Osmium, Ir, Au, Ru Rh, Pt, Pd, and Cr show enrichment, while Ni, Cu and S are slightly depleted. The mass balance assessment also shows that S, Ni and Cu have been leached out of the weathered materials. However, the PPGE are strongly enriched in some materials. Scattered plots reveal strong positive correlations between Rh, Ru, Pt and Pd with Cr in weathered amphibolites. While Cu is positively correlated with Pt, Pd and PPGE.

VI.2.Discussion

VI.2.1. Petrology of amphibolites

VI.2.1.1 Petrography

Petrographic studies suggest that studied garnet amphibolites from Akom II area are medium-grained, dark-coloured, and dense rocks with granoblastic heterogranular texture. This petrography is consistent with that of metabasite samples from the Chitrangi Region, Central Indian Tectonic Zone (Srivastava, 2012). The presence of garnet would suppose pressures of N10 kbar (e.g. Wolf and Wyllie, 1994; Shang *et al*., 2010). The presence of sulfide minerals (chalcopyrite and pyrite), sericite and to a lesser extent apatite in garnet amphibolites suggest that they might be affected by hydrothermal events (Sharrad *et al*., 2014). Also, the absence of actinolite amphibole which is a common product of retrograde metamorphism of basalts shows that these amphibolites resulted from a prograde metamorphism (Winter, 2001).

VI.2.1.2. Major and trace elements Geochemistry

Amphibolites and pyroxenites of Kolasseng II both show increasing silica content with a corresponding decrease in magnesia contents. This is a common characteristic of rocks in the Neoarchean greenstone terrains (Barnes *et al*., 2007; Manikyamba *et al*., 2008). The low CaO, Na_2O, K_2O and TiO_2 contents in amphibolites of Nyabitande are consistent with those of the ultramafic rocks of Pindar (Balaram *et al*., 2013). These contents suggest a high degree of partial melting from the depleted mantle source, which prevailed during the development of the rocks. Cr, V, Zn, Ni, Cu, and Co have significant contents. The low contents in several

major and trace elements including REE confirm the basic nature. The variability in trace element contents is probably due to the remobilization or to different levels of crustal emplacement (Ukaegbu and Ekwueme, 2007). The relatively high contents in some compatible and incompatible trace elements (Cr, Ni, Zn Zr Co, Sc and Y) may be due to remobilization during the formation of secondary minerals (Sharma and Rajamani, 2000). These contents attain several hundreds of ppm, and contents of strontium vary from 90 to 242 ppm. The differing Sr contents may be a reflection of the differences in the proportion of plagioclase in the residue during partial melting or fractional crystallization (Ukaegbu and Ekwueme, 2007). The high Sr and Ba contents are considered to be the result of partial melting of eclogite facies basaltic crust (Rapp, 1997). The light REE-enrichment and heavy REE depletion followed by high concentrations of Cr and Ni indicate that the source magmas were generated by melting in the mantle (Stern, 1981). The wide range of major oxides and large ion lithophile elements (Sr, Ba, Rb, K, Sc) confirm the involvement of post-magmatic processes like metamorphism, metasomatism and hydrothermal alteration (Srivastava, 2012). This is because LILE (such as Sr, K (alkalis), Rb, Ba, Sr, etc.) are thought to be mobile during the post-magmatic processes (Seewald and Seyfried, 1990; Verma, 1992; Condie and Sinha, 1996).

VI.2.1.3. Rare Earth Elements

REE contents in garnet amphibolites are generally low. This suggests that they are derived from a more fractionated part of melts or low degree partial melts (Shang *et al*., 2004). In fact, highly fractionated REE compositions have been reported from many areas (e.g. the central Andean rocks) and interpreted as a result of residual garnet in the sources (e.g. Kay *et al*., 1994; Mpodozis *et al*., 1995; Kay and Abbruzzi, 1996). The low values may also be linked to hydrothermal alteration processes within amphibolites. The minimal values (less than 1) for Ce/Ce* and Eu/Eu* stipulates an impoverishment in rare earth elements during hydrothermal alteration processes (Seme Mouangué, 1998).

The negative cerium anomalies may be linked to its mantellic origin, which is due to the mixture of sea water and weathered basalts in the mantle or better still due to variations in the oxidation-reduction potentials of the environment where the rocks occur (Neal and Taylor, 1989). The negative Ce-anomalies could also suggest the removal of Ce during hydrothermal alteration. While the negative Eu-anomalies could be linked to the plagioclase fractionation (Lee *et al*., 2009), The low LREE/HREE ratios observed in the rocks could be related to the

partial melting phenomena of source protoliths (Bilong *et al*., 2011) with garnet among the residual phases (Nzenti *et al*., 2006). The sample K4 with high LREE contents may not experience these phenomena. The Eu negative anomaly associated with light rare earth elements (LREE) enrichment depicts the evolution of the rocks initially through fractional crystallization (Balaram *et al*. 2013). Leybourne *et al*. (2006) showed that the negative Eu anomalies are the result of an intense fractionation of REE. The high degree of fractionation of REE is confirmed by the depletion in HREE (Nedelec *et al*., 1990). This indicates the melting of source rocks with garnet as a restite phase (Shang *et al*., 2004). Amphibolite samples show very flat REE patterns suggesting that these were derived from a melt generated from a depleted mantle source (Srivastava, 2012). In contrast, amphibolite samples from Zingui show inclined REE pattern, enriched LREE and depleted HREE suggesting their derivation from some enriched mantle source. From REE plots it is very clear that the Nyabitande and Zingui amphibolites do not have any genetic relationship but have different petrogenetic history (Srivastava, 2012). It is observed that samples derived from a crustally contamination melt show enriched LREE and flat HREE patterns (Srivastava, 2012). This is consistent with amphibolite samples from Zingui and indicates a possible contamination of their source. REE concentrations in rocks of Kolasseng II are about twice higher than those of pyroxenites of Lolodorf (Ebah Abeng, *et al* 2012) and more than ten times higher than those of serpentinites of Lomié ultramafic complex (Ndjigui, 2008).

VI.2.1.4. S, Cu, Ni and Au-PGE

The sulfur content of the investigated rocks could also be related to the S contents of the silicate magma (Wallace and Carmichael, 1992). Hydrothermal events affected the distribution of sulphur. Thus, the low sulphur contents may be due to a first episode of hydrothermal activities. However the relatively higher sulphur values (1705 ppm) suggest another episode of hydrothermal activities rich in S (Puchtel *et al*., 1995).

The samples that have undergone the maximum sulphur removal are not necessarily those that have the highest PGE and other base metal contents. These observations imply that the processes that triggered the S removal and the PGE and base metal enrichment or remobilization are probably distinct (Godel and Barnes, 2007; Godel *et al*., 2007). Otherwise, direct measurement of sulphur contents in samples has in many cases been considered unreliable because of the volatile and mobile nature of S which is lost during magma degassing or low temperature alteration (e.g., Bai *et al*., 2012; Naldrett *et al*., 2012).

The high Cu contents are also associated to different episodes of the hydrothermal fluids (Zhou *et al*., 2004) or might be result to the presence of chalcopyrite ($CuFeS_2$) (Godel *et al*., 2007). The low Ni contents and the Ni/Cr values may reflect the lack of Ni-bearing minerals like olivine in garnet amphibolites (Sababa *et al*., 2015). In addition, Ir, Pd and Cu are strongly partitioned into sulphide phases compared to Ni, Cu and Zr, respectively, under S-saturated conditions (Shellnutt *et al*., 2015). The mineralization episodes may be syn-metamorphic in origin or alternatively, they are part of a pre-metamorphic event and underwent recrystallization during metamorphism (Sharrad *et al*., 2014).

Garnet amphibolites are richer in Pd, Pt, and Au compared to other mafic-ultramafic rocks (Gueddary *et al*., 1994; Ebah Abeng *et al*., 2012; Sababa *et al*., 2015). Alard *et al*. (2000) showed that during partial melting of the mantle, base metal sulfides (BMS) melt incongruently to produce Cu-Ni-rich sulfide melt that concentrates Pd and Pt. Godel and Barnes (2007) explained the high Pd and to a lesser extent Pt enriched samples (high Pd/Pt or Pd/Ir ratios, e.g., K13). According to these authors, during hydrothermal alteration, a new fluid percolated through the cumulate pile and removed Pd and Pt from the footwall. As the fluid migrated, it could have reacted with the sulfides and precipitated Pd and Pt in the reef. This similar signature suggests that the high Pd and Pt contents in garnet amphibolites could have been leached out from other sources. This may also suggest that Pd could be distributed in sulfide minerals (Paśava *et al*., 2010) or can be transported as bisulfide complexes in acidic-neutral solutions under reduced and moderate oxidation conditions at 300 °C (Barnes and Liu, 2012) or are disseminated in the whole rocks. The large Ir depletion in the amphibolites of Zingui and the overall Ir-depleted character of other rocks from the Nuasahi Massif, may be related to multiple episodes of melt extraction from the mantle source, giving it a subchondritic character (Khatun *et al*., 2014). The garnet amphibolites of present overall low Au-PGE contents which often attain only tens of ppb, particularly low Os, Ir, Ru, and Rh contents. These contents are similar to other findings on Au-PGE in southern Cameroon (Ebah Abeng *et al*., 2012). The depletion of Au-PGE could result from the mobility of PGE during hydrothermal alteration (Ahmed *et al*., 2009). The strong depletion of these elements can also be attributed to retention of IPGE in the metal alloys of the original magma (Barnes *et al*., 1995) or, a prior segregation of a first sulphide liquid rich in PGE from the original magma leaving the remaining liquid poor in PGE (Barnes and Lightfoot, 2005).

The PGE data confirm the heterogeneity of PGE distribution in the Earth's mantle (Xu *et al*., 1998). The low PGE contents suggest that the garnet amphibolites formed from the silicate magma that had already experienced prior-sulfide separation (Song *et al*., 2009), or

the low proportion of PGE-carriers (Lorand and Alard, 2001) or to the depletion during hydrothermal events (Satyanarayanan *et al*., 2011; Hao *et al*., 2014).

Garnet amphibolites are enriched in PPGE over IPGE. According to the recent works (Ahmed *et al*., 2009; Ismail *et al*., 2010), the high difference in the contents of PPGE and IPGE may be due to PGE fractionation. All the amphibolites from Kolasseng (Nyabitande) are depleted in Ir, Ru, Rh, and and Os. These low PGE contents may be due to a low degree of partial melting (Baumgartner *et al*., 2012). The low Ir, Ru, and Rh contents could also be due to their extremely limited hydrothermal mobility (Barnes and Liu, 2012). The low IPGE contents might be also caused by an increase in oxygen fugacity (Auge and Legendre, 1994; Fonseca *et al*., 2009). The high PPGE enrichment is possibly due to partial melting of the upper mantle under ultra-high temperature metasomatic conditions. The fact that the rocks are poor in IPGE compared to Pt and Pd show that Pt and Pd were enriched by hydrothermal fluids, since the IPGE are considered as relatively immobile in fluids compared to Pt and Pd (Mountain and Wood, 1988; Hsu *et al*., 1991; Fleet and Wu, 1993). The high Pd/Ir ratios confirm a hydrothermal origin (Bleeker, 1990). The positive correlation between S and iridium does not hold for any of the other PGE or Copper. This would seem to indicate that iridium is not fractionated from sulfur minerals under a wide range of conditions that lead to the mobilization of sulfides in the rock (Good and Naldrett, 1993), the absence of correlation between Au-PGE but for Ir may suggest that Au-PGE mineralization is not associated with sulphides (Gomwe T, 2008). The contrast behaviour of Au-PGE and S seems to indicate that the garnet amphibolites were affected by another hydrothermal episode deposition containing PGE in the Green Stone Belt of Southern Cameroon. The garnet amphibolites from the Green Stone Belt are enriched in Pd and Cu, and depleted in Ni and Ir, similarly to that of the Proterozoic Donaldson West and Katiniq deposits of the Cape Smith Belt (Good and Naldrett, 1993). The amphibolites of the Green Stone Belt exhibit more fractionated Pd/(Pd+Pt) and Cu/(Cu+Ni) ratios than those of the Thompson Belt. However, both belts show similar less fractionated Pd/Ir ratios (Good and Naldrett, 1993).

The positive correlations of PGEs with MgO, and the IPGEs with Cr, show that the PGEs are immobile despite the low-grade metamorphism in the rocks (Mondal and Zhou, 2010). The Pd/Ir, Ru/Ir, and Pd/Pt ratios reflect the fractionation between the platinum -group of elements (Barnes *et al*., 1985). It can also be observed that the mobility of iridium is extremely higher than those of the other PGE and gold, while platinum is the least mobile of PGE. These high ratios have been attributed to the introduction of Pd by late magmatic–hydrothermal fluids (Djon and Barnes, 2012).

Good correlations of Ir and Ru with Cr are noted in all types of chromite occurrences like the Archean high-grade complexes, Archean greenstone belts, layered intrusions (e.g., Mathez, 1999 and references therein). The absolute concentration of the IPGE (e.g., Ir and Ru) in the ultramafic and mafic rocks and their correlation with MgO and Cr implies that both Ir and Ru were compatible and fractionated by the early crystallizing phases, namely chromite (e.g Puchtel *et al*., 2004; Barnes and Fiorentini, 2008; Mondal and Zhou, 2010), or by Ir–Ru-bearing alloys hosted within these minerals. Progressive decrease in Ru/Ir ratio with MgO for the amphibolites further implies that Ru was more compatible in chromite relative to Ir.

VI.2.2. Petrology of granodiorites

Granodiorites of Zingui form part of the Tonalite-Trondhjemite-Granodiorite (TTG) suit of rocks from the Nyong Paleoproterozoic unit (Ntem Group). The SiO_2 concentrations for granodiorites (68 wt.%) indicates their felsic composition. These concentrations are consistent with the intermediate and acidic classifications of the Sangmelima TTG suite, and indicate fractional crystallization as the origin of the rock suites (e.g., Nédélec *et al*., 1990, Shang, 2001). This silica percentage is consistent with those of the Ford Granodiorite suite described by Korhenen *et al*. (2010). They show low-MgO (1.10 wt.%) and high SiO_2 (68.07 wt.%) contents. These low MgO, high SiO_2 TTG rocks can be interpreted to be the more fractionated part of the TTG magma (Smithies, 2000). However it is generally argued that low MgO, high SiO_2 rocks might not have interacted with the peridotitic mantle wedge, implying for instance their genesis in a flat subduction regime (e.g. Smithies *et al*., 2003). The Sangmelima granodiorites also show lower MgO, higher SiO_2 composition (Shang *et al*., 2004). These were explained as consistent with melting of hydrous basaltic material at the base of the Archaean crust under a typical Archaean geotherm, a case that would be similar to the Pilbara craton (e.g. Bickle *et al*., 1993).

The Zingui granodiorites are similar to those of Sangmelima region (Shang *et al*., 2004), they are also similar to worldwide TTG complexes (e.g. Barker and Arth, 1976; Barker, 1979). They are intermediate to felsic and aluminous rocks with high Sr and Ba values, these are considered to be the result of partial melting of garnet amphibolite or eclogite facies basaltic crust (e.g. Tarney *et al*., 1976; Martin, 1986; Drummond and Defant, 1990; Rapp, 1997).

The Zingui granodiorites have an overall low REE contents, they are richer in LREE and show a strong HREE depletion. The low REE abundance and strong depletion in HREE is

probably an inherited feature from the TTG protolith (e.g. Shang *et al*., 2007). These possibly represent rocks derived from felsic melts (Shang *et al*., 2004). The low REE contents and depletion in HREE, could also represent cumulative feldspar rich fractions, or low degree partial melts as indicated by high silica content. In general granodiorites that are more felsic display LREE enrichment and this could be explained by the fact that LREEs are incompatible during fractional crystallization of tonalitic/granodioritic melts (Shang *et al*. 2004). These REE characteristics suggest that the granodiorite magmas could have been formed within the stability field of garnet.

VI.2.3 Petrology of pyroxenites

Pyroxenites are made up of moderate contents in silica and high contents Cr, V, Zn and Ni, these are characteristic of ultramafic rocks (Ndjigui et *al.,* 2008; Bilong et *al.*, 2011). They have outstanding contents in titanium and Sr, this may be due to enrichment in the source materials. The high Al_2O_3 and TiO_2 content of the rocks also suggest that the parental melt was a MORB type (Baumgartner *et al*., 2012). Pyroxenites have high LREE contents. These could be related to the enrichment of their source materials, or to a low degree of partial melting of source protoliths with garnet among the residual phases (Nzenti *et al*., 2006; Vanthangliana *et al.,* 2011). Experimental studies (e.g. Irving and Frey, 1978; Green and Pearson, 1985) have shown that garnet has high mineral/melt partition coefficients for the HREE and it is therefore considered as the key mineral to produce high $(La/Yb)_n$ ratios in pyroxenites. These REE characteristics suggest that the Nyabitande pyroxenite magmas could have been formed within the stability field of garnet from a subducted eclogitic crust. The negative Eu anomaly in pyroxenite is linked to the redox conditions of the environment (Neal and Taylor, 1989). Negative Eu anomalies within pyroxenites were also observed in Lolodorf area (Ebah Abeng, *et al*., 2012); as well as the green stone belt of Nuggihalli (Subba Rao *et al.*, 2004). This anomaly may result from a strong fractionation of plagioclases or the presence of accessory minerals like zircon, apatite and monazite (Saleh, 2007; Lee *et al.,* 2009). According to Lee *et al*. (2009), voluminous plagioclase growth removes significant Eu^{2+} from the system during magma crystallization and this reduction of total Eu limits the Eu^{3+} available to zircon, resulting in progressively more negative Eu anomalies in later grown zircon. The high value of fractionation index in pyroxenite is linked to a high rate of fractionation of REE thus depletion in HREE (Nédélec *et al*., 1990). The low contents of S and total PGE may be the result of hydrothermal alteration. Alard *et al*. (2000) showed that

during partial melting of the mantle, base metal sulfides (BMS) melt incongruently to produce a Cu–Ni-rich sulphide melt that concentrates Pd and Pt. The average Pt/Pd ratio is very low; Pd and Pt have little or no significance in pyroxenites (Godel and Barnes, 2007). The enrichment signifies that partial melting failed to completely dissolve the sulphide residue of the mantle (Subba Rao *et al.,* 2004). The low contents of IPGE may be due to the segregation of these elements within the residue issued by partial fusion of the mantle (Bockrath *et al.,* 2004; Peregoedova *et al.,* 2004). It could equally be due to the increase in oxygen fugacity or their partitioning during crystallization (Fonseca *et al.,* 2009; Fiorentini *et al.,* 2011).

VI.2.4. Petrography and base metal geochemistry of weathered amphibolite

The macroscopic aspects of the weathered blocks and the presence of primary minerals such as amphibole and feldspars indicate that the garnet amphibolites of Akom II area are in the first stage of the weathering processes (Delvigne, 1998). This is confirmed by the fresh core of several weathered samples. Weathered specimens appear to be studded with garnets owing to differential weathering, giving the impression that the rocks are composed wholly of garnet (Rajaprian *et al*., 2014). The low contents in several major and trace elements such as Si, Ca, Mg, Na, P Zn, REE are characteristic of weathering processes (Beauvais, 2009). The accumulation of Al, Fe, Mn, Ti, Cr and V might be linked to the stability of newly crystalline secondary minerals like kaolinite, gibbsite, and goethite (Manceau *et al*., 2000; Singh *et al*., 2002).

Fe_2O_3 has weak correlations with Al_2O_3 suggesting different pattern of movement in the course of weathering (Khatun *et al*., 2014). In general the positive correlations among groups of trace elements identified above may signify that (i) these group of elements were laid down under the same physic-chemical conditions; (ii) these trace elements may be hosted by the same secondary mineral phases (Sababa, 2015). Meanwhile those groups of elements with negative correlations proof that they are incompatible and consequently hosted by different mineral phases.

The weathered amphibolites have overall low contents in REE; the low contents of REE confirm the ultramafic nature of the rocks (Perelomov *et al*., 2012). The positive and negative Ce-anomalies observed from normalized patterns could result from the variability of oxidizing conditions (Neal and Taylor, 1989). The negative Eu-anomalies could be inherited from the fresh rocks or due to the weathering of plagioclase. The values of $(La/Yb)_n$ are low and variable for weathered amphibolites. The values of fractionation index are in conformity

with the ultramafic nature of the rocks (Perelomov *et al*., 2012). REE often migrate and accumulate in rocks through different ways (Perelomov *et al*., 2012). The scattered plots of REE are all positive, these suggests a common source for all samples (Bellot *et al*., 2010); and highlights a similar mechanism of REE migration and accumulation in the rocks (Perlomov *et al*., 2012). Silica has strong associations with Eu and Dy and the HREE. This confirms the slight depletion of silica in the weathered amphibolites. Silica also possess slight positive correlations with LREE and with the sum of REE as a whole, this settles the high mobility of LREE during alteration. It however has strong positive correlation with the heavy REE. This confirms the slight depletion of silica in the weathered amphibolites.

Ni and Cr contents are low in the weathered blocks. The low Ni and Cr contents may indicate fractionation of their carrier mineral (olivine), or partial melting of some mantle material containing extremely low proportions of olivine (Hoch, 1999). The low Ni contents in these samples can also be associated to a low degree of partial melting of the original magma (Barnes and Lightfoot, 2005). PGE contents are higher in the weathered samples. This could be due to the presence of goethite in which PGE can be trapped (Wimpenny *et al*., 2007). The IPGE/PPGE values are also higher in weathered samples than in the fresh ones. This is due to the high mobility of PPGE in supergene environment (Cabral *et al*., 2007). The relatively high IPGE contents might be caused by the low degree of weathering (Auge and Legendre, 1994; Fonseca *et al*., 2009). The positive Pd anomaly could suggest partial remobilization of this element during alteration. Source of Pd during alteration could be provided by PGM located in the interstitial altered silicate matrix (González-Jiménez *et al*., 2008). The positive-sloped chondrite-normalized patterns shown by some weathered samples from suggest that PPGE remobilization during metamorphism is not homogeneous but has variable spatial intensity (Gervilla *et al*., 2008).

The negative correlation between S and Ni, and S with Ni/Cr reveals the opposite behaviour of both base metals during the weathering process contrary to the correlation between S and Ir. Sulfur and iridium are highly leached in the supergene environment.

The positive correlation of Au, Ru, Rh, Pt, Pd, and Cr in the Grant's isocon diagram suggests that these base metals have similar behavior during weathering. The depletion in Ni, Cu and S means that they are more soluble in their oxidized form. Conversely, Os, Ir, Au, Ru Rh, Pt, Pd, and Cr are less soluble in their oxidized form too (Berger *et al*., 2015). According to Fu *et al*. (2015), the enrichment of Au-PGE in weathered samples could be strongly linked to the presence of organic matter.

From these ratios we can be deduced that: (1) Ir, Ru, Rh and Au are more mobile than Pd in the weathered amphibolites; (2) Ir is highly mobile compared to other Au-PGE; (3) Ru is more mobile than Rh which is in turn mobile than Au in all the weathered samples; (4) Pt is slightly more mobile than Pd, except for K7 and K18 samples. However, the Pd/Pt values are higher than 1 in some samples. This indicates the contrast Pt behavior in the supergene environment. The high values above 1 reveal a minimum fractionation of palladium compared to other PGE. The weathered materials are enriched in PPGE (16-77 ppb) than IPGE (0.26 - 2.11 ppb). The high PPGE abundance might be relative to the oxidation of primary mineral into goethite (Ahmed *et al*., 2009). The strong depletion of IPGE can be attributed to retention of IPGE in the metal alloys of the original magma (Barnes *et al*., 1995). With respect to the fresh rocks, Os, Ir and Ru are depleted. In fact PPGE are more mobile (more soluble) than IPGE in the supergene environment (Garuti, 2004). These results suggest that the processes that lead to PGE, Ni- and Cu-enrichment are quite different. Gold, Ru, Rh, Pt, Pd, and Cr are positively correlated on the Grant's isocon diagram (Grant, 1986; 2005); the diagram confirms PGE-enrichment in the weathered samples revealed by the chondrite- normalized base metal patterns. Scattered plots reveal strong positive correlations between Rh, Ru, Pt and Pd with Cr in weathered amphibolites. This confirms the findings that chromium and PGE are associated in mafic and ultramafic rocks (Garuti, 2004). Plots of nickel and platinum group elements reveal positive correlations between Ru (IPGE) and Ni. Similarly nickel has positive correlations with all the palladium –like platinum group elements. The positive correlation of Ni-PGE may suggest that these metals were originally components of a primary mineral assemblage (Zaccarini *et al*., 2014).

The mass-balance assessment shows depletion in Ni, Cu and S. This signifies that they are more soluble in their oxidized form (Berger et al., 2015). The strong depletion of S, Ni and Cu is also a consequence of weathering, it is characteristic of lateritization as observed elsewhere (e.g., Ndjigui et al., 2008; Beauvais, 2009). Also, there is strong PPGE enrichment observed in the medium and coarse grained weathered amphibolites. The PGE contents are higher in the coarse grained materials than in the other facies. This is because, the coarse grained size of this facie permits the easy release of PGE from their primary bearing phases, since coarse grained rocks easily go in to dissolution than fine grained ones (Ndjigui and Bilong, 2010). Barnes and Liu (2011) showed that Pd and Pt are much more mobile in sulphide-rich rocks than in silicates. The strong enrichment of Pd and Pt suggest that the rocks are richer in silicates. Mass balance reveals strong IPGE leaching in most samples. The

leaching of PGE could be due to (i) the removal of PGE as aqueous organic or hydroxide complexes (Barnes and Liu, 2011; Hanley, 2005); (ii) the low PGE contents in the rocks; (iii) or due to the weathering. Particularly, the high leaching of osmium, iridium and ruthenium could be extremely efficient where groundwater has an oxygen fugacity close to that of the atmosphere. Fu *et al*. (2015) explained that the accumulation of Au-PPGE in some weathered samples could be strongly linked to the presence of organic matter.

In general, the fresh and weathered garnet amphibolites from the green stone belt of the Archaean Congo Craton possess very similar geochemical features for base metals (S, Cu, Ni, and Au-PGE). These materials are at their early stage of weathering and are not too differentiated despite their variable S contents. According to several authors (Cabral *et al*., 2007; Suarez et al., 2010; Ndjigui and Bilong, 2010; Ebah Abeng *et al*., 2012; Sababa *et al*., 2015), platinum-group elements are also remobilized in geological materials in their early stage of weathering.

GENERAL CONCLUSION

GENERAL CONCLUSION

In view of determining the distribution of S, Au-PGE, a petrologic study was carried out on amphibolites and their weathered products. They are situated under the forest cover of Nyabitande and Zingui areas. The area is characterized by humid equatorial climate, while the lithology is that of the greenstone belt of the Archaean Congo Craton.

Amphibolites appear in the form of rounded and spherical blocks of different dimensions. They are medium-grained, dark-coloured, and dense, made up of green hornblende, plagioclase, garnet, biotite, quartz, apatite, chalcopyrite and pyrite. The rocks present a nemato-granoblastic heterogranular texture.

The distribution of major, trace and rare earth elements in amphibolites of Nyabitande and Zingui confirms the basic nature of these rocks. However, the rocks of Nyabitande are richer in SiO_2, V, and Cu with rather lower Fe_2O_3 and Al_2O_3 contents. The chondrite normalised REE patterns are very flat for amphibolites from Nyabitande area, while those from Zingui area are inclined. This suggests that amphibolites from Nyabitande were derived from a depleted mantle source, whereas those from Zingui were from some enriched mantle source.

Two types of amphibolites were identified, the sulphur rich and sulphur poor types. This variability is the result of hydrothermal alteration. Cu contents are high while Ni contents are low and variable. Despite the low total Au-PGE contents, the amphibolites are richer in PPGE than in IPGE. Pd and Pt are the most abundant elements, while gold contents are low and variable. Some PGE have strong positive correlations with Cr and MgO, suggesting that these elements have a common source. The Au-PGE normalised patterns show that Pd in amphibolites of Nyabitande could have been incorporated from other sources. Base metal patterns show a strong enrichment in Cu and Ni relative to Au-PGE.

The weathered amphibolite blocks are centimetric and dense, with centripetal weathering. They are made up of amphibole, feldspars, quartz, garnet kaolinite, gibbsite, goethite, hematite, and spinel. As a result of weathering, major and trace elements like SiO_2, CaO, MgO, Na_2O, TiO_2 MnO Zn, Ga, Co and Sr were depleted. Rather, there were slight enrichments in Fe_2O_3, Zr, Ba, Th, U, and Mo. Nevertheless, the contents of other trace elements were stable. Trace elements have strong affinities with some major oxides, an indication that these are held within the same secondary mineral phases. Normalized REE patterns reveal Ce- and Eu-anomalies in some samples.

The weathered samples are marked by variable S and Cu contents**.** Weathering led to some enrichment in Cu, and Au-PGE compared to the fresh rocks. The S, Ni and Cr contents are rather low, indicating that they were affected by variable degree of weathering. The chondrite-normalized base metal patterns reveal relative enrichment in Cu, and Pd. The Grant's isocon diagram shows depletion in Os, Ir and Ru and Au, Ru, Rh, Pt, Pd, and Cr align.

Pyroxenite has elevated Cu contents; low Ni and Au-PGE contents and very low sulphur contents. These contents have similar trends with those amphibolites.

Within the context of metallogeny, we note variable S contents both in the fresh and weathered rocks; high Cu and low Au-PGE contents in amphibolites. Consequently, S, and Au-PGE are not enriched enough to form workable deposits; but are significant enough to act as mineralization indices of value in a geochemical survey.

RECOMMENDATIONS

This work was a survey of sulphur, gold and platinum group elements in amphibolites and their weathered products. We identified chalcopyrite and pyrite as the carrier minerals for Au-PGE. This was realized on a few samples. It will be necessary to (i) increase the scope of this work; (ii) do more detailed analyses on sulphur, non-identified opaque minerals, and carrier minerals. Here, electron microprobes will be used to realize photographs to confirm the findings.

REFERENCES

Ahmed, H.A., Shoji, A., Yaser, M.A.-A., Moha, I., Abdellatif, R., 2009. Platinum-group elements distribution and spinel composition in podiform chromitites and associated rocks from the upper mantle section of the Neoproterozoic Bou Azzer ophiolite, Anti-Atlas Morocco. *J. Afri. Earth Sci.* **55, 92-104**.

Ako, T. A., Vishiti, A., Ateh, K. I., Kedia, A. C., Suh, C. E., 2015. Mineral Alteration and Chlorite Geothermometry in Platinum Group Element (PGE)-bearing meta-ultramafic rocks from South East Cameroon. *Journal of Geosciences and Geomatics,* **3 (4): 96-108.**

Ako, T. A., Vishiti, A., Suh, C. E., Kedia, A. C., 2017. Evaluation of Platinum Group Elements (PGE) Potentials of Ultramafic Rocks of the Paleoproterozoic Nyong Series, Southeast Cameroon. *International Journal of Mining Science,* **3, 1-20.**

Alard, O., Griffin, W.L., Lorand, J.P., Jackson, S.E., O'Reilly, S.Y., 2000. Nonchondritic distribution of the highly siderophile elements in mantle sulphides. *Nature.* 407, 891-894.

Andrade, W.O., Mackesky, M.L., Rose, A.W., 1991. Gold distribution and mobility in the surficial environment Carajás region, Brazil. *J. Geochem. Explor.* **40, 95-114**.

Anthony E.Y., Williams P.A., 1994. Thyiosulfate complexing of platinum group elements. Implications for supergene geochemistry. Proceedings of ACS Symposium series 550. *American Chem Soc, Washington DC,* **553-560**.

Asaah, A.V., 2010. Lode Gold Mineralisation in the Neoproterozoic Granitoids of Batouri, Southeastern Cameroon (Unpublished Ph.D. thesis). *Clausthal University of Technology,* p. **200.**

Asaah, A.V., Zoheir, B., Lehmann, B., Frei, D., Burgess, R., Suh, C.E., 2014. Geochemistry and geochronology of the ~620 Ma gold-associated Batouri granitoids, Cameroon. *Int. Geol.* Rev.http://dx.doi.org/10.1080/00206814.2014.951003.

Augé, T., 1985. Chromitites et minéraux du groupe du platine dans les complexes ophiolitiques. Caractérisation des séries hôtes. *Thèse Doct. d'Etat, Univ. d'Orléans*.

Auge´, T., Legendre, O., 1994. Platinum-group element oxides from the pirogues ophiolitic mineralization New Caledonia: origin and significance. *Econ. Geol.* **89, 1454– 1468.**

Auge´, T., Maurizot, P., Breton, J., Eberle´, J.-M., Gilles, C., Jezequel, P., Me´zie`re, J., Robert, M., 1995. Magmatic and supergene platinum-group minerals in the New Caledonia ophiolite. *Chronique de la Recherche Minière* **520, 3-26**.

Aye, A.B., 2010. Contribution to petrologic study of Amphibolites in the Greenstone Belt of the Nyong Unit in Nyabitande (Akom II South Cameroon): Geochemical Survey of indices of gold and Platinum Group Elements. Unpublished M.Sc. *Dissertation, University of Yaounde I*, p **96**.

Azaroual, M., Romand, B., Freyssinet, P., Disnar, J., 2001. Solubility of platinum in aqueous solutions at 25°C and phs 4 to10 under oxiding conditions. *Geochim. Cosmochim. Acta* **65 (24), 4453-4466.**

Bai, Z.-J., Zhong, H., Li, C., Zhu, W.-G., Xu, G.-W., 2012. Platinum-group elements in the oxide layers of the Hongge mafic–ultramafic intrusion, Emeishan Large Igneous Province, SW China. *Ore Geol. Rev.* **46, 149-161**.

Baker, I.A., Gamble, J.A., Graham, I.J., 1994. The age, geology and geochemistry of the Tapuaenuku Igneous Complex, Marlborough, New Zealand. *J. Geol. Geophy* **37, 3, 249-268**.

Balaram, V., Singh, S.P., Satyanarayanan, M., Anjaiah, K. V., 2013. Platinum group elements geochemistry of ultramafic and associated rocks from Pindar in Madawara Igneous Complex, Bundelkhand massif, central India. *J. of Earth Syst. Sci.***122, 1, 79 -91.**

Ballhaus, C. G., Stumpfl, E. F., 1986. Sulphide and platinum mineralization in the Merensky reef: evidence from hydrous silicates and fluid inclusions. *Contrib. Min. Petro*. **94, 193-204.**

Barakat A., Marignac C., Boiron M-C., Bouabdeli M., 2002. Caractérisation des paragèneses et des paléocirculations fluides dans l'indice d'or de Bleïda (Anti-Atlas, Moroc). *Comptes Rendus Geoscience* **334, 35-41**.

Barbosa, J.S.F., Sabaté, P., 2002. Geological features and the Paleoproterozoic collision of four Archaean crustal segments of the São Francisco craton, Bahia, Brazil. *A synthesis. Anais da Academia Brasileira de Ciências* **74 (2), 343-349**.

Barker, F., 1979. Trondhjemite. Definition, environment and hypotheses of origin. In: Barker, F. (Ed.), Trondhjemites Dacites and Related Rocks. *Elsevier, Amsterdam*, **pp. 1–12.**

Barker, F., Arth, J.G., 1976. Generation of trondhjemitic–tonalitic liquids and Achaean bimodal trondhjemites-basalt suites. *Geol* **4, 596–600.**

Barnes, S-J., Naldrett, A.J., Gorton, M.P., 1985. The origin of the fractionation of platinum-group elements in terrestrial magmas. *Chem. Geol*. **53, 303–323**.

Barnes, S.J. 1990. The use of metal ratios in prospecting for platinum group element deposits in mafic and ultramafic intrusions. *J. Geochem Explor* **37, 91-99**.

Barnes S-J, Makovicky E, Karup-Moller S, Makovicky M, Rose-Hanson J 1997. Partition coefficients for Ni, Cu, Pd, Pt, Rh and Ir between monosulfide solid solution and sulfide liquid and the implications for the formation of compositionally zoned Ni–Cu sulfide bodies by fractional crystallization of sulfide liquid. *Can. J. Earth Sci.* **34, 366–374**.

Barnes, S.-J., Boyd, R., Korneliussen, A., Nilsson, L.-P., Often, M., Pedersen, R.-B., Robins, B., 1988. The use of mantle normalization and metal ratios in discriminating between the effects of partial melting, crystal fractionation and sulphide segregation on platinum-group elements, gold, nickel and Cu: examples from Norway. *In Geo-platinum 87 Symp. Vol. (H.M. Prichard, P.J. Potts, J.F.W. Bowles & S.J. Cribbs, eds.). Elsevier, London* **(113-143).**

Barnes, S.-J., Maier, W.D., 1999. The fractionation of Ni, Cu and the noble metals in silicate and sulphide liquids. In: Keays, R.R., Lesher, C.M., Lightfoot, P.C., Farrow, C.E.G. (Eds.), Dynamic Processes in Magmatic Ore Deposits and Their Application in Mineral Exploration, Short course, Volume 13. *Geol. Asso. Can.* **69-106.**

Barnes S-J, Acterberg E, Makovicky E, Li C 2001. Proton probe results for partitioning of platinum group elements between monosulphide solid solution and sulphide liquid. *S. Afr. J. Geol.***104, 337–351**.

Barnes, S-J., Lightfoot, P.C., (2005). Formation of magmatic nickel-sulfide ore deposits and processses affecting their copper and platinum-group element contents. In Hedenquist, J.W., Thompson, J.F.H., Goldfarb, R.J. and Richards, *J.P. (eds.) Econ. Geol*. 100th Anniversary Vol, **179-213**.

Barnes, Stephan J., Liu, W., 2012. Pt and Pd mobility in hydrothermal fluids: evidence from komatiites and from thermodynamic modelling. *Ore Geol. Rev.* **44, 49-58.**

Baumgartner, R. J., Zaccarini, F., Garuti, G., Thalhammer, O. A. R., 2013. Mineralogical and geochemical investigation of layered chromitites from the Bracco–Gabbro complex, Ligurian ophiolite, Italy. *Contrib. Mineral. Petrol.* **165, 477–493**.

Bayiga, E.C., Bitom, D., Ndjigui, P-D., Bilong, P., 2011. Mineralogical and geochemical characterization of weathering products of amphibolites at SW Eséka (Northern border of the Nyong unit, SW Cameroon). *J. Geol. Min. Res* **3(10), 281-293.**

Beauvais, A., 2009. Ferricrete biochemical degradation on the rainforest–savannas boundary of Central African Republic. *Geoderma* **150, 379-388**.

Bédard, L. P., Savard, D.D., Barnes, S-J., 2008. Total sulphur concentration in geological reference materials by elemental infrared analyzer. Geostand. Geoanal. Res. 32, 203-208.

Bekoa E., 1994. Etude pétrologique et géochimique d'une couverture pédologique sur gneiss en zone forestière de l'Extrême Sud Cameroun : relation avec la dynamique du fer. *Thèse Doct. 3e cycle, Univ. de Yaoundé I*, **187** p.

Bellot, J-P., Laverne, C., Bronner, G., 2010. An early Palaeozoic supra-subduction lithosphere in the Variscides: new evidence from the Maures massif. *Int J Earth Sci* (Geol Rundsch) **99, 473–504**.

Berger A., Janots E., Gnos E., Frei R., Bernier F., 2015. Rare earth element mineralogy and geochemistry in a laterite profile from Madagascar. *Appl. Geochem*. **41, 218-228.**

Bickle, M.J., Betternay, L.F., Chapman, H.J., Groves, D.I., McNaughton, N.J., Campbell, I.H., de Laeter, J.R., 1993. Origin of the 3500–3400Ma calc-alkaline rocks in the Pilbara Archaean: isotopic and geochemical constraints from the Shaw batholith. *Precam. Res*. **60, 117–149.**

Bilong, P., Ndjigui, P.-D., Temdjim, R., Sababa, E., 2011. Geochemistry of peridotite and granite xenoliths under the early stages of weathering in the Nyos volcanic region (NWCameroon): implications for PGE exploration. *Chem. Erde Geochem.* **71, 77-86.**

Bitom D., 1988. Organisation et évolution d'une couverture ferrugineuse en zone tropicale humide (Cameroun). Genèse et transformation d'ensembles ferrugineux indurés profonds. *Thèse Doct. Univ. de Poitiers,* **164** p.

Bleeker, W., 1990. Thompson area-general geology and ore deposits. In Geology and Mineral Deposits of the Flin Flon and Thompson belts, Manitoba (A.G. Galley, A.H. Bailes E.C. Syme, W. Bleeker, J.J. Macek & T.S. Gordon, eds.). Int. Assoc. Genesis of Ore Deposits Guide Book l0; *Geol. Surv. Can., Open-File Rep*. **2165, 93-136**.

Bockrath, C., Ballhaus, C.G., Holzheid, A., 2004. Fractionation of platinum-group elements during partial melting. *Science* **305, 1951–1953**.

Boudreau, A.E., Mathez, E.A., McCallum, I.S., 1986. Halogen geochemistry of the Stillwater and Bushveld complexes: Evidence for transport of the platinum-group elements by Cl-rich fluids. *J. Petrol*. **27, 967-986.**

Boudreau, A.E., McCallum, I.S., 1992. Concentration of platinum-group elements by magmatic fluids in layered intrusions: *Econ. Geol.* **87, 1830-1848.**

Bourges, F., Debat, P., Grandin, G., Parisot, J. C., Barras, E., Ouadraogo, M. F., Tollon, F., 1994. Déformation progressive de filons de quartz en concentrations aurifères, *C. R. Acad. Sci. Paris,* 319, série II, **543-550**.

Bowell, R.J., Gize, A.P., Foster, R.P., 1993. The role of fulvic acid in the supergene migration of gold in tropical rain forest. *Geochim. Cosmochim. Acta* **57, 4179-4190.**

Bowles, J. F. W., 1986. The development of platinum-group minerals in laterites *Econ. Geol.* **81, 1278-1285.**

Bowles, J.F.W., 1987. Further studies of the development of platinun-group minerals in the laterites of the Freetown Layered Complex, Sierra Leone. In: Pritchard, H.M., Plotts, P.J., Bowles, J.F.W., Cribb, S.J. (Eds.), *Geo-Platinum, 87. Elsevier, Amsterdam*, **273-280**.

Bowles J.F.W., Gize A. P., Cowden A., 1994. The mobility of the platinum-group elements in the soils of the Freetown Peninsula, Sierra Leone. *Can. Mineral.* **62, 957-967.**

Bowles, J.F.W., Gize, A.P., Melfi, A.J., 1995. The mobility of the platinum-group elements in the soils of the Freetown Peninsula, Sierra Leone. *Can. Mineral.* **32, 957-967**.

Boyle, R. W., 1979. The geochemistry of gold and its deposits. *Geological Survey Canadian Bulletin* **280, 564.**

Braun, J-J., Pagel, M., 1990. U, Th and REE in the Akongo lateritic profile (SW Cameroon). *Chemical Geology* **84, 357-359**.

Brenan, J. M., 2008. The Platinum-Group Elements: "Admirably Adapted" for Science and Industry. *Elements* **4, 227–232.**

Butt, C.R.M., Zeegers, H., 1992. Regolith exploration geochemistry in tropical and subtropical terrains. In: Butt, C.R.M., Zeegers, H. (Eds.), Handbook of exploration geochemistry, 4, C.R.M., **607.** *Elsevier, Amsterdam*.

Cabral, A.R., 2006. Palladium gold mineralization (Ouro Petro) in Brazil Gongo Soco, Itaira and Serra Pelada. Geol Jahrb Reihe. D. Sonderheft 8 *Econ. Geol*. **103, 115.**

Cabral, A.R., Beaudoin, G., Choquette, M., Lehmann, B., Polonia, J.C., 2007. Supergene leaching and formation of platinum in alluvium: evidence from Serro, Minas Gerais, Brazil. *Min. Petrol.* **90, 141-150.**

Cabri, L.J., Laflamme, J.H.G., 1976. The mineralogy of the platinum-group elements from some copper-nickel deposits of the Subdury area, Ontario. *Econ. Geol.* **71, 1159-1195.**

Cabri, L. J., Harris, D. C., Weiser, T. W., 1996. Mineralogy and Distribution of Platinum-group Mineral (PGM) Placer Deposits of the world. *Exploration Mining Geology* **5(2), 73-167.**

Cabri, L. J., 2002. The Platinum-Group Minerals. In: Cabri, L. J. (ed.) Geology, Geochemistry, Mineralogy and Mineral Benefication of Platinum Group Element. *Can. Inst. of Min. Metall. and Petroleum, Special* **54, 13-129.**

Carville, D. P., Leckie, J. F., Moorhead, C. F., Rayner, J. G., Durbin, A. A., 1990. Coronation Hill gold-Platinum-palladium deposit. In: Hughes FE (ed) Geology of mineral deposits of Australia and Papua New Guinea. *Australasian Inst. of Min. and Metall. Melbourne,* **759-762.**

Cawthorn, R.G., 2010. The platinum group element deposits of the Bushveld Complex in South Africa. *Platin. Met. Rev.* **54 (4), 205–215.**

Champetier de Ribes, G., Aubague, M., 1956. Carte géologique de reconnaissance du Cameroun à l'échelle de 1/500 000. Feuille de Yaoundé-Est + notice explicative. *Dir. Mines Géol. Cameroun,* **35** pp.

Chu, H., Chi, G., Bosman, S., Card, C., 2015. Diagenetic and geochemical studies of sand-stones from drill core DV10-001 in the Athabasca basin, Canada, and implications for uranium mineralization. J. Geochem. Explor. **148, 206–230**.

Coakley, G. J., Mobbs, P. M. 1999. The Mineral Industries of Africa World Wide Web URL: http://minerals.usgs.gov/minerals/pubs/country/1999/africa99.pdf.Retrieved 10 November, 2002.

Colin, F., 1992. L'or dans l'alterosphere lateritique. In: Paquet, H., Clauer, N. (Eds.), *Colloques ``Sedimentologie et geochimie de la Surface'' de l'Academie des Sciences et du Cadas,* **111-125.**

Colin, F., Lecomte, P., 1988. Etude mineralogique et chimique du profil d'alteration du prospect aurifere de Megaba Mvono (Gabon). *Chron. Rech. Min.* **491, 55-65**.

Colin, F., Minko, A.E., Nahon, D., 1989. L'or particulaire residuel dans les profils lateritiques: alteration geochimique et dispersion superficielle en conditions equatoriales. *C.R. Acad. Sci. Paris 309 (Serie II),* **553-560.**

Colin, F., Vieillard, P., 1991. Behavior of gold in lateritic equatorial environment: weathering and surface dispersion of residual gold particles, at Dondo Mobi, Gabon. *Appl. Geochem*. **6, 279-290.**

Colin, F., Lecomte, P., Minko, A.E., Benedetti, M., 1993. Regional exploration strategies at Pounga, Gabon and gold dispersion under equatorial rain forest conditions. *Chron. Rech. Min.* **510, 61-68**.

Colin, F., Sanfo, Z., Brown, E., Bourles, D., Minko, A.E., 1997. Gold: a tracer of the dynamics of tropical laterites. *Geol.* **25 (1), 81-84**.

Condie, K.C. Sinha, A.K., 1996. Rare earth and other trace element mobility during mylonitization: a comparison of the Brevard and Hope Valley shear zones in the Appalachian Mountains, USA. *Jour. Met. Geol.*, **14, 213-226**.

Crocket, J. H., Teruta, Y., Garth, J., 1976. The relative importance of sulphides, spinels, and platinoid minerals as carriers of Pt, Pd, Ir and Au in the Merensky reef at Western Platinum Limited, near Marikana, South Africa. *Econ. Geol.* **71, 1308-1323**.

Dare, S.A.S., Barnes, S.–J., Prichard, H.M., Fisher, P. C., 2010a. The timing and formation of platinum-group minerals from the Creighton Ni-Cu-platinum-group element sulfide deposit, Sudbury, Canada: early crystallization of PGE-rich sulfarsenides. *Econ. Geol.* **105, 1071–1096**.

Dare, S.A.S., Barnes, S.–J., Prichard, H.M., 2010b. The distribution of platinum group elements and other chalcophile elements among sulfides from the Creighton Ni–Cu–PGE sulfide deposit, Sudbury, Canada, and the origin of Pd in pentlandite. *Miner. Depos.* **45,765–793.**

Dare, S. A. S., Barnes, S.-J., Prichard, H. M., Fisher, P. C. 2011. Chalcophile and platinum-group element (PGE) concentrations in the sulfide minerals from the McCreedy East deposit, Sudbury, Canada, and the origin of PGE in pyrite. *Miner. Depos*. **46, 381–407**.

Delvigne, J.E., 1998. Atlas of micromorphology of mineral alteration and weathering. *Can. Min.* **3, 494**.

Dillon-Leitch, H.C.H., Watkinson, D.H., Coats, C.J.A., 1986. Distribution of platinum-group elements in the Donaldson West deposit, Cape Smith belt, Quebec, *Econ. Geol.* **81 (5), 1147-1158.**

Djon, M. L. N., 2010. Changement de la minéralogie des sulfures, des minéraux du groupe du platine et des textures avec le degree d'altération des zones Roby, Twilight et High-Grade du Complex du Lac-Des-Iles (Ontario, Canada). *Unpublished M.Sc. thesis, Univ. du Québec à Chicoutimi,* **95**.

Drummond, M.S., Defant, M.J., 1990. A model for trondhjemite–tonalite–dacite genesis and crustal growth via slab melting: Archaean to modern comparisons. *J. Geophy. Res.* **95B, 21503–21521.**

Ebah Abeng A. S., 2006. Les pyroxénites à grenat de l'unité du Bas-Nyong dans le secteur de Lolodorf (Département de l'Océan, Région du Sud) : pétrographie, géochimie et prospection géochimique du platine, palladium et or. *Memoire DEA, Université de Yaoundé I,* **65**.

Ebah Abeng, S.A., Ndjigui, P.-D., Aye, A.B., Tessontsap, T., Bilong, P. 2012. Geochemistry of pyroxenites, amphibolites and their weathered products in the Nyong unit, SW Cameroon (NW border of Congo craton): implications for Au-PGE exploration. J. *Geochem. Explor*. **114, 1-19.**

Edou Minko, A., Colin, F., Trescases, J.J., Lecomte, P., 1995. Les mécanismes de dispersion et d'accumulation d'or. *J. afro Géol.* **322-326.**

Eno Belinga, S. M., 1984. Géologie du Cameroun. Librarie Universitaire. *Univ. Ydé. Rep. Unie du Cameroun.* **281**.

Feybesse, J. L., Johan, V., Maurizot, P., Abessol, A., 1986. Evolution tectono-métamorphique libérenne et éburnéenne á la partie NW du craton zaïrọis (SW Cameroon). Current Research in *Africa Journal of Earth Sciences, Matheis and Schandelmeier (eds) Balkema, Rotterdam*: **9 – 12**.

Fleet, M.E., Wu, T.W., 1993. Volatile mass transfer of platinum-group elements in sulfide-chloride assemblages at 1000°C. *Geochim. Cosmochim. Acta* **57, 3519-3531**.

Fonseca, R.O.C., Campbell, I.H., O'Neill, H. St. C., Allen, C.M., 2009. Solubility of Pt in sulphide mattes: implications for the genesis of PGE-rich horizons in layered intrusions. *Geochim. Cosmochim. Acta* **73, 5764-5777**.

Freyssinet, P., Lecomte, P., Edimo, A., 1989. Dispersion of gold and base metals in the Mborguene lateritic profile, East Cameroun. *J. Geochem. Explor.* **32, 99-116**.

Freyssinet, P., 1994. Gold mass balance in lateritic profiles from savana and rain forest zones. *Catena* **21, 159-172**.

Frey, F.A., Suen, C.J., Stockman, H.M., 1985. The Ronda high temperature peridotite: geochemistry and petrogenesis. *Geochim. Cosmochim. Acta* **49, 2469–2491**.

Fuchs, W.A., Rose A. W., 1974. The geochemical behavior of platinum and palladium in the weathering cycle in the Stillwater Complex, Montana. *Econ. Geol.* **69 (3), 332-346.**

Fu, X., Wanga, J., Yuhong, Z., Tan, F., Wenbinga, C., Feng, X., 2015. The geochemistry of platinum group elements in marine oil shale-A case study from the Bilong Co oil shale, northern Tibet, China. *Chem. Erde Geochem.* **75, 55-63.**

Ganno, S., Ngnotue, T., Kouankap, N.G.D., Nzenti, J.P., Notsa, F.M., 2015. Petrography and geochemistry of the banded iron-formations from Ntem complexes belt, Elom area, Southern Cameroon: implications for the origin and depositional environment. *Chem. Erde Geochem.* **75, 375-387**.

Ganno, S. Njiosseu, T.E.L., Kouankap N.G.D., Djoukouo S.A., Moudioh, C., Ngnotue, T., Nzenti, J.P., 2017. A mixed seawater and hydrothermal origin of superior-type Banded Iron Formation (BIF)-hosted Kouambo iron deposit, Palaeoproterozoic Nyong series, Southwestern Cameroon: constraints from petrography and geochemistry. *Ore Geol. Rev.* **80, 860-875**.

Garuti, G., 2004. Chromite-Platinum Group Element MagmaticD. In: De Vivo, B., Stüwe, K. (eds). Geology Encyclopedia of Life Support Systems (EOLSS). *Oxford (United Kingdom), Eolss Pub. http://www.eolss.net*.

Gasquet, D., Levresse, G., Cheilletz, A., Azizi-Samir M.R., Mouttaqi, A., 2005. Contribution to a geodynamic reconstruction of the Anti-Atlas (Morocco) during Pan-African times, with the emphasis on inversion tectonics and metallogenic activity at the Precambrian-Cambrian transition. *Precamb Res* **140, 157-182**.

Genkin A.D., Evstigneeva T.L., 1986. Associations of Platinum-Group Minerals from Noril'sk Sulphide Ores. *Econ. Geol*., **81, 1203-1212.**

Gervilla, F., Fanlo, I., Kerestedjian, T., Castroviejo, R., Padrón, J. A., Rodrigues, J. F., González-Jiménez, J. M., 2011. Origin of Ferrian Chromite in Metamorphosed Podiform Chromitites: a Two-Stage Process. *Contrib Mineral Petr.* **150, 589-607**.

Ghorfi, El. M., Oberthür, T., Melcher, F., Lüders, V., Maacha, L., Ziadi, R., Baoutoul, H., 2006. Gold- palladium mineralization at Bleïda Far West, Bou Azzer-El Graara Inlier, Anti-Atlas, Morocco. *Miner Dep.* **41, 549-564**.

Godel, B., Barnes, S.-J., 2007. Platinum-group elements in sulphide minerals and the whole rocks of the J-M reef (Stillwater Complex): implication for the formation of the reef. *Chem. Geol.* **248 (3-4), 272-294.**

Godel, B., Barnes, S.J., 2008. Platinum-group elements in sulfide minerals and the whole rocks of the J-M Reef (Stillwater Complex): implication for the formation of the reef. *Chem. Geol.* **248, 272–294**

Godel, B., Barnes, S.-J., Maier, W.D., 2007. Platinum-group elements in sulphide minerals, platinum-group minerals, and whole-rocks of Merensky Reef (Bushveld complex, South Africa): implications for the formation of the Reef. *J. Petrol.* **48, 1569-1684**.

Gomwe, S.T., 2008. The formation of the Palladium-Rich Roby, Twilight and High-Grade Zones of the Lac Des Iles Complex, Ontario. *Doctorate thesis*. **191**.

Gonzalez-Jiménez, J.M., Kerestedjian, T., Proenza, J.A., Gervilla, F., 2008. Metamorphism of Chromite ores from the Dobromirtsi Ultramafic Massif, Rhodope Mountains (SE Bulgaria). *Geologica Acta,* **7, 4, 413-429**.

Good, D.J., Naldrett. A.J., 1993. Geology and distribution of platinum-group elements, Bucko Lake intrusion. Thompson belt, Manitoba. *Can. Mineral*. **31, 45-60**.

Goodwin, A.M., 1991. Precambrian Geology-The dynamic evolution of the continental crust. *Academic Press, New York*.

Grant, J.A., 1986. The isocon diagram – a single solution to Gresens' equation for metasomatic alteration. *Econ. Geol.* **81, 1976-1982**.

Grant, J.A., 2005. Isocon analysis: a brief review of the method and applications. *Phys. Chem. Earth* **30, 997-1004**.

Gray F., Page. N. J., Carlson C. A., Wilson S. A., Carlson R. R., 1986. Platinum group elements geochemistry of zoned ultramafic intrusive suites, Klamath Mountains, Carlefornia and Oregon. *Econ. Geol.* **81, 5, 1252-1260**.

Green, T.H., Pearson, N.J., 1985. Experimental determination of REE partition coefficients between amphibole and basaltic to andesitic liquids at high pressure. *Geochim. Cosmochim. Acta* **49, 1465–1468**.

Gruenevaldt, G. V., Hatton, C. J., Merkle, R. K. W. and Gains, S. B., 1986. Platinum group elements-chromitite associations in the Bushveld Complex. *Econ. Geol.* **81, 5, 1067-1079**.

Gueddari, K., Piboule, M., Amosse, J., 1994. Comportement des éléments du groupe du platine (PGE) dans les ultrabasites des Beni Bousera (Rif, Maroc): données préliminaires. *C. R. Acad. Sci. Paris*. **318, 79-86**.

Helmy, H.M., Ballhaus C., Wohlgemuth-Ueberwasser C., Fonseca, R.O.C, Laurenz, V., 2010. Partitioning of Se, As, Sb, Te and Bi between monosulfide solid solution and sulfide melt—application to magmatic sulfide deposits. *Geochim. Cosmochim. Acta* **74, 6174–6179**

Handler R. M., Bennett C V., 1999. Behaviour of platinum–group elements in the subcontinental mantle of eastern Australia during variable metasomatism and melt depletion. *Geochim Cosmochim. Acta* **63, 3597-3618**.

Hanley, J. J., Mungall, J. E., Pettke, T., Spooner, E. T. C., Bray C. J., 2005. Fluid and Halide melt inclusions of magmatic origin in the ultramafic and lower banded series, Stillwater Complex, Montana, USA. *J. Petrol.* **49, 1133-1160.**

Harney D M. W., Roland K. W. Merkle., Gerhard Von Gruenewaldt., 1990. Platinum-group element behavior in the lower part of the upper zone, eastern Bushveld. *Econ. Geol.* **85, 1777-1789.**

Hao, L., Zhao, X., Boorder, de, H., Lu, J., Zhao, Y., Wei, Q., 2014. Origin of PGE depletion of Triassic magmatic Cu-Ni sulfide deposits in the central-southern area of Jilin province, NE China. *Ore Geol. Rev.* **63, 226-237**.

Hoch. M., 1999. Geochemistry and Petrology of Ultramafic Lamprophyres from Schirmacher Oasis East Antarctica. *Min. and Petrol.* **65, 51-67**.

Hsu, L.C., Lechler, P.J., Nelson, J.H., 1991. Hydrothermal solubility of palladium in chloride solutions from 300° to 700°C: preliminary experimental results. *Econ. Geol.* **86, 422-428**.

Huminicki MAE, Sylvester PJ, Cabri LJ, Lesher CM, Tubrett M 2005. Quantitative mass balance of platinum-group elements in the Kelly Lake Ni–Cu–PGE deposit, Copper Cliff Offset, Sudbury. *Econ. Geol.* **100, 1631–1646.**

Ismail, S.A., Mirza, T.M., Carr, P.F., 2010. Platinum-group elements geochemistry in podiform chromitites and associated peridotites of the Mawat ophiolite, north eastern Iraq. *J. Asian Earth Sci.* **37, 31-41**.

Irving, A.J., Frey, F.A., 1978. Distribution of trace elements between garnet megacrysts and host volcanic liquids of kimberlitic and rhyolitic composition. *Geochim. Cosmochim. Acta* **42, 771–787**.

Irvine, T.N. Sharpe, M. R., 1982. Source-rock compositions and depths of origin Bushveld and Stillwater magmas. *Carnegie Institution of Washington.* **294-303.**

Kamgang Kabeyene Beyala, V., Onana, V. L., Ndome Effoudou Priso, E., Parisot, J-C., Ekodeck, G. E., 2009. Behaviour of REE and mass balance calculations in a lateritic profile over chlorite schists in South Cameroon. *Chemie der Erde* **69, 61-73**.

Kay, S.M., Coira, B., Viramonte, J., 1994. Young mafic back arc volcanic rocks as indicators of continental lithospheric delamina-tion beneath the Argentine Puna plateau, Central Andes. *J. Geophy. Res.* **99 (B12), 24323–24339**.

Kay, S.M., Abbruzzi, J.M., 1996. Magmatic evidence for Neogene lithospheric evolution of the central Andean ‘‘flat-slab’’ between 30°S and 32°S. *Tectonophysics* **259, 15–28**.

Keays, R.R., 1995. The role of komatiitic and picritic magmatism and S-saturation in the formation of ore dep. *Lithos* **34, 1–18.**

Khatun, S., Mondal, S. K., Zhou, M-F., Balaram, V., Prichard, H. M., 2014. Platinum-group element geochemistry of Mesoarchean ultramafic–mafic cumulate rocks and chromitites from the Nuasahi Massif, Singhbhum Craton (India). *Lithos* **205, 322-340**.

Korhonen, F. J., Saito, S., Brown, M., Siddoway, C. S., Day J. M. D., 2010. Multiple Generations of Granite in the Fosdick Mountains, Marie Byrd Land, West Antarctica: Implications for Polyphase Intracrustal Differentiation in a Continental Margin Setting. *J. Petrol.* **51 (3), 627-670.**

Krupp, R.E., Weiser, T., 1992. On the stability of gold-silver alloys in the weathering environment. *Mineral. Depos.* **27, 268-275**.

Lauder, W. R., 1970. Origin of Merensky reef. *Nat.* **227, 355-356**.

Lee, R.G., Dilles, J.H., Mazdab, F.K., Wooden, J.L., 2009. Europium anomalies in zircon from granodirorite porphyry intrusions at the El Salvador porphyry copper deposit, Chile. *The Geol. Soc. of America,* **158-8**.

Lerouge, C., Cochérie, A., Toteu, F.S., Penaye, J., Milési, J.P., Tchameni, R., Nsifa, E.N., Fanning, C.M., Deloule, E., 2006. SHRIMP U-Pb zircon age evidence for Paleoproterozoic sedimentation and 2.05 Ga syntectonic plutonism in the Nyong Group, Southwestern Cameroon: consequences for the Eburnean-Transamazonian belt of NE Brazil and Central Africa. *J. Afri. Earth Sci.* **44, 413-427**.

Lee, R.G., Dilles, J.H., Mazdab, F.K., Wooden, J.L., 2009. Europium anomalies in zircon from granodirorite porphyry intrusions at the El Salvador porphyry copper deposit, Chile. *The Geol. Soc. of America*, **158-8**.

Lesher, C.M., Stone, W.E., 1996. Exploration geochemistry of komatiites. In Wyman, D.A. (ed.), Igneous trace elements geochemistry, application for massive sulphide exploration. *Geol. Association of Canada, short course notes,* **12, 153-204**.

Letouzey R., 1985. Notice explicative de la carte phytogéographique du Cameroun à l'échelle de 1/500 000. Fascicules 1, 2, 3, 4 et 5. *Institut de la Carte Internationale de la Végétation, Toulouse*, **240**.

Le Fur, Y., 1964. Rapport special Roches basiques. *Yao 64 A 15. Arch. B.R.G.M*.

Li, C., Naldrett, A.J., Coat, C.J.A., Johannessen P., 1992. Platinum, palladium, gold and copper-rich stringers at the Strathcona Mine, Sudbury: their enrichment by fractionation of a sulfide liquid. *Econ. Geol.* **87, 1584–1598.**

Li, C., Naldrett, A. J., Rucklidge, J. C., Kilius, L. R., 1993. Concentration of platinum-group elements and gold in sulfides from the Strathcona deposit, Sudbury, Ontario. *Can. Mineral*. **31, 523–531**.

Li, C., Barnes, S-J., Makovicky, E., Rose-Hansen, J., Makovicky M., 1996. Partitioning of Ni, Cu, Ir, Rh, Pt and Pd between monosulfide solid solution and sulfide liquid: effects of com-position and temperature. *Geochim. Cosmochim. Acta* **60, 1231–1238**.

Lorand, J.P., Alard, O., 2001. Platinum-group abundances in the upper mantle: new constraints from in-situ and whole rock analyses of massive central xenoliths (France). *Geochim. Cosmochim. Acta* **65, 2789-2806**.

Lorand, J. P., Luguet, A., Alard, O., Bezos, A., Meisel, T., 2007. Abundance and distribution of platinum-group elements in organic Iherzolites; a case study in a Fontete Rouge Iherzolite (French Pyrénées). *Chem. Geol.* **248, 174-194.**

Lauguet A., Shirey S. B., Lorand J. –P., Horan M. F., Carlson R. W., 2007. Residual platinum-group minerals from highly depleted harzburgites of Lherz massif (France) and their role in HSE fractionation of mantle. *Geochim. Cosmochim. Acta* **71, 3082-3097**.

Maier, W. D., Barnes, S.-J., Gartz, V., Andrews, G., 2003. Pt-Pd reefs in magnetitites of the Stella layered intrusion, South Africa: A World of new exploration opportunities for platinum group elements. *Geol.* **31, 885-888**.

Manceau, A., Schlegel, M.L., Musso, M., Sole, V.A., Gauthier, C., Petit, P.E., Trolard, F., 2000. Crystal chemistry of trace elements in natural and synthetic goethite. *Geochim. Cosmochim. Acta* **64, 3643-3661**.

Mann, A.W., 1984. Mobility of gold and silver in lateritic weathering profiles: some observations from Western Australia. *Econ. Geol.* **79, 38-49.**

Martin, H., 1986. Effect of steeper Archaean geothermal gradient on geochemistry of subduction-zone magmas. *Geol.* **14, 753–756.**

Martin, H., Moyen, J.-P., 2002. Secular changes in tonalite–trondhjemite–granodiorite composition as markers of the progressive cooling of Earth. *Geol*. **30, 319–322**.

Matthey, J., 1999. Annual Report & Accounts 1999 – Johnson Matthey. *www.matthey.com/AR99/1999annualrep*.

Maurizot, P., Abessolo, A., Feybesse, A., Johan, J.L., Lecomte, P., 1986. Etude et prospection minières du Sud-Ouest Cameroun. *Synthèse des travaux de 1978 à 1985*. **85-**CMR 066. BRGM.

Maurizot, P., 2000. Geological map of south, west Cameroon. Edition BRGM, Orleans.

McCready, A.J., Parnell, J., Castro, L., 2003. Crystalline placer gold from the Rio Neuquén, Argentina: implications for the gold budget in placer gold formation. Econ. *Geol.* **98, 623-633**.

McDonough, W.F., Sun, S.-S., 1995. The composition of the Earth. *Chem. Geol*. **120, 223-253**.

Minyemeck, A. E., 2006 Les amphibolites et talcshistes du secteur du Pouth-Kellé (plaine côtière du Cameroun) petrography, mineralogy, géochimie et prospection géochimique du platine, palladium et or. *Mém. D.E.A., Univ. de Yaoundé I*, **82** p.

Minyem D., Nédélec A., 1990. Origine et évolution métamorphique des gneiss d'Eséka (SW Cameroun). *15th Colloquium of Afr. Geol. CIFEG. Univ. Nancy I*.

Mitchell, R. H., Keays, R.R., 1981. Abundance and distribution of gold, palladium and iridium in some spinel and garnet Iherzolites: implication for the nature and origin of precious metal-rich intergranular components in the upper mantle. *Geochim. Cosmochim. Acta* **45, 2425-2442**.

Mota-e-Silva, J., Ferreira Filho, C.F., Giustina, M.E.S.D., 2013. The Limoeiro deposit: Ni-Cu-PGE sulfide mineralization hosted within an ultramafic tabular magma conduit in the Borborema Province, Northeastern Brazil. *Econ Geol.* **108, 1753-1771**.

Mota-e-Silva, J., Prichard, H. M., Ferreira Filho, C.F., Fisher, P.C., McDonald, I., 2015. Platinum-group minerals in the Limoeiro deposit: Ni- Cu-PGE sulfide deposit, Brazil: the effect of magmatic and amphibolite upper to granulite metamorphic processes on PGM formation. *Miner Dep.* **50, 1007-1029**.

Mountain, B.W., Wood, S.A., 1988. Chemical controls on the solubility, transport, and deposition of platinum and palladium in hydrothermal solutions: a thermodynamic approach. *Econ. Geol.* **83, 492-510**.

Mpodozis, C., Cornejo, P., Kay, S.M., Titler, A., 1995. La Franja de Maricunga: Sintesis de la evolucion del Frente Volcanico Oligo-ceno-Mioceno de la zona sur de los Andes Centrales. *Rev. Geol. Chile* **21, 273–313**.

Mungall, JE, Andrews, R, Cabri, LJ, Sylvester, PJ, Tubrett, M 2005. Partitioning of Cu, Ni, An, and platinum-group elements between monosulfide solid solution and sulfide melt under controlled oxygen and sulfur fugacities. *Geochim. Cosmochim. Acta* **69, 4349–4360.**

Naldrett AJ, Innes DG, Sowa J, Gorton MP. 1982. Compositional variations within and between five Sudbury ore deposits. *Econ. Geol.* **77, 1519–153**.

Naldrett, A. J., Gasparrini, E. C., Barnes, S. J., Von Gruenewaldt, G. Sharpe, M. S. 1986. The upper critical view of the Bushveld Complex and the origin of Merensky-type Ores. *Econ. Geol.* **81, 1105-1117**.

Naldrett, A.J., 2004. Magmatic sulfide deposits: geology, geochemistry and exploration. *Springer, Berlin*, **727.**

Naldrett, T., Kinnaird, J., Wilson, A., Chunnett, G., 2008. Concentration of PGE in the earth's crust with special reference to the Bushveld Complex. *Earth Sci. Front.* **15 (5), 264-297.**

Naldrett, A.J., Wilson, A., Kinnaird, J., Chunnett, G., 2009. PGE tenor and metal ratios within and below the Meren-sky Reef, Bushveld Complex: Implications for its genesis; *J. Petrol.* **50, 625–659**.

Naldrett, A.J., Wilson, A., Kinnaird, J., Yudovskaya, M., Chunnett, G., 2012. The origin of chromitites and related PGE mineralization in the Bushveld Complex: new mineralogical and petrological constraints. *Miner. Dep.* **47, 209-232.**

Nana, R., 2001. Pétrologie des péridotites en enclaves dans les basaltes alcalins récents de Nyos: apport à la connaissance du manteau supérieur de la ligne du Cameroun. *Thèse Doct d'Etat, Univ. Yaoundé I,* pp **220**.

Ndema Mbongue, J. L., Ngnotue, T., Ngo Nlend, C. D., Nzenti, J. P., Cheo Suh, E. 2015. Origin and Evolution of the Formation of the Cameroon Nyong Series in the Western Border of the Congo Craton. *Journal of Geosciences and Geomatics* **2(2): 62- 75**.

Ndjigui, P.-D., Bilong, P., Nyeck, B., Eno Belinga, S. M., Vicat, J. P., Gerard M., 1998. Les produits d'alteration du gneiss à biotite et amphibolite dans la plaine côtière de Douala. *Ann. Fac. Sci., Univ. Ydé Série Sci. Nat. et Vie*, **34, 191-216**.

Ndjigui P.-D., Bilong P., Nyeck B., Eno Belinga S. M., Vicat J. P., Gerard M., 1999. Etude morphologique et géochimique de deux profils latéritiques dans la plaine côtière de Douala (Cameroun). Géol. et Environ. au Cameroun, Vicat J.P. et Bilong P. éd. collect. GEOCAM 2, *Press. Univ. Yaoundé I,* **189-201**.

Ndjigui P.-D., Bitom D., Bilong P., Colin F., Hendratta Ntalla A., 2002. Correlation between metallic oxides (Fe_2O_3, Cr_2O_3, and NiO) platinum and palladium in the laterites from South-East Cameroon (Central Africa): Perspectives of PGE survey in weathering mantles. *In the Extended Abtracts volume of the 9th International Platinum Symposium, Billings, Montana (USA), 21-25th July 2002*, **500** p.

Ndjigui, P.-D., Mungall, J. E. Bilong, P., 2004. Behaviour of PGE in the Mang North weathering profiles on serpentinites in the Lomié ultramafic complex, (South-East Cameroon). *Proceedings of Recent Advances in Magmatic Ore Systems of Mafic Ultramafic Rocks, IGCP 479 Hong Kong*, **129-134**.

Ndjigui P.-D., 2008. Altération supergène des serpentinites et distribution des éléments du group du platine dans les profils latéritiques du complexe ultrabasique de Lomié (Sud-Est Cameroun). *Thèse Doct/PhD. Univ. de Yaoundé I,* **284** p.

Ndjigui P.-D., Bitom D., Bilong P., Colin F., Hendratta Ntalla A., 2003. Influence des oxydes métalliques (Fe_2O_3, Cr_2O_3, NiO) sur le comportement du platine et du palladium dans les manteaux d'altération des roches ultrabasiques serpentinisées en zone forestière humides d'Afrique Centrale. *Annales de la Fac. des Sci., Série Sciences de la Terre et de la Vie, Univ. de Yaoundé I,* **35**, n° 2, **7-16.**

Ndjigui, P.-D., Bilong, P., 2010. Platinum-group elements in the serpentinite lateritic mantles of the Kongo-Nkamouna ultramafic massif (Lomié region, South-East Cameroon). *J. Geochem. Explor.* **107, 63–76**.

Ndjigui, P.-D., Bilong, P., Bitom, D., Dia, A., 2008. Mobilization and redistribution of major and trace elements in two weathering profiles developed on serpentinites in the Lomié ultramafic complex, South-East Cameroon. *J. Afr. Earth Sci*. **50, 305–328**.

Ndjigui, P.-D., Yongue-Fouateu, R., Bilong, P., Bayiga, E.C., Oumarou, M., 2009. Geochemical surveys of Pt, Pd and Au in talcschists and hornblendites, and their weathered equivalents at Pouth-Kellé, Southern Cameroon. *J. Cameroon Acad. Sci.* **8, 115-128**.

Nesbitt, H.W., Wilson, R.E., 1992. Recent chemical weathering of basalts. *American Journal Sciences* **292, 740-777**.

Neal, C.R., Taylor, L.A., 1989. A negative Ce anomaly in a peridotite xenolith: evidence for crustal recycling into the mantle or mantle metasomatism. *Geochim. Cosmochim. Acta* **53, 1035-1040**.

Nédélec, A., Nsifa, E.N., Martin, H., 1990. Major and trace element geochemistry of the Archaean Ntem plutonic complex (South Cameroon): petrogenesis and crustal evolution. *Prec. Res.* **47, 35–50**.

Ngo Bidjeck, L.M., 2004. L'altération des roches basiques et ultrabasiques du Sud-Ouest Cameroun et ses implications métallogéniques. Cas du complexe d'Abiété-Yenjok. *Thèse de Doct. /Ph.D, Univ. de Yaoundé I,* **267** p.

Nguetnkam J. -P., 1994. Etude d'une toposéquence des sols sur granite dans la région de Mvangan (Sud-Cameroun). Caractérisation de deux domaines de pédogenèse différenciés. *Thèse Doct. 3^e cycle, Univ. de Yaoundé I,* **165** p.

Nkoumbou, C., Villieras, F., Njopwouo, D., Yonta Ngoune, C., Barres, O., Pelletier, M., Razafitianamaharavo, A., Yvon, J., 2008. Physicochemical properties of talc ore from three deposits of Lamal Pougué area (Yaoundé Pan-African Belt, Cameroon), in relation to industrial uses. *Applied Clay Science* **41, 113-132**.

Ntep Gweth, P., Dupuy, J. J., Matip, O., Fombutu, Fogakoh, A., Kalngui, E., 2001. Ressources minérales du Cameroun : *Notice explicative de la carte thématique des ressources minérales du Cameroun sur un fond Géologique. Edition Sopecam, Ydé,* **153-170.**

Nzenti, J.P., Barbey, P., Macaudière, J., Soba, D., 1988. Origin and evolution of the late Precambrian high-grade Yaounde gneisses (Cameroon). *Prec. Res.* **38, 91–109**.

Nzenti, J.P., Kapajika, B., Wörner, G., Lubala, T.R., 2006. Synkinematic emplacement of granitoïds in a Pan-African shear zone in Central Cameroon. *J. Afri. Earth Sci*. **45, 74-86**.

Oberthur, T., Weiser, T.W., Gast, L., 2003. Geochemistry and mineralogy of platinum-group elements at Hartley Platinum Mine Zimbabwe. *Mineral. Depos.* **38, 344–355**.

Oumarou M., 2006. Prospection géochimique du Pt, Pd et Au dans les boules altérées de talcschistes et d'amphibolites contenues dans les produits d'altération des gneiss à biotite de la localité de Pouth-Kelle (Plaine côtière du Cameroun). *Mémoire DEA, Univ. de Ydé I,* **60**.

Owona, S. 2008. Archaean, Eburnean and Pan-African Features and Relationships in their Junction Zone in the South of Yaounde (Cameroon). *PhD Thesis, University of Douala*, pp **232**.

Owona, S., Schulz, B., Ratschbacher, L., Ondoa, J. M., Ekodeck, G. E., Tchoua, F. M., Affaton, P., 2011. Pan-African Metamorphism evolution in the southern Yaounde Group (Oubannguide Complex, Cameroon) as revealed by EMP-Monazite dating and thermobarometry of garnet metapelites. *Journal of African Earth Sciences* **59, 125-139**.

Owona, S., Mvondo, J. O., Ekodeck, G. E., 2013. Evidence of quartz, feldspar and amphibole crystal plastic deformation in the Paleoproterozoic Nyong complex shear zones under amphibolites to granulite conditions (West Central African Fold Belt, SW Cameroon). *Journal of Geography and Geology* **5(3), 186-201**.

Paśava, J., Vymazalov, A., Košler, J., Koneev, R.I., Jukov, A.V., Khalmatov, R.A., 2010. Platinum-group elements in ores from the Kalmakyr porphyry Cu-Au-Mo deposit,

Uzbekistan: bulk geochemical and laser ablation ICP-MS data. *Miner. Depos.* **45 (5), 411-418.**

Penaye, J., Toteu, S.F., Tchameni, R., Van Schmus, W. R., Tchakounté, J., Ganwa, A., Minyem, D., Nsifa, N.E., 2004. The 2.1 Ga West African belt in Cameroon: extension and evolution. *J. Afri. Earth Sci.* **39, 1196-1202**.

Prichard, H., Neary, C., Potts, P.J., 1986. Platinum group minerals in the Shetland ophiolite. In Gallagher M.J. et al. (eds). Metallogeny of basic and ultrabasic rocks. *Inst. Min. Metall. London* **395-414**.

Prichard, H.M., Sά J. H.S., Fisher, P.C., 2001. Platinum-group mineral assemblages and chromite composition in the altered and deformed Bacuri Complex, Amapa, Northeastern Brazil. *Can Mineral.* **39, 377-396**.

Prichard, H.M., Hutchinson, D., Fisher, P.C., 2004. Petrology and crystallization history of multiphase sulfide droplets in a mafic dike from Uruguay: implications for the origin of Cu–Ni–PGE sulfide deposits. *Econ. Geol.* **99, 365–376.**

Puchtel, H., Prichard, H.M., Berner, Z., Maynard, J., 1995. Sulfide mineralogy, sulfur content, and sulfur isotope composition of mafic and ultramafic rocks from leg 147. *Proceedings of the Ocean Drilling Program, Scientific Results*, **147, 4227-4242**.

Puchtel, I. S., Brandon, A. D., Humayun, M., 2004. Precise Pt–Re–Os isotope systematics of the mantle from 2.7-Ga komatiites. *Earth and Planetary Science Letters*, **224, 157–174**.

Peck, D.C., Keays, R. R., 1990. Insights into the behaviour of precious metals in primitive S-undersaturated magmas: evidence from the Heazlewood River complex, Tasmania. *Can. Mineral.* **28, 553–577**.

Peregoedova, A., Barnes, S-J., Baker, D.R., 2004. The formation of Pt-Ir alloys and Cu-Pd rich Sulfide melts by partial desulfurization of Fe-Ni-Cu sulfides: results of experiments and implications for natural systems. *Chem. Geol.* **208, 247-264**.

Perelomov, L. V., Asainova Zh. S., Yoshida, S., Ivanov, I. V., 2012. Concentrations of Rare- Earth Elements in Soils of the Prioksko-Terrasnyi State Biospheric Reserve Eurasian Soil *Sci.* **45, 10, 983–994**.

Piña R, Gervilla, F., Barnes, S-J, Ortega, L., Lunar, R., 2011. Distribution of platinum-group and chalcophile elements in the Aguablanca Ni–Cu sulfide deposit (SW Spain): evidence from a LA-ICP-MS study. *Chem. Geol.*

Rajaprian, K., Kuldeep, Singh, Vinoth, Kumar, M., Kumar, R S., 2014. Metamorphism and deformation of mafic and felsic rocks in Bhavani Shear Zone, Tamilnadu, India: *International J. of Adv. Geosci*. **2 (1) 13-19**.

Rapp, P.R., 1997. Heterogeneous source regions for Archaean granitoids. In: de Wit, M.J., Ashwal, L.D. (Eds.), Greenstone Belts. *Oxford University Press*, **267–279**.

Sababa, E., Ndjigui, P.-D., Ebah Abeng, S.A., Bilong, P., 2015. Geochemistry of peridotite xenoliths from the Kumba and Nyos areas (southern part of the Cameroon Volcanic Line): implications for Au-PGE exploration. *J. Geochem. Explor.* **152, 75-90.**

Saleh, G.M., 2007. Geology and rare-earth element geochemistry of highly evolved, molybdenite-bearing granitic plutons, Southeastern Desert, Egypt. *Chinese J. Geochem*. **26 (4), 333–344.**

Sanfo, Z., Colin, F., Delaune, M., Boulange, B., Parisot, J.C., Bradley, R., Bratt, J., 1993. Gold: a useful tracer in sub-Sahelian laterites. *Chem. Geol*. **107, 323-326**.

Santosh, M., Omana, P.K., 1991. Very high purity gold from lateritic weathering profiles of Nilambur, southern India. *Geol.* **19, 746-749**.

Salpéteur, I., Martel-Jantin, B., Rakotomanana, D., 1995. Pt and Pd mobility in ferralitic soils of the West Andriamena area (Madagascar). Evidence of a supergene origin of some Pt and Pd minerals. *Chronologie de la Recherche Minière* **520, 27-45**.

Satyanarayanan, M., Balaram, V., Sylvester, P.J., Subba Rao, D.V., Charan, S.N., Shaffer, M., Ali Mohammed Dar., Anbarasu, K., 2011. Geochemistry of late-Archean Bhavani mafic/ultramafic complex, southern India: implications for PGE metallogeny. *Appl. Geochem.* **13, 1-14.**

Savard, D., Barnes, S.-J., Meisel, T., 2010. Comparison between Nickel–Sulfur Fire Assay Te co-precipitation and Isotope Dilution with High-Pressure Asher acid digestion for the determination of Platinum-Group Elements, rhenium and gold. Geostan. *Geoanal. Res.* **34 (3), 281-291.**

Seabrook, C.L., Prichard, H. M., Fisher, P. C., 2004. Platinum-group minerals in the Raglan Ni-Cu (PGE) sulfide deposit, Cape Smith, Quebec, Canada. *Can. Mineral.* **42 (2), 485-497**.

Seewald, J.S., Seyfried, W.E. 1990. The effect of temperature on metal mobility in sub-seafloor hydrothermal systems: constraints from basalt alteration experiments. Earth Planet. *Sci. Lett.* **101, 388-403**.

Segalen, P., 1967. Les sols et la géomorphologie du Cameroun. *Cah. ORSTOM, sér. Pédol*., **2, 137-187**.

Shang, C.K., 2001. Geology, Geochemistry and Geochronology of Archaean Rocks from the Sangmelima Region, Ntem complex, NW Congo craton, South Cameroon. *Ph.D. Thesis, University of Tübingen, Germany*, **313**.

Shang, C.K., Liégeois, J.-P., Satir, M., Nsifa, E.N., 2010. Late Archaean high-K granite geochronology of the northern metacratonic margin of the Archaean Congo craton. Southern Cameroon: evidence for Pb-loss due to non-metamorphic causes. *Gond. Res.* **18, 337-355**.

Shang CK, Satir M, Siebel W, Nsifa EN, Taubald H, Lie´geois JP, Tchoua FM (2004). Major and trace element geo-chemistry, Rb–Sr and Sm–Nd systematics of TTG magma-tism in the Congo craton: case of the Sangmelima region, Ntem complex, southern Cameroon. *J Afr Earth Sci* **40, 61–79**.

Shang, C.K., Satir, M., Nsifa, E.N., Liégois, J.-P., Siebel, W., Taubald, H., 2007. Archaean high-K granitoids produced by remelting of earlier Tonalite-Trondhjemite–Granodiorite (TTG) in the Sangmelima region of the Ntem complex of the Congo craton. *Int. J. Earth Sci*. **96, 817-841**.

Sharpe, M. R.1985. Strongtium-isotope evidence for preserved density stratification in the main zone of the Bushveld Complex, South Africa. *Nat*. **316, 119-126.**

Sharrad, K.A., McKinnon-Matthews, J., Cook, N.J., Ciobanu, C.L., Hand, M., 2014. The basil Cu-Co deposit, Eastern Arunta region, Northern Territory, Australia: a metamorphosed volcanic-hosted massive sulphide deposit. Ore Geol. Rev. 56, 141-158.

Shellnutt, J.G., Mab, G.S.-K., Qi, L., 2015. Platinum-group elemental chemistry of the Baima and Taihe Fe-Ti oxide bearing gabbroic intrusions of the Emeishan large igneous province, SW China. *Chem. Erde Geochem*. **75, 35-49**.

Shepherd, T. J., Bouch, J. E., Gunn, A. G., Mckervey, J. A., Naden, J. Scrivener, R. C., Styles, M. T., Large, D. E., 2005. Permo-Triassic unconformity-related Au-Pd

mineralization, South Devon, UK: new insights and the European perspective. *Miner Deposita* **40, 24-44**.

Singh, B., Sherman, D.M., Gilkes, R.J., Wells, M.A., Mosselmans, J.F.W., 2002. Incorporation of Cr, Mn and Ni into goethite (α-FeOOH): mechanism from extended X-ray absorption fine structure spectroscopy. *Clay Min.* **37, 639-649**.

Sinyakova, E.F., Kosyakov, VI 2007. Experimental modeling of zoning in copper–nickel sulfide ores. *Dokl Earth Sci* **417A, 1380–1385**.

Smithies, R.H., 2000. The Archaean tonalite–trondhjemite–granodi-orite (TTG) series is not an analogue of Cenozoic adakite. *Earth and Planetary Science Letters* **182, 115–125**.

Smithies, R.H., Champion, D.C., Cassidy, K.F., 2003. Formation of Earth's early Archaean continental crust. *Prec. Res.* **127, 89–101**.

Song, X.Y., Keays, R.R., Zhou, M.F., Qi, L., Ihlenfeld, C., Xiao, J.F., 2009. Siderophile and chacophile elemental constraints on the origin of the Jinchuan Ni-C-(PGE) sulfide deposit, NW China. *Geochim. Cosmochim. Acta* **73, 404-424**.

Srivastava, R.K., 2012. Petrological and Geochemical Studies of Paleoproterozoic Mafic Dykes from the Chitrangi Region, Mahakoshal Supracrustal Belt, Central Indian Tectonic Zone: Petrogenetic and Tectonic Significance. *J. Geol. Soc. India* **80, 369-381**.

Stanienda, K. 2016. Strontium and barium in the Triassic Limestone of the Opole Silesia Deposits. *Arch. Min. Sci.* **61, 29-46**.

Stanley, C. 2009. Chromite composition and PGE content of Bushveld chromitites. 1. The Lower and Middle groups. Trans. Inst. Mining Metall., Sect. B: *Appl. Earth Sci.* **118, 131-161**.

Stern, R.J., 1981. Petrogenesis and tectonic setting of Late Precambrian ensimatic volcanic rocks, central eastern desert of Egypt. *Prec. Res.* **16, 195-230**.

Suarez, S., Prichard, H.M., Valasco, F., Fisher, P.C., McDonald, I., 2010. Alteration of platinum-group minerals and dispersion of platinum-group elements during progressive weathering of the Aguablanca Ni–Cu deposit, SW Spain. *Miner. Depos*. **45 (4), 331-350.**

Subba Rao, D.V., Sridhar, D.N., Charan, S.N., Balaran, V., Graneshwara, T., Govinda Rajulu, B., 2004. Petrology, trace, rare earth and platinum-group elements geochemistry of Archaean layered mafic–ultramafic magmatic intrusions from Nuggihalli greenstone belt, Southern India. *Proceedings of the "Recent Advances in Magmatic Ore Systems of Mafic–Ultramafic Rocks*", **118–122**.

Suchel J.-B., 1988. Les climats du Cameroun. *Thèse Doct. ès-Lettres, Univ. de Bordeaux III*, **1186**.

Suh, C.E., Lehmann, B., Mafany, G.T., 2006. Geology and geochemical aspects of lode gold mineralization at Dimako- Mboscorro SE Cameroon. Geochem. *Explor. Environ. Anal. 6, 295-309*.

Taborda, C. M.M., 2010. Distribution of platinum-group elements in the Ebay Claim, central part of the Bell River Complex, Matagami, Quebec. *Dissertation, University of Quebec at Chicoutimi*, **206**.

Takam, T., Arima, M., Kokonyangi, J., Dunkley, D.J., Nsifa, E.N., 2009. Paleoarchaean charnockites in the Ntem complex, Congo craton, Cameroon: insights from SHRIMP zircon U–Pb ages. *J. Mineralogical and Petrological Sciences* **104, 1–11**.

Tarney, J., Dalziel, I.W.D., De Wit, M.J., 1976. Marginal basin rocasverdes complex from southern chile: a model for Arhaean greenstone belt formation. In: Windley, B.F. (Ed.), *The Early History of the Earth. Wiley, London*, **131–146**.

Taufen P.M., Marchetto C.M.L., 1989. Tropical weathering control of Ni, Cu, Co and platinum group element distributions at the O'Toole Ni-Cu sulphidedeposit, Minas Gerais, Brazil. *J. of Geochem. Explor.* **32,185-197**.

Tchameni, R., 1997. Géochemie et geochronology des formations de l'Archéen et du paléoprotérozoïque du sud-Cameroun (groupe du Ntem, craton du Congo). *Thès. Univ. Orléans*, **356**.

Tchameni, R., Pouclet, A., Mezger, K., Nsifa, E.N., Vicat, J.P., 2004. Single zircon Pb-Pb and Sm-Nd whole rock ages for the Ebolowa greenstone belts: evidence for pre-2.9 Ga terranes in the Ntem Complex (South Cameroon). *J. Cameroon Acad. Sci.* 4, **235-246**.

Tessontsap Teutsong, 2010. Contribution à l'étude pétrologique des latérites développées sur amphibolites dans l'Unité du Bas-Nyong à Nyabitandé (Akom II, Sud Cameroun): recherche géochimique des indices d'Or et des Eléments du Groupe du Platine. *Mém. Master, Univ. de Yaoundé I,* **85** p.

Teutsong T., Bontognali, R.R.T., Ndjigui, P.-D., Vrijmoed, J.C., Teagle, D., Cooper, M., Vance, D., 2017. Petrography and geochemistry of the Mesoarchean Bikoula banded iron formation in the Ntem complex (Congo craton), Southern Cameroon: implications for its origin. *Ore Geol. Rev.* **80, 267-288**.

Tolstykh, N. D., Sidorov, E. G., Laajoki, K. V. O., Krivenko, A. P., Podlipskiy, M., 2002. The association of platinum-group minerals in placers of the Pustaya River, Kamchatka, Russia. *Can Mineral* **38, 1251-1264**.

Tomkins A. G., Pattison, D. R., Frost, B. R., 2007. On the initiation of metamorphic sulfide anatexis. ***J. Petrol.* 48 (3), 511-535**.

Toteu, S.F., Van Schmus, W.R., Penaye, J., Nyobe, J.B., 1994. U-Pb and Sm-Nd evidence for Eburnean and Pan-African high-grade metamorphism in cratonic rocks of southern Cameroon. *Prec. Res.* **67, 321-347**.

Toteu, S.F., Yongue, R.F., Penaye, J., Tchakounte, J., Seme Mouangue, A.C., Van Schmus, W.R., Deloule, E., Stendal, H., 2006. U–Pb dating of plutonic rocks involved in the nappe tectonic in southern Cameroon: consequence for the Pan-African orogenic evolution of the central African fold belt. *J. Afri. Earth Sci.* **44, 479–493**.

Traore´, D. 2005. Serpentinisation hydrothermale et alteration lateritique des roches ultrabasiques en milieu tropical: evolution mineralogique et geochimique de la mineralisation en platine de la Riviere des Pirogues, Nouvelle-Caledonie. *PhD thesis, Universite´ de la Nouvelle-Caledonie,* **193**.

Traoré D., Beauvais A., Augé T., Chabaux F., Parisot J.-C., Cathelineau M., Peiffert C., Colin F., 2006. Platinum and palladium mobility in supergene environment: the residual origin of the Pirogues River mineralization, New Caledonia. *J. Geochem. Explor.* **88, 350-354.**

Traoré, D., Beauvais, A., Augé, T., Parisot, J.-C., Colin, F., Cathelineau, M., 2008. Chemical and physical transfers in an ultramafic rock weathering profile: Part 2. Dissolution vs. accumulation of platinum group minerals. *Amer. Miner.* **93, 31-38**.

Travis G. A., Keays R. R., Davidson R. M., 1976. Palladium and iridium in the evaluation of nickel Gossans in Western Australia. *Econ. Geol.* **71, 1229-1243**.

Tuomo Karimen. 2010. The Koillismaa intrusion, Northeastern Finland-evidence for PGE reef forming processes in the layered series, Bull. *Geol. sol. Finland.* **176.**

Ukaegbu, V.U., Ekwueme, B. N., 2007. Geochemistry of the Precambrian Nigeria. *Global Journal of Geological Sciences* **5 (1& 2), 77- 99**.

Vanthangliana, V., Hussain, M.F., Lalnunmawia, J., 2011. Petrochemical studies metapelites of the area around Sonapahar, Meghalaya, India. *Science Vision* **11(2), 77-89**.

Varajao, C.A.C., Colin, F., Vieillard, P., Melfi, A.J., Nahon, D., 2000. Early weathering of palladium gold under lateritic conditions, Maquine Mine, Minas Gerais: Brazil. *Applied Geochemistry* **15, 245–263**.

Verma, S.P. 1992. Seawater alteration effects on REE, K, Rb, Cs, Sr, U, Th, Pb, and Sr-Nd-Pb isotope systematic of mid-ocean ridge basalts. *Geochem. Journ.* **26, 159-177**.

Vermaak, C. F. 1976. The Merensky reef-thoughts on its environment and genesis. *Econ. Geol*. **71, 1270-1298**.

Vicat, J.P., Pouclet, A., Nsifa, E., (1998). Les dolérites du groupe du Ntem (Sud-Cameroun) et des régions voisines (Centrafrique, Gabon, Congo, Bas-Zaïre). Caractéristiques géochimiques et place dans l'évolution du craton du Congo au Protérozoïque. *GEOCAM,* **1, 305-3.**

Vishiti, A., 2009. Primary and Eluvial Gold in the Batouri North Gold District, Southeastern Cameroon (*Unpublished M.Sc. thesis). University of Buea*, p. 75.

Vishiti, A., Suh, C.E., Lehmann, B., Egbe, J.A., Shemang, E.M., 2015. Gold grade variation and particle microchemistry in exploration pits of the Batouri gold district, SE Cameroon. *Journal of African Earth Sciences*, **111, 1-13**.

Wallace, P., Carmichael, I.S.E., 1992. Sulfur in basaltic magmas. *Geochim. Cosmochim. Acta* **56, 1863–1874**.

Wang, C.Y., Zhou, M.-F., Prichard, H.M., Fisher, P.C., 2008. Platinum-group minerals from the Jinbaoshan Pd–Pt deposit, SW China: evidence for magmatic origin and hydrothermal alteration. *Miner. Depos.* **43, 791–803**.

Whalen, J.B., Zwanzig, H.V., Percival, J.A., Rayner, N., 2008. Geochemistry of an alkaline, ca. 1885 Ma K-feldspar-porphyritic, monzonitic to syenogranitic suite northeastern Kisseynew Domain, Monitoba (parts of NTS 63O); in Reports of Activities 2008, Monitoba Science, Technology, Energy and Mines. *Monitoba geological survey*, **66-78**.

Whitten, D. G. A., with Brooks, J. R. V., 1972. The Penguin dictionary of Geology, **495** p.

Wilson, A.F., 1984. Origin of quartz-free gold nuggets and supergene gold found in laterites and soils-a review and some new observations. *Austral. J. Earth Sci.* **31, 303-316**.

Wilson, A.H., Murahwv, C. Z., Coghill, B., 2000. Stratigraphy, geochemistry and platinum group element mineralization of the central zone of the selukwe Subchamber of the Great Dyke, Zimbabwe. *J. Afr. Earth Sci* **30 (4), 633-653**.

Wimpenny, J., Gannoun, A., Burton, K.W., Widdowson, M., James, R.H., Gislason, S.R., 2007. Rhenium and osmium isotope and elemental behaviour accompanying laterite formation in the Deccan region of India. *Earth Planet. Sci. Lett.* **261, 239-258**.

Winter, J. D., 2001. An introduction to igneous and metamorphic petrology, 695, *Prentice Hall,* **ISBN 0-13-240342-0.**

Wolf, M.B., Wyllie, P.J., 1994. Dehydration melting of solid amphibolite at 10 kbar: the effect of temperature and time. *Contrib. Min. Petrol.* **115, 369–383.**

Wood, S.A., 1990. The interaction of dissolved platinum with fulvic acid and simple organic acid analogues in aqueous solutions. *Can. Mineral.* **28, 665-673**.

Wood, S.A., 1996. The role of humic substances in the transport and fixation of metals of economic interest (Au, Pt, Pd, U, V). *Ore Geol. Rev.* **11, 1-31**.

Xu, Y., Orberger, B., Reeves, S.J., 1998. Fractionation of platinum group elements in upper mantle: evidence from peridotite xenoliths from Wangqing. *Sci. China* **41 (4), 354-361**.

Ying, J., Zhang, H., Sun, M., Tang, Y., Zhou, X., Liu, X., 2007. Petrology and geochemistryof Zijinshan alkaline intrususive complexin Shanxi Province, western North China Craton: Implication for magma mixing of different sources in an extensional regime. *Lithos* **98, 45-66**.

Yongué, R., 1986. Contribution à l'étude pétrologique de l'altération et des faciès de cuirassement ferrugineux des gneiss migmatitiques de la région de Yaoundé. *Thèse. Doct. 3ème cycle. Univ. Yaoundé*, **214** p.

Yongue Fouateu, R., Yemefack, M., Wouatong, A. S. L., Ndjigui, P. D., Bilong, P., 2009. Contrasted mineralogical composition of the laterite cover on serpentinites of Nkamouna-Kongo, southeast Cameroon. *ClayMinerals,* **44, 221–237**.

Zaccarini, F., Proenza, J.A., Ortega-Gutiérrez, F., Garuti, G., 2005. Platinum group minerals in ophiolitic chromitites from Tehuitzingo (Acatlán complex, southern Mexico): implications for post-magmatic modification. *Mineral. Petrol.* **84, 147-168**.

Zaccarini, F., Garuti, G., Proenza, J.A., Campos, L., Thalhammer, O. A.R., Aiglsperger, T., Lewis, J.F., 2011. Chromiteand platinumgroup elementsmineralisation in the Santa Elena UltramaficNappe (Costa Rica): geodynamic implications. *Geol. Acta* 9, **3-4, 407-423**.

Zaccarini 2014. The occurrence of platinum group element and gold minerals in the Bon Accord Ni-oxide body, *S. Afr. American Mineralogist*, **99, 1774–1782**.

Zeegers, H., Leduc, C., 1991. Geochemical exploration in temperate, arid and tropical rainforest terrain, in Foster, R. P., éditeur, *Gold mettalogeny and exploration, Glasgow, Blackie and Sons*, **309-355**.

Zhou, H., McKeegan, K.D., Xu, X., Zindler, A., 2004. Fe-Al-rich tridymite-hercynite xenoliths with positive cerium anomalies: preserved lateritic paleosols and implications for Miocene climate. *Chem. Geol*. **207, 101-116**.

Appendix

Table 1 : Mass-balance assessment of major elements in weathered amphibolites.

	Fine grained					Medium grained			Coarse Grained				
	K1	K3	K6	K7	K17	K2	K9	K12	K14	KI5	K16	K8W	K18
SiO_2	-92.5219	-73.4697	-70.2364	-94.7395	-78.324	-78.5269	-12.2435	8.731313	-84.3912	-81.2589	-80.1743	-72.6602	-84.5637
Al_2O_3	-80.5253	-65.9629	-77.064	-93.2169	-69.8927	-72.8927	-17.1328	-4.45736	-61.8441	-62.5607	-81.9065	-64.6516	-83.5447
Fe_2O3	-75.8054	-38.0551	-51.2452	-83.9407	-55.4179	-55.8953	-8.21732	25.39785	-39.198	-35.4639	-71.2272	-44.7461	-71.6472
CaO	-98.8649	-90.5556	-99.8857	-99.6743	-95.0628	-90.5511	-17.7694	0.273016	-97.0624	-98.6474	-91.4638	-79.4265	-92.2837
MgO	-96.2436	-78.8432	-96.1316	-99.2199	-87.5376	-80.0518	17.49307	81.92982	-93.1689	-96.2625	-80.5252	-52.0677	-87.626
Na_2O	-98.9991	-91.7361	-99.6667	-99.7466	-96.7308	-91.02	-15.9942	-20.6667	-97.7944	-99.1034	-93.7305	-83.8095	-95.6797
K_2O	-4.375	-15	143	-68.8376	-41.1538	-47.0492	52.10526	92.66667	-54.1916	-3.16456	-30.5532	-12.5714	-25.8511
TiO_2	-70.2571	-44.9679	-54.7692	-82.8694	-59.4759	-45.9773	-7.77328	11.58974	-23.6527	-26.0078	-70.6187	-55.4451	-62.7169
MnO	-86.8342	-68.125	-77.5	-97.7198	-87.3901	-74.918	-1.57895	41.66667	-87.7844	-95.1582	-80.4681	-67.2143	-70.1596
P_2O_5	-65.3533	-39.7917	-55	-81.7586	-69.1758	-58.1967	-37.3684	-9.33333	-32.8144	-25.7595	-80.4681	-70.8571	-72.8723

Table 2 : Mass-balance assessment of trace elements in weathered amphibolites.

	Fine grained					*Medium grained*			*Coarse grained*				
	K1	K3	K6	K7	K17	K2	K9	K12	K14	K15	K16	K8W	K18
Cr	-31.3511	194.8643	-58.1395	-76.8447	30.33478	91.19329	45.65483	153.0233	175.5605	106.4321	20.62345	121.113	-73.5032
V	-83.6697	-58.267	-90.1019	-91.0439	-66.9805	-67.1609	5.430774	28.3482	-64.0146	-61.9648	-75.6024	-57.0746	-78.6895
Zn	-91.0908	-70.0645	-81.7857	-96.5616	-76.3148	-67.4863	6.516291	41.66667	-83.6399	-86.5506	-82.4316	-60.5357	-66.6287
Co	-87.9334	-74.0405	-88.0711	-90.6336	-78.7238	-74.2573	-3.25658	26.49856	-91.3649	-93.3426	-85.482	-65.6519	-86.2686
Sc	-82.2853	-61.2661	-71.9008	-90.7243	-60.3987	-67.1409	-2.14586	45.17906	-53.14	-52.516	-77.4011	-52.6328	-77.6303
Ga	-77.6327	-49.3624	-62.6047	-86.8633	-59.4789	-63.3816	-14.2301	-4.06202	-49.4332	-43.4751	-77.0058	-54.2355	-81.671
Zr	-50.162	-27.1234	6.730769	-69.4515	-49.8838	-9.42623	-13.9676	-12.8205	-26.0018	13.59542	-62.0213	-54.4643	-67.6555
Sr	-99.2067	-94.8707	-99.1517	-99.6016	-97.7969	-92.7925	-38.9111	-55.2138	-98.0202	-97.0838	-96.4828	-95.2266	-95.248
Y	-97.491	-82.3312	-98.1041	-99.0026	-93.5102	-82.8643	-32.9114	-12.8302	-94.1874	-90.9164	-88.0275	-86.1057	-87.8245
Nb	-59.139	-50.5733	-40.2948	-78.8229	-38.93	-45.9057	-19.9793	0.802621	-23.9153	-27.9881	-70.0329	-59.3647	-70.0063
Pb	293.9829	590.625	285.7143	30.83883	246.2716	2103.63	40.6015	94.28571	321.0009	312.7034	56.56535	326.7347	47.26444
Mo	-37.6359	-12.5	-6.47059	-70.0447	-62.0879	-22.1311	-34.2105	6.666667	1100.898	41.4557	-40	-14.2857	-80.3191
Li	-69.6607	-67.455	-14.0541	-94.4536	-65.9192	-69.1183	16.07397	22.52252	-90.0955	-86.0417	-85.9229	-75.3861	-68.7177
Rb	-86.2403	12.70089	395.3214	-74.4023	-42.1546	13.56557	19.19173	12.52381	-71.4243	-8.46745	-57.4483	-48.6097	-41.4172
Ba	-36.7744	11.22748	395.4054	-51.767	58.13484	93.72619	19.9431	67.24324	-25.5511	67.49914	-29.3801	-18.8726	-48.1886
Hf	-57.5789	-33.0539	-8.71951	-73.9541	-51.4741	-24.7201	-17.0732	-6.70732	-30.1701	-3.36138	-64.5355	-54.4643	-71.4388
U	7.404891	48.30729	89.375	-24.4691	57.62363	35.86066	-10.5263	-0.83333	39.33383	73.49684	-3.69681	18.39286	-2.79255
Ta	-61.8886	-50.6696	-55	-78.284	-30.9458	-49.2389	-23.3083	1.190476	-31.2874	-35.443	-69.772	-59.6684	-70.9347

Table 3 : Mass-balance assessment of rare earth elements in weathered amphibolites.

	Fine grained					Medium grained			Coarse grained				
	K1	K3	K6	K7	K17	K2	K9	K12	K14	K15	K16	K8W	K18
La	-96.196	-71.139	-81.106	-94.324	-59.577	-43.491	-15.095	-10.298	-80.442	-40.869	-28.06	-86.979	-72.834
Ce	-84.312	-68.851	-80.918	-91.309	-78.731	-39.511	-22.627	-14.071	-77.621	-56.609	-67.198	-77.187	-71.627
Pr	-96.397	-80.167	-90.25	-96.542	-75.481	-66.975	-23.947	-16.133	-86.105	-57.07	-58.332	-86.886	-81.553
Nd	-96.652	-82.537	-93.287	-97.291	-81.467	-72.462	-27.269	-14.944	-87.422	-63.279	-66.458	-87.016	-84.314
Sm	-96.439	-84.32	-95.635	-97.741	-84.471	-77.826	-26.593	-12.982	-88.182	-69.52	-75.342	-86.466	-86.282
Eu	-97.441	-89.375	-97	-98.538	-87.929	-83.707	-31.174	-25.897	-91.778	-77.405	-83.306	-86.83	-88.036
Gd	-96.945	-85.62	-97.355	-98.589	-89.792	-80.86	-29.833	-17.169	-91.214	-77.383	-81.722	-86.899	-87.999
Tb	-96.816	-84.206	-97.162	-98.562	-89.776	-81.17	-31.081	-14.234	-90.921	-80.371	-83.577	-85.724	-87.78
Dy	-96.628	-83.058	-97.155	-98.637	-90.062	-81.612	-31.004	-13.072	-91.374	-83.428	-84.831	-85.429	-87.359
Ho	-96.64	-81.04	-97.273	-98.695	-90.942	-82.265	-32.217	-10.707	-91.98	-86.958	-85.97	-84.913	-87.03
Er	-96.19	-79.31	-96.907	-98.694	-90.756	-82.474	-31.127	-8.866	-92.129	-88.908	-86.501	-84.227	-86.825
Tm	-95.71	-78.075	-95.714	-98.552	-89.992	-82.748	-33.96	-8.254	-92.002	-89.241	-86.049	-84.388	-86.651
Yb	-95.26	-76.038	-95.093	-98.361	-89.062	-82.699	-31.481	-2.2553	-91.145	-89.68	-85.72	-83.885	-86.352
Lu	-94.803	-76.094	-94.75	-98.29	-89.492	-82.582	-30.658	-3.6667	-91.602	-90.316	-86.436	-83.607	-86.888

Table 4 : Mass-balance assessment of base metals in weathered amphibolites.

	Fine grained					Medium grained			Coarse grained				
	K1	K3	K6	K7	K17	K2	K9	K12	K14	KI5	K16	K8W	K18
S	-92.31	-83.19	-91.17	-94.78	-86.95	-91.16	-65.73	-67.75	-78.13	-79.23	-94.01	-86.44	-96.57
Ni	-85.24	-36.81	-87.64	-92.88	-39.18	-42.77	30.22	119.26	-56.58	-46.31	-54.06	-17.55	-82.27
Cu	-85.51	-68.50	-92.16	-96.37	-80.99	-69.89	-32.56	-21.41	-76.98	-76.97	-83.10	-84.26	-85.64
Os	\	\	\	\	-59.04	\	-51.82	-21.54	\	\	\	\	\
Ir	-62.58	\	\	\	-57.97	\	-37.37	70.00	\	\	\	-19.86	\
Ru	-65.35	17.32	-56.88	\	-24.69	-32.07	-21.71	27.50	-2.66	21.04	-26.76	18.39	\
Rh	-31.73	36.42	-43.33	-95.50	-38.77	-0.91	-40.35	114.07	48.17	80.52	12.53	5.24	-82.58
Pt	22.04	210.69	-0.62	-64.05	142.24	57.18	105.66	787.87	118.84	182.09	135.23	280.51	45.71
Pd	-0.48	372.97	54.86	-87.58	62.74	157.56	42.32	558.83	257.15	392.96	176.11	134.68	-65.52
Au	-46.81	770.75	38.79	-89.41	-54.15	70.87	-19.56	0.74	-70.69	-42.94	482.89	-38.18	-85.39